

2016

Dosimetry, Activation, and Robotic Instrumentation Damage Modeling of the Holtec HI-STORM 100 Spent Nuclear Fuel System

C. Ryan Priest

University of South Carolina

Follow this and additional works at: <https://scholarcommons.sc.edu/etd>

 Part of the [Nuclear Engineering Commons](#)

Recommended Citation

Priest, C. R. (2016). *Dosimetry, Activation, and Robotic Instrumentation Damage Modeling of the Holtec HI-STORM 100 Spent Nuclear Fuel System*. (Master's thesis). Retrieved from <https://scholarcommons.sc.edu/etd/3832>

This Open Access Thesis is brought to you by Scholar Commons. It has been accepted for inclusion in Theses and Dissertations by an authorized administrator of Scholar Commons. For more information, please contact dillarda@mailbox.sc.edu.

DOSIMETRY, ACTIVATION, AND ROBOTIC INSTRUMENTATION DAMAGE MODELING
OF THE HOLTEC HI-STORM 100 SPENT NUCLEAR FUEL SYSTEM

by

C. Ryan Priest

Bachelor of Science
North Carolina State University, 2014

Submitted in Partial Fulfillment of the Requirements
for the Degree of Master of Science in
Nuclear Engineering
College of Engineering and Computing
University of South Carolina
2016

Accepted by:

Travis W. Knight, Director of Thesis

Elwyn Roberts, Reader

Lacy Ford, Senior Vice Provost and Dean of Graduate Studies

© Copyright by C. Ryan Priest, 2016
All Rights Reserved.

DEDICATION

This thesis is dedicated to my family and friends, whose sacrifice and support have made my educational pursuits possible.

ACKNOWLEDGMENTS

Funding for this work was provided by the Nuclear Energy Institute in the form of a National Academy for Nuclear Training fellowship. This material is based upon work performed under an Integrated Research Project by the DoE Nuclear Energy University Program under award number DE-NE0008266. The computational modeling of this research required the use of MAXWELL and BOLDEN, high performance computing clusters located at the University of South Carolina, and administered by Paul Sagona.

Great contributions to this project were made in the form of the review and instruction of Dr. Travis W. Knight and Dr. Elwyn Roberts. Their guidance was a constant asset in focusing and directing my research. I must also express my most profound gratitude to Dr. Travis W. Knight for his unwavering support, as well as his dedication to my development as a student and a professional while under his tutelage.

I would also like to thank my colleagues at the University of South Carolina; Aaren Rice, Jonathon Gardner, Donald Shurtliff, Kallie Metzger, JunLiang Liu, Joshua Ramsey, Dr. Mark Noordhoek, Austin Freeman, David Mason, Kyle Singer, and Nafis Reza. At times I have sought council from them all, and their thoughts have helped me shape my own.

ABSTRACT

The Holtec HI-STORM 100 spent fuel storage system is an intermediate storage mechanism for SNF assemblies. Long term licensing and storage requires consideration of material degradation of the stainless steel multi-purpose canister holding the spent fuel. This material degradation is predicted to take the form of environmentally assisted cracking on weld interfaces of the stainless steel cylinder. Several of these spent fuel storage arrays are located in coastal environments. These sites include both the Hope Creek and Diablo Canyon nuclear power stations. A multi-sensory robotic package is being designed for non-destructive assay of the cask annular environment. It will be necessarily exposed to radiation and high temperature. To inform the design of the robotic probe, radiation strength and spectra are modeled in SCALE 6.2 utilizing both ORIGEN-ARP and ORIGAMI for 0-D and 1-D characterization of spent fuel assembly radiation. Radiation transport is modeled within MCNP 6.1 for the case of both photons and neutrons in the annular environment and beyond. Radiation dose rate to operators and electronics was finely considered in regards to the insertion and operation of the probe within the cask annulus. This allows predictive quantification of radiation damage within components of the robotic probe. When planning robotic inspection procedure, accurate depiction of radiation source terms and transported radiation fields is a major concern. Predictions are made in relation to the shielded field of mixed species radiation for the purpose of operator and robotic interaction within the HI-STORM 100 system at different points in storage life.

TABLE OF CONTENTS

DEDICATION	iii
ACKNOWLEDGMENTS	iv
ABSTRACT	v
LIST OF TABLES	viii
LIST OF FIGURES	xvi
LIST OF ABBREVIATIONS	xxvii
CHAPTER 1 INTRODUCTION	1
CHAPTER 2 BACKGROUND	8
2.1 Software	8
2.2 Holtec Design	12
CHAPTER 3 METHODOLOGY	26
3.1 ORIGEN-ARP	26
3.2 ORIGAMI	29
3.3 Source Strength Comparison	38
3.4 Cobalt Activation	42
3.5 MCNP Mathematics	45
3.6 MCNP Geometry	49
3.7 MCNP Materials	57

3.8 MCNP Model Assumptions	57
3.9 MCNP Vent Tallying	61
3.10 Response Functions	61
3.11 Neutron-Photon Coupled Transport	62
CHAPTER 4 RESULTS	71
CHAPTER 5 DISCUSSION	132
CHAPTER 6 CONCLUSIONS	139
6.1 Future Work	140
REFERENCES	142
APPENDIX A NPS DATA	145
APPENDIX B ORIGEN-ARP BWR DATA	146
APPENDIX C ORIGEN-ARP PWR DATA	181
APPENDIX D ORIGAMI PWR DATA	216
APPENDIX E SUMMARY NEUTRON TABLES	251
APPENDIX F SUMMARY PHOTON TABLES	253

LIST OF TABLES

Table 1.1	This table categorizes the design variants encompassed within the HI-STORM storage system. With the exception of the project incompatible HI-STORM 100 METCON, all variations are represented within the MCNP geometry.	3
Table 1.2	The fuel inventory of each multi-purpose canister listed in metric tons of uranium (MTU), where it is extrapolated from the number of loaded assemblies.	3
Table 3.1	The cycle data for the reference PWR assembly used within ORIGEN-ARP details a V.C. Summer Nuclear Station cycle of a Westinghouse 17x17 assembly burned to $57.535 \frac{MWd}{kg}$. [10]	26
Table 3.2	The cycle data for the reference BWR assembly used within ORIGEN-ARP details a Cooper Power Station cycle of a General Electric 8x8 assembly burned to $25.388 \frac{MWd}{kg}$. [3]	27
Table 3.3	ARP source calculation options for reference PWR and BWR assemblies.	28
Table 3.4	The radially averaged, EoC, axial, Virgil C. Summer Nuclear Station burnup data used to generate the curve shown in figure 3.3.	31
Table 3.5	ORIGAMI source calculation options for the reference PWR assembly.	34
Table 3.6	The photon source strength comparison for the reference PWR assembly.	41
Table 3.7	The neutron source strength comparison for the reference PWR assembly.	42
Table 3.8	The photon source strength comparison for the reference BWR assembly.	42

Table 3.9	The neutron source strength comparison for the reference BWR assembly.	42
Table 3.10	The following tables detail the elemental breakdown of materials used within the models described.	58
Table 3.11	Continued from table 3.10.	59
Table 3.12	Continued from table 3.11.	60
Table 3.13	This details the ANSI 6.1.1 1977 flux to dose response function utilized to derive Rem/hr from neutron flux tallies.[22]	64
Table 3.14	This details the ANSI 6.1.1 1977 flux to dose response function utilized to derive Rem/hr from photon flux tallies.[22]	65
Table 3.15	This details the JPL flux to dose response function utilized to derive Rad(Si)/sec from neutron flux tallies.[29]	66
Table 3.16	This details the JPL flux to dose response function utilized to derive Rad(Si)/sec from photon flux tallies.[29]	67
Table 3.17	This is a function taken from the mass energy attenuation coefficient. From it, a flux to dose response function was utilized to derive Rad(Si)/sec from photon flux tallies.[26]	68
Table 3.18	Photon results for coupled neutron-photon transport data of the HI-STORM 100S and MPC-24, populated with Westinghouse 17x17 assemblies enriched to 3.5%, with an ORIGAMI axial emission profile, a discharge burnup of $57.535 \frac{MWd}{kg}$, and cooled for 25yr.	69
Table 3.19	Photon results for comparison to the nominal photon source case values for the same system, where the NP run results are given as a percentage of the nominal photon source case values.	69
Table 3.20	Explanation of individual photon tallies considered within separate MCNP cases.	70
Table 3.21	Explanation of individual neutron tallies considered within separate MCNP cases.	70

Table 4.1	The photon transport data for the HI-STORM 100S and MPC-24, populated with Westinghouse 17x17 assemblies enriched to 3.5%, with an ORIGAMI axial emission profile, a discharge burnup of $57.535 \frac{MWd}{kg}$, and cooled for 5yr.	72
Table 4.2	The photon transport data for the HI-STORM 100S and MPC-24, populated with Westinghouse 17x17 assemblies enriched to 3.5%, with an ORIGAMI axial emission profile, a discharge burnup of $57.535 \frac{MWd}{kg}$, and cooled for 25yr.	76
Table 4.3	The photon transport data for the HI-STORM 100S and MPC-32, populated with Westinghouse 17x17 assemblies enriched to 3.5%, with an ORIGAMI axial emission profile, a discharge burnup of $57.535 \frac{MWd}{kg}$, and cooled for 5yr.	80
Table 4.4	The photon transport data for the HI-STORM 100S and MPC-32, populated with Westinghouse 17x17 assemblies enriched to 3.5%, with an ORIGAMI axial emission profile, a discharge burnup of $57.535 \frac{MWd}{kg}$, and cooled for 15yr.	84
Table 4.5	The photon transport data for the HI-STORM 100S and MPC-32, populated with Westinghouse 17x17 assemblies enriched to 3.5%, with an ORIGAMI axial emission profile, a discharge burnup of $57.535 \frac{MWd}{kg}$, and cooled for 25yr.	88
Table 4.6	The photon transport data is given for the HI-STORM 100S and MPC-68, populated with General Electric assemblies, enriched to 3.5%, burned in ORIGIN-ARP to $25.344 \frac{MWd}{kg}$, and cooled for 5yr.	92
Table 4.7	The photon transport data is given for the HI-STORM 100S and MPC-68, populated with General Electric assemblies, enriched to 3.5%, burned in ORIGIN-ARP to $25.344 \frac{MWd}{kg}$, and cooled for 15yr.	96
Table 4.8	The photon transport data is given for the HI-STORM 100S and MPC-68, populated with General Electric assemblies, enriched to 3.5%, burned in ORIGIN-ARP to $25.344 \frac{MWd}{kg}$, and cooled for 25yr.	100
Table 4.9	The neutron transport data for the HI-STORM 100S and MPC-24, populated with Westinghouse 17x17 assemblies enriched to 3.5%, with an ORIGAMI axial emission profile, a discharge burnup of $57.535 \frac{MWd}{kg}$, and cooled for 5yr.	104

Table 4.10	The neutron transport data for the HI-STORM 100S and MPC-24, populated with Westinghouse 17x17 assemblies enriched to 3.5%, with an ORIGAMI axial emission profile, a discharge burnup of $57.535 \frac{MWd}{kg}$, and cooled for 25yr.	108
Table 4.11	The neutron transport data for the HI-STORM 100S and MPC-32, populated with Westinghouse 17x17 assemblies enriched to 3.5%, with an ORIGAMI axial emission profile, a discharge burnup of $57.535 \frac{MWd}{kg}$, and cooled for 5yr.	112
Table 4.12	The neutron transport data for the HI-STORM 100S and MPC-32, populated with Westinghouse 17x17 assemblies enriched to 3.5%, with an ORIGAMI axial emission profile, a discharge burnup of $57.535 \frac{MWd}{kg}$, and cooled for 15yr.	115
Table 4.13	The neutron transport data for the HI-STORM 100S and MPC-32, populated with Westinghouse 17x17 assemblies enriched to 3.5%, with an ORIGAMI axial emission profile, a discharge burnup of $57.535 \frac{MWd}{kg}$, and cooled for 25yr.	118
Table 4.14	The neutron transport data is given for the HI-STORM 100S and MPC-68, populated with General Electric assemblies, enriched to 3.5%, burned in ORIGEN-ARP to $25.344 \frac{MWd}{kg}$, and cooled for 5yr.	122
Table 4.15	The neutron transport data is given for the HI-STORM 100S and MPC-68, populated with General Electric assemblies, enriched to 3.5%, burned in ORIGEN-ARP to $25.344 \frac{MWd}{kg}$, and cooled for 15yr.	125
Table 4.16	The neutron transport data is given for the HI-STORM 100S and MPC-68, populated with General Electric assemblies, enriched to 3.5%, burned in ORIGEN-ARP to $25.344 \frac{MWd}{kg}$, and cooled for 25yr.	128
Table A.1	The number of histories, NPS, for each given MCNP run.	145
Table B.1	ORIGEN-ARP photon results for a GE 8×8 BWR assembly burned to $25.344 \frac{MWd}{kg}$ and cooled for a combined time period of 5yr.	146

Table B.2	ORIGEN-ARP neutron results for a GE 8 × 8 BWR assembly burned to 25.344 $\frac{MWd}{kg}$ and cooled for a combined time period of 5yr.	147
Table B.3	ORIGEN-ARP photon results for a GE 8 × 8 BWR assembly burned to 25.344 $\frac{MWd}{kg}$ and cooled for a combined time period of 15yr.	153
Table B.4	ORIGEN-ARP neutron results for a GE 8 × 8 BWR assembly burned to 25.344 $\frac{MWd}{kg}$ and cooled for a combined time period of 15yr.	154
Table B.5	ORIGEN-ARP photon results for a GE 8 × 8 BWR assembly burned to 25.344 $\frac{MWd}{kg}$ and cooled for a combined time period of 25yr.	160
Table B.6	ORIGEN-ARP neutron results for a GE 8 × 8 BWR assembly burned to 25.344 $\frac{MWd}{kg}$ and cooled for a combined time period of 25yr.	161
Table B.7	ORIGEN-ARP photon results for a GE 8 × 8 BWR assembly burned to 25.344 $\frac{MWd}{kg}$ and cooled for a combined time period of 35yr.	167
Table B.8	ORIGEN-ARP neutron results for a GE 8 × 8 BWR assembly burned to 25.344 $\frac{MWd}{kg}$ and cooled for a combined time period of 35yr.	168
Table B.9	ORIGEN-ARP photon results for a GE 8 × 8 BWR assembly burned to 25.344 $\frac{MWd}{kg}$ and cooled for a combined time period of 45yr.	174
Table B.10	ORIGEN-ARP neutron results for a GE 8 × 8 BWR assembly burned to 25.344 $\frac{MWd}{kg}$ and cooled for a combined time period of 45yr.	175
Table C.1	ORIGEN-ARP photon results for a Westinghouse 17 × 17 PWR assembly burned to 57.535 $\frac{MWd}{kg}$ and cooled for a combined time period of 5yr.	181
Table C.2	ORIGEN-ARP photon results for a Westinghouse 17 × 17 PWR assembly burned to 57.535 $\frac{MWd}{kg}$ and cooled for a combined time period of 5yr.	182

Table C.3	ORIGEN-ARP photon results for a Westinghouse 17×17 PWR assembly burned to $57.535 \frac{MWd}{kg}$ and cooled for a combined time period of 15yr.	188
Table C.4	ORIGEN-ARP photon results for a Westinghouse 17×17 PWR assembly burned to $57.535 \frac{MWd}{kg}$ and cooled for a combined time period of 15yr.	189
Table C.5	ORIGEN-ARP photon results for a Westinghouse 17×17 PWR assembly burned to $57.535 \frac{MWd}{kg}$ and cooled for a combined time period of 25yr.	195
Table C.6	ORIGEN-ARP photon results for a Westinghouse 17×17 PWR assembly burned to $57.535 \frac{MWd}{kg}$ and cooled for a combined time period of 25yr.	196
Table C.7	ORIGEN-ARP photon results for a Westinghouse 17×17 PWR assembly burned to $57.535 \frac{MWd}{kg}$ and cooled for a combined time period of 35yr.	202
Table C.8	ORIGEN-ARP photon results for a Westinghouse 17×17 PWR assembly burned to $57.535 \frac{MWd}{kg}$ and cooled for a combined time period of 35yr.	203
Table C.9	ORIGEN-ARP photon results for a Westinghouse 17×17 PWR assembly burned to $57.535 \frac{MWd}{kg}$ and cooled for a combined time period of 45yr.	209
Table C.10	ORIGEN-ARP photon results for a Westinghouse 17×17 PWR assembly burned to $57.535 \frac{MWd}{kg}$ and cooled for a combined time period of 45yr.	210
Table D.1	ORIGAMI photon results for a Westinghouse 17×17 PWR assembly burned to $57.535 \frac{MWd}{kg}$ and cooled for a combined time period of 5yr.	216
Table D.2	ORIGAMI photon results for a Westinghouse 17×17 PWR assembly burned to $57.535 \frac{MWd}{kg}$ and cooled for a combined time period of 5yr.	217
Table D.3	ORIGAMI photon results for a Westinghouse 17×17 PWR assembly burned to $57.535 \frac{MWd}{kg}$ and cooled for a combined time period of 15yr.	223

Table D.4	ORIGAMI photon results for a Westinghouse 17×17 PWR assembly burned to $57.535 \frac{MWd}{kg}$ and cooled for a combined time period of 15yr.	224
Table D.5	ORIGAMI photon results for a Westinghouse 17×17 PWR assembly burned to $57.535 \frac{MWd}{kg}$ and cooled for a combined time period of 25yr.	230
Table D.6	ORIGAMI photon results for a Westinghouse 17×17 PWR assembly burned to $57.535 \frac{MWd}{kg}$ and cooled for a combined time period of 25yr.	231
Table D.7	ORIGAMI photon results for a Westinghouse 17×17 PWR assembly burned to $57.535 \frac{MWd}{kg}$ and cooled for a combined time period of 35yr.	237
Table D.8	ORIGAMI photon results for a Westinghouse 17×17 PWR assembly burned to $57.535 \frac{MWd}{kg}$ and cooled for a combined time period of 35yr.	238
Table D.9	ORIGAMI photon results for a Westinghouse 17×17 PWR assembly burned to $57.535 \frac{MWd}{kg}$ and cooled for a combined time period of 45yr.	244
Table D.10	ORIGAMI photon results for a Westinghouse 17×17 PWR assembly burned to $57.535 \frac{MWd}{kg}$ and cooled for a combined time period of 45yr.	245
Table E.1	Dose from neutrons in $\frac{Rad(Si)}{hr}$ taken as an average on the multi-purpose canister wall.	251
Table E.2	Cobalt activation from neutrons in $\frac{Bq}{gm}$ per hr exposure taken as an average on the multi-purpose canister wall.	251
Table E.3	Dose from neutrons in $\frac{Rem}{hr}$ taken as an average on the METCON wall.	251
Table E.4	Dose from neutrons in $\frac{Rad(Si)}{hr}$ taken as an average on the multi-purpose canister lid.	252
Table E.5	Dose from neutrons in $\frac{Rad(Si)}{hr}$ taken behind a 4-side, 5mm, Pb shield as an F4 tally in the annulus formed by the multi-purpose canister and the METCON.	252

Table F.1	Dose from photons in $\frac{Rad(Si)}{hr}$ taken as an average on the multi-purpose canister wall.	253
Table F.2	Dose from photons in $\frac{Rem}{hr}$ taken as an average on the METCON wall.	253
Table F.3	Dose from photons in $\frac{Rad(Si)}{hr}$ taken as an average on the multi-purpose canister lid.	253
Table F.4	Dose from photons in $\frac{Rad(Si)}{hr}$ taken behind a 4-side, 5mm, Pb shield as an F4 tally in the annulus formed by the multi-purpose canister and the METCON.	254

LIST OF FIGURES

Figure 1.1	The γ -ray emission intensity of a TMI-1, Babcock and Wilcox designed, 15×15 Mark B8V with initial enrichment of 4.013 wt% burned to $50 \frac{MWd}{kg}$ and compared to predicted detector response.[14]	5
Figure 1.2	A representation of a Westinghouse 17×17 PWR assembly.[13]	6
Figure 1.3	A representation of a General Electric GNF2 BWR assembly.[16]	7
Figure 2.1	The code path used to simulate spent nuclear fuel radiation transport through the HI-STORM 100 design.	10
Figure 2.2	The data path used to simulate spent nuclear fuel radiation transport through the HI-STORM 100 design.	11
Figure 2.3	An XZ cross section of the HI-STORM 100 METCON with installed MPC.[7]	14
Figure 2.4	An XZ cross section of the HI-STORM 100 METCON without an installed MPC.[7]	15
Figure 2.5	An XY cross section of the default HI-STORM METCON displaying annular channels.[7]	16
Figure 2.6	Cross sectional view of the Holtec HI-STORM 100S design with cutaway section showing structure between overpack and MPC walls.[7]	17
Figure 2.7	Cross sectional view of the Holtec HI-STORM 100S v.B design with cutaway section showing structure between overpack and MPC walls.[7]	18
Figure 2.8	The XY cross section of the MPC-24 design.[7]	19
Figure 2.9	The XY cross section of the MPC-32 design.[7]	20

Figure 2.10	The XY cross section of the MPC-68 design.[7] . . .	21
Figure 2.11	The indexing of BORAL sheets along the axial height of the MPC, allowing for clearance of top and bottom scallops of the honeycomb.[7]	22
Figure 2.12	A MPC-24 cell of the basket honeycomb displaying spacing between assembly, channel, and BORAL plates.[7] . .	23
Figure 2.13	A MPC-32 cell of the basket honeycomb displaying spacing between assembly, channel, and BORAL plates.[7] . .	24
Figure 2.14	A MPC-68 cell of the basket honeycomb displaying spacing between assembly, channel, and BORAL plates.[7] . .	25
Figure 3.1	The SemiLog spectra of the neutron source is shown after a cooling period of 25 years. This is for 1 MTU of the reference BWR assembly in ORIGEN-ARP, and details a Cooper Power Station cycle of a General Electric 8x8 assembly burned to $25.388 \frac{MWd}{kg}$	28
Figure 3.2	The SemiLog spectra of the photon source is shown after a cooling period of 25 years. This is for 1 MTU of the reference BWR assembly in ORIGEN-ARP, and details a Cooper Power Station cycle of a General Electric 8x8 assembly burned to $25.388 \frac{MWd}{kg}$	29
Figure 3.3	The radially averaged axial burnup and end of cycle power for a reference Virgil C. Summer Nuclear Generating Station cycle.	30
Figure 3.4	The axial photon (p) and neutron (n) emission profiles calculated within ORIGAMI in SCALE6.2 for a Westinghouse 17x17 irradiated to $57.535 \frac{MWd}{kg}$ to the axial power density.	32
Figure 3.5	The axial photon (p) and neutron (n) emission profiles from a composite average of US legacy fuel assemblies appropriate for the 1970-1980 time period. The profile is normalized to max source strength over the height of a fuel assembly.[19]	33
Figure 3.6	The Semilog photon spectra for 1 MTU of W17x17 computed for ORIGAMI, ARP, and compared to Literature.[11]	34

Figure 3.7	The LogLog photon spectra for 1 MTU of W17x17 computed for ORIGAMI, ARP, and compared to Literature.[11]	35
Figure 3.8	Comparison of different neutron spectra sections as described in table 3.4 and calculated within ORIGAMI for an axial discretized depletion run on 1 MTU of a Westinghouse 17×17 burned to $57.535 \frac{MWd}{kg}$ and cooled for 25 years.	36
Figure 3.9	Normalized comparison of different neutron spectra sections as described in table 3.4 and calculated within ORIGAMI for an axial discretized depletion run on 1 MTU of a Westinghouse 17×17 burned to $57.535 \frac{MWd}{kg}$ and cooled for 25 years.	37
Figure 3.10	Comparison of different photon spectra sections as described in table 3.4 and calculated within ORIGAMI for an axial discretized depletion run on 1 MTU of a Westinghouse 17×17 burned to $57.535 \frac{MWd}{kg}$ and cooled for 25 years.	38
Figure 3.11	Normalized comparison of different photon spectra sections as described in table 3.4 and calculated within ORIGAMI for an axial discretized depletion run on 1 MTU of a Westinghouse 17×17 burned to $57.535 \frac{MWd}{kg}$ and cooled for 25 years.	39
Figure 3.12	The multizone blended neutron spectra as described in table 3.4 and calculated within ORIGAMI for an axial discretized depletion run on 1 MTU of a Westinghouse 17×17 burned to $57.535 \frac{MWd}{kg}$ and cooled for 25 years.	40
Figure 3.13	The multizone blended photon spectra as described in table 3.4 and calculated within ORIGAMI for an axial discretized depletion run on 1 MTU of a Westinghouse 17×17 burned to $57.535 \frac{MWd}{kg}$ and cooled for 25 years.	41
Figure 3.14	The decay diagram for cobalt.	44
Figure 3.15	The externally proposed multi-sensory robot design.	45
Figure 3.16	A Log-Log representation of both the neutron and photon flux to dose functions described above.[18]	48
Figure 3.17	A representation of both the neutron and photon flux to dose functions described above.[28]	49

Figure 3.18	MCNP rendering of quartered cutaway of the HI-STORM 100S and MPC-24E as designed in MCNP.	50
Figure 3.19	MCNP rendered cross section in the XY plane of the MPC-24E canister and the open annulus space.	51
Figure 3.20	MCNP rendered detailed cross section in the XY plane of the MPC-24E basket.	51
Figure 3.21	MCNP rendering of quartered cutaway of the HI-STORM 100S and MPC-32 as designed in MCNP.	52
Figure 3.22	MCNP rendered cross section in the XY plane of the MPC-32 canister and the open annulus space.	53
Figure 3.23	MCNP rendered detailed cross section in the XY plane of the MPC-32 basket.	53
Figure 3.24	MCNP rendering of quartered cutaway of the HI-STORM 100S and MPC-68 as designed in MCNP.	54
Figure 3.25	MCNP rendered cross section in the XY plane of the MPC-68 canister and the open annulus space.	55
Figure 3.26	MCNP rendered detailed cross section in the XY plane of the MPC-68 basket.	55
Figure 3.27	MCNP rendered detailed cross section in the XZ plane of the MPC-24E basket and HI-STORM 100S METCON.	56
Figure 3.28	The photon and neutron dose is detailed within the vicinity of both the inlet and outlet vents for the HI-STORM 100S. Results are detailed as show for their corresponding points and expressed in units of Rem/hr taken from a 3 cm radius F5 tally.	62
Figure 3.29	The annular thermosiphon developed by way of axial channels and natural circulation.	63
Figure 4.1	The transported photon spectra taken as a surface average for the MPC-24, housed in a 100S METCON, and cooled for 5 yr.	73

Figure 4.2	The MPC wall photon dose rate for a $6\text{cm} \cdot 6\text{cm}$ coaxial FMESH wrapped around the outside of a MPC-24, housed in a 100S METCON, and cooled for 5 yr. The y-axis spans the bottom to the top of the MPC and the x-axis spans 0 to 2π . This details a V.C. Summer cycle of a Westinghouse 17×17 assembly burned to $57.535 \frac{\text{MWd}}{\text{kg}}$ and includes an ORIGAMI 28 zone axial emission profile.	74
Figure 4.3	The MPC lid photon dose rate for a $45 \cdot 45$ FMESH in a plane at the lid surface for a MPC-24, housed in a 100S METCON, and cooled for 5 yr. Dose is in $\frac{\text{mRad}(Si)}{\text{hr}}$ for the matrix of 4 cm cells. This is the proposed deployment surface for the delivery system of the robotic instrumentation.	75
Figure 4.4	The transported photon spectra taken as a surface average for the MPC-24, housed in a 100S METCON, and cooled for 25 yr.	77
Figure 4.5	The MPC wall photon dose rate for a $6\text{cm} \cdot 6\text{cm}$ coaxial FMESH wrapped around the outside of a MPC-24, housed in a 100S METCON, and cooled for 25 yr. The y-axis spans the bottom to the top of the MPC and the x-axis spans 0 to 2π . This details a V.C. Summer cycle of a Westinghouse 17×17 assembly burned to $57.535 \frac{\text{MWd}}{\text{kg}}$ and includes an ORIGAMI 28 zone axial emission profile.	78
Figure 4.6	The MPC lid photon dose rate for a $45 \cdot 45$ FMESH in a plane at the lid surface for a MPC-24, housed in a 100S METCON, and cooled for 25 yr. Dose is in $\frac{\text{mRad}(Si)}{\text{hr}}$ for the matrix of 4 cm cells. This is the proposed deployment surface for the delivery system of the robotic instrumentation.	79
Figure 4.7	The transported photon spectra taken as a surface average for the MPC-32, housed in a 100S METCON, and cooled for 5 yr.	81
Figure 4.8	The MPC wall photon dose rate for a $6\text{cm} \cdot 6\text{cm}$ coaxial FMESH wrapped around the outside of a MPC-32, housed in a 100S METCON, and cooled for 5 yr. The y-axis spans the bottom to the top of the MPC and the x-axis spans 0 to 2π . This details a V.C. Summer cycle of a Westinghouse 17×17 assembly burned to $57.535 \frac{\text{MWd}}{\text{kg}}$ and includes an ORIGAMI 28 zone axial emission profile.	82

Figure 4.9	The MPC lid photon dose rate for a 45·45 FMESH in a plane at the lid surface for a MPC-32, housed in a 100S METCON, and cooled for 5 yr. Dose is in $\frac{mRad(Si)}{hr}$ for the matrix of 4 cm cells. This is the proposed deployment surface for the delivery system of the robotic instrumentation.	83
Figure 4.10	The transported photon spectra taken as a surface average for the MPC-32, housed in a 100S METCON, and cooled for 15 yr.	85
Figure 4.11	The MPC wall photon dose rate for a 6cm·6cm coaxial FMESH wrapped around the outside of a MPC-32, housed in a 100S METCON, and cooled for 15 yr. The y-axis spans the bottom to the top of the MPC and the x-axis spans 0 to 2π . This details a V.C. Summer cycle of a Westinghouse 17×17 assembly burned to $57.535 \frac{MWd}{kg}$ and includes an ORIGAMI 28 zone axial emission profile.	86
Figure 4.12	The MPC lid photon dose rate for a 45·45 FMESH in a plane at the lid surface for a MPC-32, housed in a 100S METCON, and cooled for 15 yr. Dose is in $\frac{mRad(Si)}{hr}$ for the matrix of 4 cm cells. This is the proposed deployment surface for the delivery system of the robotic instrumentation.	87
Figure 4.13	The transported photon spectra taken as a surface average for the MPC-32, housed in a 100S METCON, and cooled for 25 yr.	89
Figure 4.14	The MPC wall photon dose rate for a 6cm·6cm coaxial FMESH wrapped around the outside of a MPC-32, housed in a 100S METCON, and cooled for 25 yr. The y-axis spans the bottom to the top of the MPC and the x-axis spans 0 to 2π . This details a V.C. Summer cycle of a Westinghouse 17×17 assembly burned to $57.535 \frac{MWd}{kg}$ and includes an ORIGAMI 28 zone axial emission profile.	90
Figure 4.15	The MPC lid photon dose rate for a 45·45 FMESH in a plane at the lid surface for a MPC-32, housed in a 100S METCON, and cooled for 25 yr. Dose is in $\frac{mRad(Si)}{hr}$ for the matrix of 4 cm cells. This is the proposed deployment surface for the delivery system of the robotic instrumentation.	91

Figure 4.16	The transported photon spectra taken as a surface average for the MPC-68, housed in a 100S METCON, and cooled for 5 yr.	93
Figure 4.17	The MPC wall photon dose rate for a 6cm·6cm coaxial FMESH wrapped around the outside of a MPC-68, housed in a 100S METCON, and cooled for 5 yr. The y-axis spans the bottom to the top of the MPC and the x-axis spans 0 to 2π. This details a Cooper Nuclear Station cycle of a of a General Electric 8 × 8 assembly burned to 25.344 $\frac{MWd}{kg}$ and includes an ORIGEN-ARP source term.	94
Figure 4.18	The MPC lid photon dose rate for a 45·45 FMESH in a plane at the lid surface for a MPC-68, housed in a 100S METCON, and cooled for 5 yr. Dose is in $\frac{mRad(Si)}{hr}$ for the matrix of 4 cm cells. This is the proposed deployment surface for the delivery system of the robotic instrumentation.	95
Figure 4.19	The transported photon spectra taken as a surface average for the MPC-68, housed in a 100S METCON, and cooled for 15 yr.	97
Figure 4.20	The MPC wall photon dose rate for a 6cm·6cm coaxial FMESH wrapped around the outside of a MPC-68, housed in a 100S METCON, and cooled for 15 yr. The y-axis spans the bottom to the top of the MPC and the x-axis spans 0 to 2π. This details a Cooper Nuclear Station cycle of a of a General Electric 8 × 8 assembly burned to 25.344 $\frac{MWd}{kg}$ and includes an ORIGEN-ARP source term.	98
Figure 4.21	The MPC lid photon dose rate for a 45·45 FMESH in a plane at the lid surface for a MPC-68, housed in a 100S METCON, and cooled for 15 yr. Dose is in $\frac{mRad(Si)}{hr}$ for the matrix of 4 cm cells. This is the proposed deployment surface for the delivery system of the robotic instrumentation.	99
Figure 4.22	The transported photon spectra taken as a surface average for the MPC-68, housed in a 100S METCON, and cooled for 25 yr.	101

Figure 4.23	The MPC wall photon dose rate for a 6cm·6cm coaxial FMESH wrapped around the outside of a MPC-68, housed in a 100S METCON, and cooled for 25 yr. The y-axis spans the bottom to the top of the MPC and the x-axis spans 0 to 2π. This details a Cooper Nuclear Station cycle of a of a General Electric 8 × 8 assembly burned to 25.344 $\frac{MWd}{kg}$ and includes an ORIGEN-ARP source term.	102
Figure 4.24	The MPC lid photon dose rate for a 45·45 FMESH in a plane at the lid surface for a MPC-68, housed in a 100S METCON, and cooled for 25 yr. Dose is in $\frac{mRad(Si)}{hr}$ for the matrix of 4 cm cells. This is the proposed deployment surface for the delivery system of the robotic instrumentation.	103
Figure 4.25	The transported neutron spectra taken as a surface average for the MPC-24, housed within a 100S METCON, and cooled for 5 yr.	105
Figure 4.26	The MPC lid neutron dose rate for a 45·45 FMESH in a plane at the lid surface for a MPC-24, housed in a 100S METCON, and cooled for 5 yr. Dose is in $\frac{mRad(Si)}{hr}$ for the matrix of 4 cm cells. This is the proposed deployment surface for the delivery system of the robotic instrumentation.	106
Figure 4.27	The MPC wall neutron dose rate for a 6cm·6cm coaxial FMESH wrapped around the outside of a MPC-24, housed in a 100S METCON, and cooled for 5 yr. The y-axis spans the bottom to the top of the MPC and the x-axis spans 0 to 2π. This details a V.C. Summer cycle of a Westinghouse 17 × 17 assembly burned to 57.535 $\frac{MWd}{kg}$ and includes an ORIGAMI 28 zone axial emission profile.	107
Figure 4.28	The transported neutron spectra taken as a surface average for the MPC-24, housed in a 100S METCON, and cooled for 25 yr.	109
Figure 4.29	The MPC lid neutron dose rate for a 45·45 FMESH in a plane at the lid surface for a MPC-24, housed in a 100S METCON, and cooled for 25 yr. Dose is in $\frac{mRad(Si)}{hr}$ for the matrix of 4 cm cells. This is the proposed deployment surface for the delivery system of the robotic instrumentation.	110

Figure 4.30	The MPC wall neutron dose rate for a 6cm·6cm coaxial FMESH wrapped around the outside of a MPC-24, housed in a 100S METCON, and cooled for 25 yr. The y-axis spans the bottom to the top of the MPC and the x-axis spans 0 to 2π. This details a V.C. Summer cycle of a Westinghouse 17 × 17 assembly burned to 57.535 $\frac{MWd}{kg}$ and includes an ORIGAMI 28 zone axial emission profile.	111
Figure 4.31	The transported neutron spectra taken as a surface average for the MPC-32, housed in a 100S METCON, and cooled for 5 yr.	113
Figure 4.32	The MPC lid neutron dose rate for a 45·45 FMESH in a plane at the lid surface for a MPC-32, housed in a 100S METCON, and cooled for 5 yr. Dose is in $\frac{mRad(Si)}{hr}$ for the matrix of 4 cm cells. This is the proposed deployment surface for the delivery system of the robotic instrumentation.	114
Figure 4.33	The transported neutron spectra taken as a surface average for the MPC-32, housed in a 100S METCON, and cooled for 15 yr.	116
Figure 4.34	The MPC lid neutron dose rate for a 45·45 FMESH in a plane at the lid surface for a MPC-32, housed in a 100S METCON, and cooled for 15 yr. Dose is in $\frac{mRad(Si)}{hr}$ for the matrix of 4 cm cells. This is the proposed deployment surface for the delivery system of the robotic instrumentation.	117
Figure 4.35	The transported neutron spectra taken as a surface average for the MPC-32, housed in a 100S METCON, and cooled for 25 yr.	119
Figure 4.36	The MPC lid neutron dose rate for a 45·45 FMESH in a plane at the lid surface for a MPC-32, housed in a 100S METCON, and cooled for 25 yr. Dose is in $\frac{mRad(Si)}{hr}$ for the matrix of 4 cm cells. This is the proposed deployment surface for the delivery system of the robotic instrumentation.	120

Figure 4.37	The MPC wall neutron dose rate for a 6cm·6cm coaxial FMESH wrapped around the outside of a MPC-32, housed in a 100S METCON, and cooled for 25 yr. The y-axis spans the bottom to the top of the MPC and the x-axis spans 0 to 2π. This details a V.C. Summer cycle of a Westinghouse 17 × 17 assembly burned to 57.535 $\frac{MWd}{kg}$ and includes an ORIGAMI 28 zone axial emission profile.	121
Figure 4.38	The transported neutron spectra taken as a surface average for the MPC-68, housed in a 100S METCON, and cooled for 5 yr.	123
Figure 4.39	The MPC lid neutron dose rate for a 45·45 FMESH in a plane at the lid surface for a MPC-68, housed in a 100S METCON, and cooled for 5 yr. Dose is in $\frac{mRad(Si)}{hr}$ for the matrix of 4 cm cells. This is the proposed deployment surface for the delivery system of the robotic instrumentation.	124
Figure 4.40	The transported neutron spectra taken as a surface average for the MPC-68, housed in a 100S METCON, and cooled for 15 yr.	126
Figure 4.41	The MPC lid neutron dose rate for a 45·45 FMESH in a plane at the lid surface for a MPC-68, housed in a 100S METCON, and cooled for 15 yr. Dose is in $\frac{mRad(Si)}{hr}$ for the matrix of 4 cm cells. This is the proposed deployment surface for the delivery system of the robotic instrumentation.	127
Figure 4.42	The transported neutron spectra taken as a surface average for the MPC-68, housed in a 100S METCON, and cooled for 25 yr.	129
Figure 4.43	The MPC lid neutron dose rate for a 45·45 FMESH in a plane at the lid surface for a MPC-68, housed in a 100S METCON, and cooled for 25 yr. Dose is in $\frac{mRad(Si)}{hr}$ for the matrix of 4 cm cells. This is the proposed deployment surface for the delivery system of the robotic instrumentation.	130

Figure 4.44	The MPC wall neutron dose rate for a 6cm·6cm coaxial FMESH wrapped around the outside of a MPC-68, housed in a 100S METCON, and cooled for 25 yr. The y-axis spans the bottom to the top of the MPC and the x-axis spans 0 to 2π. This details a Cooper Nuclear Station cycle of a of a General Electric 8 × 8 assembly burned to 25.344 $\frac{MWd}{kg}$ and includes an ORIGEN-ARP source term.	131
Figure 5.1	The composite of both neutron and photon dose rates taken for a 3 cm F5 Tally positioned within the upper, outlet vent.	133
Figure 5.2	The composite of both neutron and photon dose rates taken for a 3 cm F5 Tally positioned within the lower, inlet vent.	134
Figure 5.3	Time variant, segmented, photon tallies modified by a dose response function and divided into axial increments of 30 cm on the outer shell of the MPC-24.	135
Figure 5.4	Time variant, segmented, photon tallies modified by a dose response function and divided into axial increments of 30 cm on the outer shell of the MPC-32. Note the y-axis has a multiplicative factor of 10 ⁴	136
Figure 5.5	Time variant, segmented, photon tallies modified by a dose response function and divided into axial increments of 30 cm on the outer shell of the MPC-68.	137
Figure 5.6	Time variant, segmented, neutron tallies modified by a dose response function and divided into axial increments of 30 cm on the outer shell of the MPC-24.	138

LIST OF ABBREVIATIONS

ARP	Automatic Rapid Processing
BWR	Boiling Water Reactor
DOE	Department of Energy
EAC	Environmentally Assisted Cracking
FSAR	Final Safety Analysis Report
HI-STORM	Holtec International STORAge Module
HPC	High Performance Computing
ISFSI	Independent Spent Fuel Storage Installation
IRP	Integrated Research Project
MCNP	Monte Carlo n Particle
METCON	MEtal CONcrete overpack
MPC	Multi-Purpose Canister
NANT	National Academy for Nuclear Training
NEI	Nuclear Energy Institute
ORIGAMI	ORIGEN Assembly Isotopics
ORIGEN	Oak Ridge Isotope Generation
PWR	Pressurized Water Reactor
SCALE	Standardized Computer Analyses for Licensing Evaluation

CHAPTER 1

INTRODUCTION

With the initial construction of the primary and secondary waves of Gen II LWRs, plant sights and spent fuel pools were designed with the intent of periodic removal of cooled spent fuel to off site storage. Spent fuel handling is limited by current government policy on reprocessing, reprocessing economics, and the lack of a national geological disposal site. Spent nuclear fuel is largely restricted to on site storage at existing nuclear facilities. This limits operator options to extended wet storage, or the movement of spent fuel to specially designed dry storage casks on site. This storage occurs on site near operators for a relatively short time span as compared to ultimate disposal within a geological repository. Based on initial placement of the HI-STORM system at sites not limited to Vogtle, Diablo Canyon, and Arkansas Nuclear One, primary focus was placed on evaluating the variants designed to house PWR assemblies.[15]

Both the MPC-24 and MPC-32 family of multi-purpose canisters are designed to exclusively house PWR assemblies. However, with the Vermont Yankee purchase of the BWR version of the design, further justification exists for full modeling on the numerous variants within the MPC-68 family. Current use is evenly divided between PWR and BWR models. Several of these ISFSIs are located in coastal environments. These coastal sites include both the Hope Creek and Diablo Canyon nuclear power stations. This exacerbates the existing potential for degradation of storage canisters. Prolonged on site storage container may present a regulatory concern in regards to

potential canister failure.[25] This may assume the form of environmentally assisted cracking (*EAC*) of the stainless steel canister or degradation and delamination of the concrete METCON.[6] However, the degradation of the concrete METCON does not increase the risk of radionuclide release.

With this in mind, motivation exists for the development of robotic instrumentation to be used for inspection of cask integrity. This reality brings about the need for evaluation of transported radiation with regard to the use of this robotic instrumentation. Concern is directed towards potential $^{59}_{27}\text{Co}$ activation within the portion of instrumentation inserted into the annular gap between the multi-purpose canister (*MPC*) and the overpack wall. In addition, evaluation of electronics damage in the form of Si damage in the instrumentation is required. Furthermore, the use of the proposed robotic equipment will require operator interaction with vents, so dosimetry at vents is also required.

These interests listed, a fine definition of both transported neutron and photon spectra is desired within and in the vicinity of our selected cask environment. This is achieved within this work through the use of MCNP 6.1 for source terms calculated within SCALE 6.1 (ORIGEN-ARP) and SCALE 6.2 (ORIGAMI). Our modeling interest centers on the Holtec HI-STORM 100 system of vertical spent fuel storage casks. Given this cask system, licensing limits the scope of modeling to approximately 5 to 45 years, where this work evaluates the spent fuel strength and spectra at 10 year increments along said continuum. Furthermore, both a PWR and BWR assembly design are evaluated within ORIGAMI and ORIGEN-ARP as described below. Where appropriate, these were inserted within their associated multi-purpose canister as described within table 1.1.

Table 1.1: This table categorizes the design variants encompassed within the HI-STORM storage system. With the exception of the project incompatible HI-STORM 100 METCON, all variations are represented within the MCNP geometry.

METCON	24 Assembly	32 Assembly	68 Assembly
HI-STORM 100	MPC-24	MPC-32	MPC-68
HI-STORM 100S	MPC-24E	MPC-32F	MPC-68F
HI-STORM 100S v.B	MPC-24EF	-	MPC-68FF
-	-	-	MPC-68M

Table 1.2: The fuel inventory of each multi-purpose canister listed in metric tons of uranium (MTU), where it is extrapolated from the number of loaded assemblies.

Canister	Mass, MTU
MPC-24	11.232
MPC-32	14.976
MPC-68	12.9336

As can be seen, the HI-STORM system hosts three primary METCON variants capable of housing three principal Multi-Purpose Canister families. These are fully geometrically compatible and interchangeable by design.[23] By nature, BWR assemblies are considerably smaller than PWR assemblies. This can be observed in the MPC-68 group, as they all house a larger number of BWR assemblies when compared to the same size PWR fuel MPC designs. The MPC loading is calculated from assembly number and assembly mass, where each PWR assembly is assumed to be 468 kg heavy metal, and each BWR assembly is assumed to be 190.2 kg heavy metal.[8]

Each multi-purpose canister houses a different assembly number, different assembly type, or both. Throughout the course of this research, it is useful and standard practice to report particle emission rate normalized to 1 MTU. In this manner, fuel of the same type may be characterized and then modified by the mass loaded into each unique multi-purpose canister. Table 1.2 shows the comparatively tight packed loading of the MPC-32 design, and explains why it is chosen as the limiting case.

Concordant with the general geometric interchangeability of these designs, a set of standardized tallies have been developed for the characterization of transported photons and neutrons at points of interest throughout the geometry modeled within MCNP. As a novel element in this project, fine dose rate maps are generated via independent mesh tallies oriented around the MPC in the METCON annular space. This capability prompted a companion effort to evaluate emission rate of neutrons and photons within the limiting case of a high burnup PWR assembly, and prompted the use of a 28 zone, axially characterized spent fuel assembly generated within ORIGAMI.

At present there are approximately 70,000 tons of discharged fuel in either spent fuel pools or dry cask storage. Discharges from current reactors amount to nearly 2,000 tons per year. This used fuel is initially stored in spent fuel pools for a period not less than 5 years. In all likelihood, this used fuel will be placed into dry cask storage for a period of time that could extend from 20 years to more than 100 years. At present, this fuel is stored in 34 states. While submerged in the spent fuel pool, 24 - 68 of these assemblies are loaded into casks with consideration of burnup and linear heat rate. More radioactive assemblies are generally placed in a central positions, while assemblies with a high thermal power in kW are more generously spaced.[7] Possible radiation doses from gamma rays in particular are anticipated to be as high as $2.71 \times 10^4 \frac{\text{Rad}}{\text{hr}}$ within the annular space between the multi-purpose canister and the overpack.[18] Detailed exploration of this region will be required for investigation with robotic equipment and sensors. These estimates are developed from the most conservative assumptions of $62 \frac{\text{MWd}}{\text{kgU}}$ following a cooling period of 5 years. Semiconductors are vulnerable to radiation damage, and functional issues may be expected to manifest after $10^4 - 10^5 \text{ Rad(Si)}$. [18] Hardened microelectronics are generally categorized as capable of withstanding on the order of 10^6 Rad(Si) , or a MRad(Si).

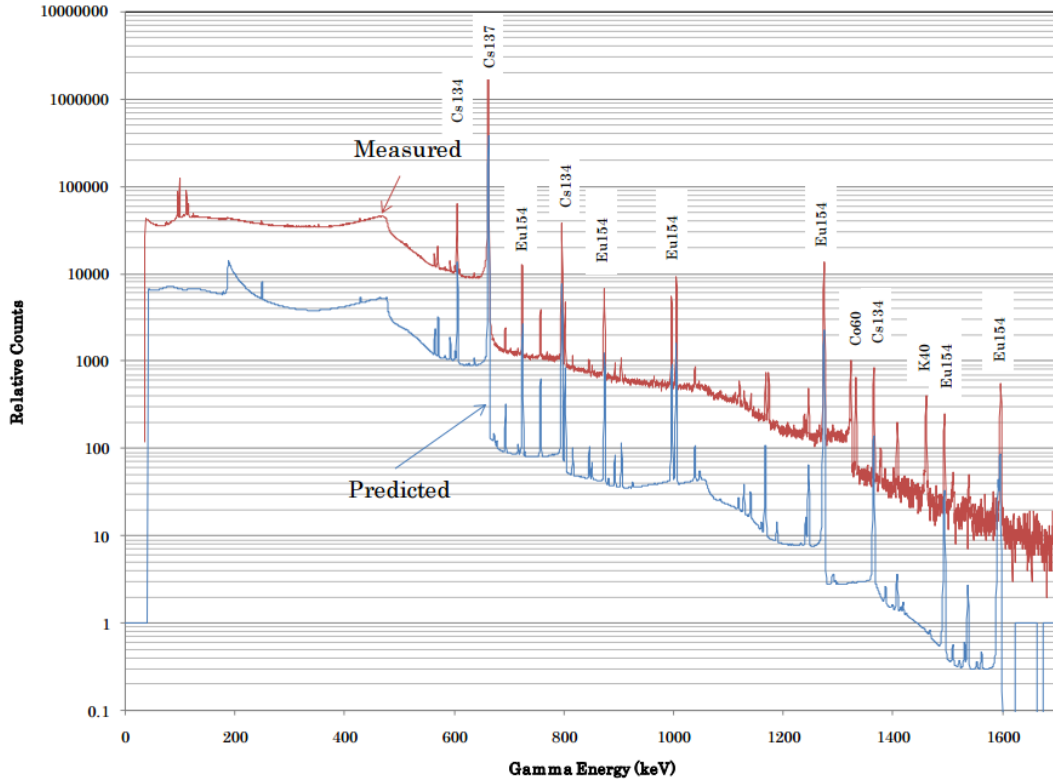


Figure 1.1: The γ -ray emission intensity of a TMI-1, Babcock and Wilcox designed, 15×15 Mark B8V with initial enrichment of 4.013 wt% burned to $50 \frac{MWd}{kg}$ and compared to predicted detector response.[14]

This research focuses on simulation of sources and transport of both neutrons and γ -rays. However, γ -rays are known to be the most significant contributor to radiation damage within the annulus of these spent fuel storage casks. Consideration of neutron dose is, however, pertinent. Crystalline defects from neutron irradiation typically consist of interstitials and vacancy clusters within crystalline Si, which behaves similarly to SiC.[33]

Both α particles and β particles will fail to escape the 304 Stainless canister.[15] Therefore, α particles and β particles will not contribute to radiation damage outside the light shielding of the MPC wall. High energy γ -rays are produced in decay of fission products, exemplified by the 662 keV emission of ^{137}Cs . Neutrons are produced in the cask from (α ,n) reactions and from spontaneous fission of transuranic isotopes

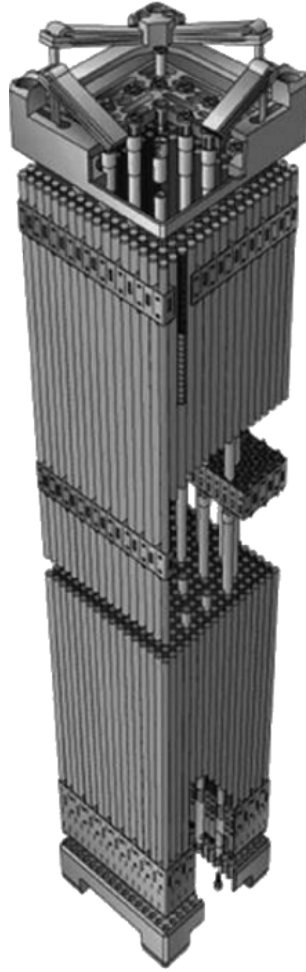


Figure 1.2: A representation of a Westinghouse 17×17 PWR assembly.[13]

within the spent nuclear fuel. The principle emissions expected prior to the shielding effect of both the surrounding spent fuel and stainless steel multi-purpose canister are detailed in figure 1.1. Unshielded spent nuclear fuel γ -ray emissions are attributable to six primary fission products. These consist of ^{134}Cs , ^{137}Cs , ^{154}Eu , ^{125}Sb , ^{106}Rh , and ^{85}Kr . [14]

Housed within the HI-STORM storage system, inside the multi-purpose canister, sorted within a honeycomb basket, is a matrix of spent fuel assemblies like the geometry shown in figures 1.2 and 1.3. The consideration of these assemblies as a homogeneous parallelepiped and source term is described subsequently. The concise explanation of



Figure 1.3: A representation of a General Electric GNF2 BWR assembly.[16]

their treatment is that a homogenized assembly material is substituted for the external geometry of the parallelepiped, and ORIGAMI/ORIGEN-ARP characterized neutron and γ -ray emissions are transported with MCNP. This is an industry standard for shielding and dose calculations due to the muted effect of fuel assembly heterogeneity on transported radiation fields.

CHAPTER 2

BACKGROUND

2.1 SOFTWARE

MCNP 6.1 provides a stochastic solution of spatially transported particles through use of the Monte Carlo method. This references known databases detailing probability distributions for a given interaction, where this interaction is that of a neutral particle of known direction and energy. MCNP6 analyzes neutral particle transport and coupled transport of secondary gamma rays resultant from neutron interactions within a system. This technique offers high accuracy at the cost of computational intensiveness. To this end, both the MAXWELL and BOLDEN cluster were utilized interchangeably for extended calculations with MCNP6. BOLDEN is the more modern of the pair, and offers 20 core nodes - each providing 64 GB of RAM.

MCNP 6.1 stands for Monte Carlo N-Particle transport code, and is maintained by Oak Ridge National Laboratory (ORNL). Within this body of work, MCNP6 was utilized to build models representing the range of storage solutions in the Holtec HI-STORM 100 system. The tallying and meshes supported by the code package were utilized in order to gather data regarding transported radiation. This code package is the primary suite for building Boolean geometry through definitions of surfaces, cells, and materials. MCNP uses the Monte Carlo method to estimate particle flux by following the histories of many particles sampled within the defined geometry and materials. With the numerous tool packages and capabilities of the program, the phenomena of interest within the defined transported radiation fields may be

used to predict and output neutron interactions. Output values are post processed in order to yield dosimetry around selected geometry or surfaces. MCNP models for radiation transport approach real world accuracy with respect to geometry and material specifications. Furthermore, its source distributions were populated with SCALE in order to characterize the spent nuclear fuel housed within the casks.

SCALE 6.1 / 6.2 stands for Standardized Computer Analyses for Licensing Evaluation, and is maintained by Oak Ridge National Laboratory. It houses multiple packages related to neutronics and shielding analysis. In this work, source evaluation for various spent nuclear fuel assemblies is performed with both ORIGEN-ARP and ORIGAMI. ORIGEN-ARP allows users to rapidly evaluate a 0-dimensional source term for a given mass of fuel irradiated homogeneously at a given specific power.

ORIGEN-ARP is an isotopic depletion and decay analysis sequence which sets up a SCALE 6.2 input file in order to execute both ARP and ORIGEN. ARP designates automatic rapid processing in terms of pre-populated data, where in this case we utilize it to burn a known assembly design to be inserted into the MCNP design in the form of a volumetric source term. The input conditions are defined for both the assembly and a power history. This power history allows time dependent definition of neutron flux. A cooling period is defined for it to endure and thusly populate the spent fuel of our current design as a radiation source term generated by ORIGEN-ARP. It operates chiefly through cross section interpolation based on burnup, enrichment, and moderator density. Thusly, it avoids generating models and cross sections for transport and depletion calculations. As mentioned, this module operates within SCALE 6.1 or SCALE 6.2. ORIGEN-ARP may be used in order to generate source terms for both photon and neutron radiation as well as isotopic abundances and heat generation rates.

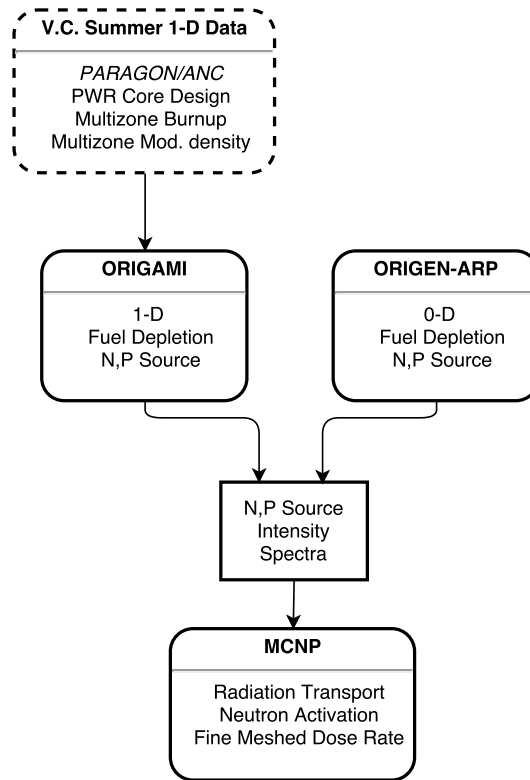


Figure 2.1: The code path used to simulate spent nuclear fuel radiation transport through the HI-STORM 100 design.

In contrast, ORIGAMI is an object oriented code that may call ORIGEN for multiple unique regions. This allows multi-dimensional definition of a radiation source term by way of multi-dimensional definition of qualities such as specific power and moderator density. Cross section data for radiation transport and dose calculation are the most up to date and thoroughly evaluated datasets.

In the manner described within figure 2.1, the most novel data path extracts a 28 bin axial burnup structure from an ANC (Advanced Nodal Code) simulation run associated with a V. C. Summer 17×17 assembly. This 28 zone axial burnup and axial moderator density was exported to ORIGAMI in order to generate a 28 zone depletion calculation for the cycle described in table 3.1.

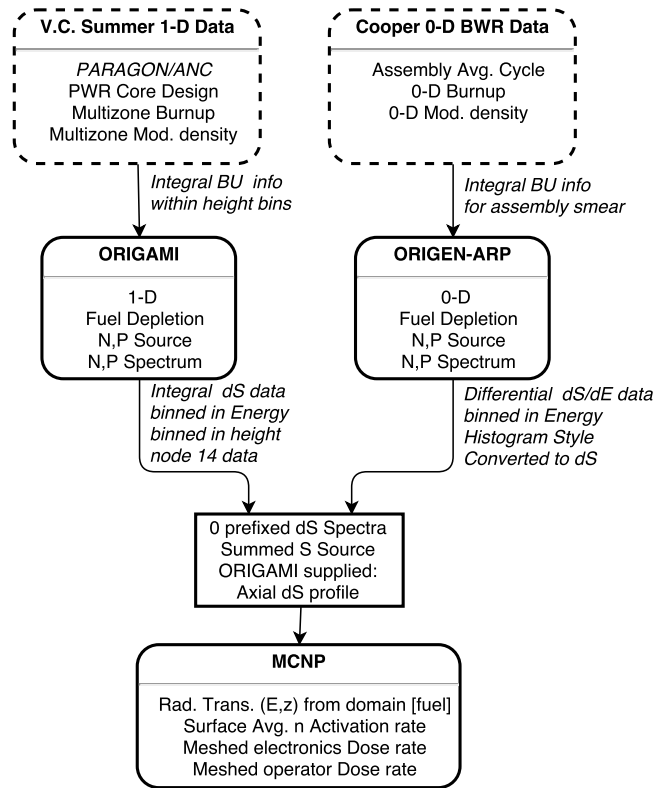


Figure 2.2: The data path used to simulate spent nuclear fuel radiation transport through the HI-STORM 100 design.

As is shown in figure 3.4, a normalized emission function was generated in 28 zones over axial height for both neutrons and photons. In addition to the 1 MTU normalized source strength and spectrum, this was used to characterize neutron and photon emission for a 1-D assembly model. Concordantly, this informed the transport and fine meshing of particles through the geometry of the HI-STORM storage system, where particle flux is modified in MCNP to quantities of interest. These quantities can include dose rate in $\frac{Rem}{hr}$, $\frac{Rad(Si)}{hr}$, or ^{59}Co activation results in $\frac{Bq}{gm}$ per hr exposure.

As is shown in figure 2.2, data is appropriately handled as it is transferred from source, ORIGAMI or ORIGEN-ARP, and then to MCNP. The data path from the supplied V.C. Summer data inputs integral values for moderator density and burnup binned in terms of height as shown in figure 3.4. These are output and binned princi-

pally in height as defined by the burnup bins. From this, the 28 zone integral values of source strength may be used to construct an axial profile of emission like that in figure 3.4. For each bin, a spectrum is also produced, where node 14, the midplane, is input as an integral distribution for the fuel.

2.2 HOLTEC DESIGN

In order to construct a set of geometric and material models encompassing the Holtec HI-STORM 100 system, the released FSAR was utilized in order to gather information. Industry representatives associated with the storage of spent nuclear fuel suggest it is likely that most PWR purchases will be the MPC-32 design due to the space and economics of more dense fuel storage. However, the design of the MPC-24 allows for higher linear heat rate assembly storage. This is a definite asset in the case where it may be sought to store fresh fuel with a shorter cooling time.

All MPC variants are designed by Holtec such that they interchange within all METCON overpacks. In the work, the minor flanged variants of the overpacks designed for earthquake performance are neglected as modeling variations in current plans due to extremely minor external dissimilarity irrelevant to internal particle transport.

The MCNP geometry models generated for this research were extracted from all available revisions of the Holtec HI-STORM 100 final safety analysis report. Both qualitative and labeled diagrams listed within the FSAR have been used in order to construct a thorough picture of the geometry required for modeling. Where gaps in documentation exist, they have extrapolated from the system of known measurements. In this case, the well known dimensions of the multi-purpose canister, basket plates, BORAL plates, and the selected fuel assemblies allowed close approximations of the

dimensions of the basket supports indexed within the MPC-24, MPC-32, and MPC-68 designs. Likewise, the specification of the METCON inner and outer diameter, combined with knowledge of the laminating sheet stainless allowed boolean modeling of the METCON.

Within the annulus, the symmetry of stainless steel channels was utilized in order to accurately place them in the model. In the case of both inlet and outlet vents, the external dimensions of the fitted γ -ray cross plates allowed a strong approximation of the vent mouth dimensions. The amount of known data shown within the numerous diagrams included within the released FSAR have allowed reasonable extrapolation of any unknown measurement. This has allowed design of a highly detailed representation of the designs that is novel in complexity. A sampling of the diagrams detailing the MPC and METCON are included for comparison to the MCNP geometry.

The METCON overpacks are detailed with cross sectional views found in the FSAR. The figures show the preliminary METCON within the FSAR, the HI-STORM 100. These structures are a heterogeneous layers of concrete and stainless steel. The assembled METCON and MPC shows the HI-STORM 100 with a MPC-68 installed. METCON modeling was expanded to include both the HI-STORM 100 and the HI-STORM 100S shown in figure 2.6. The primary difference between the 100 and 100S consists of the replacement of the top shield ring and internal lid bottom plug in the HI-STORM 100 with an external shield disk in the HI-STORM 100S variant. It is notable to comment that the order of METCON development appears to be 100 \rightarrow 100S \rightarrow 100S v.B. METCON modeling was not expanded to include the HI-STORM 100S v.B design. This is related to expressed incompatibility with the internal shield plug and the clearance required for robotics on the lid of the multi-purpose canister.

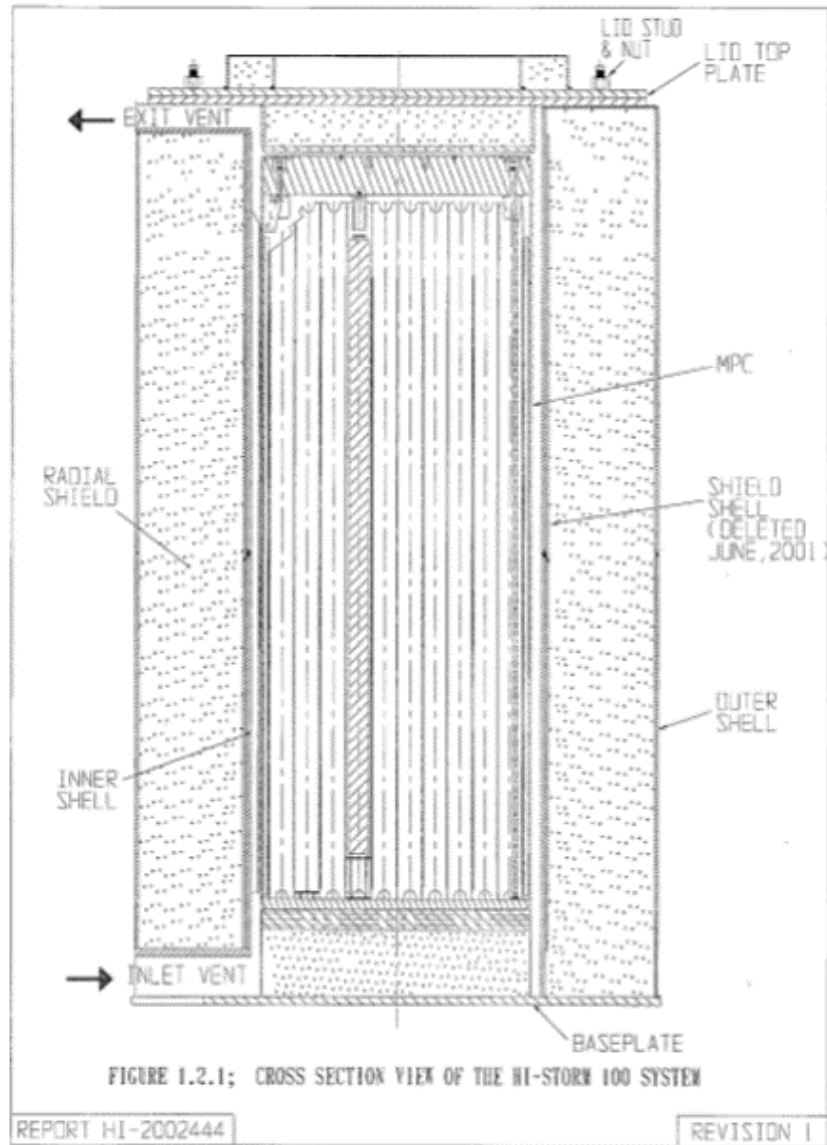


Figure 2.3: An XZ cross section of the HI-STORM 100 METCON with installed MPC.[7]

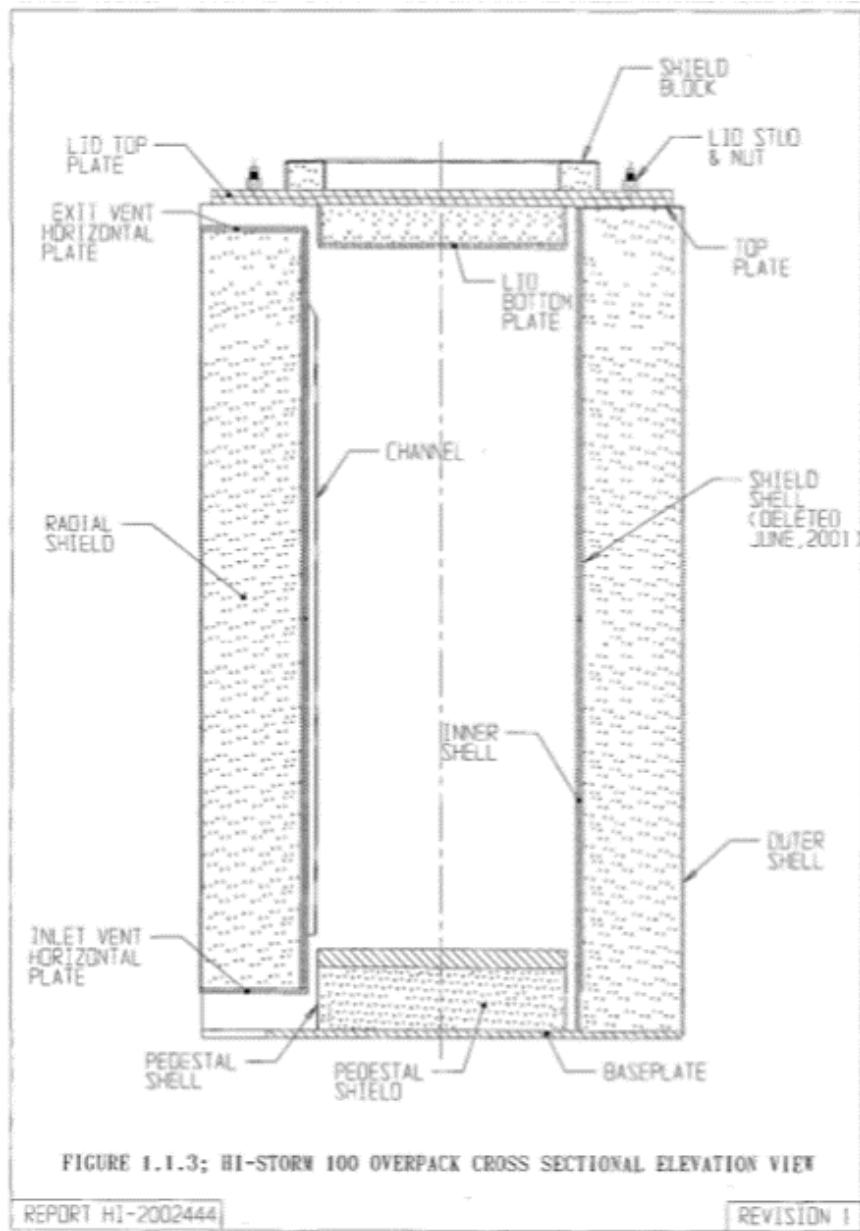


Figure 2.4: An XZ cross section of the HI-STORM 100 METCON without an installed MPC.[7]

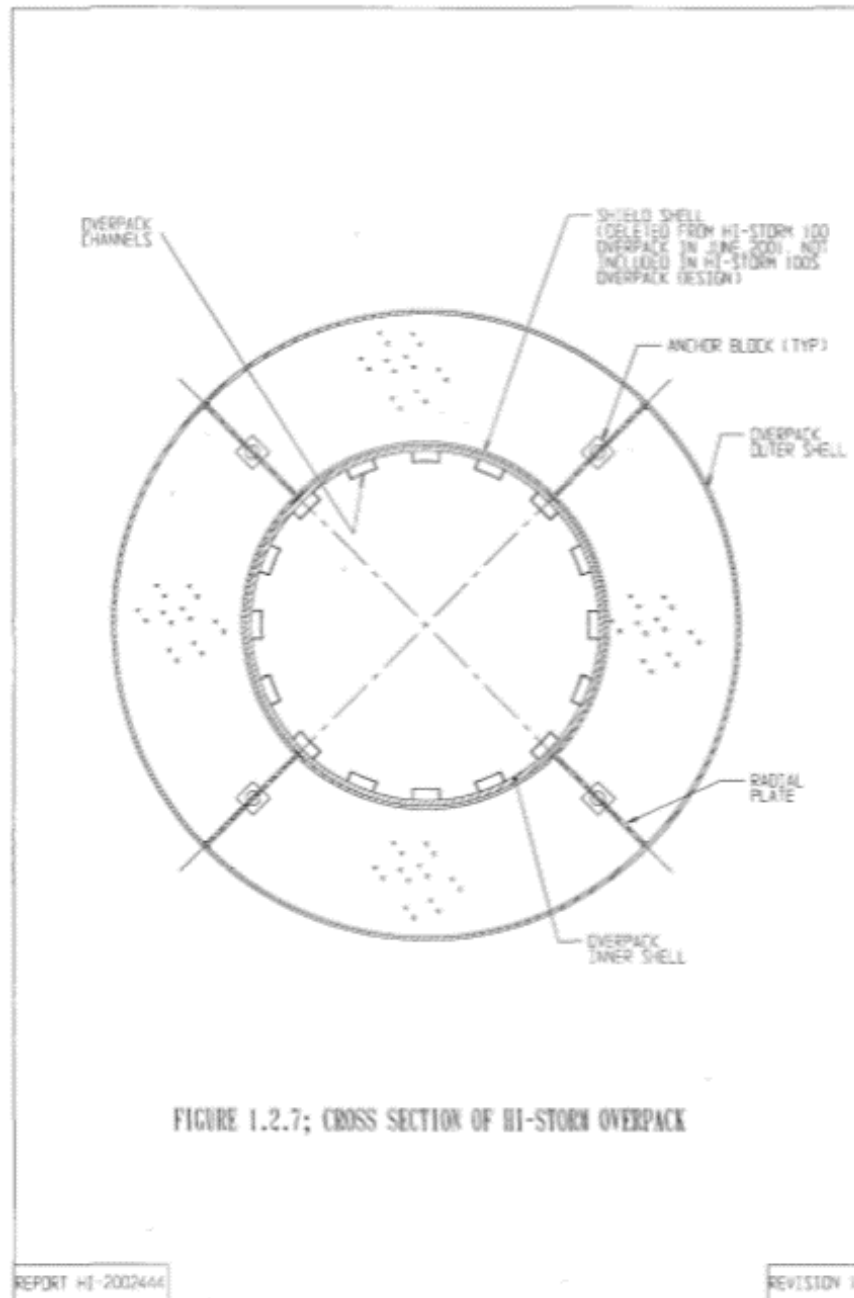


Figure 2.5: An XY cross section of the default HI-STORM METCON displaying annular channels.[7]

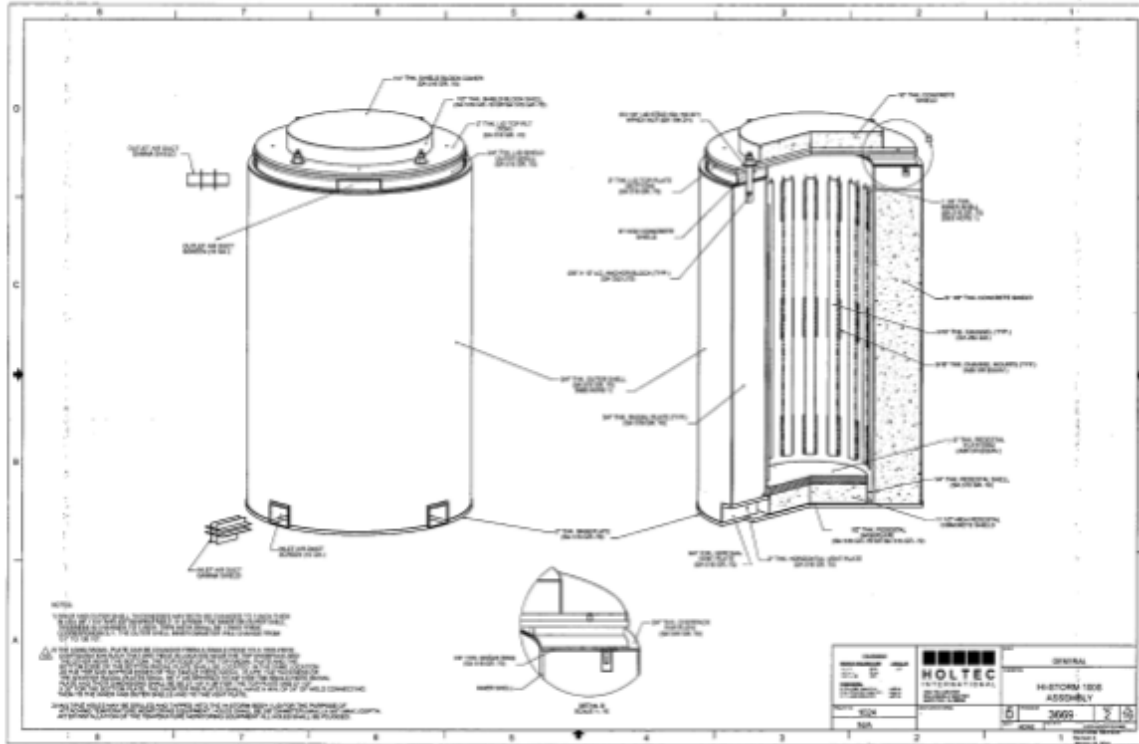


Figure 2.6: Cross sectional view of the Holtec HI-STORM 100S design with cutaway section showing structure between overpack and MPC walls.[7]

The 3D diagram shown in figure 2.7 is that of the HI-STORM 100S v.B METCON. Preliminary examination and dialogue with the robotics design group has eliminated this geometry as a target for radiation transport modeling in this research. A generous clearance between the multi-purpose canister top and the bottom of the METCON lid is required for the current pre-deployment staging of the multi-sensory probe. As such, results focus on the HI-STORM 100S METCON design. The MPC-24 and MPC-32 family are exemplified by both figure 2.8 and figure 2.9 taken directly from the final safety analysis report. The more complex of the designs exists in the form of the MPC-24, where it has numerous assembly offsets and flux traps forming an intricate basket structure that required detailed modeling attention.

The MPC-32 and MPC-68 designs are such that their basket geometry is comparably simpler than that of the MPC-24 group. However, the MPC-68 group shown in

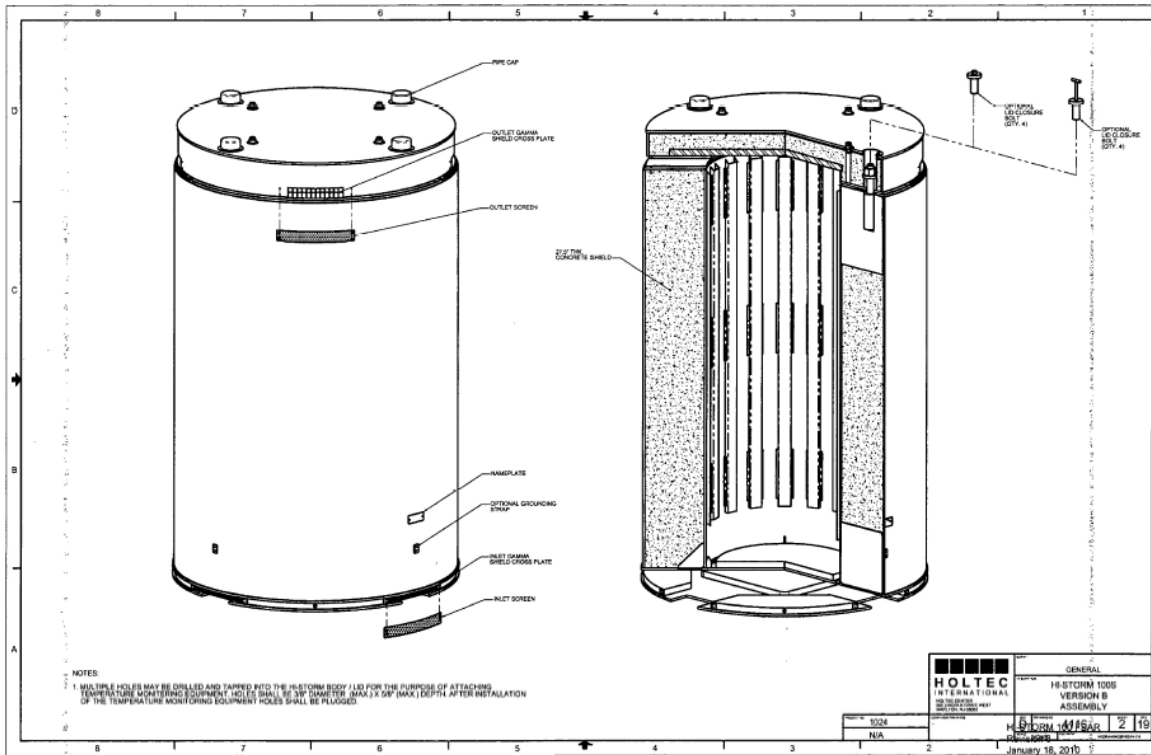


Figure 2.7: Cross sectional view of the Holtec HI-STORM 100S v.B design with cutaway section showing structure between overpack and MPC walls.[7]

figure 2.10 is designed to house smaller BWR assemblies. In this manner, it requires a unique set of BWR appropriate source term inputs channeled from SCALE 6.2 and ORIGEN-ARP as is detailed. In accordance with the complexity of design and nature of the MPC-24, it was the initial model constructed. Subsequent models required some azimuthal repeated geometry in order to minimize input complexity. This azimuthally repeating structure allowed more efficient geometry definition through the use of quarters in the MPC-32 and octants in the MPC-68. The MCNP model of the MPC-24 group is novel in that it is more finely constructed than the Nuclear Regulatory Commission approved FSAR calculations for the similarly designed Holtec HI-TRAC system. This degree of modeling complexity was required in order to justify the fidelity of the fine meshing of radiation dose rates on the shell and lid of the multi-purpose canister.

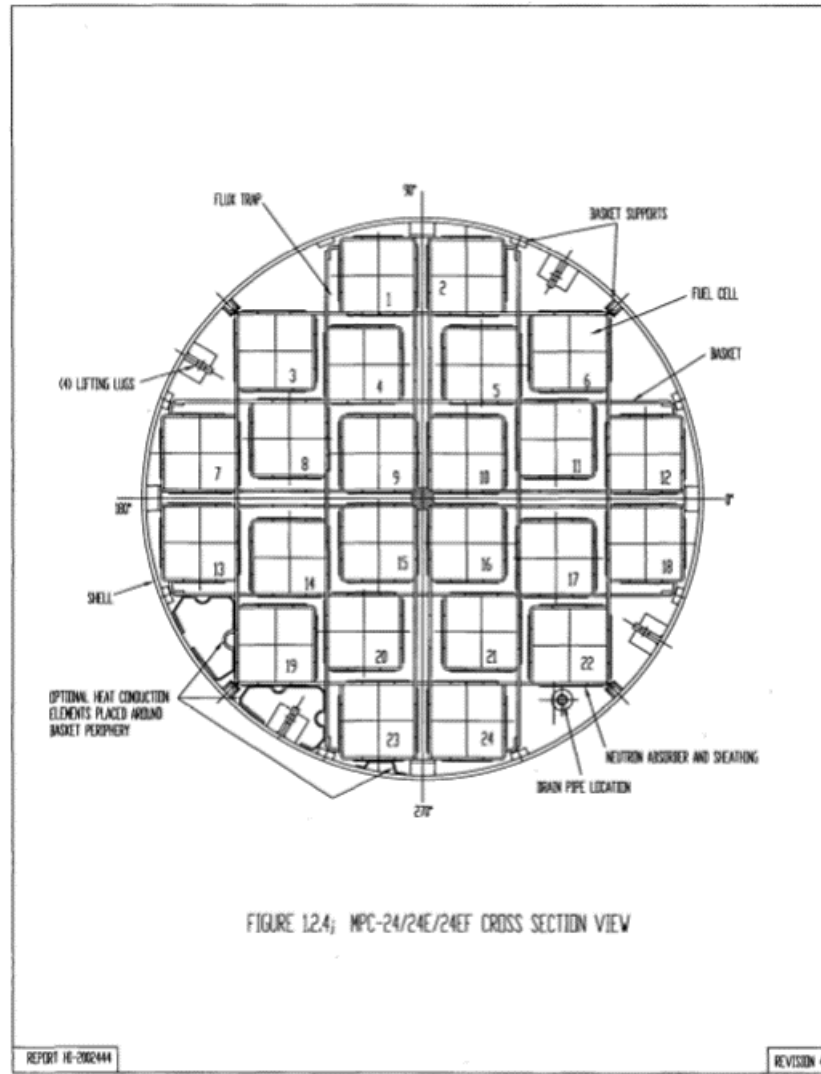


Figure 2.8: The XY cross section of the MPC-24 design.[7]

The FSAR submitted to the Nuclear Regulatory Commission has allowed for refined geometric models to be generated. These address precise orientation and spacing of components within each multi-purpose canister. When consideration is taken to each design family, a total of 6 distinct permutations are represented by modeled MCNP geometry. This considers the two principle METCONs, and 3 principle MPC models. Subsumed within the MPC-24, MPC-32, and MPC-68 are all non-distinct variants differentiated by nomenclature. The designs are summarized in figure 1.1.

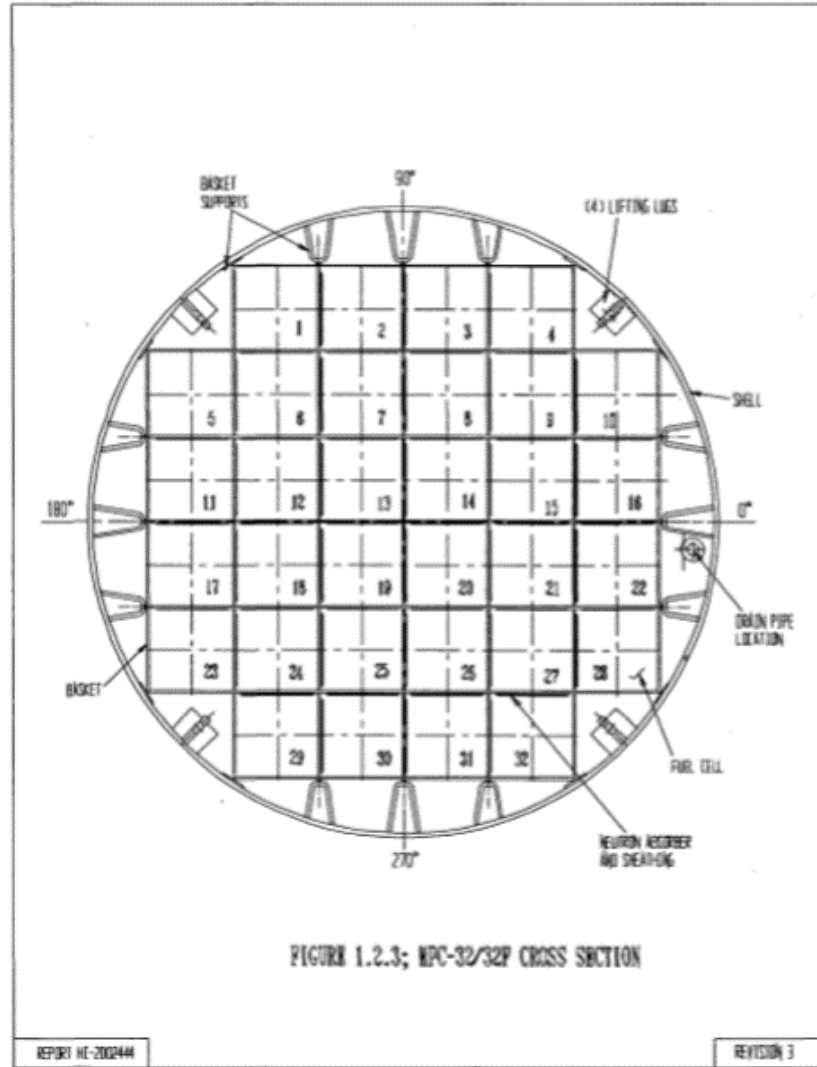


Figure 2.9: The XY cross section of the MPC-32 design.[7]

Spent fuel assemblies were centered within their channel in both the MPC-32 and MPC-68 designs. Measurements were taken from the FSAR in order to define the honeycomb cell and the BORAL plates. With the exception of the wide BORAL plates shown in figure 2.11, their dimensions are $0.076in \cdot 7.5in \cdot 156in$ with a prescribed ^{10}B loading of $0.0267 \frac{gm}{cm^3}$. [7] Demonstrating their interchangeability, the METAMIC plates are $0.077in \cdot 7.5in \cdot 156in$ with a prescribed ^{10}B loading of $0.0223 \frac{gm}{cm^3}$. [7] This constitutes a volume averaged density for the domain of the entire neutron absorbing sheet.

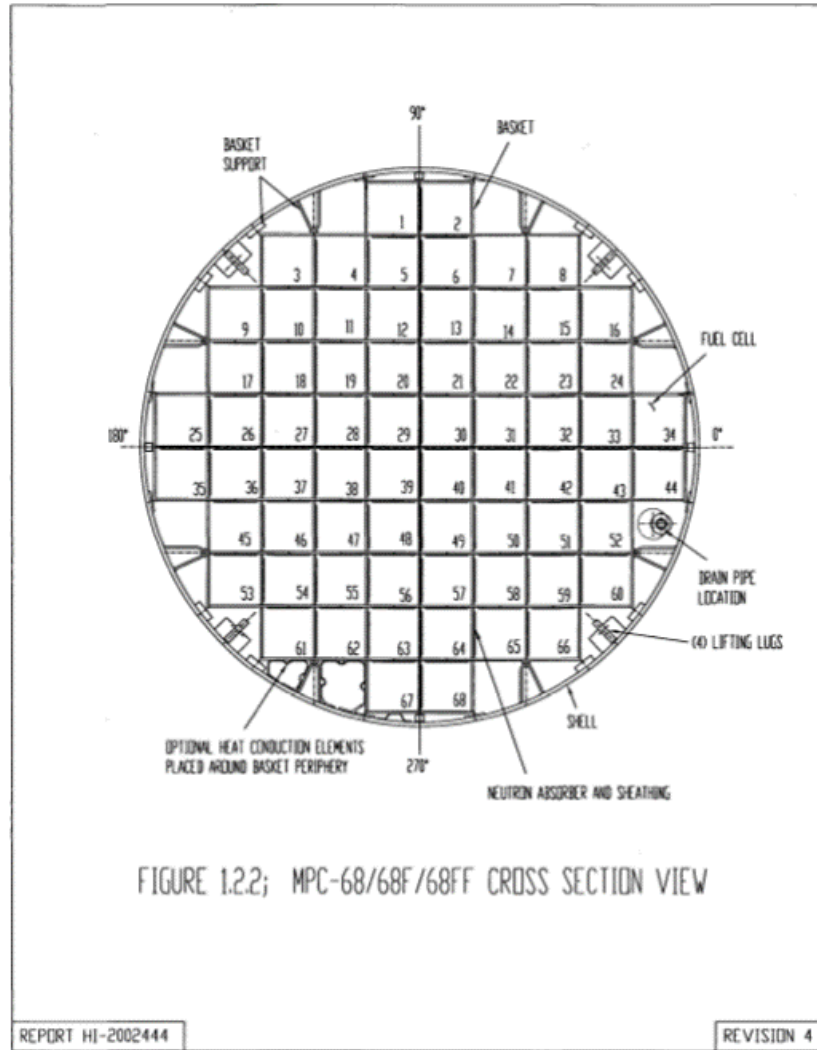


Figure 2.10: The XY cross section of the MPC-68 design.[7]

While modeling the multi-purpose canisters throughout the course of this project, reference was taken from some of the preliminary schematics related to the released FSAR as shown in the basket cells diagrams. Notably, the BORAL and sheathing regions were homogenized as modeled within MCNP.

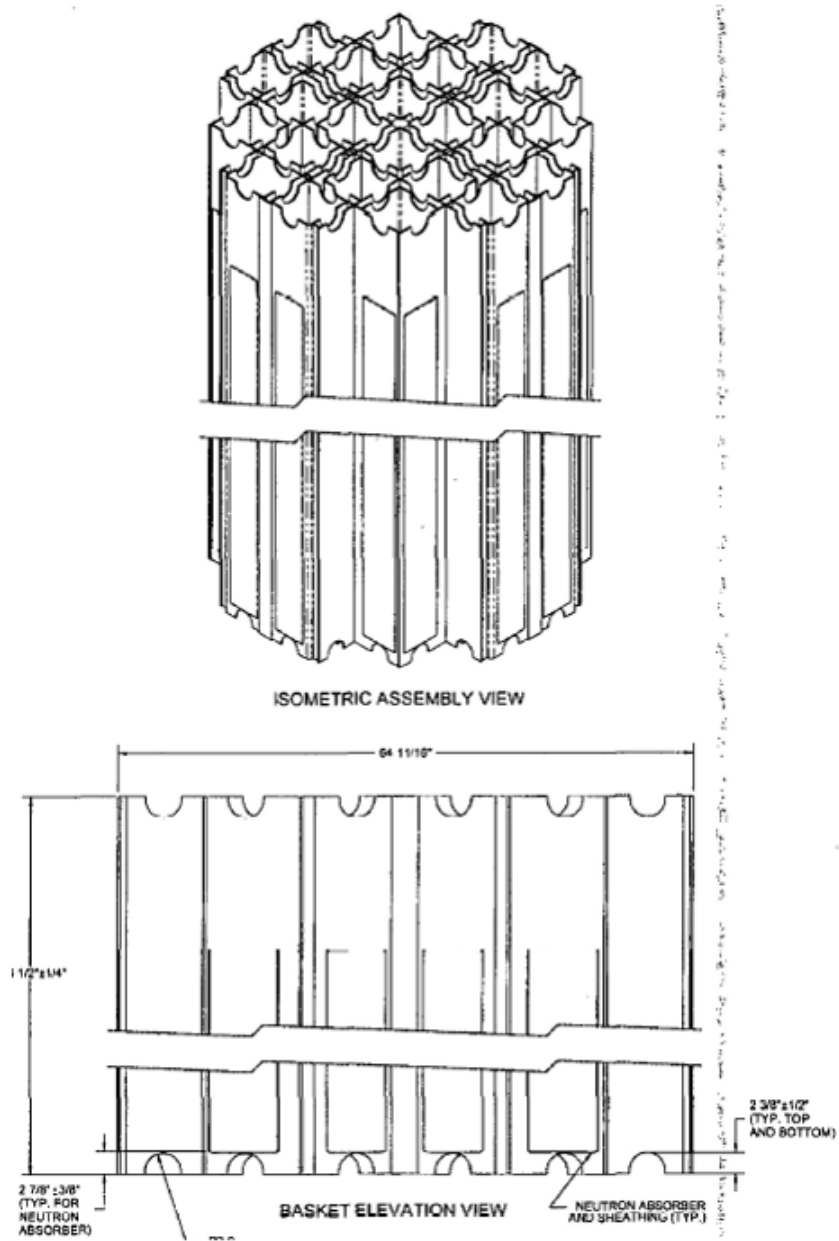


Figure 2.11: The indexing of BORAL sheets along the axial height of the MPC, allowing for clearance of top and bottom scallops of the honeycomb.[7]

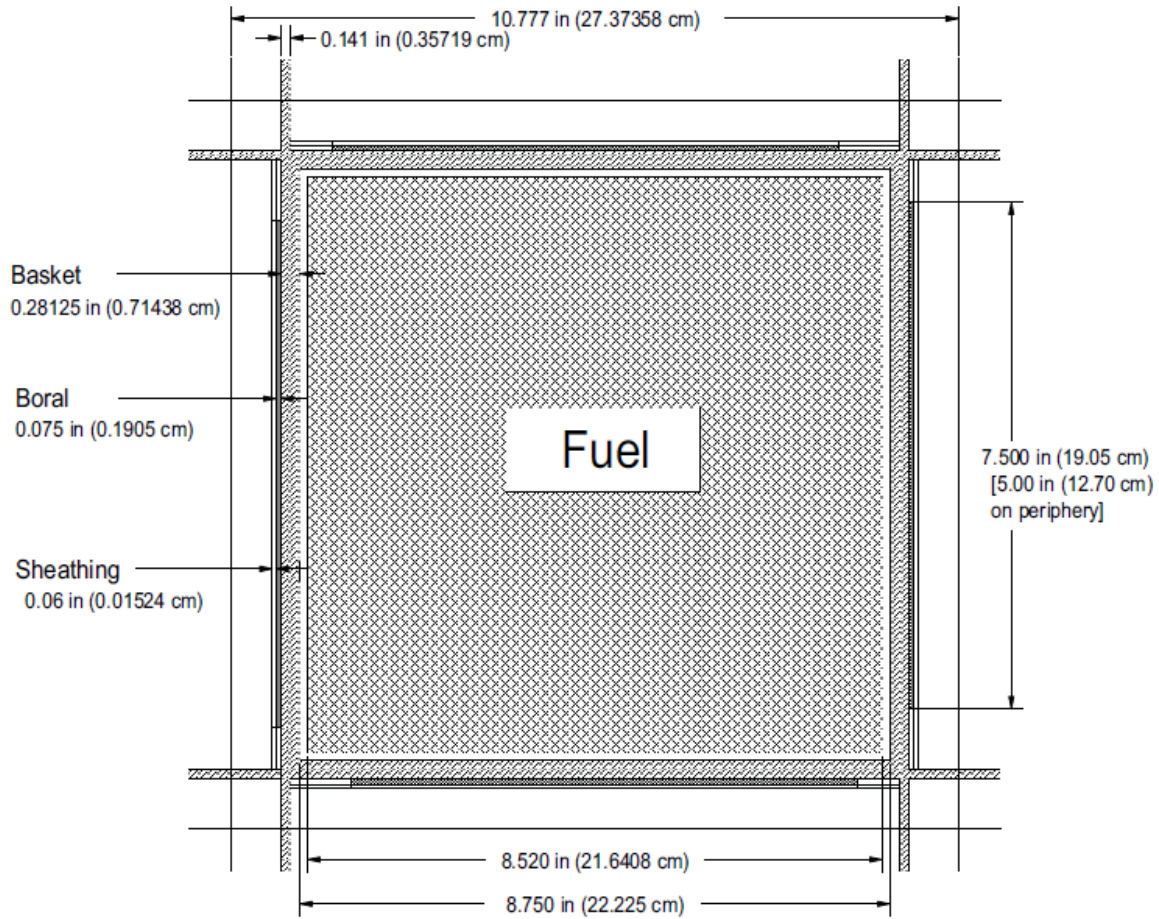


Figure 2.12: A MPC-24 cell of the basket honeycomb displaying spacing between assembly, channel, and BORAL plates.[7]

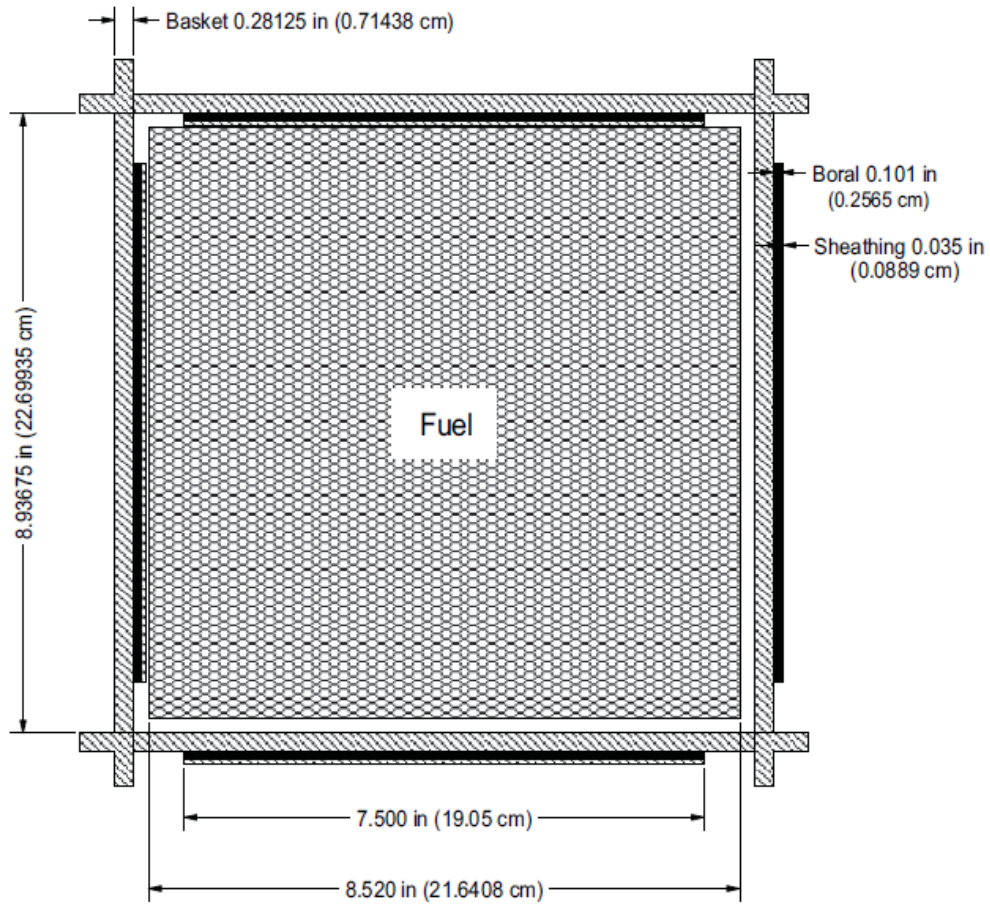


Figure 2.13: A MPC-32 cell of the basket honeycomb displaying spacing between assembly, channel, and BORAL plates.[7]

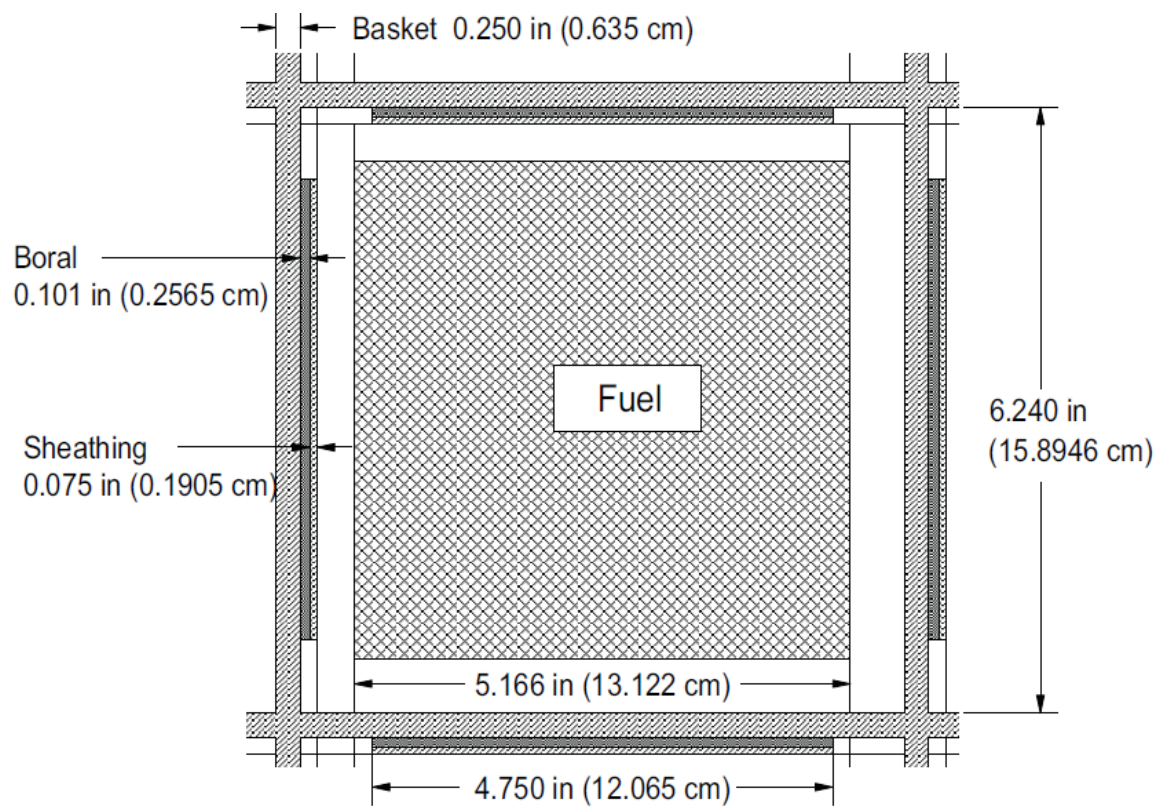


Figure 2.14: A MPC-68 cell of the basket honeycomb displaying spacing between assembly, channel, and BORAL plates.[7]

CHAPTER 3

METHODOLOGY

3.1 ORIGEN-ARP

This section details the procedure for establishing an ORIGEN-ARP case, where this methodology was used in order to characterize a homogeneous neutron and photon source strength and spectra for all BWR assemblies modeled within this body of work. As a companion, ORIGEN-ARP was used in order to validate preliminary data generated within the beta release of SCALE 6.2. In order to achieve preliminary 0-dimensional modeling of both neutron and gamma emission from the spent fuel assembly source blocks, ORIGEN-ARP was utilized. Given known burn cycles for both a PWR and BWR reference assembly, depletion calculations were performed on an assembly averaged basis. The cycle data utilized within ORIGEN-ARP is detailed below within tables 3.1 and 3.2. PWR assemblies were considered to account for 0.468 MTU while BWR assemblies were considered to be 0.190 MTU.

Within ORIGEN-ARP, the "enrich" option was utilized in order to populate the initial heavy metal within the Uranium dioxide fuel. All source characterizations are computed for 1 MTU. With the mentioned option, an initial ^{235}U at% dictates the

Table 3.1: The cycle data for the reference PWR assembly used within ORIGEN-ARP details a V.C. Summer Nuclear Station cycle of a Westinghouse 17x17 assembly burned to $57.535 \frac{\text{MWd}}{\text{kg}}$. [10]

Cycle No.	Cycle 1	Cycle 2	Cycle 3
Time (days)	522.6	504.8	521.8
Power (MW/MTU)	53.2	43.9	15.0
Down Period (days)	30	30	<i>variable</i>

Table 3.2: The cycle data for the reference BWR assembly used within ORIGEN-ARP details a Cooper Power Station cycle of a General Electric 8x8 assembly burned to $25.388 \frac{MWd}{kg}$. [3]

Binary Burnup Data					
<i>Data for Cooper BWR assembly CZ05</i>					
Fuel Loading	Cycle No.	Power (MW/asmby.)	Burnup (MWd/kg)	Cycle (days)	Outage (days)
Basis = 1 assembly (0.1902 MTU)	1	2.427	10.298	807	59
	2	4.608	7.414	306	31
	3	3.464	2.987	164	35
^{234}U wt% = 0.022	4	0.0	0	370	-
^{235}U wt% = 2.500	5	0.0	0	394	-
^{236}U wt% = 0.012	6	1.118	1.864	317	48
^{238}U wt% = 97.466	7	1.520	2.781	348	-

inventory of ^{234}U , ^{236}U and ^{238}U . Furthermore, standard moderator density of $0.7332 \frac{gm}{cm^3}$, 238 group neutron spectra, and 47 group photon spectra were chosen within ORIGEN-ARP. The selected output of neutron and photon spectra is given as a set of differential values. For consideration of source strength, this set of differential values is converted to integral values, a product of the energy bin width.

The data represented in figures 3.1 and 3.2 where output from ORIGEN-ARP is used to characterize energy dependent photon and neutron emission for the reference General Electric 8x8 assembly used in the MPC-68 design.

In the manner prescribed within table 3.3, selections were made within ORIGEN-ARP. These specify consideration of (α, n) generation of neutron emission and Bremsstrahlung generation within UO_2 in the ORIGEN assembly model. User input also dictated the energy binning of both neutron and photon output spectra. Input relevant to the (α, n) neutron source included the target material and energy cutoff. The spontaneous fission neutron source dominates the neutron spectrum of the spent fuel.

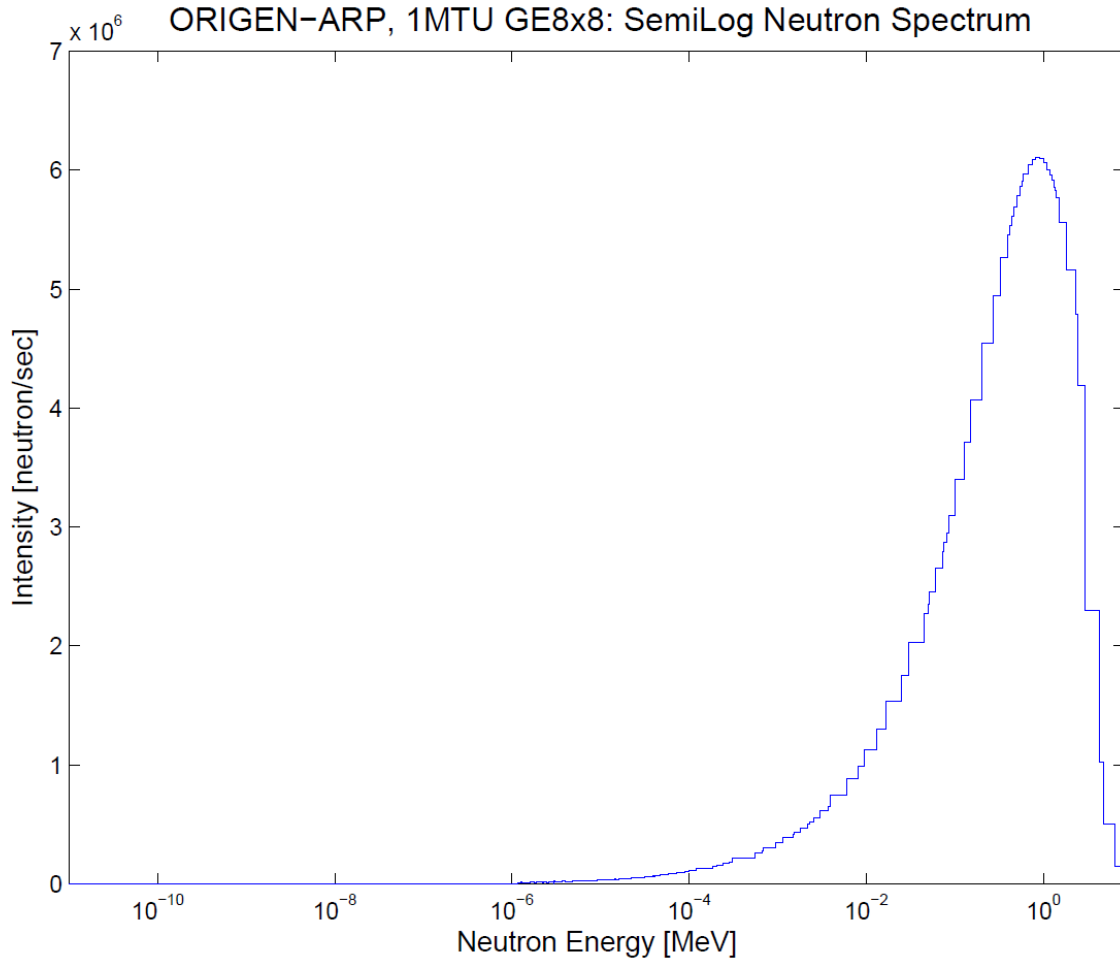


Figure 3.1: The SemiLog spectra of the neutron source is shown after a cooling period of 25 years. This is for 1 MTU of the reference BWR assembly in ORIGEN-ARP, and details a Cooper Power Station cycle of a General Electric 8x8 assembly burned to $25.388 \frac{MWd}{kg}$.

Table 3.3: ARP source calculation options for reference PWR and BWR assemblies.

Assembly	BWR	PWR
$\rho_{moderator}$	$0.723 \frac{gm}{cm^3}$	auto
Enrich = Auto	3.5% U-235	3.5% U-235
Structure, neutron	238G SCALE	238G SCALE
Structure, photon	47G SCALE6	47G SCALE6
(α,n) material	UO_2	UO_2
(α,n) cutoff	$1 \cdot 10^{-5}$	$1 \cdot 10^{-5}$
(α,n) groups	200	200
Bremmstrahlung material	UO_2	UO_2
Gamma Library	total	total

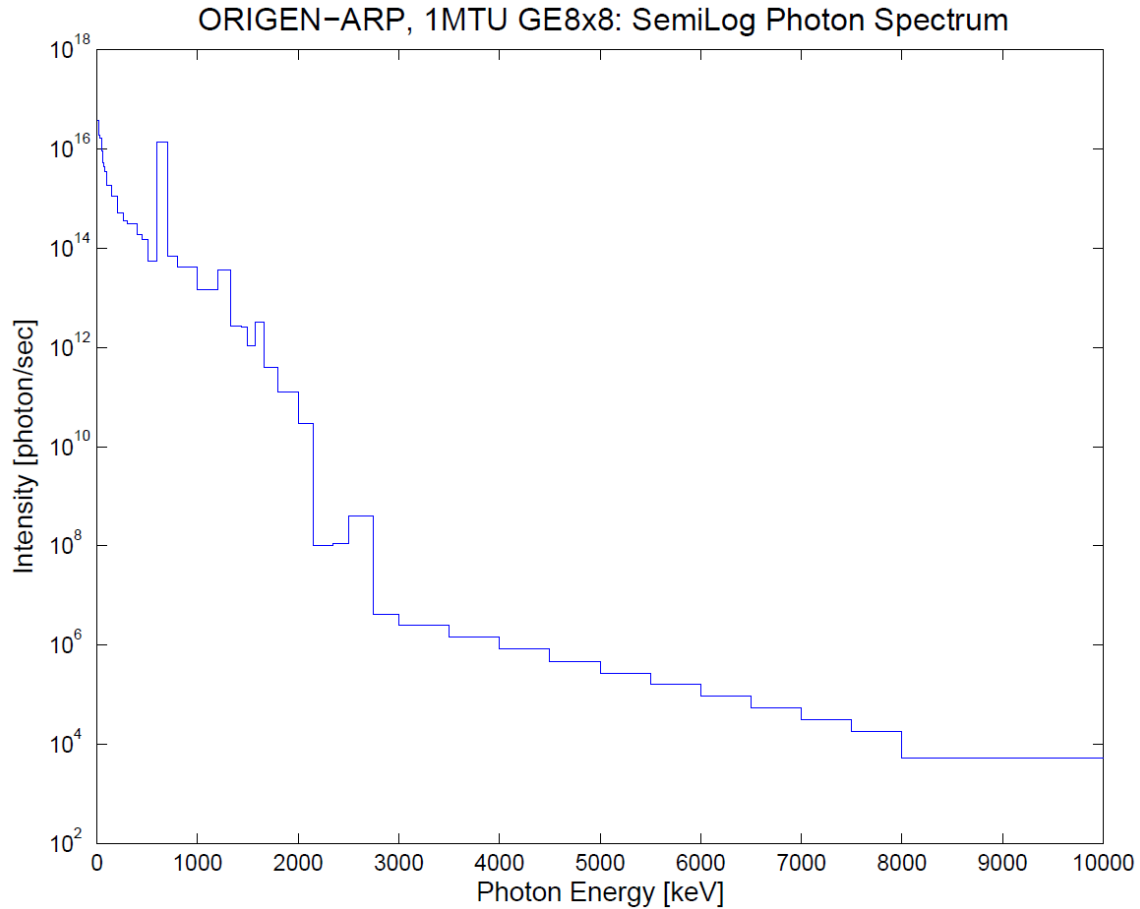


Figure 3.2: The SemiLog spectra of the photon source is shown after a cooling period of 25 years. This is for 1 MTU of the reference BWR assembly in ORIGIN-ARP, and details a Cooper Power Station cycle of a General Electric 8x8 assembly burned to $25.388 \frac{MWd}{kg}$.

3.2 ORIGAMI

ORIGAMI is utilized in order to provide a 28 zone 1D characterization of a Westinghouse 17x17 assembly, where both moderator density and discharge burnup were quantified within this 28 zone structure. As can be observed within figures 3.4 and 3.5, the curve generated with the supplied industry data closely matches the literature values of K_0 .

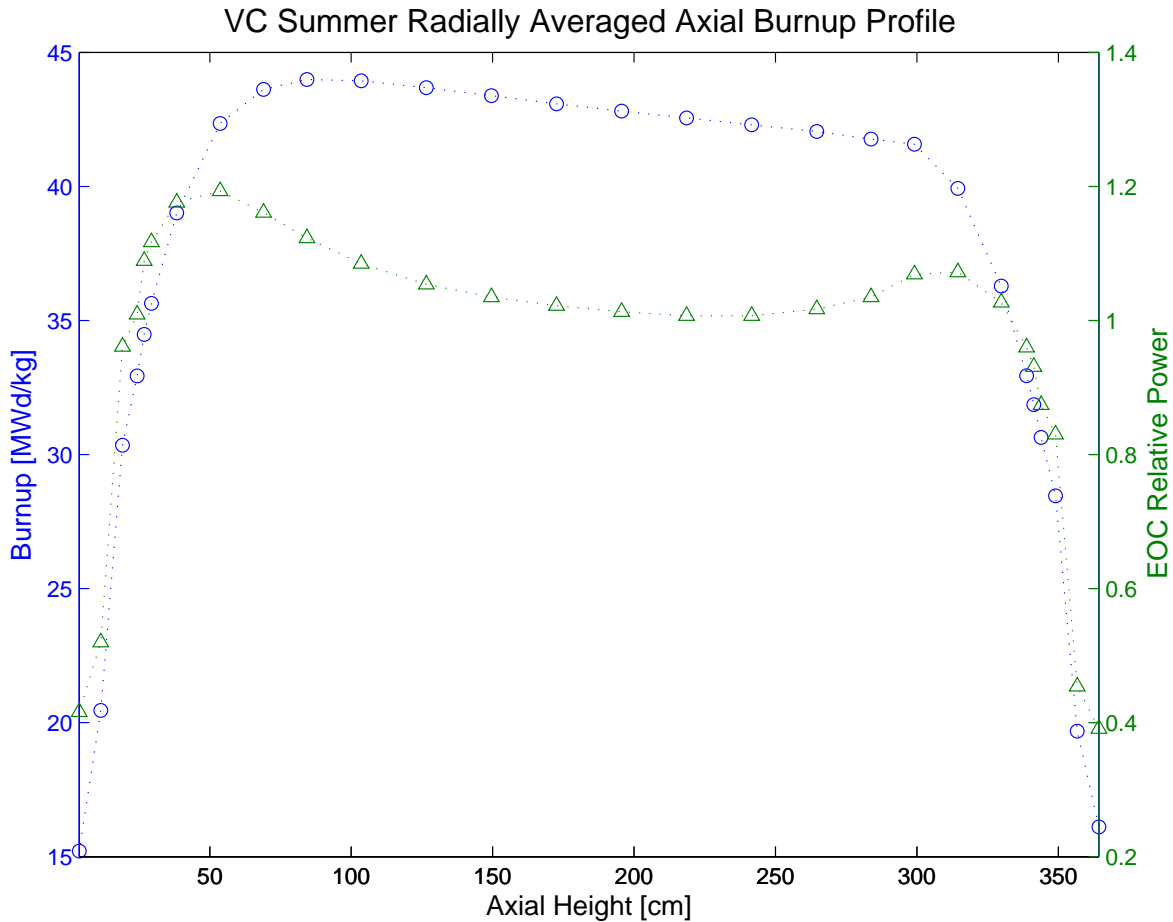


Figure 3.3: The radially averaged axial burnup and end of cycle power for a reference Virgil C. Summer Nuclear Generating Station cycle.

As a further mechanism of validation, the photon spectra generated within ORIGEN-ARP, ORIGAMI, and ORIGEN2 were compared within figure 3.6 in order to demonstrate validity of the simulated photon spectra generated within ORIGAMI. Given the data shown within figure 3.3, a 28 zone axial burnup profile was used in order to generate a 28 zone depletion calculation on the irradiated fuel. This characterization of energy release over time allowed definition of thermal and neutron power on a unique bin by bin basis within ORIGAMI, in combination with an axial moderator density profile. The results are shown in figure 3.4.

Table 3.4: The radially averaged, EoC, axial, Virgil C. Summer Nuclear Station burnup data used to generate the curve shown in figure 3.3.

Row No.	Height [cm]	BU [MWd/MTU]
28	364.29	16108
27	356.63	19684
26	348.96	28460
25	343.84	30637
24	341.29	31859
23	338.73	32937
22	329.78	36284
21	314.44	39930
20	299.11	41576
19	283.77	41764
18	264.59	42049
17	241.59	42301
16	218.58	42551
15	195.57	42806
14	172.56	43081
13	149.55	43384
12	126.54	43685
11	103.54	43942
10	84.36	43987
9	69.02	43620
8	53.69	42348
7	38.35	39011
6	29.4	35637
5	26.84	34482
4	24.29	32933
3	19.17	30347
2	11.5	20458
1	3.83	15207

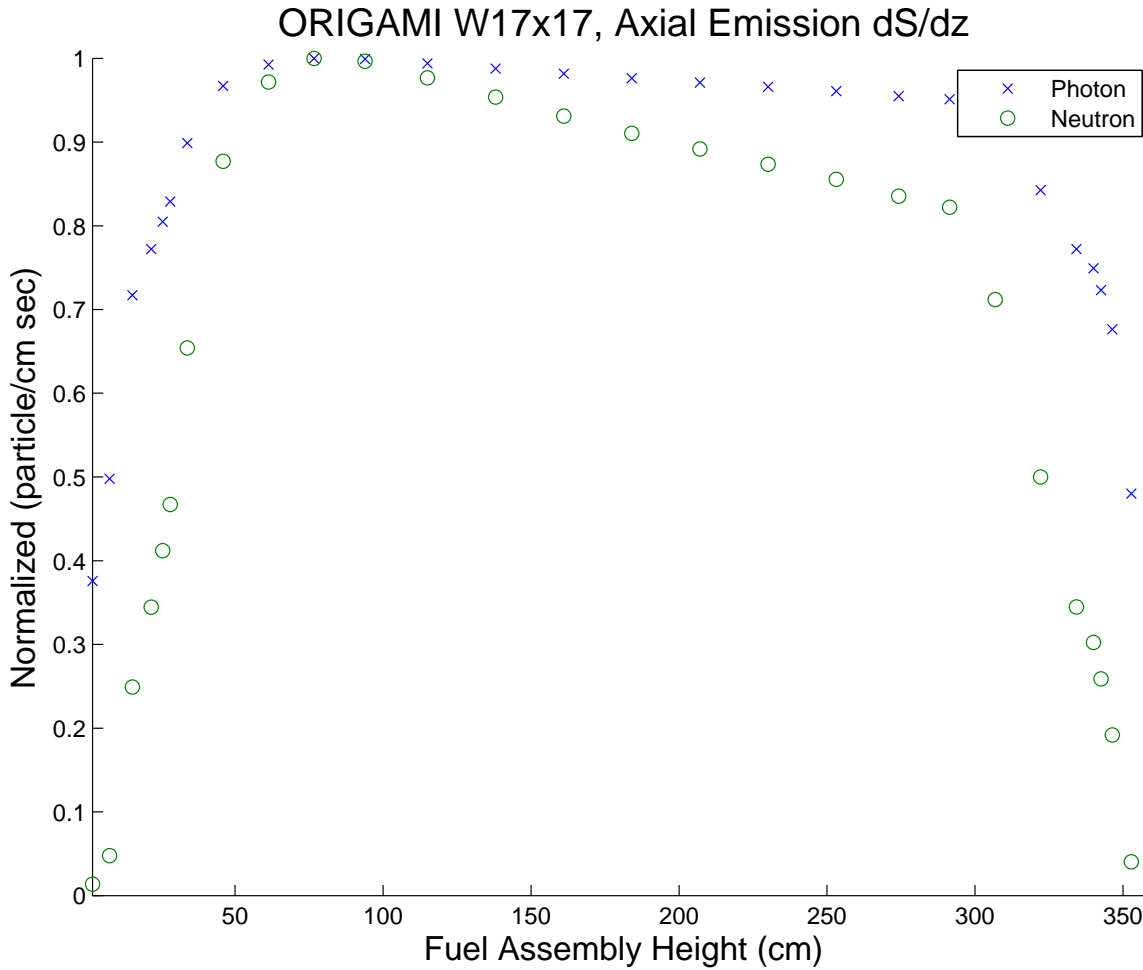


Figure 3.4: The axial photon (p) and neutron (n) emission profiles calculated within ORIGAMI in SCALE6.2 for a Westinghouse 17x17 irradiated to $57.535 \frac{MWd}{kg}$ to the axial power density.

The information in table 3.4 represents the expected discharge burnup for an assembly calculated by the core design engineers at VC Summer Nuclear Station. This curve generated and shown in figure 3.4 compares favorably with known literature data shown in figure 3.5 when both are normalized to a maximum value of unity. Modeling of the spent nuclear fuel photon spectra may be undertaken through multiple different code packages. A Semilogarithmic spectra is shown in figure 3.6, and a Log-Log spectra is shown in figure 3.7. A photon spectra for 1 MTU of a PWR assembly is generated within ORIGAMI, ORIGIN-ARP, and ORIGIN2.

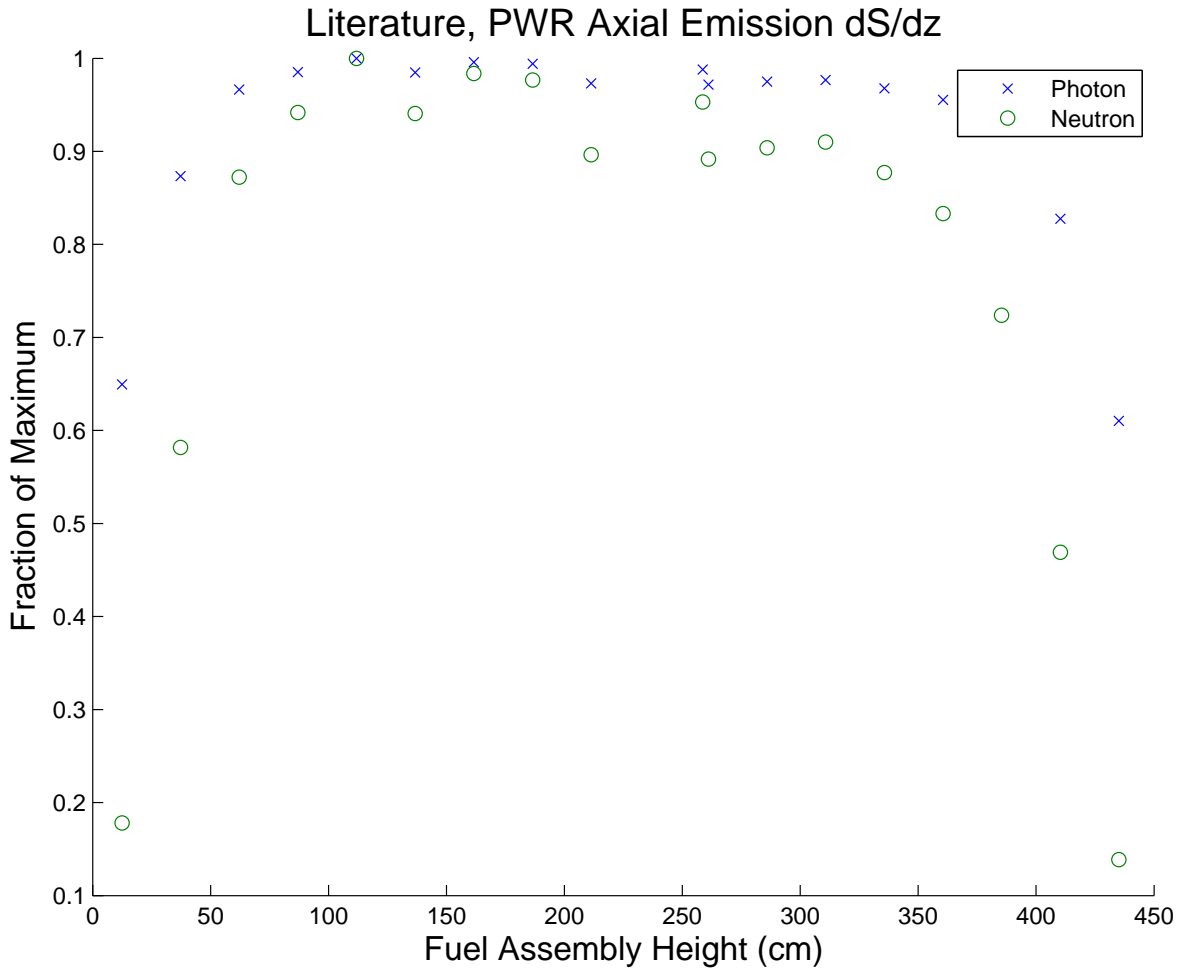


Figure 3.5: The axial photon (p) and neutron (n) emission profiles from a composite average of US legacy fuel assemblies appropriate for the 1970-1980 time period. The profile is normalized to max source strength over the height of a fuel assembly.[19]

ORIGEN-ARP was ran for 1 MTU of a Westinghouse 17x17 assembly with BU of $57.535 \frac{MWd}{kg}$ enriched to 3.5% with a cooling period of 5yr. Does not consider axially variant power density. Options chosen include the auto enrich option that populates minor isotopes of uranium given a target enrichment of $^{235}_{92}U$.

ORIGAMI was ran for 1 MTU of a Westinghouse 17x17 assembly with BU of $57.535 \frac{MWd}{kg}$ enriched to 3.5% with a cooling period of 5yr. Includes an axial variation in power density extrapolated from terminal BU axial profile taken from V.C. Summer Nuclear Station. The averaged BU for the assembly is the same as in the

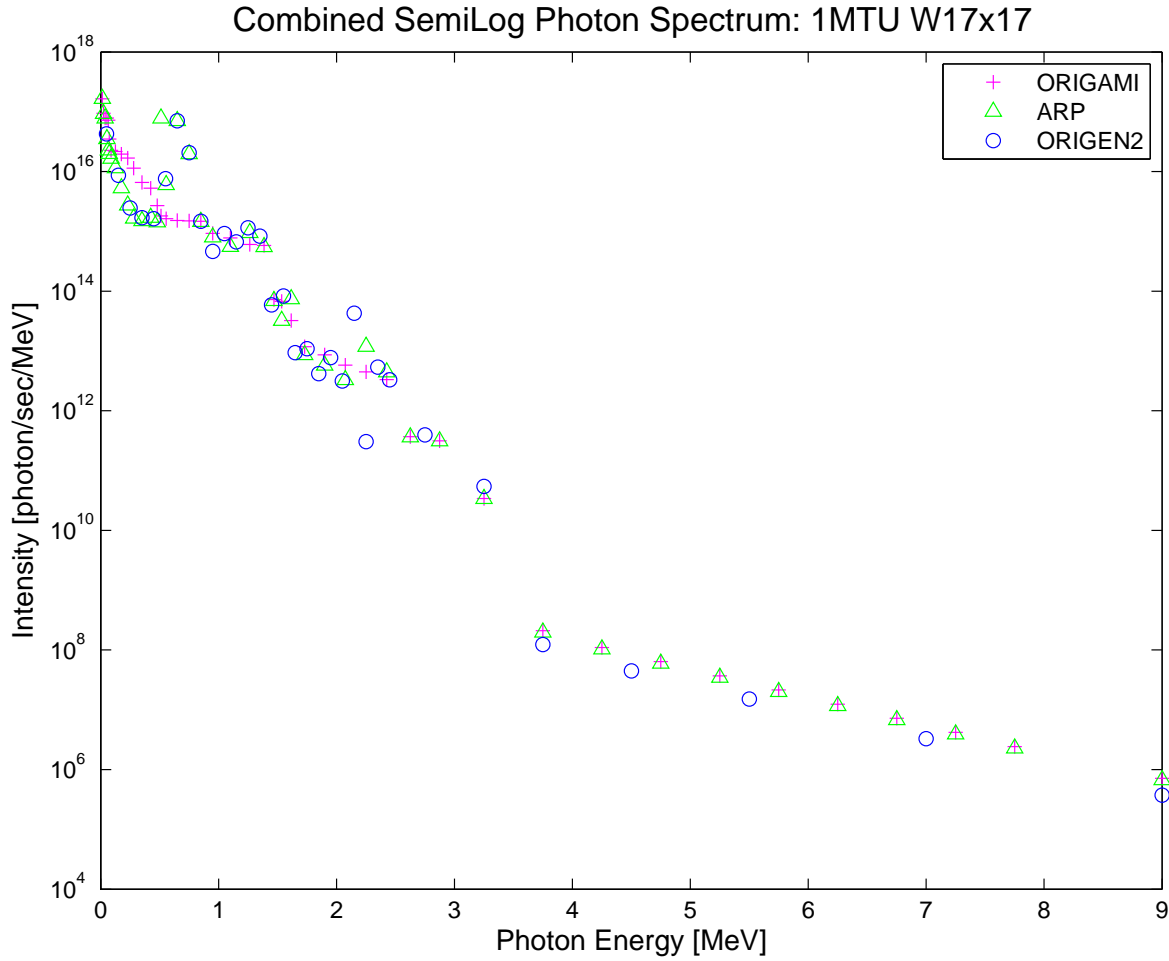


Figure 3.6: The Semilog photon spectra for 1 MTU of W17x17 computed for ORIGAMI, ARP, and compared to Literature.[11]

Table 3.5: ORIGAMI source calculation options for the reference PWR assembly.

Option	Selection
MTU	1
nburn	15
ndecay	12
Temper	565.25 K
Relnorm	yes
decayheat	yes
output	last
Libs	[w17x17]
Fuel	UOX
Enrich	3.5
Comps	fuel = 100
$\rho_{\text{moderator}}$	axial function

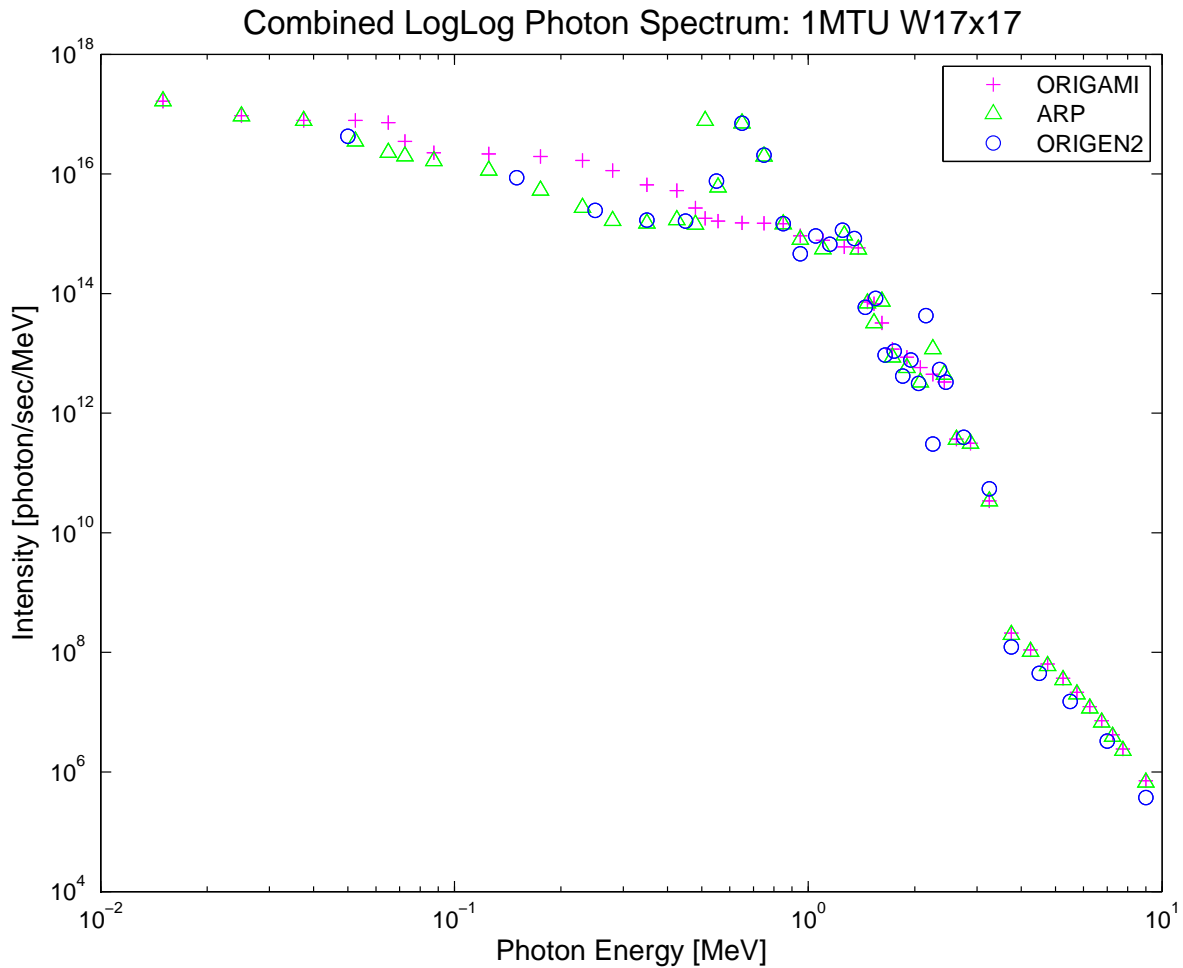


Figure 3.7: The LogLog photon spectra for 1 MTU of W17x17 computed for ORIGAMI, ARP, and compared to Literature.[11]

ORIGEN-ARP run. Options are detailed within table 3.5, and include the UOXfuel and enrich=3.5 options given within ORIGAMI in the SCALE 6.2 release. For comparison, ORIGEN2 data was taken from literature and spectra was calculated for 1 MTU of fuel with a BU of $50 \frac{MWd}{kg}$ and enriched to 3.6% over a cooling period of 5yr. This data was selected from a data set in order to closely match the previously mentioned conditions.

From figure 3.8, the various binned spectra are shown for the ORIGAMI depletion run on 1 MTU of a Westinghouse PWR assembly. For this research, the spectra was taken at zone 14, for the domain listed in table 3.4. The general curve of the

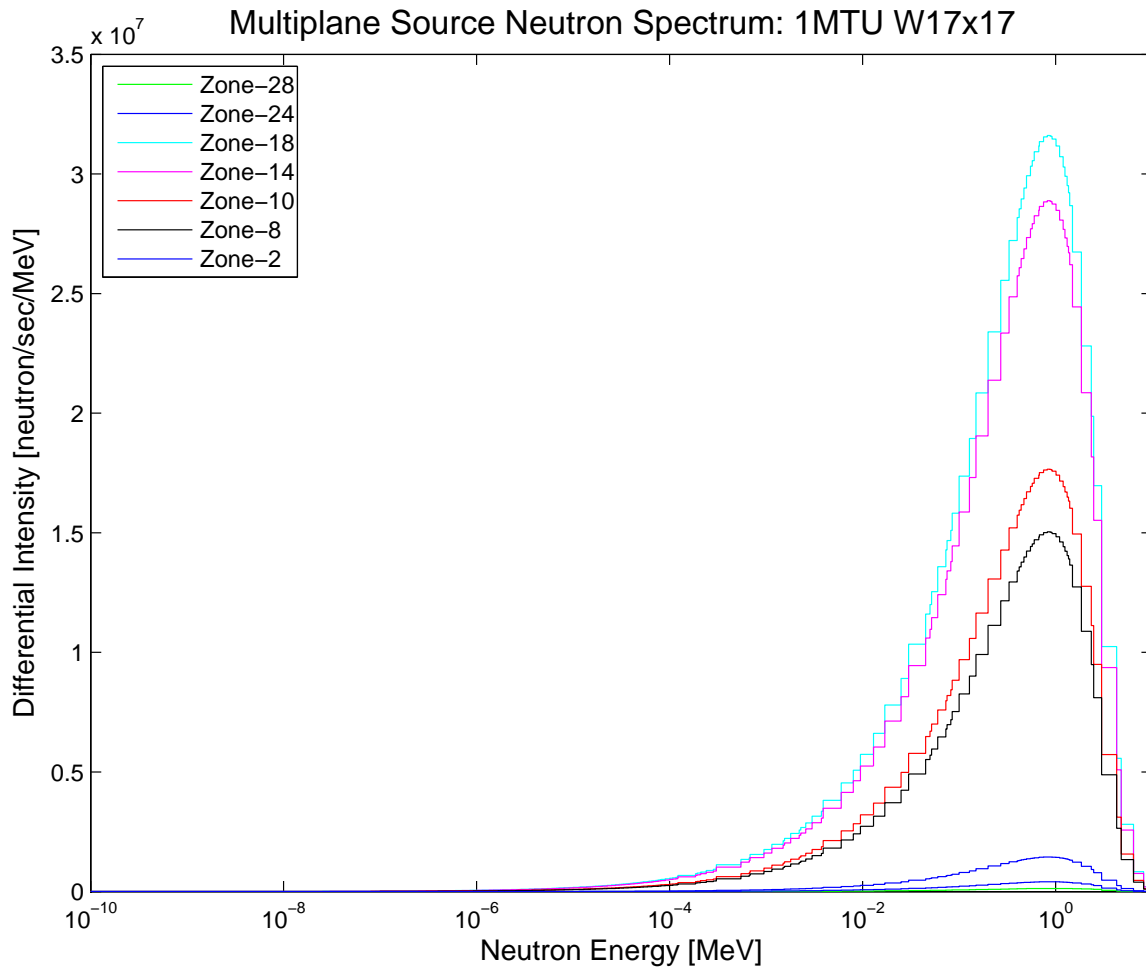


Figure 3.8: Comparison of different neutron spectra sections as described in table 3.4 and calculated within ORIGAMI for an axial discretized depletion run on 1 MTU of a Westinghouse 17×17 burned to $57.535 \frac{MWd}{kg}$ and cooled for 25 years.

individual zone by zone spectra show good agreement for one another over the major active height of the fuel assembly.

To justify spectral characterization at node-14, the normalized neutron spectra are shown in figure 3.9. It may be noted that the output spectra at each nodal bin is similar across the height of the fuel assembly, where the midplane nodes will be largely indistinguishable from lower burnup nodes. This constitutes the conservative approach desired for characterization of emitted neutron spectrum.

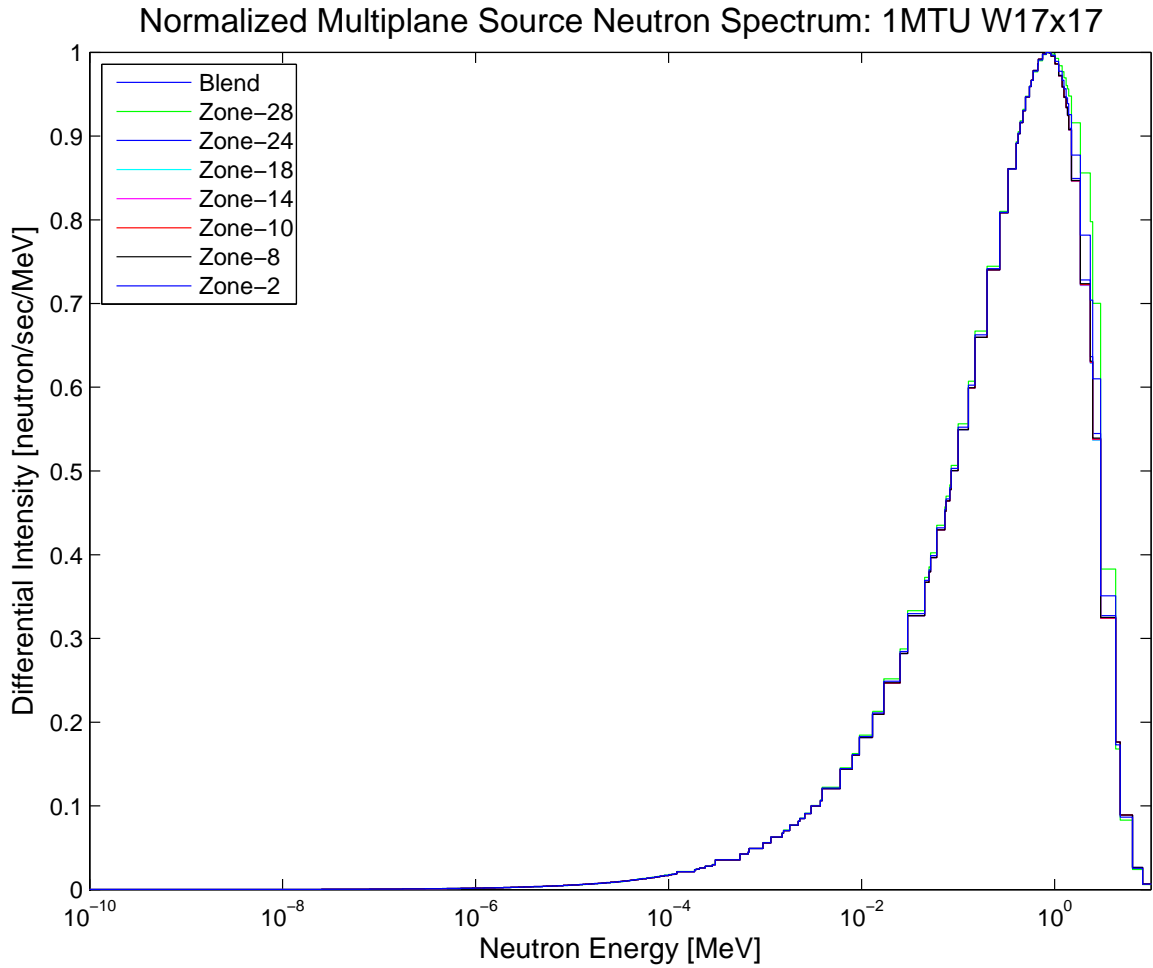


Figure 3.9: Normalized comparison of different neutron spectra sections as described in table 3.4 and calculated within ORIGAMI for an axial discretized depletion run on 1 MTU of a Westinghouse 17×17 burned to $57.535 \frac{MWd}{kg}$ and cooled for 25 years.

For the case of zoned photon spectra shown in 3.10, strong agreement is shown between the individual spectra zones located along the axis of the PWR fuel assembly modeled in ORIGAMI. This provides justification for using the spectra of zone 14 in order to characterize the assembly photon emissions. To further illustrate this agreement, the normalized multizone photon spectra are shown in figure 3.11. The lower energy, higher intensity photon emissions are largely the same across the various zones considered.

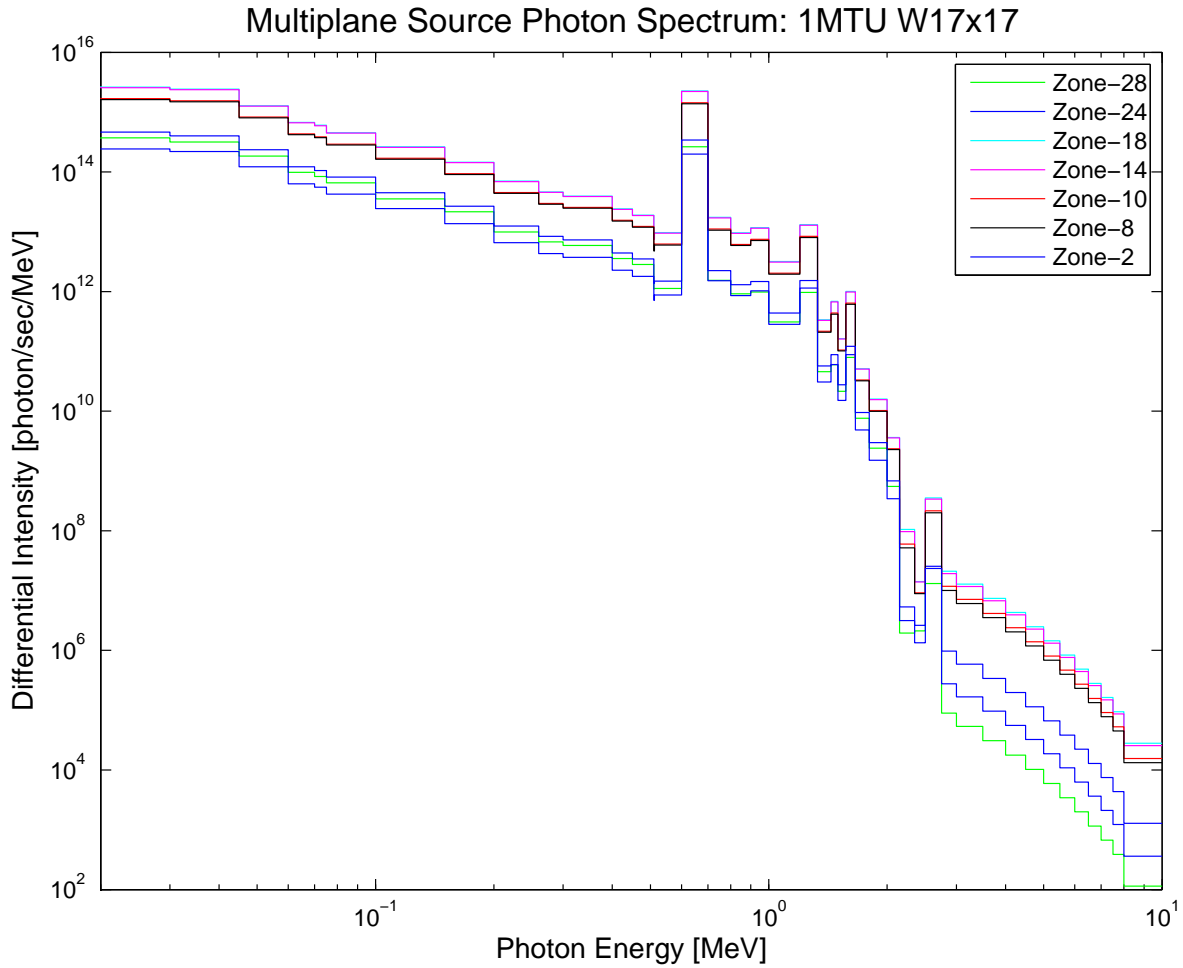


Figure 3.10: Comparison of different photon spectra sections as described in table 3.4 and calculated within ORIGAMI for an axial discretized depletion run on 1 MTU of a Westinghouse 17×17 burned to $57.535 \frac{MWd}{kg}$ and cooled for 25 years.

The ORIGAMI combined zone photon and neutron spectra are listed in figures 3.12 and 3.13 for the described case. These spectra are not normalized, and taken for the blend of the 28 zone depletion structure shown in figures 3.8 and 3.11.

3.3 SOURCE STRENGTH COMPARISON

As a validation method, both ARP and ORIGAMI were compared to literature values and themselves. In this instance, the bulk and local impact of axial discretization of depletion was observed. Fine consideration of burnup is pertinent for neutron emission,

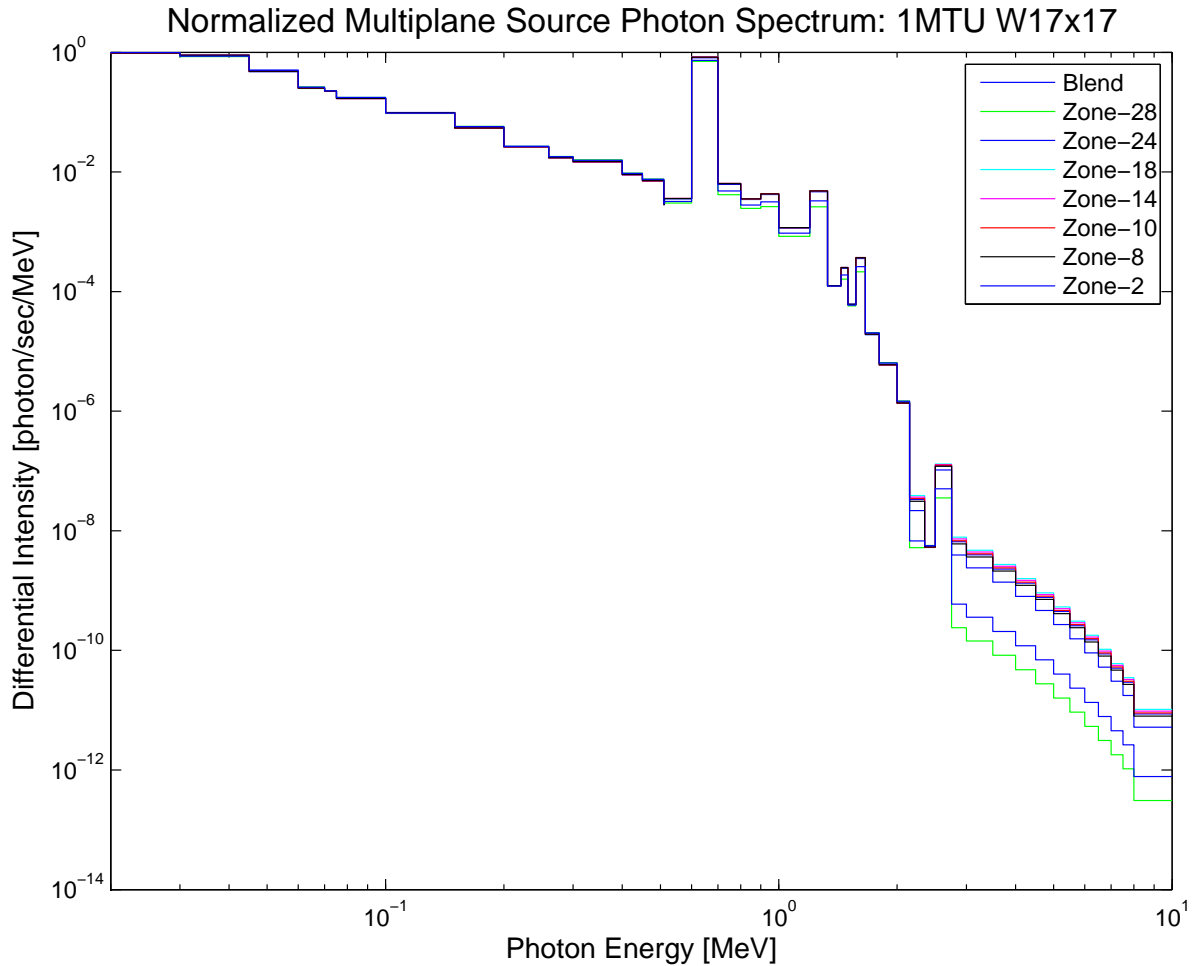


Figure 3.11: Normalized comparison of different photon spectra sections as described in table 3.4 and calculated within ORIGAMI for an axial discretized depletion run on 1 MTU of a Westinghouse 17×17 burned to $57.535 \frac{MWd}{kg}$ and cooled for 25 years.

as it is known that neutron source strength is proportional to burnup raised to the fourth power.[4] In the case of the bulk source strength, considering the low power density extrema of the fuel assembly had only a small impact on the assembly averaged source strength. However, this discretization in height prompted an expected spatial variation in dose rate over height on the outside of the cask. With the use of ORIGEN, sources from fission products, transuranics, (α, n) reactions, and Bremsstrahlung in UO_2 are given consideration. Specific energy cutoffs are detailed within table 3.3. The values for source strength detailed within tables 3.6 and 3.7 are implemented within MCNP 6.1 in the form of a FM multiplier in units of $\frac{particle}{sec}$ for the fuel

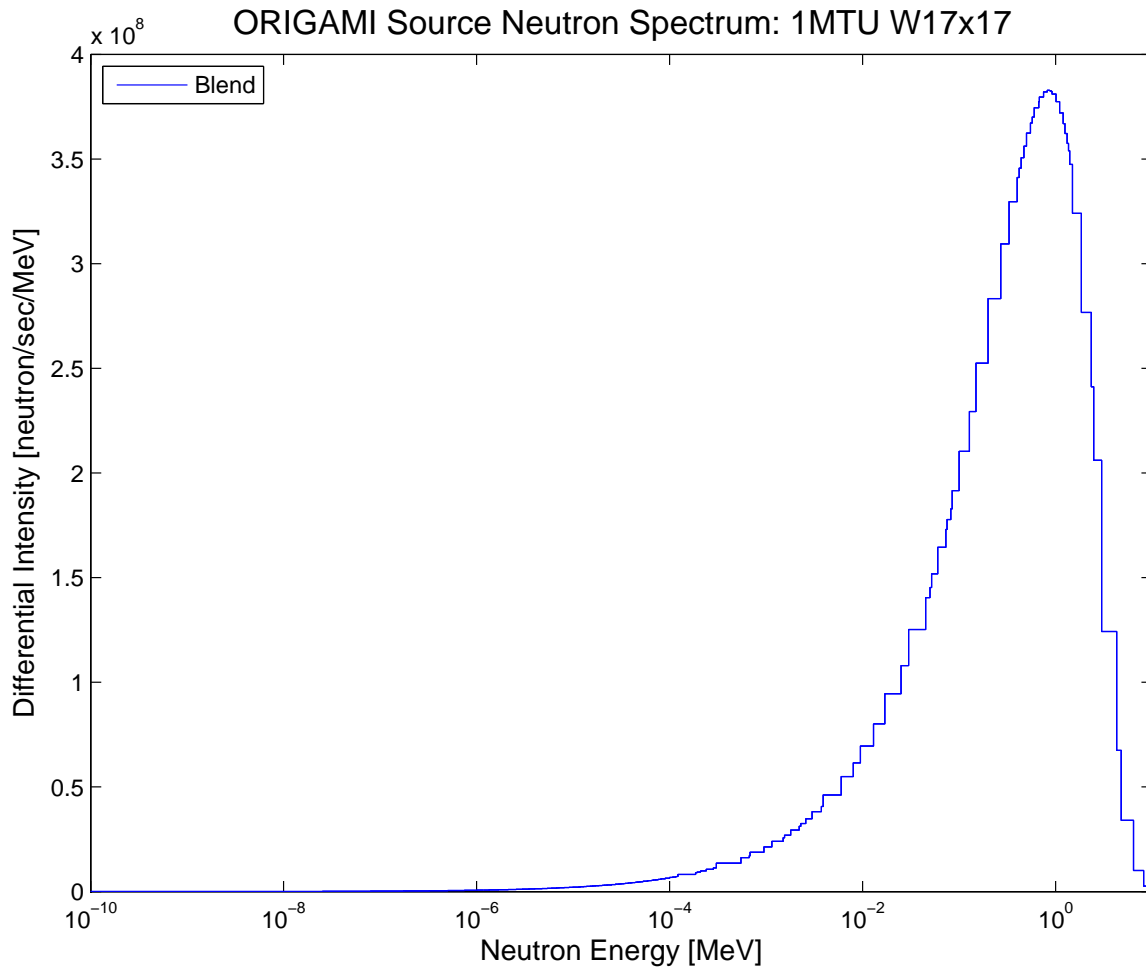


Figure 3.12: The multizone blended neutron spectra as described in table 3.4 and calculated within ORIGAMI for an axial discretized depletion run on 1 MTU of a Westinghouse 17×17 burned to $57.535 \frac{MWd}{kg}$ and cooled for 25 years.

mass. Within the internal radius and height of the multi-purpose canister, rectangular parallelepipeds representing a homogenous fuel assembly are sampled. In the case of an ORIGEN-ARP characterized source, they are sampled uniformly in height and over a power law in radius. In the case of ORIGAMI, they are characterized by an axial power distribution as well as the same power law over radius.

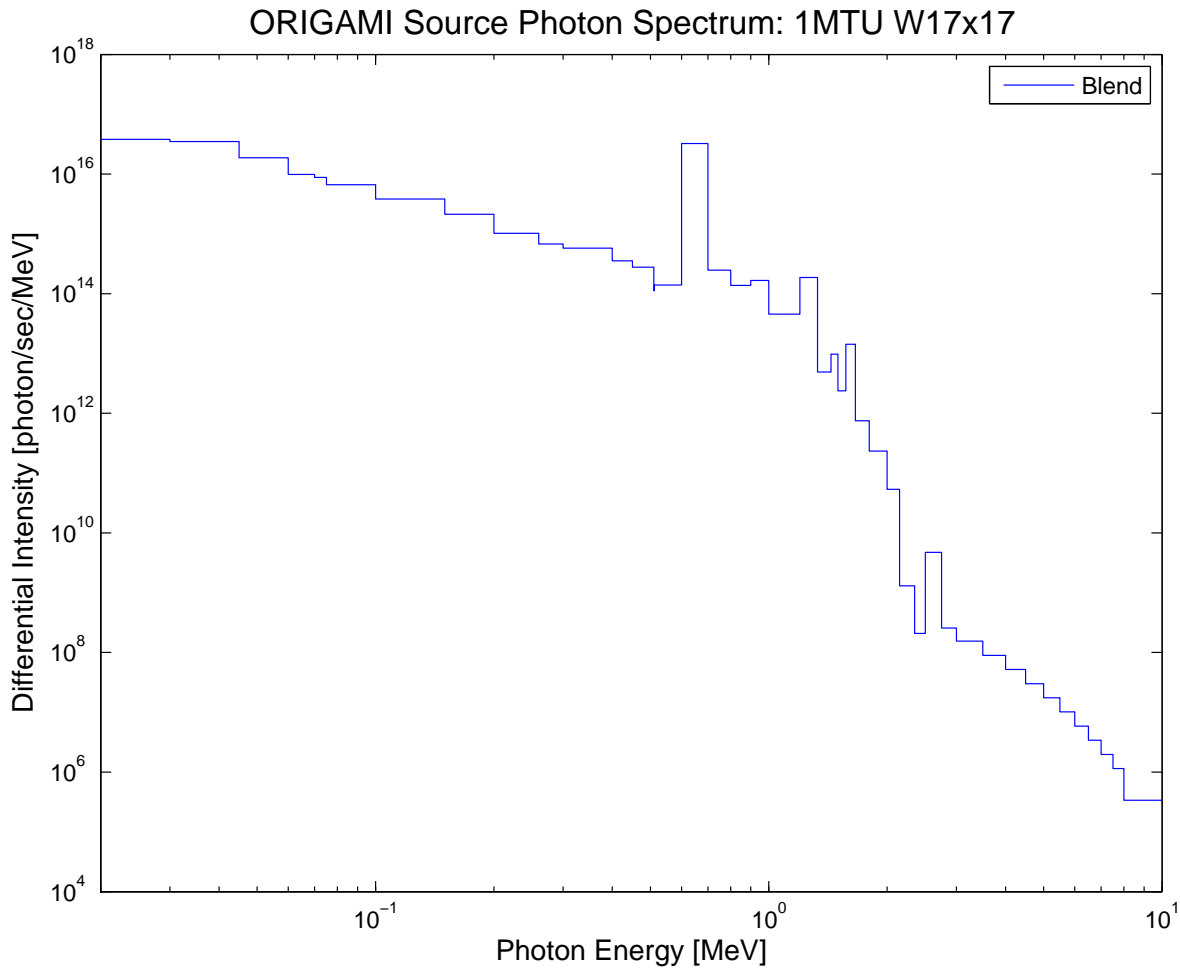


Figure 3.13: The multizone blended photon spectra as described in table 3.4 and calculated within ORIGAMI for an axial discretized depletion run on 1 MTU of a Westinghouse 17×17 burned to $57.535 \frac{MWd}{kg}$ and cooled for 25 years.

Table 3.6: The photon source strength comparison for the reference PWR assembly.

Assembly	Cooling Time	Basis [MTU]	BU {MWD/MTU}	Temp	Enrichment	Method	Particle	S [photon/sec]
W 17x17	5 yr	1	57,535	565.25	3.50%	ORIGAMI	gamma	1.70890E+16
W 17x17	15 yr	1	57,535	565.25	3.50%	ORIGAMI	gamma	7.98610E+15
W 17x17	25 yr	1	57,535	565.25	3.50%	ORIGAMI	gamma	6.09490E+15
W 17x17	35 yr	1	57,535	565.25	3.50%	ORIGAMI	gamma	4.80840E+15
W 17x17	45 yr	1	57,535	565.25	3.50%	ORIGAMI	gamma	3.82260E+15
W 17x17	5 yr	1	57,535	-	3.50%	ARP	gamma	1.66665E+16
W 17x17	15 yr	1	57,535	-	3.50%	ARP	gamma	8.02924E+15
W 17x17	25 yr	1	57,535	-	3.50%	ARP	gamma	6.13660E+15
W 17x17	35 yr	1	57,535	-	3.50%	ARP	gamma	4.83584E+15
W 17x17	45 yr	1	57,535	-	3.50%	ARP	gamma	3.84028E+15
W 15x15	3 yr	1	45,000	-	3.60%	FSAR p.1115[7]	gamma	1.44909E+16
W 15x15	5 yr	1	69,000	-	4.80%	FSAR p.1115[7]	gamma	1.48138E+16
W 15x15	3 yr	1	60,000	-	4.50%	FSAR p.1116[7]	gamma	1.98593E+16
W 15x15	5 yr	1	75,000	-	5.00%	FSAR p.1116[7]	gamma	1.61862E+16
-	5 yr	1	33,000	-	3.20%	Herman, ORIGEN[1]	gamma	1.33500E+16
-	4.9 yr	1	30,000	-	3.00%	Cuta, ORIGEN2[11]	gamma	7.81053E+15

Table 3.7: The neutron source strength comparison for the reference PWR assembly.

Assembly	Cooling Time	Basis [MTU]	BU {MWD/MTU}	Temp	Enrichment	Method	Particle	S [neutron/sec]
W 17x17	5 yr	1	57,535	565.25	3.50%	ORIGAMI	neutron	2.46400E+09
W 17x17	15 yr	1	57,535	565.25	3.50%	ORIGAMI	neutron	1.68230E+09
W 17x17	25 yr	1	57,535	565.25	3.50%	ORIGAMI	neutron	1.16740E+09
W 17x17	35 yr	1	57,535	565.25	3.50%	ORIGAMI	neutron	8.17180E+08
W 17x17	45 yr	1	57,535	565.25	3.50%	ORIGAMI	neutron	5.78190E+08
W 17x17	5 yr	1	57,535	-	3.50%	ARP	neutron	2.30002E+09
W 17x17	15 yr	1	57,535	-	3.50%	ARP	neutron	1.57811E+09
W 17x17	25 yr	1	57,535	-	3.50%	ARP	neutron	1.08927E+09
W 17x17	35 yr	1	57,535	-	3.50%	ARP	neutron	7.55817E+08
W 17x17	45 yr	1	57,535	-	3.50%	ARP	neutron	5.28295E+08
W 15x15	3 yr	1	45,000	-	3.50%	FSAR p.1117[7]	neutron	9.38474E+08
W 15x15	5 yr	1	69,000	-	3.50%	FSAR p.1117[7]	neutron	2.80533E+09
W 15x15	3 yr	1	60,000	-	3.50%	FSAR p.1118[7]	neutron	1.99602E+09
W 15x15	5 yr	1	75,000	-	3.50%	FSAR p.1118[7]	neutron	3.61262E+09
-	90 days	1	-	-	-	Herman, SAS2[1]	neutron	1.02328E+09
-	4.9 yr	1	30,000	-	3.00%	Cuta, ORIGEN2[11]	neutron	1.84668E+08

Table 3.8: The photon source strength comparison for the reference BWR assembly.

Assembly	Cooling Time	Basis [MTU]	BU {MWD/MTU}	Temp	Enrichment	Method	Particle	S [photon/sec]
GE 8x8	5 yr	1	25,388	-	3.50%	ARP	gamma	5.46012E+15
GE 8x8	15 yr	1	25,388	-	3.50%	ARP	gamma	3.51926E+15
GE 8x8	25 yr	1	25,388	-	3.50%	ARP	gamma	2.75137E+15
GE 8x8	35 yr	1	25,388	-	3.50%	ARP	gamma	2.17603E+15
GE 8x8	45 yr	1	25,388	-	3.50%	ARP	gamma	1.72815E+15
GE 7x7	3 yr	1	50,000	-	3.50%	FSAR p.1117[7]	gamma	1.51625E+16
GE 6x6	18 yr	1	30,000	-	3.50%	FSAR p.1118[7]	gamma	2.39054E+15

Table 3.9: The neutron source strength comparison for the reference BWR assembly.

Assembly	Cooling Time	Basis [MTU]	BU {MWD/MTU}	Temp	Enrichment	Method	Particle	S [neutron/sec]
GE 8x8	5 yr	1	25,388	-	3.50%	ARP	neutron	3.71048E+07
GE 8x8	15 yr	1	25,388	-	3.50%	ARP	neutron	2.70052E+07
GE 8x8	25 yr	1	25,388	-	3.50%	ARP	neutron	2.01070E+07
GE 8x8	35 yr	1	25,388	-	3.50%	ARP	neutron	1.53529E+07
GE 8x8	45 yr	1	25,388	-	3.50%	ARP	neutron	1.20686E+07
GE 7x7	3 yr	1	50,000	-	3.50%	FSAR p.1128[7]	neutron	1.29461E+09
GE 6x6	18 yr	1	30,000	-	3.50%	FSAR p.1129[7]	neutron	1.92644E+08
-	6 yr	1	27,400	-	3.50%	CRWM p.18[30]	neutron	7.46400E+07

3.4 COBALT ACTIVATION

In-annulus instrumentation may have some $^{59}_{27}\text{Co}$ within its components. Interconnections on some electronic chips may contain CoSi_2 , and electrical contacts are typically an Au-Co alloy that may contain up to 15% cobalt. Semiconductors may contain a Co bearing Au or Pt material. Some rare earth magnets designed for both high temperature and nuclear magnetic resonance spectrometry are composed of a system of SmCo. Outdated magnetic recording materials will also bear cobalt. Cobalt is common in Nickel-Cadmium, Nickel-Metal Hydride, and Lithium alloy batteries.

Cobalt production and loss:

$$\frac{d}{dt}N_{27}^{60}\text{Co} = \sigma_c(E)\Phi(E)N_{27}^{59}\text{Co} - \lambda_{27}^{60}\text{Co}N_{27}^{60}\text{Co} \quad (3.1)$$

where:

$\sigma_c(E)$ is the capture cross section, cm^2

$\Phi(E)$ is surface flux, $\frac{1}{cm^2 \cdot sec}$

N_{Co} is atom number

$\lambda_{27}^{60}\text{Co}$ is the decay constant, $\frac{1}{sec}$

This activation within the annulus will follow a rate equation of the form shown. For the purpose of this research, it is assumed that the loiter time within the annular environment is such that no saturation of ^{60}Co is reached within a cobalt sample. That states that $T_{annulus}$ is much smaller than the half-life of cobalt, which is 5.2715 years.[31] This method effectively considers a thin section of pure cobalt in intimate contact with the outer radius of the multi-purpose canister constitutes a conservative approach. This layer is not physically present within the model, rather, it is a consideration of MCNP alone in the form of a modified tally. This modified tally considers the (n, γ) reaction within pure Co. This cobalt is a virtual material, and does result in perturbation of transported flux.

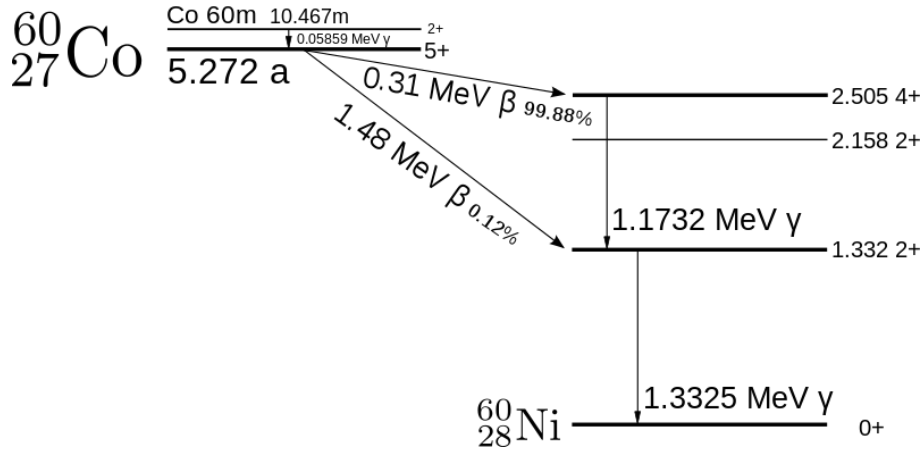


Figure 3.14: The decay diagram for cobalt.

It can be discerned from figure 3.14 that activated $^{60}_{27}\text{Co}$ presents an operator hazard in the form of principal daughter γ -rays of both 1.1732 MeV and 1.3325 MeV. This presents a health physics concern, and additional ALARA consideration may be necessary. These emissions are both preceded by both a low energy γ decay of $^{60\text{m}}_{27}\text{Co}$ and a β decay of $^{60}_{27}\text{Co}$.

$^{60}_{27}\text{Co}$ activation rate converted to radioactivity:

$$A_{Co} = N_{Co} S_o [FM12] \lambda_{Co} \frac{1}{\rho_{Co}} \left[\frac{3600 \text{ sec}}{\text{hr}} \right], \frac{Bq}{gm} \text{ per hr exposure} \quad (3.2)$$

where:

N_{Co} is cobalt number density for converting barns, $\frac{\text{atom}}{\text{barn}\cdot\text{cm}}$

S_o is source strength, $\frac{\text{neutron}}{\text{sec}}$

FM12 is a Co (n, γ) reaction modified F2 tally, $\frac{\text{barn}}{\text{cm}^2\cdot\text{neutron}}$

λ_{Co} is the decay constant, $\frac{1}{\text{sec}}$

$\frac{1}{\rho_{Co}}$ is the density, $\frac{\text{gm}}{\text{cm}^3}$

The $^{60}_{27}\text{Co}$ activation rate conversion equation is utilized within the master MCNP input in order to perform in code conversion of $^{60}_{27}\text{Co}$ activation rate into radioactivity density per hour of annulus loiter time. The activation reaction was considered via

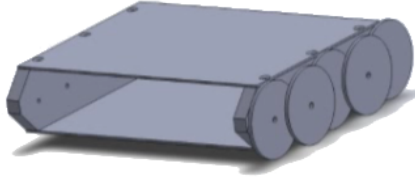


Figure 3.15: The externally proposed multi-sensory robot design.

the 102 MT card, which references the ENDF/B neutron continuous energy (n, γ) reaction. In this manner, a conservative approach to any potential for neutron activation of various Cobalt bearing semiconductors, magnets, or batteries may be calculated.

With further estimates of cobalt mass installed within the multi-sensory robotic probe, activation radioactivity may be predicted for used robotic components. This is a conservative estimate of activation rate for an unshielded geometry of $^{60}_{27}\text{Co}$. Ultimately, this may inform health physics personnel when combined with field measurement of any neutron activation within a shielded robotic component.

This multi-sensory robotic probe will take the form of a train of cars as seen in figure 3.15, where the potential exists for amelioration of dose via use of lead shield plates on the sides of these cars. The critical measurement consisting of 5 mm in thickness. As is shown within the results section, simple shielding in the form of these 5 mm shield plates is capable of reducing γ -ray dose by approximately half.

3.5 MCNP MATHEMATICS

The Holtec HI-STORM 100 family of spent nuclear fuel casks exist such that they may be installed into ISFSI arrays for extended periods of time under conditions where they are subjected to incremental damage. With this in mind, robotic instrumentation related to inspection is to be utilized to inspect the external MPC

wall for corrosion and cracking, and the internal METCON wall for degradation and liner delamination. MCNP utilizes several base calculations, referred to as tallies. They output transport data in terms of a starting particle and a given window for the particle to pass through. In this manner, an MCNP tally may be modified in order to relate to the rate of particle emission and their subsequent passage through a 2D or 3D mesh. Equations for the fundamental MCNP tallies are subsequently shown.

Surface Current Tally:

$$F1 = \int_A dA \int_E dE \int_{4\pi} d\omega \cdot n \cdot J(\vec{r}, E, \omega), \quad \frac{1}{cm^2} \quad (3.3)$$

Averaged Surface Flux Tally:

$$F2 = \frac{1}{A} \int_A dA \int_E dE \int_{4\pi} d\omega \cdot n \cdot \Phi(\vec{r}, E, \omega), \quad \frac{1}{cm^2} \quad (3.4)$$

Averaged Cell Flux Tally:

$$F4 = \frac{1}{V} \int_V dV \int_E dE \int_{4\pi} d\omega \cdot n \cdot \Phi(\vec{r}, E, \omega), \quad \frac{1}{cm^2} \quad (3.5)$$

The nature of the annular environment of the spent fuel storage system may prove to be challenging for complex electronics and machinery to survive for an indefinite period. Operator insertion of this equipment will likely involve interacting with and maintaining some presence in the vicinity of the vent mouths of the cask. Additionally, any insertion of robotics of unknown geometry would reasonably involve operator immersion past the plane of the vent mouth while removing the photon attenuating grating. With this in mind, methods for quantification of dose to electronic components within the proposed robotic instrumentation were developed from literature. Dose rate in Si is calculated utilizing both a mass energy absorption coefficient and a dose response function for comparison purposes. The dose response function utilized within this research was initially developed by the Jet Propulsion Laboratory to independently quantify mixed species radiation damage to spacecraft. These measurements take different approaches to assess Si dose, and both agree on energy deposition within Si. Relevant equations convert MCNP output in the following manner.

Photon dose rate from $\frac{\mu_{en}}{\rho}$:

$$D_{Si} = C_1 S_o \left[\frac{\mu_{en}}{\rho} \right] [*F2], \frac{Rad(Si)}{sec} \quad (3.6)$$

where:

C_1 is a conversion factor, $\frac{Rad(Si)}{\frac{MeV}{gm}}$

S_o is source strength, $\frac{photon}{sec}$

$\frac{\mu_{en}}{\rho}$ is the mass energy absorption coefficient, $\frac{cm^2}{gm}$

*F2=E ϕ is MCNP calculated energy flux, $\frac{MeV}{cm^2}$

After validating methods with a $\frac{\mu_{en}}{\rho}$ based photon dose rate calculation, this method was used as a companion to subsequent calculations involving the use of a straightforward flux to dose conversion for both neutron and photon flux.

Dose function dose rate from neutron or γ -rays:

$$D_{Si} = S_o [DF2] [F2], \frac{Rad(Si)}{sec} \quad (3.7)$$

where:

S_o is source strength, $\frac{particle}{sec}$

DF2 a dose response function, $\frac{Rad(Si)}{\frac{particle}{cm^2}}$

*F2 = E Φ is MCNP calculated flux, $\frac{particle}{cm^2}$

The above algorithms are utilized for conversions of particle flux to dose rate within MCNP, and allows onboard calculations. This generates output for comparison of radiation field related damage in Si, a major constituent of microelectronics. Ionization and disruption of Si components constitute a primary failure mechanism. It is logical to assume electronics failure will be resultant from high fluence as opposed to high flux electrical upset. Dose in Si will be expressed in terms of Rad(Si), where comparison may be drawn between existing data on electronics failure and predicted Si dose.

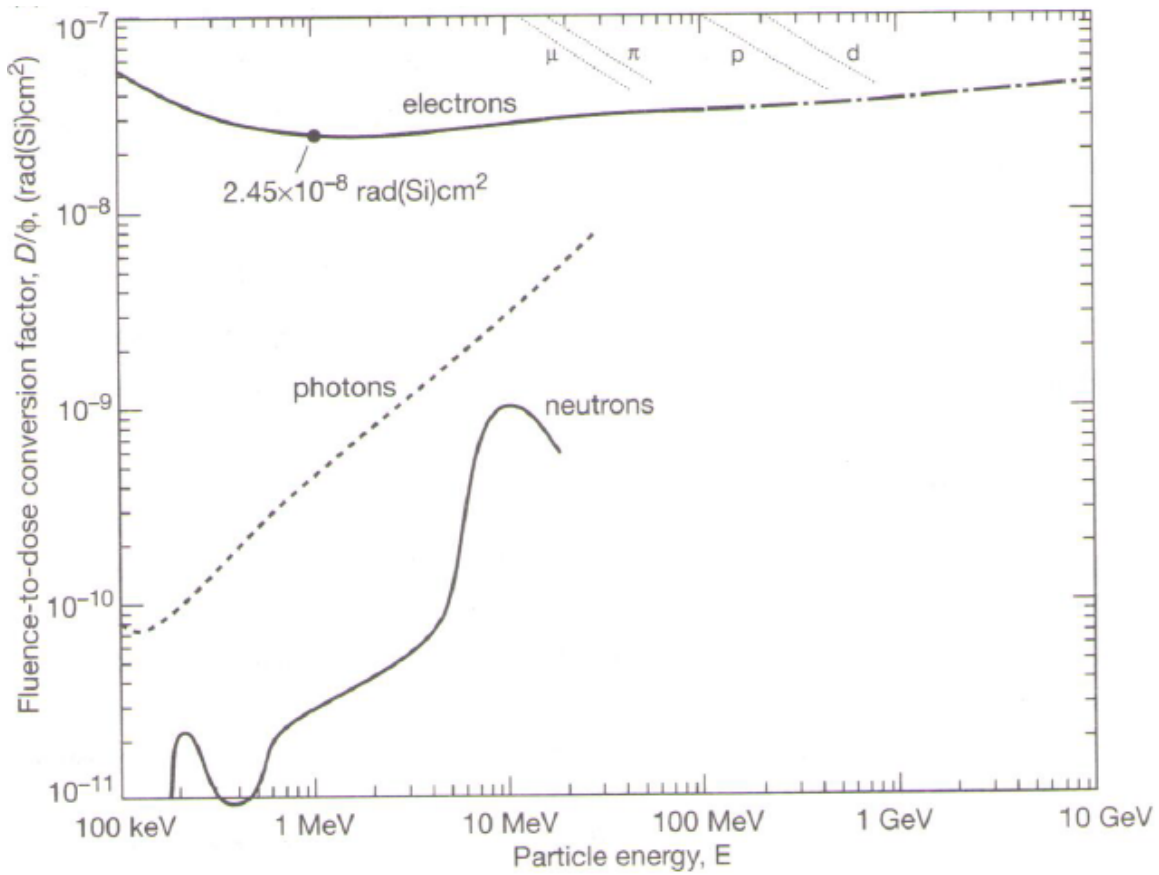


Figure 3.16: A Log-Log representation of both the neutron and photon flux to dose functions described above.[18]

Figure 3.16 demonstrates the suitability of log interpolation within the photon flux to dose response function. Likewise, the requirement for logarithmic interpolation of the neutron flux to dose response function is demonstrated.

As is shown within figure 3.17, mass energy absorption coefficients from NIST demonstrate a finely energy binned approximation of dose in terms of Rad(Si) for an unshielded undefined geometry of Si existing within the annulus of our MCNP model. Assuming an unshielded configuration is by far the most conservative approximation given current knowledge concerning final geometry of proposed robotic instrumentation. In the annulus of a dry spent fuel storage cask, the proportions and magnitude of neutrons to γ -rays will be dominated by fission product gamma-rays. This prompted

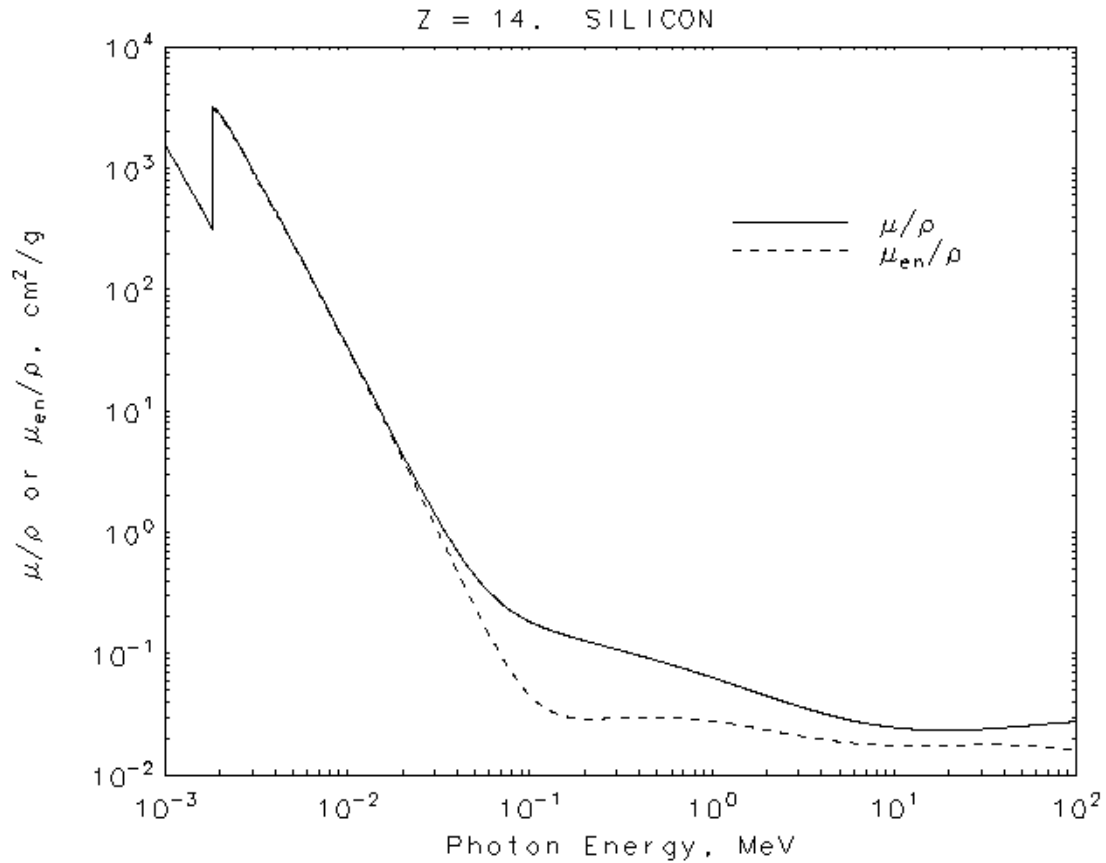


Figure 3.17: A representation of both the neutron and photon flux to dose functions described above.[28]

the decision to pursue independent evaluation of dose in Si in terms of separately computed both photon and neutron fields. The overall goal of the research being to provide advisement on both required radiation hardening and suggested loiter time within the annulus.

3.6 MCNP GEOMETRY

This section details the generation of the unique METCON and multi-purpose canister models, with boolean geometry in a MCNP input deck. True to the design, all of these components are geometrically interchangeable. In the case of all quartered cutaway

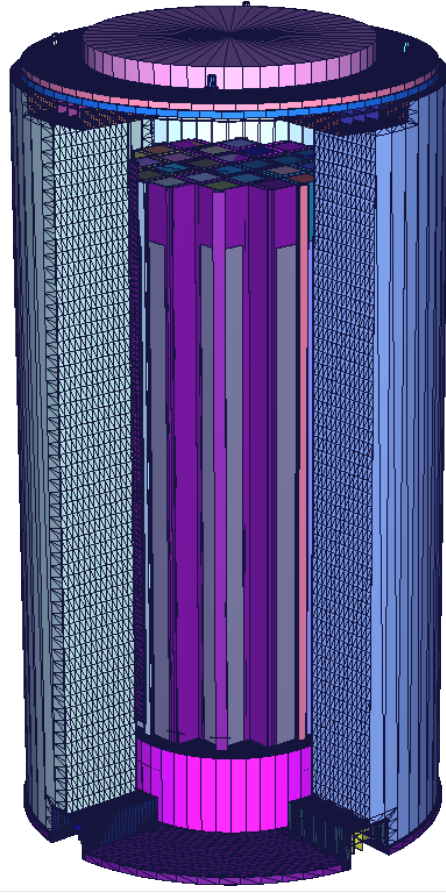


Figure 3.18: MCNP rendering of quartered cutaway of the HI-STORM 100S and MPC-24E as designed in MCNP.

diagrams, the MPC shell is removed for clarity and viewing. Within the actual model, a 304 stainless steel cylinder obfuscates view of the basket and contained fuel assemblies.

The MPC-24E and MPC-24EF are complex within the XY plane as shown in figure 3.19. This includes the various housed offsets within the MPC-24E basket and the generously space individual fuel assemblies. This model includes the flux traps on the periphery of the basket and the basket supports between the basket and MPC internal wall. Externally facing walls in the MPC-24E basket host a neutron absorbing BORAL plate. The flux traps of the MPC-24 basket are shown in figure 3.20.

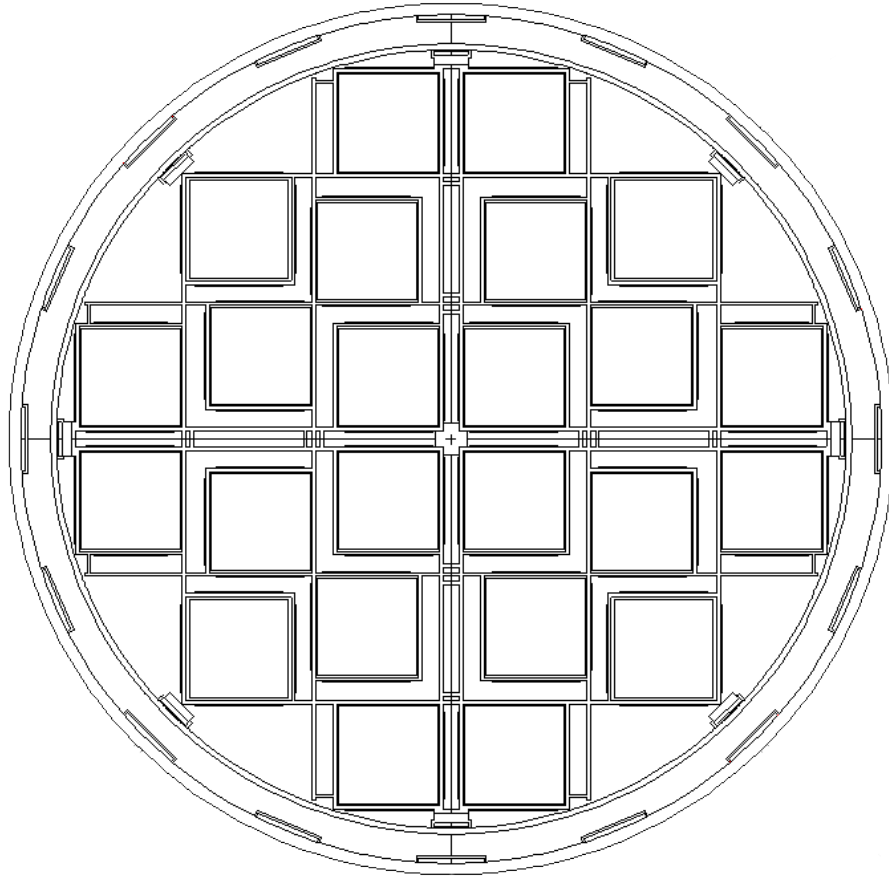


Figure 3.19: MCNP rendered cross section in the XY plane of the MPC-24E canister and the open annulus space.

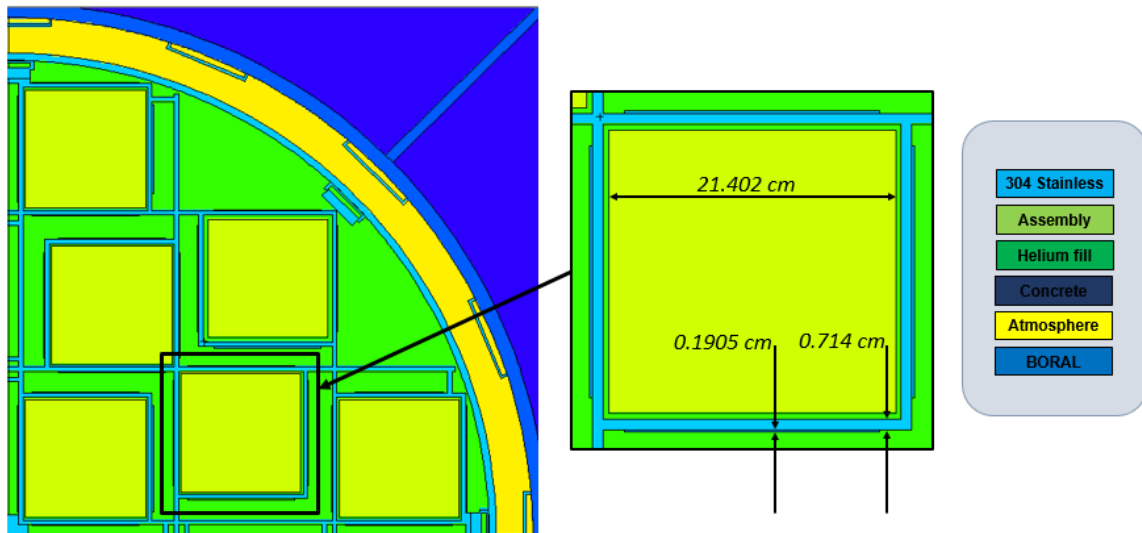


Figure 3.20: MCNP rendered detailed cross section in the XY plane of the MPC-24E basket.

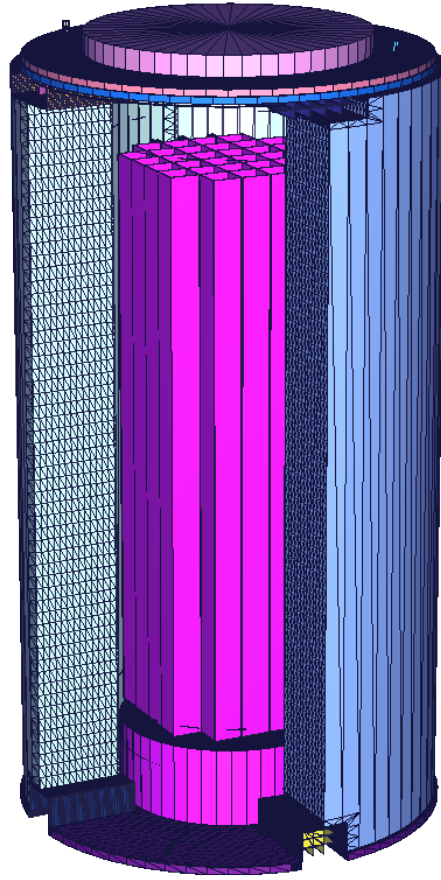


Figure 3.21: MCNP rendering of quartered cutaway of the HI-STORM 100S and MPC-32 as designed in MCNP.

From figure 3.22, the more homogeneous design of the less generously spaced MPC-32 design is apparent as modeled within MCNP. In contrast to the MPC-24E, multiple points of the MPC-32 basket closely approach the internal surface of the multi-purpose canister wall. Furthermore, the positioning of thin BORAL sheets is such that the external faces of the basket are not covered. While modeling this canister, 1/4 symmetry was used in order to simplify validation and manipulation of input geometry. Compared to the MPC-24 basket pattern in figure 3.20, the MPC-32 allows for denser packing. The differences in location of BORAL sheets is evident in figure 3.23.

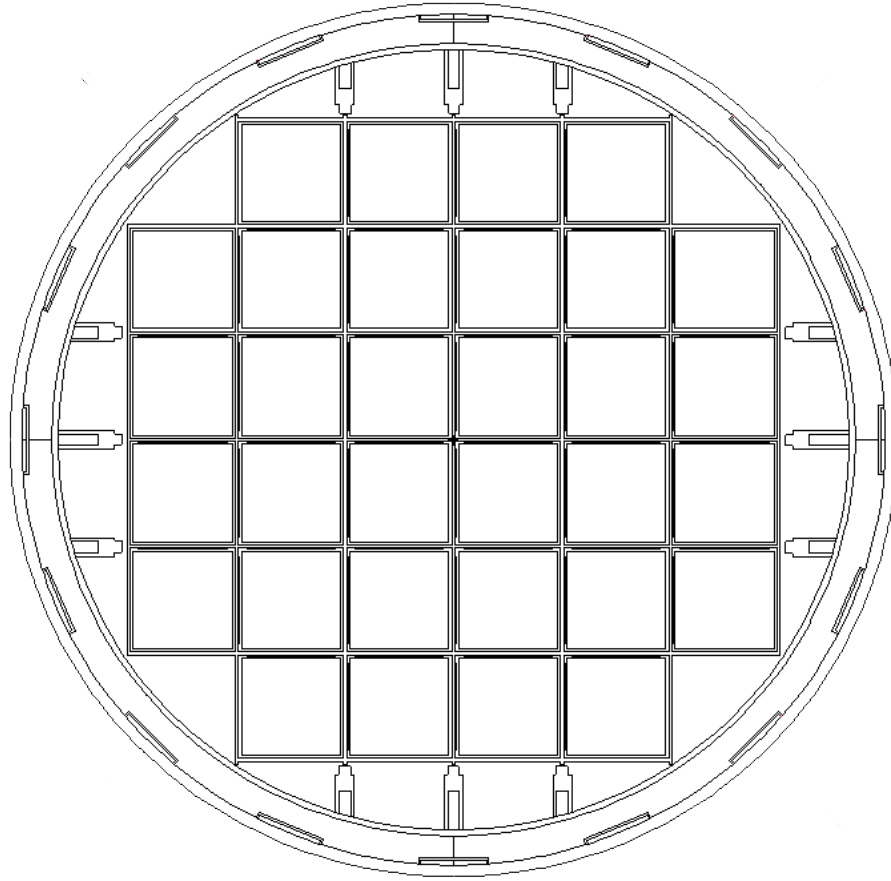


Figure 3.22: MCNP rendered cross section in the XY plane of the MPC-32 canister and the open annulus space.

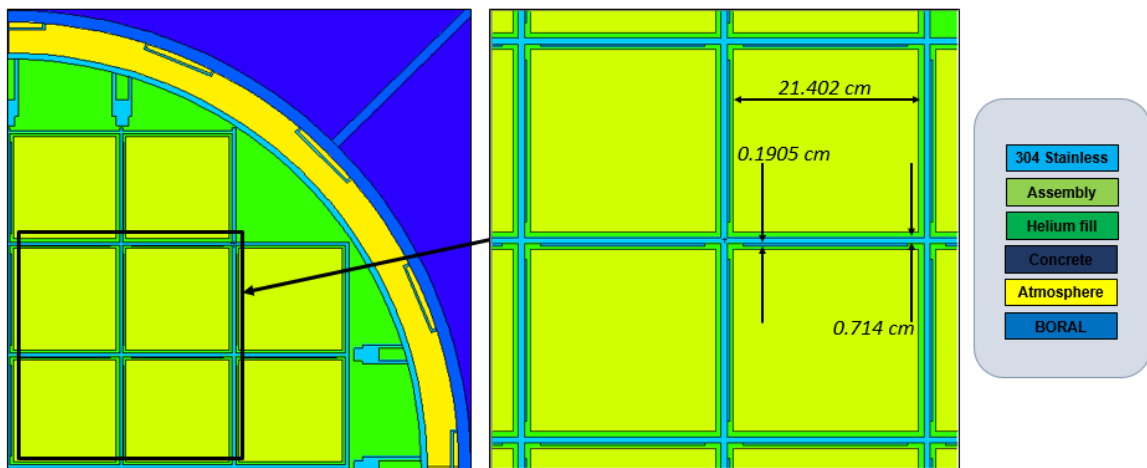


Figure 3.23: MCNP rendered detailed cross section in the XY plane of the MPC-32 basket.

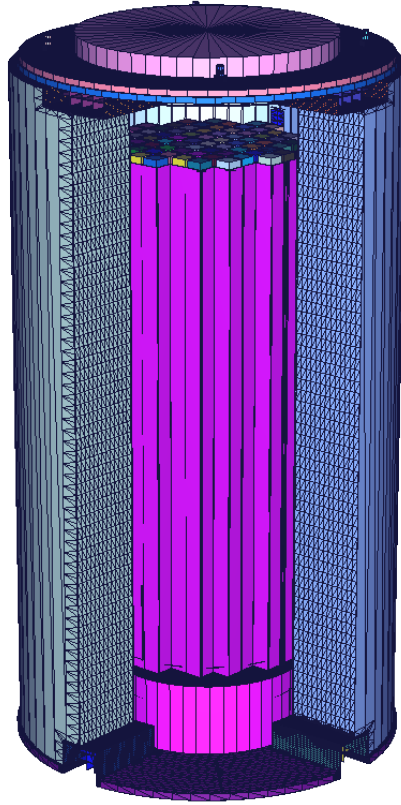


Figure 3.24: MCNP rendering of quartered cutaway of the HI-STORM 100S and MPC-68 as designed in MCNP.

As shown in figure 3.25, the BWR specific MPC-68 canister houses a multitude of smaller BWR assemblies packed closely together. Much like the MPC-32, BORAL sheets are not indexed on the outermost faces of the 304 stainless steel basket. Due to the complexity of this model, 1/8 symmetry was used in the case of BORAL plates in order to define them in an efficient manner within the boolean geometry of the MCNP input deck. By comparison, the MPC-68 hosts many basket supports between the basket and the inner surface of the multi-purpose canister wall. With few exceptions, assemblies are centered identically within each honeycomb basket channel. Figure 3.26 shows the orientation of BORAL sheets within a section of the MPC-68 basket. For each cell completely surrounded by other channels, each side hosts a BORAL plate.

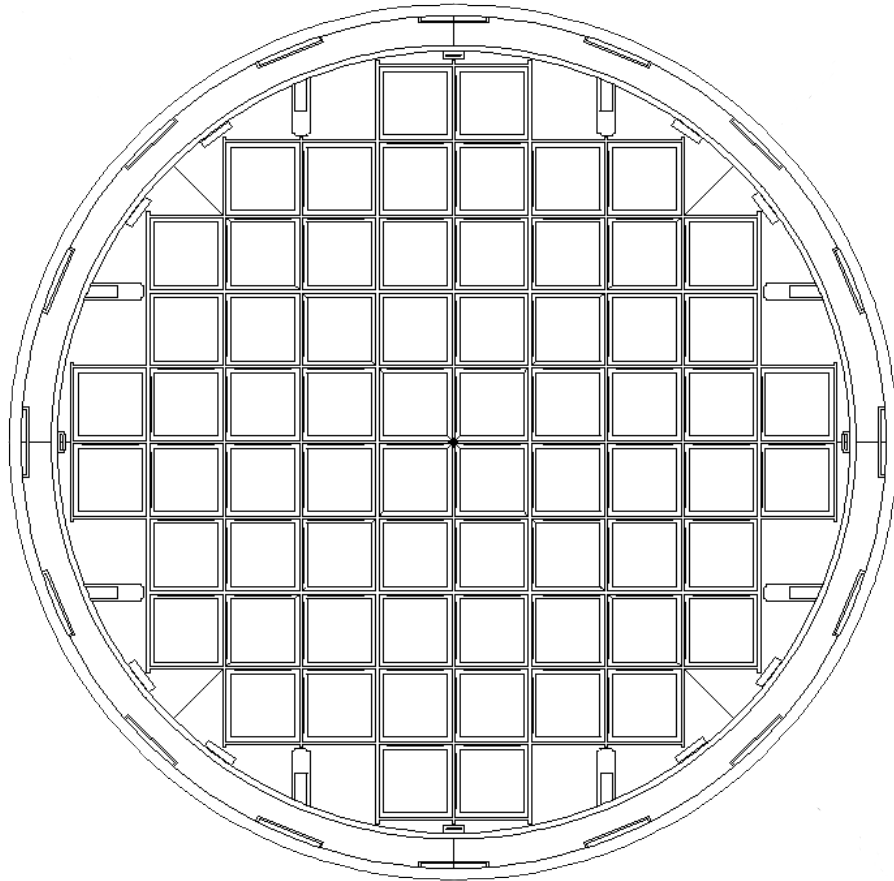


Figure 3.25: MCNP rendered cross section in the XY plane of the MPC-68 canister and the open annulus space.

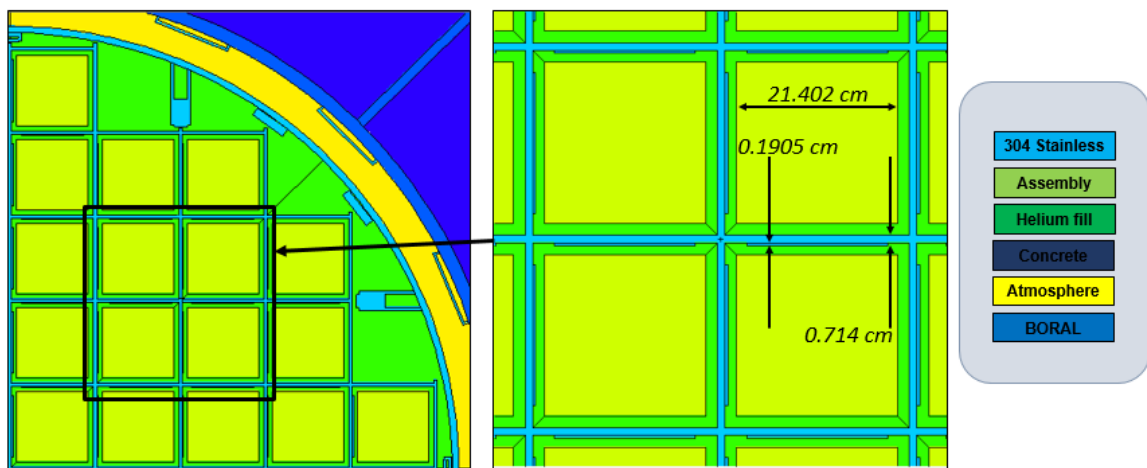


Figure 3.26: MCNP rendered detailed cross section in the XY plane of the MPC-68 basket.

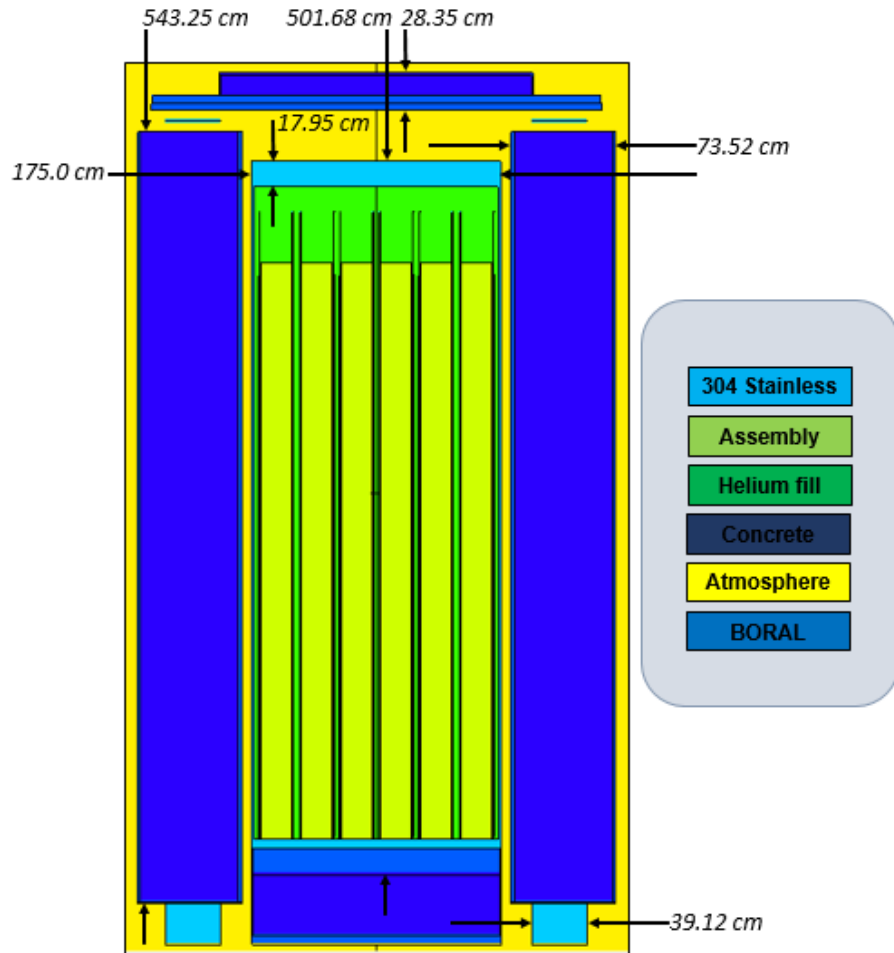


Figure 3.27: MCNP rendered detailed cross section in the XZ plane of the MPC-24E basket and HI-STORM 100S METCON.

The vertical cross section of the HI-STORM 100S METCON paired with the MPC-24 is shown in figure 3.27. Due to the interchangeability of the system, external measurements for the multi-purpose canister are indistinguishable for different canisters. As is shown, the gamma cross plates are installed within both the inlet and outlet vents. Measurements are given for the geometry in MCNP.

3.7 MCNP MATERIALS

In order to define physical cells defined by boolean geometry, MCNP utilizes material cards in order to generate a homogeneous fill material to occupy the mentioned cell. The user is presented with the ability to define a homogeneous media on a by element basis, where MCNP references given cross section data for the selected ENDF/B-VII database at the given weight percent at a density to be prescribed on a cell by cell basis. Materials were defined with use of continuous data sets, noted in MCNP input with the C suffix. These material cards allow independent generation of a material, however standardized material specification is available due to their required use. The primary resource utilized within this work has been both the NRC released Holtec HI-STORM 100 FSAR and a PNNL MCNP material database.[7][32]

3.8 MCNP MODEL ASSUMPTIONS

This research makes some assumptions and simplifications of geometry to facilitate a finely modeled geometry that is also justifiable in time expenditure related to the modeled geometry. With regards to geometry within the multipurpose canister, the basket scallops shown within figure 2.11 were not modeled. However, careful consideration was taken to indexing the BORAL plates with the vertical offsets shown within the FSAR and visible within figure 2.11. The BORAL plates modeled within each model were simplified to a homogeneous structure as was done in the HI-STAR FSAR. In reality, plates like the METAMIC design are a heterogeneous sandwich of Type 1 ASTM C-750 graded B_4C powder between 6061 Aluminum plates. For thermal considerations, anodized METAMIC will be more emissive and contribute more to heat transfer, but the impact on radiation transport of an anodization thin oxide layer is irrelevant. The Boron loading of both BORAL and METAMIC are nearly indistinguishable in atom density of the neutron absorber, and are considered to be

Table 3.10: The following tables detail the elemental breakdown of materials used within the models described.

Material	ZAID	wt%	Isotope
Concrete, Lid $\rho = 2.35 \frac{gm}{cm^3}$	1001.70C	0.006	^1H
	8016.70C	0.50	^{16}O
	14000.50C	0.315	Nat. Si
	13027.50C	0.048	^{27}Al
	11023.50C	0.017	^{23}Na
	20000.50C	0.083	Nat. Ca
	26000.55C	0.012	Nat. Fe
	19000.50C	0.019	Nat. K
Carbon Steel $\rho = 7.82 \frac{gm}{cm^3}$	6000.70C	0.0026	Nat. C
	15031.50C	0.0004	^{31}P
	16000.62C	0.0005	Nat. S
	25055.70C	0.0075	^{55}Mn
	26000.55C	0.987	Nat. Fe
	29000.50C	0.002	Nat. Cu
304 Stainless $\rho = 7.92 \frac{gm}{cm^3}$	24000.50C	0.19	Nat. Cr
	25055.70C	0.02	^{55}Mn
	26000.55C	0.695	Nat. Fe
	28000.50C	0.095	Nat. Ni
NS4R Shielding $\rho = 1.693 \frac{gm}{cm^3}$	1001.70C	0.0594	^1H
	5010.70C	0.00143	^{10}B
	5011.70C	0.00639	^{11}B
	6000.70C	0.2719	Nat. C
	7014.70C	0.01942	^{14}N
	7015.70C	0.00008	^{15}N
	13027.50C	0.2146	^{27}Al
Helium gas $\rho = 0.000164 \frac{gm}{cm^3}$	2004.50C	0.99999866	^4He
	2003.50C	0.00000134	^3He
NaI Detector	11023.70C	0.15337	^{23}Na
	53127.70C	0.84663	^{127}I

Table 3.11: Continued from table 3.10.

Homogeneous W17[7] $\rho = 3.26 \frac{gm}{cm^3}$	40000.57C	0.034312	Nat. Zr
	8016.70C	0.114451	¹⁶ O
	92235.70C	0.00824	²³⁵ U
	92236.70C	0.004009	²³⁶ U
	92238.70C	0.838988	²³⁸ U
Air, Dry $\rho = 0.001205 \frac{gm}{cm^3}$	6000.70C	0.000124	Nat. C
	7014.70C	0.755268	¹⁴ N
	8016.70C	0.231781	¹⁶ O
	18000.35C	0.012827	Nat. Ar
Polyethylene $\rho = 0.93 \frac{gm}{cm^3}$	1001.70C	0.143716	¹ H
	6000.70C	0.856284	Nat. C
Cobalt $\rho = 8.86 \frac{gm}{cm^3}$	27059.60C	1	Nat. Co
Silicon $\rho = 2.329 \frac{gm}{cm^3}$	14000.42C	1	Nat. Si
BORAL[7][20] $\rho = 2.644 \frac{gm}{cm^3}$	5010.70C	0.044226	¹⁰ B
	5011.42C	0.201474	¹¹ B
	13027.70C	0.6861	²⁷ Al
	6000.70C	0.0682	Nat. C
ZIRLO[12] $\rho = 6.5 \frac{gm}{cm^3}$	50000.40C	0.01	Nat. Sn
	41093.24C	0.01	⁹³ Nb
	26000.55C	0.001	Nat. Fe
	8016.70C	0.00125	¹⁶ O
	40000.57C	0.97775	Nat. Zr
UO ₂ $\rho = 10.97 \frac{gm}{cm^3}$	92234.70C	0.00010166	²³⁴ U
	92235.70C	0.00998899	²³⁵ U
	92238.70C	0.32324266	²³⁸ U
	8016.70C	0.66666666	¹⁶ O
Concrete, Body[26] $\rho = 2.48 \frac{gm}{cm^3}$	1001.70C	0.00569	¹ H
	8016.70C	0.49884	¹⁶ O
	14000.50C	0.31594	Nat. Si
	13027.50C	0.04814	²⁷ Al
	11023.50C	0.01705	²³ Na
	20000.50C	0.08325	Nat. Ca
	26000.55C	0.01204	Nat. Fe
	19000.50C	0.01905	Nat. K

Table 3.12: Continued from table 3.11.

INCONEL, Alloy 718	28000.50C	0.5	Nat. Ni
$\rho = 8.1932 \frac{gm}{cm^3}$	24000.50C	0.17	Nat. Cr
	26000.55C	0.22484	Nat. Fe
	42000.42C	0.028	Nat. Mo
	41093.24C	0.0475	⁹³ Nb
	27059.60C	0.01	⁵⁹ Co
	25055.70C	0.02	⁵⁵ Mn
	29000.50C	0.002	Nat. Cu
	13027.24C	0.0065	²⁷ Al
	22000.42C	0.003	Nat. Ti
	14000.42C	0.0035	Nat. Si
	16000.62C	0.00015	Nat. S
	15031.24C	0.00015	³¹ P
	5010.70C	0.00001194	¹⁰ B
	5011.70C	0.00004806	¹¹ B

one and the same in the MCNP model. Within the MPC, homogeneous fuel regions are modeled in lieu of a pin by pin geometry for each assembly. This is standard practice for dosimetric evaluation of spent fuel storage, and greatly simplifies boolean models with little loss in fidelity of surface averaged dose rate.

In the case of BWR assemblies, lift handles were omitted from the MCNP model. The penetrations known to exist in the top portion of the MPC lid were omitted due to the knowledge that they are threaded and occupied with large bolts. With regards to the concrete within the METCON, distinction is made between the elemental composition of the concrete within the lid and shell as suggested by the FSAR. However, these material cards are homogeneous in nature, and do not consider porosity or aggregate within the concrete housed between stainless steel sheathing of the METCON. Considering a 2 MeV γ -ray in standard concrete, it would have a mean free path of approximately 4 cm. This means that the path from the internal to external surface of the METCON accounts for about 17 mean free paths for a relatively high energy γ -ray.

External to the METCON, any layer of anti corrosion paint is neglected from the model geometry. Both the inlet and outlet vents have fine 0.01 gauge screens for the purpose of isolating foreign biological matter or contaminants from the annular environment of the spent fuel storage cask, these are neglected within our model. The rationale behind this centers around the fact that they would by necessity be removed during special interaction with the vents in order to deploy the robotic probe. Therefore, relevant dosimetry would necessitate them being excluded.

3.9 MCNP VENT TALLYING

For the purpose of dose rate evaluation external to the spent fuel storage cask in $\frac{Rem}{hr}$, a set of F5 detector tallies are arranged in and around the vicinity of the inlet and outlet vent mouths. This tallying method differs from a standard F4 tally through consideration of a spherical detector volume as opposed to an arbitrarily defined F4 volume. The operation of the tally is defined by the following equation.

Detector Tally:

$$F5 = \int_E dE \int_t dt \int_\omega d\omega \cdot \psi(\vec{r}, \omega, E, t), \frac{1}{cm^2} \quad (3.8)$$

For reference, figure 3.29 labels both the inlet and outlet vents of the Holtec HI-STORM design with focus on the dynamics of natural circulation cooling within the annulus of the spent fuel storage cask.

3.10 RESPONSE FUNCTIONS

MCNP6 provides a Monte Carlo approximation of 3-dimensional particle transport, and the general output of an unmodified tally is generally $\frac{1}{cm^2}$. Typically, this probability of passing through this "gate" is modified by the frequency of particle emission, in our case, source strength in $\frac{particle}{sec}$. Further, it is useful to transform $\frac{particle}{cm^2 \cdot sec}$ to some quantity. This is done via way of a dose response function, which is an energy binned

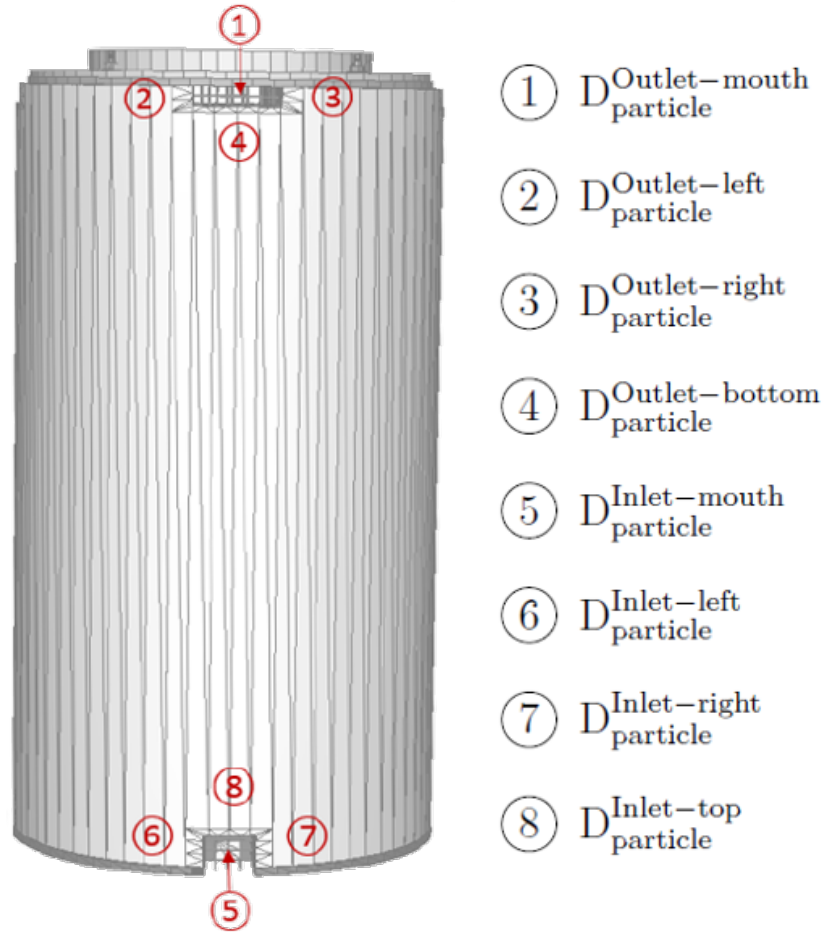


Figure 3.28: The photon and neutron dose is detailed within the vicinity of both the inlet and outlet vents for the HI-STORM 100S. Results are detailed as show for their corresponding points and expressed in units of Rem/hr taken from a 3 cm radius F5 tally.

transform of flux to dose. Those utilized within this project are detailed below. This response function shown within table 3.17 is utilized as a validation mechanism for the JPL photon flux to dose response function.

3.11 NEUTRON-PHOTON COUPLED TRANSPORT

For the majority of the results presented for this work, generation of photon flux as a result of neutron interactions was treated with the default MCNP approximation of

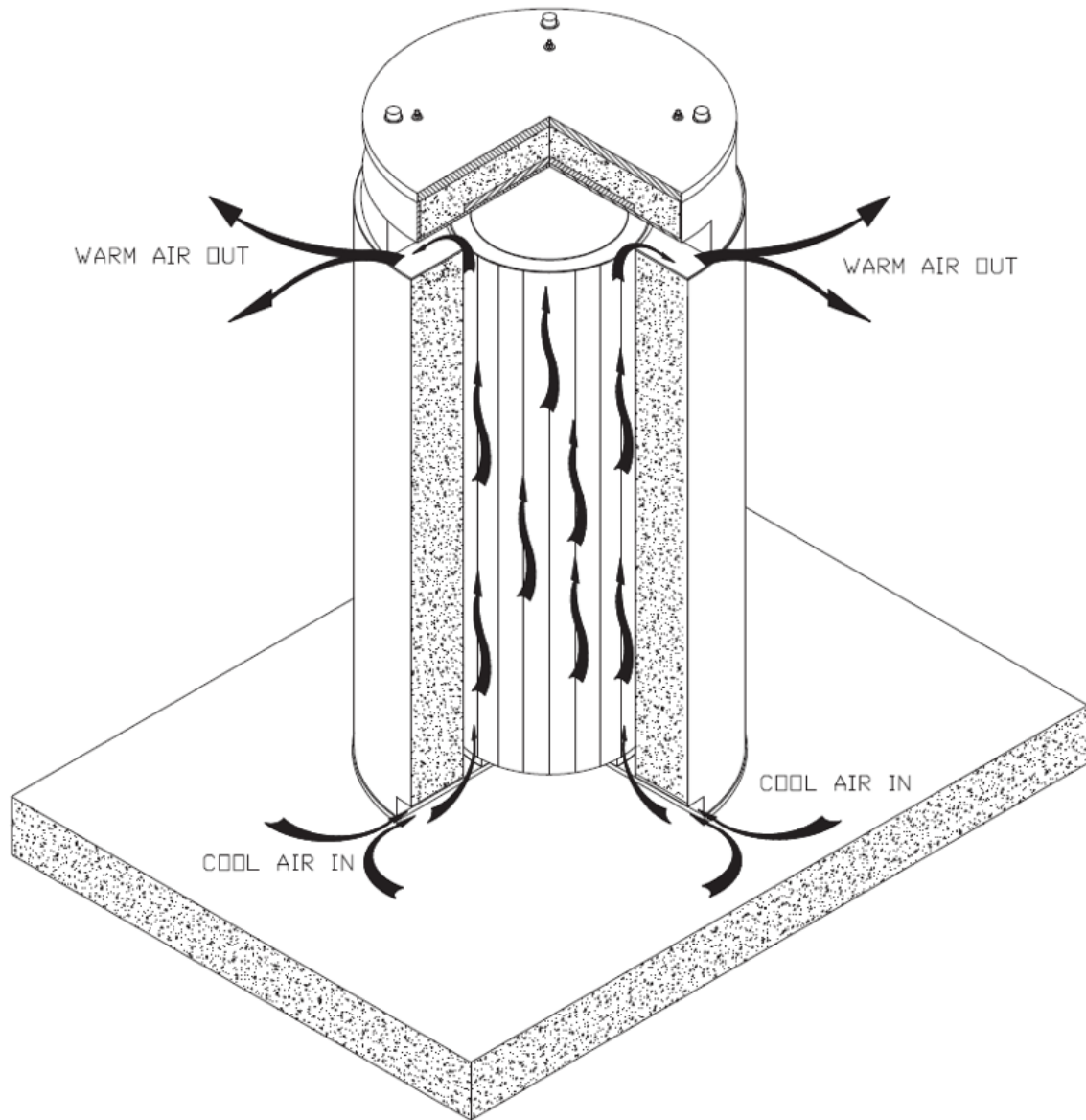


Figure 3.29: The annular thermosiphon developed by way of axial channels and natural circulation.

Table 3.13: This details the ANSI 6.1.1 1977 flux to dose response function utilized to derive Rem/hr from neutron flux tallies.[22]

Neutron Energy (MeV)	Conversion Factors (Rem/hr)/(n/cm ² .sec)
2.50E-08	3.67E-06
1.00E-07	3.67E-06
1.00E-06	4.46E-06
1.00E-05	4.54E-06
1.00E-04	4.18E-06
1.00E-03	3.76E-06
1.00E-02	3.56E-06
1.00E-01	2.17E-05
5.00E-01	9.26E-05
1.0	1.32E-04
2.5	1.25E-04
5.0	1.56E-04
7.0	1.47E-04
10.0	1.47E-04
14.0	2.08E-04
20.0	2.27E-04

local deposition. However, for the case of a MPC-24 housed in a 100S and cooled for a period of 25 years, the coupled neutron-photon flux is compared to a pure photon transport simulation. This is an example case for the purpose of evaluation of coupled neutron and photon flux. This considers capture γ -rays, where activation gamma is considered a minimal level concern for dose outside of the METCON due to low primary neutron source intensity.[9]

As can be observed within table 3.19, the impact of coupling neutron and photon transport is minimal within the annular space. As may be expected, neutron production of photons becomes more prominent where the native photon flux is lowest. External to the METCON, the contributions of neutron bred photons becomes noticeable, however native photon flux still overwhelms neutron produced photons.

Table 3.14: This details the ANSI 6.1.1 1977 flux to dose response function utilized to derive Rem/hr from photon flux tallies.[22]

Photon Energy (MeV)	Conversion Factors (Rem/hr)/(p/cm ² ·sec)
0.01	3.96E-06
0.03	5.82E-07
0.05	2.90E-07
0.07	2.58E-07
0.1	2.83E-07
0.15	3.79E-07
0.2	5.01E-07
0.25	6.31E-07
0.3	7.59E-07
0.35	8.78E-07
0.4	9.85E-07
0.45	1.08E-06
0.5	1.17E-06
0.55	1.27E-06
0.6	1.36E-06
0.65	1.44E-06
0.7	1.52E-06
0.8	1.68E-06
1	1.98E-06
1.4	2.51E-06
1.8	2.99E-06
2.2	3.42E-06
2.6	3.82E-06
2.8	4.01E-06
3.25	4.41E-06
3.75	4.83E-06
4.25	5.23E-06
4.75	5.60E-06
5	5.80E-06
5.25	6.01E-06
5.75	6.37E-06
6.25	6.74E-06
6.75	7.11E-06
7.5	7.66E-06
9	8.77E-06
11	1.03E-05
13	1.18E-05
15	1.33E-05

Table 3.15: This details the JPL flux to dose response function utilized to derive Rad(Si)/sec from neutron flux tallies.[29]

Neutron Energy (MeV)	Conversion Factor (Rad(Si))/(n/cm ²)
0.045	1.00E-12
0.065	1.10E-12
0.1	1.0-12
0.15	5.00E-13
0.2	1.70E-11
0.3	1.00E-11
0.45	1.10E-11
0.65	1.70E-11
1	2.00E-11
1.5	2.70E-11
2	3.20E-11
3	5.60E-11
4.5	8.40E-11
6.5	6.00E-10
10	1.00E-09
15	7.00E-10

Neutron attenuation within the cask shielding will occur through neutron scattering and neutron capture resulting in prompt secondary γ -ray emission.[9] The majority of capture gamma sources are typically found inside of the multi-purpose canister, in the fuel region. The information in table 3.20 provides explanation of the data methods used in MCNP photon runs beyond the data label and output units. This information details the tally type and any further information unique to the individual tally. Similarly, table 3.21 provides explanation of the data methods used in MCNP neutron runs. For all photon results, the dose rate derived from mass attenuation coefficients is compared to that derived from a dose function as described. The data derived from a flux to dose conversion function is labeled with DF. Unique to the case of neutron transport data, the first tally in the output tables is a cobalt activation rate as opposed to a predicted dose rate on the multi-purpose canister.

Table 3.16: This details the JPL flux to dose response function utilized to derive Rad(Si)/sec from photon flux tallies.[29]

Photon Energy (MeV)	Conversion Factor Rad(Si)/(photon/cm ²)
0.01	5.35E-09
0.015	2.10E-09
0.02	1.10E-09
0.03	5.00E-10
0.045	2.35E-10
0.065	1.31E-10
0.1	7.35E-11
0.15	7.49E-11
0.2	9.37E-11
0.3	1.47E-10
0.45	2.15E-10
0.65	3.06E-10
1	4.43E-10
1.5	6.07E-10
2	7.70E-10
3	1.05E-09
4.5	1.45E-09
6.5	1.88E-09
10	2.60E-09
15	4.18E-09
20	5.54E-09
30	8.40E-09

Table 3.17: This is a function taken from the mass energy attenuation coefficient. From it, a flux to dose response function was utilized to derive Rad(Si)/sec from photon flux tallies.[26]

Photon Energy (MeV)	$\frac{\mu_{en}}{\rho}$ (cm^2/gm)
1.00E-03	1.57E+03
1.50E-03	5.33E+02
1.84E-03	3.07E+02
1.84E-03	3.06E+03
2.00E-03	2.67E+03
3.00E-03	9.52E+02
4.00E-03	4.43E+02
5.00E-03	2.40E+02
6.00E-03	1.44E+02
8.00E-03	6.31E+01
1.00E-02	3.29E+01
1.50E-02	9.79E+00
2.00E-02	4.08E+00
3.00E-02	1.16E+00
4.00E-02	4.78E-01
5.00E-02	2.43E-01
6.00E-02	1.43E-01
8.00E-02	6.90E-02
1.00E-01	4.51E-02
1.50E-01	3.09E-02
2.00E-01	2.91E-02
3.00E-01	2.93E-02
4.00E-01	2.97E-02
5.00E-01	2.97E-02
6.00E-01	2.95E-02
8.00E-01	2.88E-02
1.00E+00	2.78E-02
1.25E+00	2.65E-02
1.50E+00	2.54E-02
2.00E+00	2.35E-02
3.00E+00	2.10E-02
4.00E+00	1.96E-02
5.00E+00	1.88E-02
6.00E+00	1.83E-02
8.00E+00	1.77E-02
1.00E+01	1.75E-02
1.50E+01	1.75E-02
2.00E+01	1.76E-02

Table 3.18: Photon results for coupled neutron-photon transport data of the HI-STORM 100S and MPC-24, populated with Westinghouse 17x17 assemblies enriched to 3.5%, with an ORIGAMI axial emission profile, a discharge burnup of 57.535 $\frac{MWd}{kg}$, and cooled for 25yr.

Tally	Out	RE	Units
P: Si Dose, MPC Wall	4.5207E+06	0.0011	Rad(Si)/hr
P: Si Dose, MPC Wall, DF	8.1867E-02	0.0010	Rad(Si)/hr
P: Flux, MPC Wall	4.2779E+04	0.0008	photon/cm ² .sec
P: Flux, METCON Wall	5.9164E+02	0.0029	photon/cm ² .sec
P: Dose, outlet vent	7.1441E-04	0.0458	Rem/hr
P: Dose, inlet vent	4.3458E-04	0.0637	Rem/hr
P: Dose, METCON Wall	1.6611E-03	0.0033	Rem/hr
P: Dose, MPC Lid	6.6387E-03	0.0127	Rad(Si)/hr
P: Flux, MPC Lid	2.9883E+03	0.0094	photon/cm ² .sec
P: Dose, w/o Pb shield	1.0899E-01	0.0346	Rad(Si)/hr
P: Dose, 4-side Pb shield	7.3296E-02	0.0347	Rad(Si)/hr
P: Dose, 6-side Pb Shield	6.4787E-02	0.0395	Rad(Si)/hr
P: Dose, METCON ext. 15cm	2.2050E-04	0.0302	Rem/hr
P: Dose, METCON ext. 45cm	1.7333E-04	0.0150	Rem/hr
P: Dose, METCON ext. 75cm	1.7308E-04	0.0116	Rem/hr
P: Dose, METCON ext. 105cm	1.7316E-04	0.0180	Rem/hr

Table 3.19: Photon results for comparison to the nominal photon source case values for the same system, where the NP run results are given as a percentage of the nominal photon source case values.

Tally	Out [% Nominal]	RE, NP	Units
P: Si Dose, MPC Wall, DF	0.00%	0.0010	Rad(Si)/hr
P: Flux, MPC Wall	0.00%	0.0008	photon/cm ² .sec
P: Flux, METCON Wall	15.99%	0.0029	photon/cm ² .sec
P: Dose, outlet vent	16.00%	0.0458	Rem/hr
P: Dose, inlet vent	13.00%	0.0637	Rem/hr
P: Dose, METCON Wall	41.17%	0.0033	Rem/hr
P: Dose, MPC Lid	1.52%	0.0127	Rad(Si)/hr
P: Flux, MPC Lid	0.24%	0.0094	photon/cm ² .sec
P: Dose, w/o Pb shield	0.01%	0.0346	Rad(Si)/hr
P: Dose, 4-side Pb shield	0.01%	0.0347	Rad(Si)/hr
P: Dose, 6-side Pb Shield	0.01%	0.0395	Rad(Si)/hr
P: Dose, METCON ext. 15cm	8.33%	0.0302	Rem/hr
P: Dose, METCON ext. 45cm	3.98%	0.0150	Rem/hr
P: Dose, METCON ext. 75cm	4.68%	0.0116	Rem/hr
P: Dose, METCON ext. 105cm	5.83%	0.0180	Rem/hr

Table 3.20: Explanation of individual photon tallies considered within separate MCNP cases.

Tally Description	No.	Description
P: Si Dose, MPC Wall	F112	F2 surface tally on the MPC wall, modified with mass attenuation coefficients
P: Si Dose, MPC Wall, DF	F132	F2 surface tally on the MPC wall, modified with dose function
P: Flux, MPC Wall	F152	F2 surface tally on the MPC wall
P: Flux, METCON Wall	F162	F2 surface tally on the METCON wall
P: Dose, outlet vent	F195	F5 detector tally, 3cm in radius, located 5cm inside the vent mouth
P: Dose, inlet ven4t	F205	F5 detector tally, 3cm in radius, located 5cm inside the vent mouth
P: Dose, METCON Wall	F212	F2 surface tally on the METCON wall, modified with dose function
P: Dose, MPC Lid	F222	F2 surface tally on the MPC lid, modified with dose function
P: Flux, MPC Lid	F302	F2 surface tally on the MPC lid
P: Dose, left outlet	F405	F5 detector tally, 3cm in radius, 15cm left of vent mouth
P: Dose, right outlet	F415	F5 detector tally, 3cm in radius, 15cm right of vent mouth
P: Dose, bottom outlet	F425	F5 detector tally, 3cm in radius, 15cm below of vent mouth
P: Dose, left inlet	F435	F5 detector tally, 3cm in radius, 15cm left of vent mouth
P: Dose, right inlet	F445	F5 detector tally, 3cm in radius, 15cm right of vent mouth
P: Dose, above inlet	F455	F5 detector tally, 3cm in radius, 15cm above vent mouth
P: Dose, w/o Pb shield	F684	F4 volume tally, in annulus of canister
P: Dose, 4-side Pb shield	F694	F4 volume tally, with 4-side 5mm Pb sheets, in annulus of canister
P: Dose, 6-side Pb Shield	F704	F4 volume tally, with 6-side 5mm Pb sheets, in annulus of canister
P: Dose, METCON ext. 15cm	F815	F5 detector tally, 30cm in radius, 15cm outside of inlet vent
P: Dose, METCON ext. 45cm	F825	F5 detector tally, 30cm in radius, 45cm outside of inlet vent
P: Dose, METCON ext. 75cm	F835	F5 detector tally, 30cm in radius, 75cm outside of inlet vent
P: Dose, METCON ext. 105cm	F845	F5 detector tally, 30cm in radius, 105cm outside of inlet vent

Table 3.21: Explanation of individual neutron tallies considered within separate MCNP cases.

Tally Description	No.	Description
N: Co-60 Activation	F12	Modified activation tally on the MPC wall
N: Si Dose, MPC Wall, DF	F22	F2 surface tally on the MPC wall, modified with dose function
N: Dose, outlet vent	F35	F5 detector tally, 3cm in radius, located 5cm inside the vent mouth
N: Dose, inlet vent	F45	F5 detector tally, 3cm in radius, located 5cm inside the vent mouth
N: Dose, METCON Wall	F52	F2 surface tally on the METCON wall, modified with dose function
N: Flux, MPC Wall	F62	F2 surface tally on the MPC wall
N: Flux, METCON Wall	F72	F2 surface tally on the METCON wall
N: Flux, MPC Lid	F282	F2 surface tally on the MPC lid
N: Dose, MPC Lid	F312	F2 surface tally on the MPC lid, modified with dose function
N: Dose, left outlet	F725	F5 detector tally, 3cm in radius, 15cm left of vent mouth
N: Dose, right outlet	F735	F5 detector tally, 3cm in radius, 15cm right of vent mouth
N: Dose, bottom outlet	F745	F5 detector tally, 3cm in radius, 15cm below of vent mouth
N: Dose, left inlet	F755	F5 detector tally, 3cm in radius, 15cm left of vent mouth
N: Dose, right inlet	F765	F5 detector tally, 3cm in radius, 15cm right of vent mouth
N: Dose, above inlet	F775	F5 detector tally, 3cm in radius, 15cm above vent mouth
N: Dose, w/o Pb shield	F784	F4 volume tally, in annulus of canister
N: Dose, 4-side Pb shield	F794	F4 volume tally, with 4-side 5mm Pb sheets, in annulus of canister
N: Dose, 6-side Pb Shield	F804	F4 volume tally, with 6-side 5mm Pb sheets, in annulus of canister
N: Dose, METCON ext. 15cm	F855	F5 detector tally, 30cm in radius, 15cm outside of inlet vent
N: Dose, METCON ext. 45cm	F865	F5 detector tally, 30cm in radius, 45cm outside of inlet vent
N: Dose, METCON ext. 75cm	F875	F5 detector tally, 30cm in radius, 75cm outside of inlet vent
N: Dose, METCON ext. 105cm	F885	F5 detector tally, 30cm in radius, 105cm outside of inlet vent

CHAPTER 4

RESULTS

The following data is separated into unique MCNP runs, and details output results of transported neutrons and photons. These cases represent the three canister variants: MPC-24, MPC-32, and MPC-68. In each case, they are housed within the HI-STORM 100S METCON. Each run considers the standard γ -ray cross plates installed within both the inlet and outlet vents of the METCON. In all cases, the tally is briefly described before output and RE are provided along with appropriate units. Evaluation of radiation dose rate within the annulus of the HI-STORM 100 design constitutes the raison d'être of this research, and as such is the primary consideration of the output.

For the case of all PWR runs, photon and neutron source spectra and strength are uniquely characterized as a function of cooling time. Axial emission profiles generated in ORIGAMI describe photon and neutron emission probability over axial height. These cases represent a modern, high burnup assembly that would constitute a limiting case for radiation dose rates in the cask.

For the case of the BWR specific MPC-68, photon and neutron source spectra are also uniquely characterized as a function of cooling time. ORIGEN-ARP is used for this characterization, and axial emission variation was not modeled. The BWR cases represent a legacy fuel of lower burnup, and offer a comparison case that approximates a less limiting radiation shielding concern.

Table 4.1: The photon transport data for the HI-STORM 100S and MPC-24, populated with Westinghouse 17x17 assemblies enriched to 3.5%, with an ORIGAMI axial emission profile, a discharge burnup of $57.535 \frac{MWd}{kg}$, and cooled for 5yr.

Tally	Out	RE	Units
P: Si Dose, MPC Wall	7.9110E+03	0.0004	Rad(Si)/hr
P: Si Dose, MPC Wall, DF	8.9607E+03	0.0004	Rad(Si)/hr
P: Flux, MPC Wall	1.2543E+10	0.0004	photon/cm ² ·sec
P: Flux, METCON Wall	3.3158E+04	0.1008	photon/cm ² ·sec
P: Dose, outlet vent	1.8159E-02	0.2000	Rem/hr
P: Dose, inlet vent	1.1754E-02	0.1705	Rem/hr
P: Dose, METCON Wall	3.9488E-02	0.1015	Rem/hr
P: Dose, MPC Lid	1.6617E+00	0.0864	Rad(Si)/hr
P: Flux, MPC Lid	4.0640E+06	0.0929	photon/cm ² ·sec
P: Dose, left outlet	9.0879E-05	0.4198	Rem/hr
P: Dose, right outlet	8.1553E-05	0.3438	Rem/hr
P: Dose, bottom outlet	1.3066E-04	0.2495	Rem/hr
P: Dose, left inlet	6.1087E-04	0.4432	Rem/hr
P: Dose, right inlet	8.2179E-04	0.4620	Rem/hr
P: Dose, above inlet	1.0171E-03	0.1933	Rem/hr
P: Dose, w/o Pb shield	7.1024E+03	0.0211	Rad(Si)/hr
P: Dose, 4-side Pb shield	3.1470E+03	0.0326	Rad(Si)/hr
P: Dose, 6-side Pb Shield	2.2794E+03	0.0370	Rad(Si)/hr
P: Dose, METCON ext. 15cm	9.2543E-03	0.2536	Rem/hr
P: Dose, METCON ext. 45cm	9.1917E-03	0.2139	Rem/hr
P: Dose, METCON ext. 75cm	9.5263E-03	0.1878	Rem/hr
P: Dose, METCON ext. 105cm	8.9989E-03	0.1797	Rem/hr

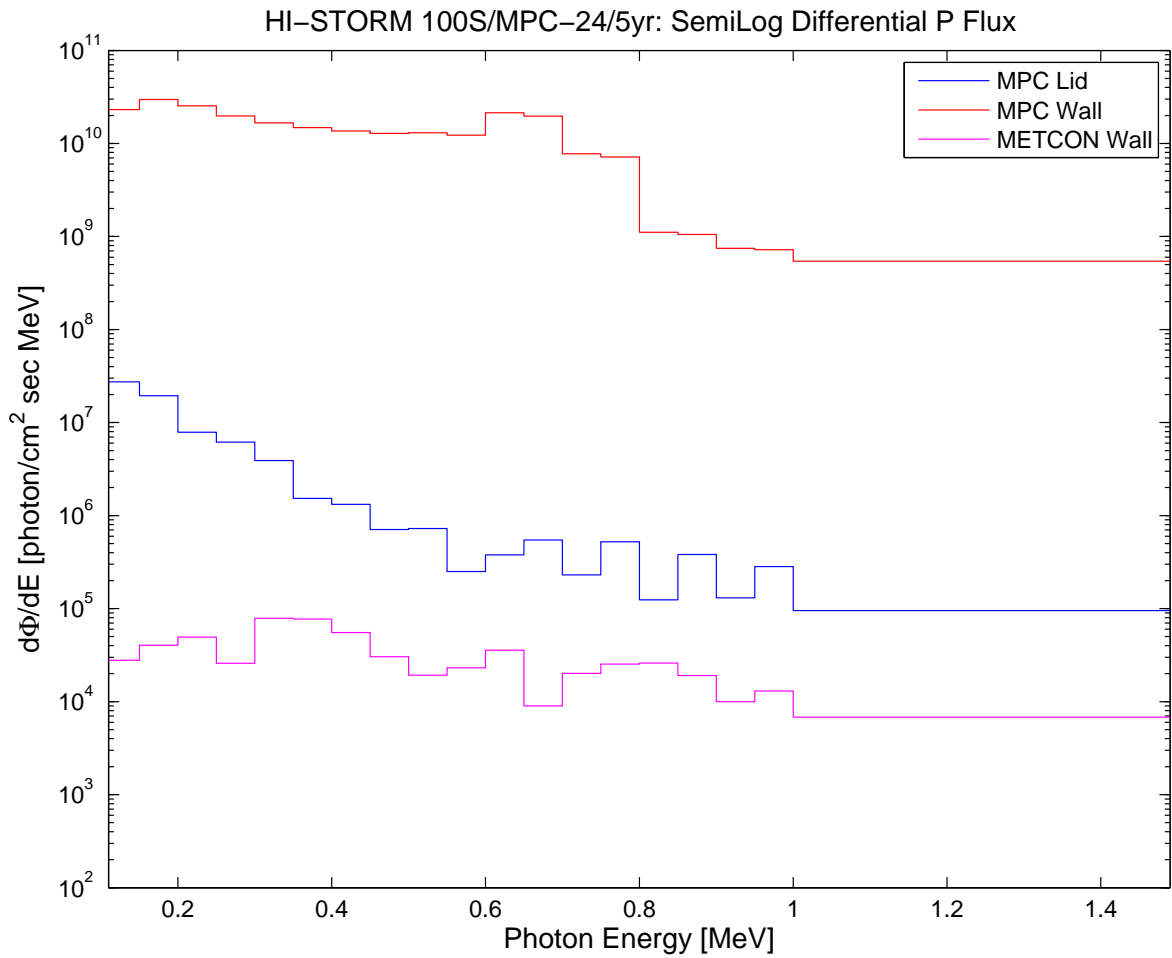


Figure 4.1: The transported photon spectra taken as a surface average for the MPC-24, housed in a 100S METCON, and cooled for 5 yr.

HI-STORM 100S/MPC-24/5yr: P Dose(θ,z), MPC shell in kiloRad(Si)/hr

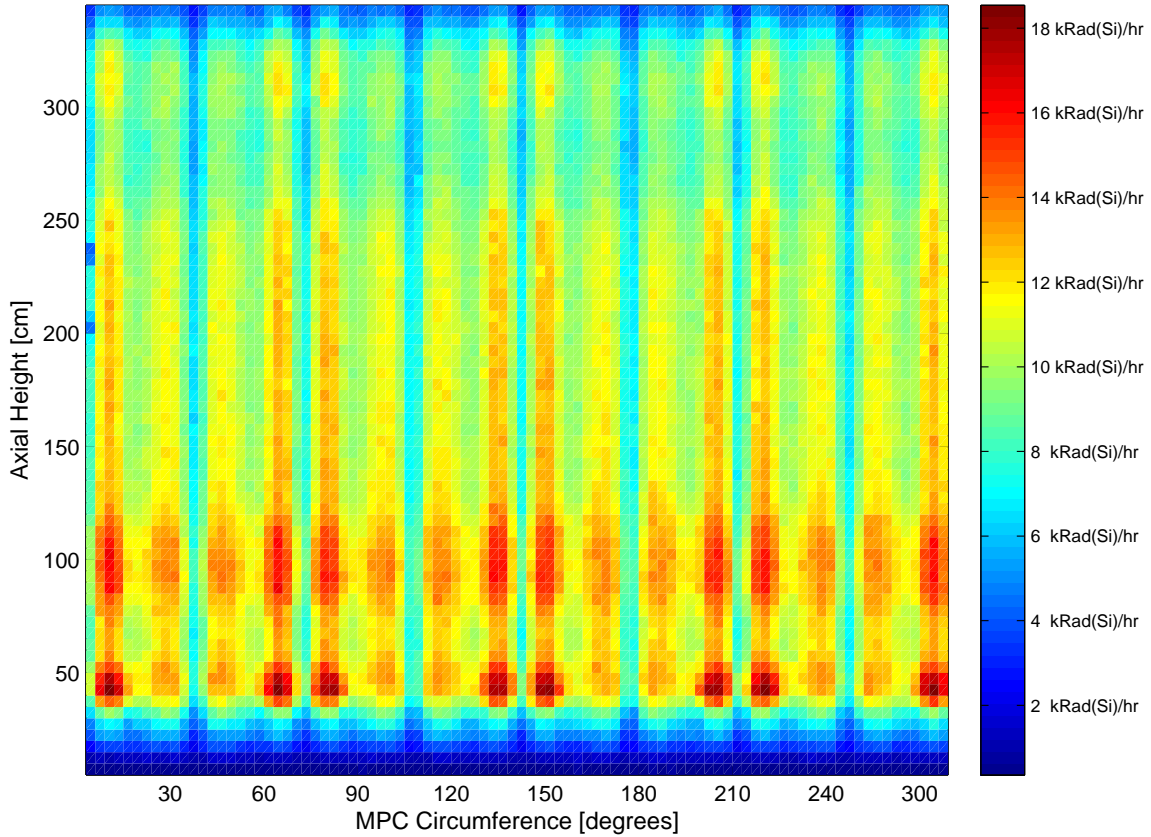


Figure 4.2: The MPC wall photon dose rate for a $6\text{ cm} \cdot 6\text{ cm}$ coaxial FMESH wrapped around the outside of a MPC-24, housed in a 100S METCON, and cooled for 5 yr. The y-axis spans the bottom to the top of the MPC and the x-axis spans 0 to 2π . This details a V.C. Summer cycle of a Westinghouse 17×17 assembly burned to $57.535 \frac{\text{MWd}}{\text{kg}}$ and includes an ORIGAMI 28 zone axial emission profile.

HI-STORM 100S/MPC-24/5yr: P Dose(x,y), MPC Lid in Rad(Si)/hr

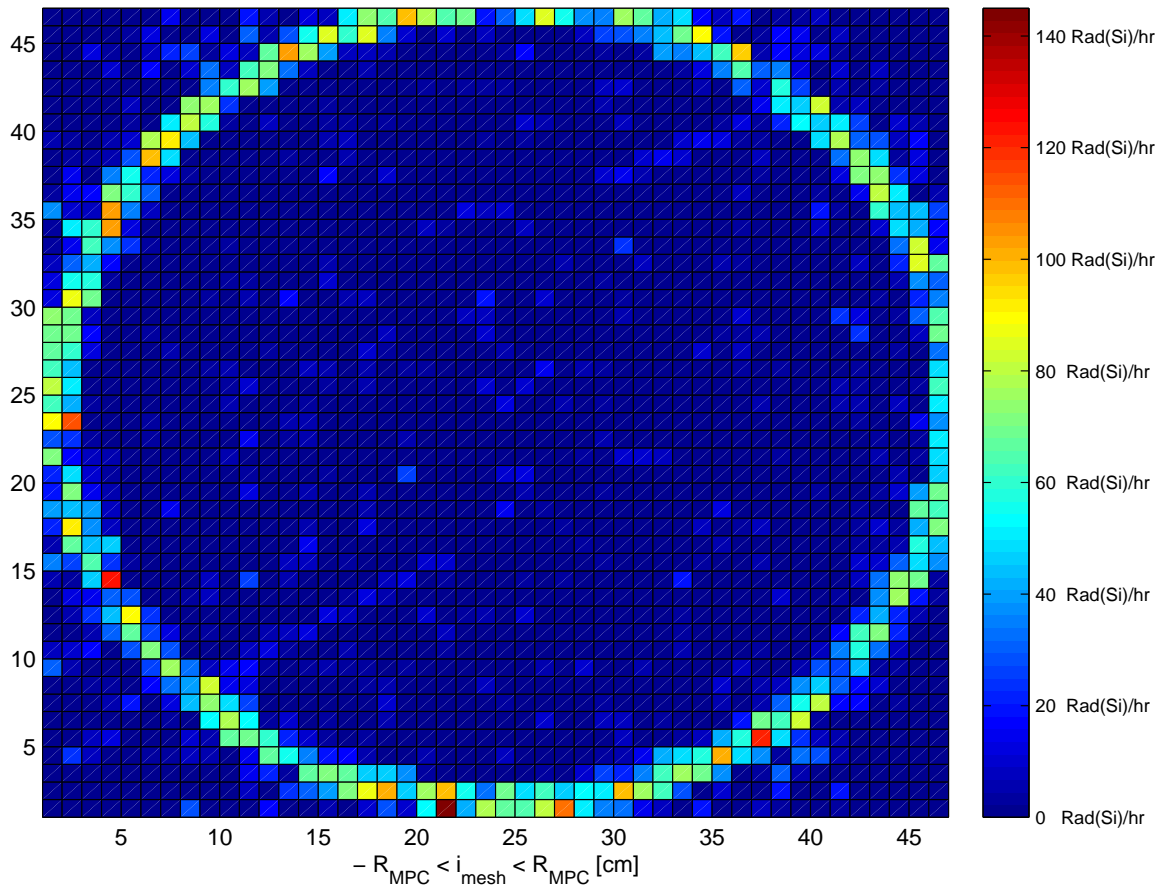


Figure 4.3: The MPC lid photon dose rate for a 45·45 FMESH in a plane at the lid surface for a MPC-24, housed in a 100S METCON, and cooled for 5 yr. Dose is in $\frac{mRad(Si)}{hr}$ for the matrix of 4 cm cells. This is the proposed deployment surface for the delivery system of the robotic instrumentation.

Table 4.2: The photon transport data for the HI-STORM 100S and MPC-24, populated with Westinghouse 17x17 assemblies enriched to 3.5%, with an ORIGAMI axial emission profile, a discharge burnup of $57.535 \frac{MWd}{kg}$, and cooled for 25yr.

Tally	Out	RE	Units
P: Si Dose, MPC Wall	2.1590E+03	0.0004	Rad(Si)/hr
P: Si Dose, MPC Wall, DF	2.4484E+03	0.0004	Rad(Si)/hr
P: Flux, MPC Wall	3.6014E+09	0.0004	photon/cm ² ·sec
P: Flux, METCON Wall	3.7005E+03	0.1666	photon/cm ² ·sec
P: Dose, outlet vent	4.4640E-03	0.3853	Rem/hr
P: Dose, inlet vent	3.3427E-03	0.2766	Rem/hr
P: Dose, METCON Wall	4.0346E-03	0.1750	Rem/hr
P: Dose, MPC Lid	4.3578E-01	0.1000	Rad(Si)/hr
P: Flux, MPC Lid	1.2392E+06	0.1024	photon/cm ² ·sec
P: Dose, left outlet	5.1771E-06	0.4235	Rem/hr
P: Dose, right outlet	9.2683E-05	0.9289	Rem/hr
P: Dose, bottom outlet	4.6385E-06	0.0825	Rem/hr
P: Dose, left inlet	3.1539E-05	0.7974	Rem/hr
P: Dose, right inlet	2.3440E-04	0.9021	Rem/hr
P: Dose, above inlet	4.6171E-04	0.8255	Rem/hr
P: Dose, w/o Pb shield	1.8224E+03	0.0222	Rad(Si)/hr
P: Dose, 4-side Pb shield	7.6926E+02	0.0353	Rad(Si)/hr
P: Dose, 6-side Pb Shield	5.3783E+02	0.0366	Rad(Si)/hr
P: Dose, METCON ext. 15cm	2.6470E-03	0.3167	Rem/hr
P: Dose, METCON ext. 45cm	4.3536E-03	0.4224	Rem/hr
P: Dose, METCON ext. 75cm	3.6943E-03	0.3816	Rem/hr
P: Dose, METCON ext. 105cm	2.9696E-03	0.3382	Rem/hr

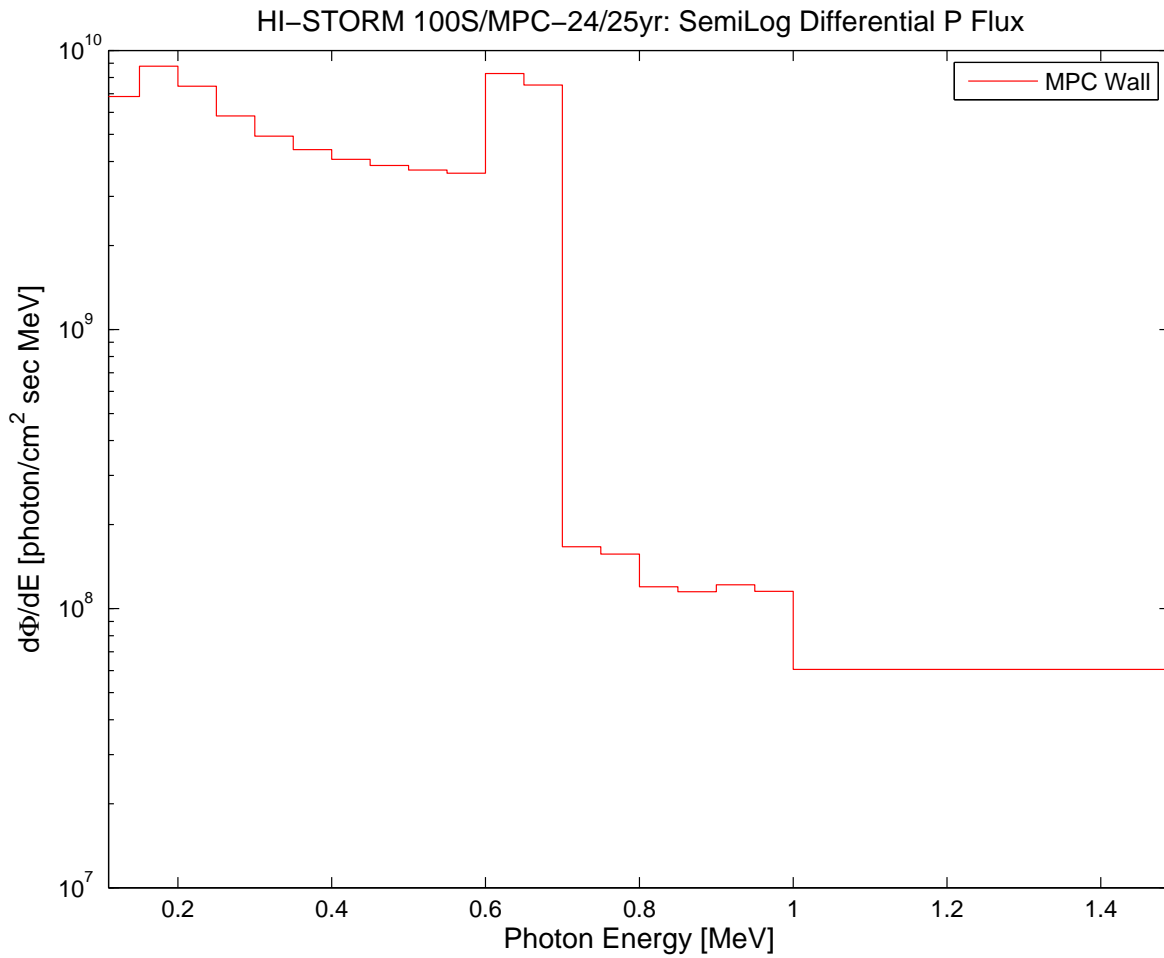


Figure 4.4: The transported photon spectra taken as a surface average for the MPC-24, housed in a 100S METCON, and cooled for 25 yr.

HI-STORM 100S/MPC-24/25yr: P Dose(θ,z), MPC shell in kiloRad(Si)/hr

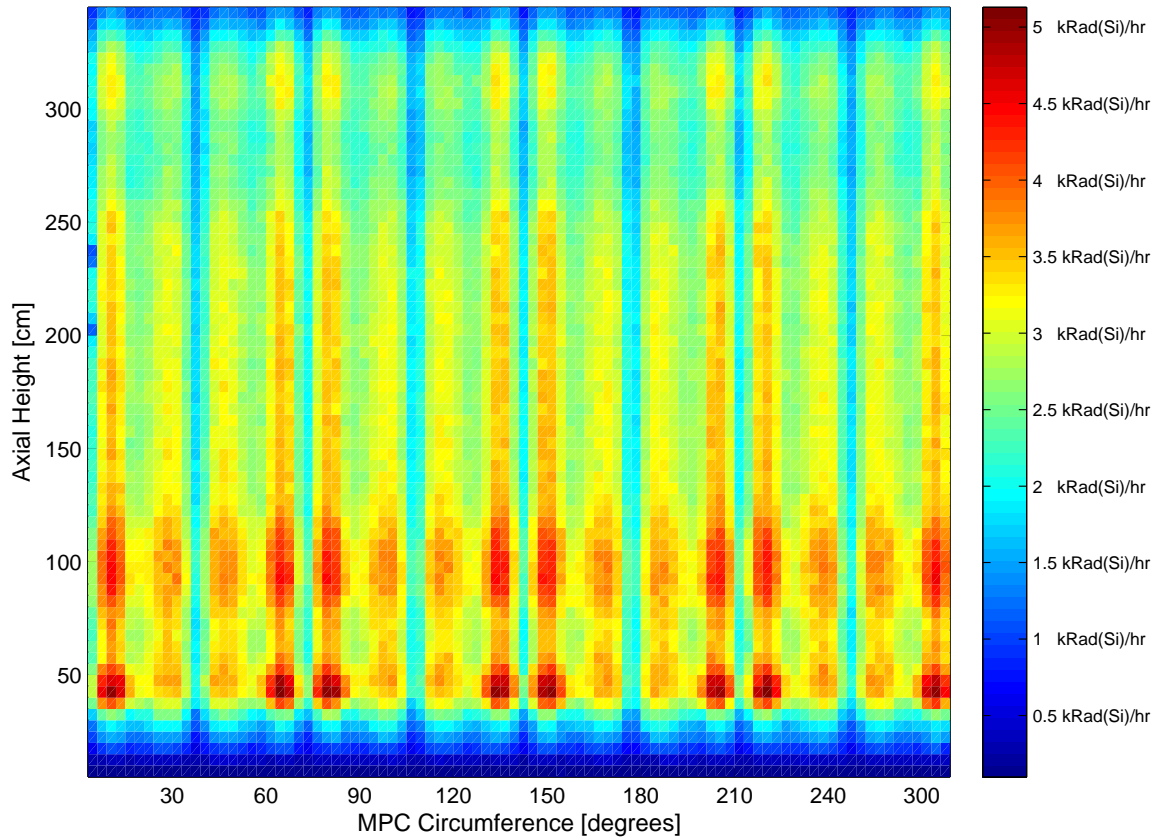


Figure 4.5: The MPC wall photon dose rate for a $6\text{ cm} \cdot 6\text{ cm}$ coaxial FMESH wrapped around the outside of a MPC-24, housed in a 100S METCON, and cooled for 25 yr. The y-axis spans the bottom to the top of the MPC and the x-axis spans 0 to 2π . This details a V.C. Summer cycle of a Westinghouse 17×17 assembly burned to $57.535 \frac{\text{MWd}}{\text{kg}}$ and includes an ORIGAMI 28 zone axial emission profile.

HI-STORM 100S/MPC-24/25yr: P Dose(x,y), MPC Lid in Rad(Si)/hr

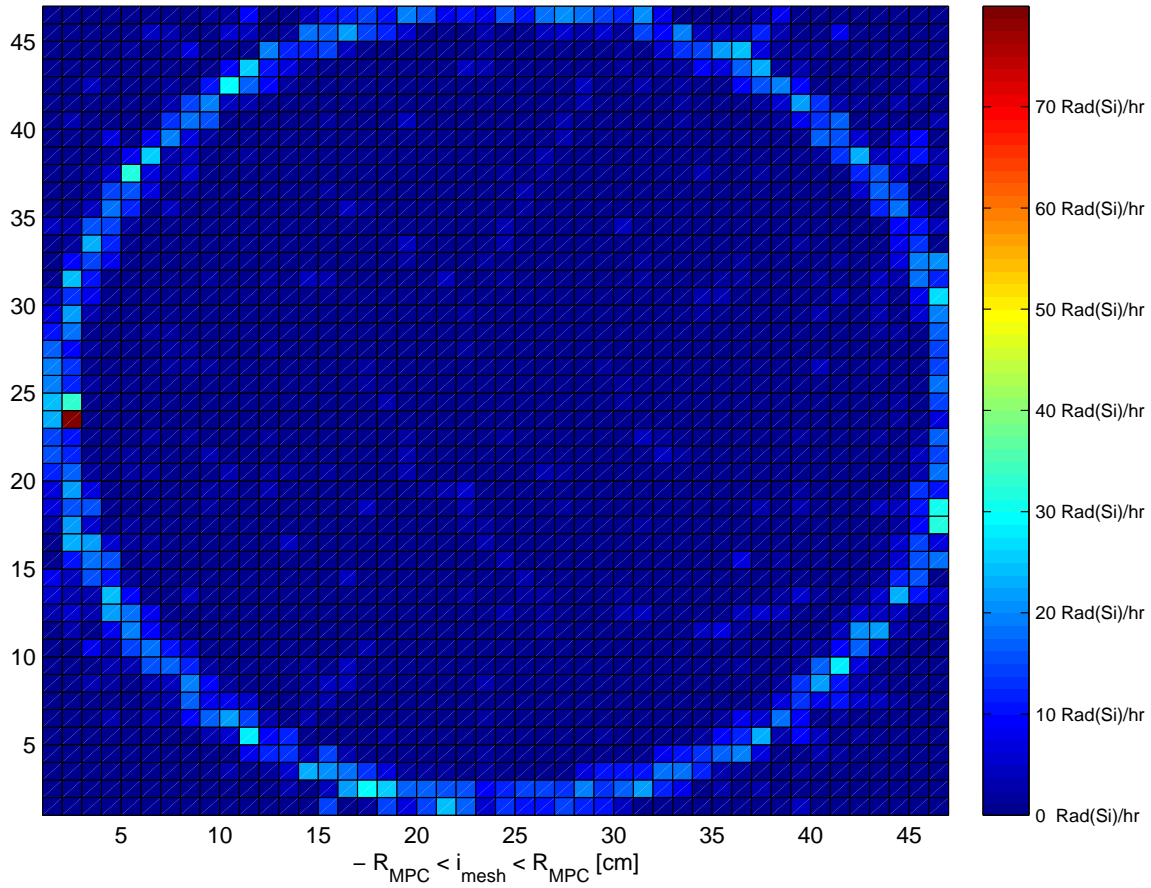


Figure 4.6: The MPC lid photon dose rate for a 45·45 FMESH in a plane at the lid surface for a MPC-24, housed in a 100S METCON, and cooled for 25 yr. Dose is in $\frac{mRad(Si)}{hr}$ for the matrix of 4 cm cells. This is the proposed deployment surface for the delivery system of the robotic instrumentation.

Table 4.3: The photon transport data for the HI-STORM 100S and MPC-32, populated with Westinghouse 17x17 assemblies enriched to 3.5%, with an ORIGAMI axial emission profile, a discharge burnup of $57.535 \frac{MWd}{kg}$, and cooled for 5yr.

Tally	Out	RE	Units
P: Si Dose, MPC Wall	1.2678E+04	0.0002	Rad(Si)/hr
P: Si Dose, MPC Wall, DF	1.4349E+04	0.0002	Rad(Si)/hr
P: Flux, MPC Wall	1.8989E+10	0.0002	photon/cm ² ·sec
P: Flux, METCON Wall	5.4437E+04	0.0728	photon/cm ² ·sec
P: Dose, outlet vent	4.8895E-02	0.0998	Rem/hr
P: Dose, inlet vent	3.6772E-02	0.1614	Rem/hr
P: Dose, METCON Wall	6.3160E-02	0.0737	Rem/hr
P: Dose, MPC Lid	5.2404E+00	0.0322	Rad(Si)/hr
P: Flux, MPC Lid	1.3287E+07	0.0344	photon/cm ² ·sec
P: Dose, left outlet	4.1029E-03	0.8441	Rem/hr
P: Dose, right outlet	7.1717E-04	0.4135	Rem/hr
P: Dose, bottom outlet	1.3247E-03	0.3459	Rem/hr
P: Dose, left inlet	1.2449E-03	0.2427	Rem/hr
P: Dose, right inlet	1.1623E-03	0.2396	Rem/hr
P: Dose, above inlet	2.4104E-03	0.1151	Rem/hr
P: Dose, w/o Pb shield	1.3772E+04	0.0101	Rad(Si)/hr
P: Dose, 4-side Pb shield	6.6186E+03	0.0133	Rad(Si)/hr
P: Dose, 6-side Pb Shield	5.0383E+03	0.0148	Rad(Si)/hr
P: Dose, METCON ext. 15cm	1.5466E-02	0.1303	Rem/hr
P: Dose, METCON ext. 45cm	1.7092E-02	0.0882	Rem/hr
P: Dose, METCON ext. 75cm	1.8250E-02	0.0851	Rem/hr
P: Dose, METCON ext. 105cm	1.8495E-02	0.0991	Rem/hr

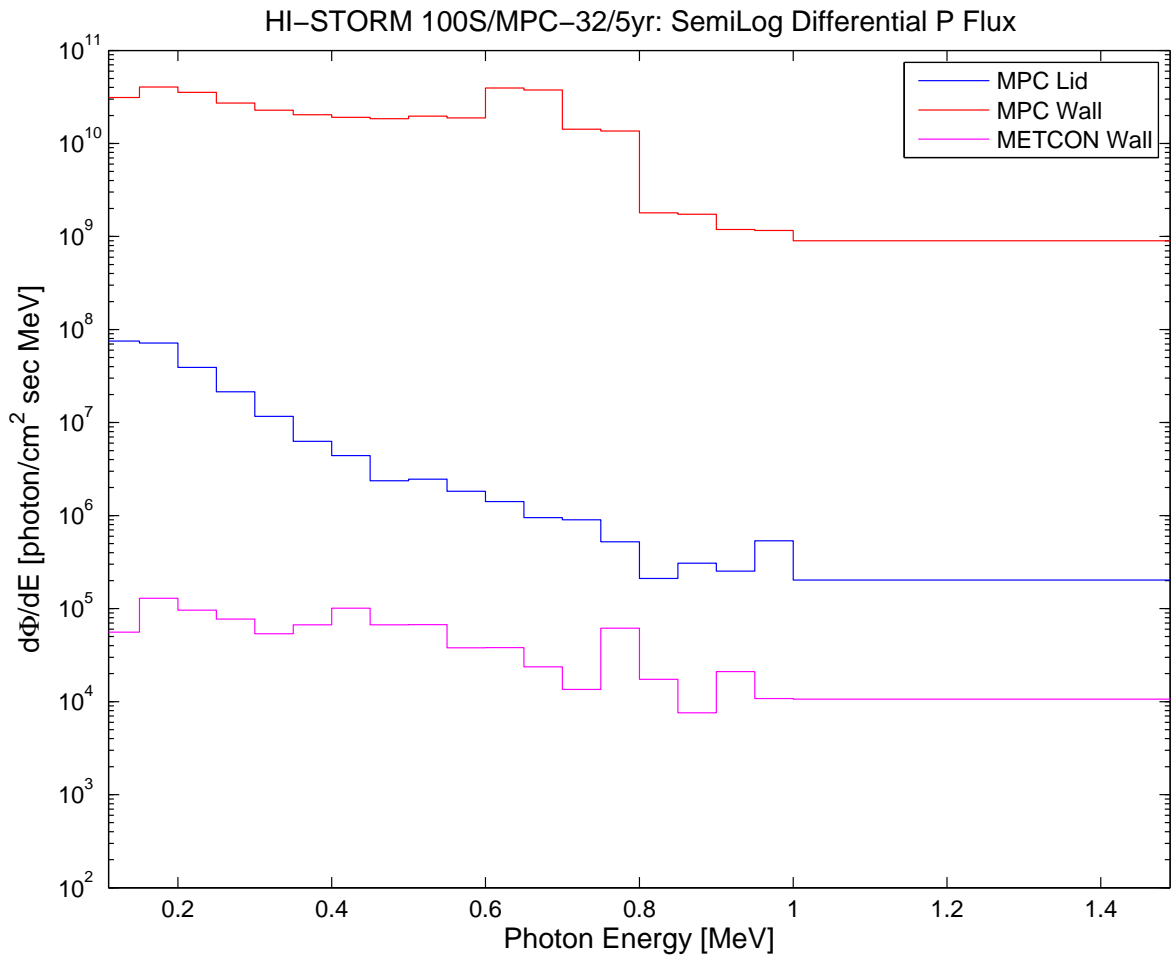


Figure 4.7: The transported photon spectra taken as a surface average for the MPC-32, housed in a 100S METCON, and cooled for 5 yr.

HI-STORM 100S/MPC-32/5yr: P Dose(θ,z), MPC shell in kiloRad(Si)/hr

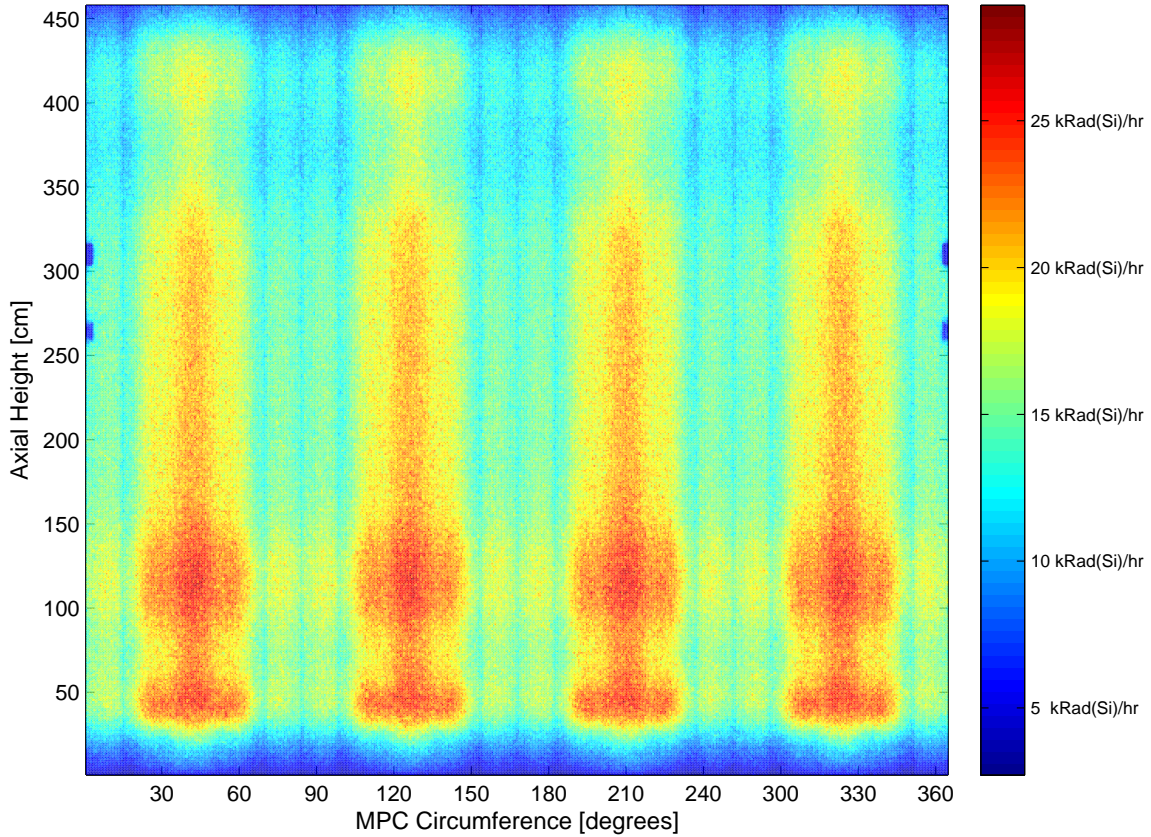


Figure 4.8: The MPC wall photon dose rate for a $6\text{ cm} \cdot 6\text{ cm}$ coaxial FMESH wrapped around the outside of a MPC-32, housed in a 100S METCON, and cooled for 5 yr. The y-axis spans the bottom to the top of the MPC and the x-axis spans 0 to 2π . This details a V.C. Summer cycle of a Westinghouse 17×17 assembly burned to $57.535 \frac{\text{MWd}}{\text{kg}}$ and includes an ORIGAMI 28 zone axial emission profile.

HI-STORM 100S/MPC-32/5yr: P Dose(x,y), MPC Lid in Rad(Si)/hr

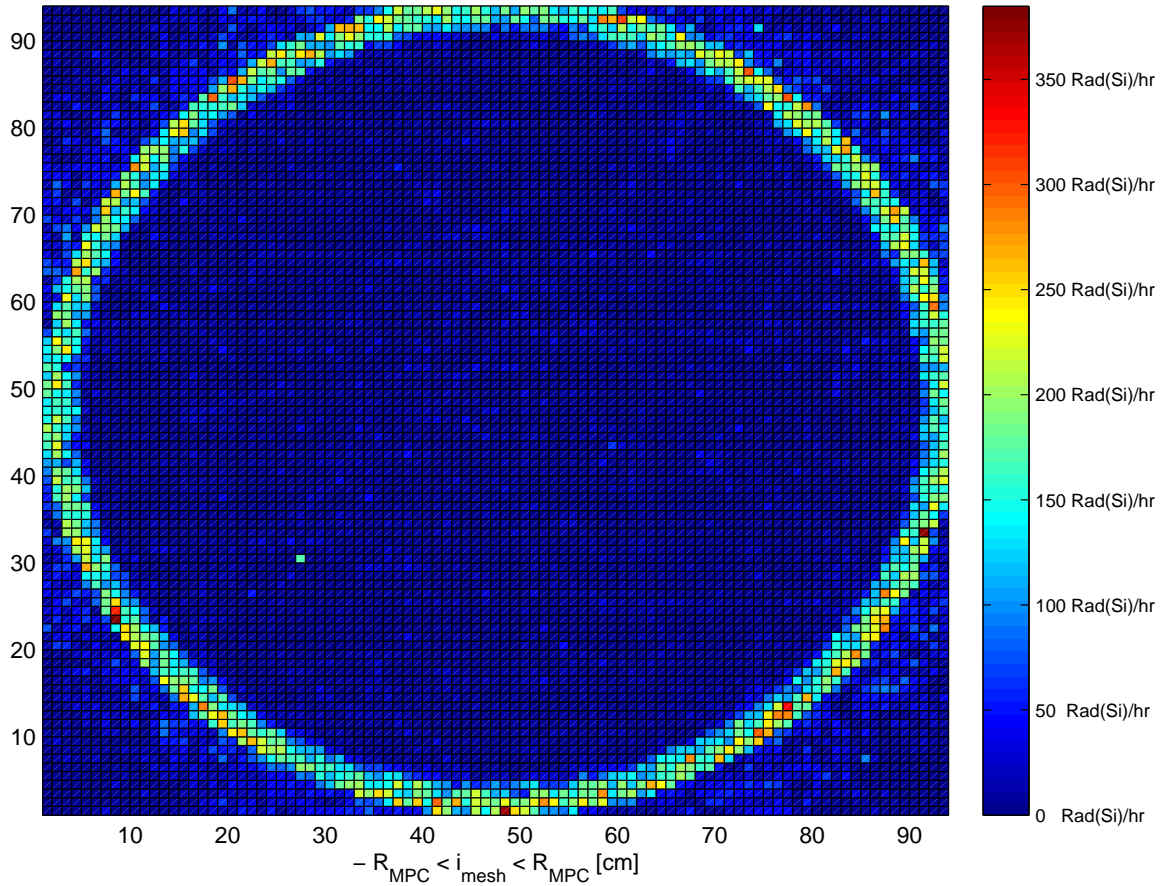


Figure 4.9: The MPC lid photon dose rate for a 45·45 FMESH in a plane at the lid surface for a MPC-32, housed in a 100S METCON, and cooled for 5 yr. Dose is in $\frac{mRad(Si)}{hr}$ for the matrix of 4 cm cells. This is the proposed deployment surface for the delivery system of the robotic instrumentation.

Table 4.4: The photon transport data for the HI-STORM 100S and MPC-32, populated with Westinghouse 17x17 assemblies enriched to 3.5%, with an ORIGAMI axial emission profile, a discharge burnup of $57.535 \frac{MWd}{kg}$, and cooled for 15yr.

Tally	Out	RE	Units
P: Si Dose, MPC Wall	4.8069E+03	0.0002	Rad(Si)/hr
P: Si Dose, MPC Wall, DF	5.4464E+03	0.0002	Rad(Si)/hr
P: Flux, MPC Wall	7.4555E+09	0.0002	photon/cm ² .sec
P: Flux, METCON Wall	1.1665E+04	0.0734	photon/cm ² .sec
P: Dose, outlet vent	1.9561E-02	0.2623	Rem/hr
P: Dose, inlet vent	1.7019E-02	0.5096	Rem/hr
P: Dose, METCON Wall	1.2339E-02	0.0751	Rem/hr
P: Dose, MPC Lid	1.9089E+00	0.0365	Rad(Si)/hr
P: Flux, MPC Lid	4.9962E+06	0.0385	photon/cm ² .sec
P: Dose, left outlet	1.2595E-04	0.3871	Rem/hr
P: Dose, right outlet	6.4508E-05	0.3094	Rem/hr
P: Dose, bottom outlet	1.5704E-04	0.2249	Rem/hr
P: Dose, left inlet	5.3907E-03	0.9577	Rem/hr
P: Dose, right inlet	7.6135E-04	0.6414	Rem/hr
P: Dose, above inlet	2.9609E-03	0.7332	Rem/hr
P: Dose, w/o Pb shield	5.2002E+03	0.0109	Rad(Si)/hr
P: Dose, 4-side Pb shield	2.3785E+03	0.0136	Rad(Si)/hr
P: Dose, 6-side Pb Shield	1.7588E+03	0.0165	Rad(Si)/hr
P: Dose, METCON ext. 15cm	2.1650E-02	0.7002	Rem/hr
P: Dose, METCON ext. 45cm	6.9485E-03	0.1653	Rem/hr
P: Dose, METCON ext. 75cm	5.4974E-03	0.1184	Rem/hr
P: Dose, METCON ext. 105cm	4.6324E-03	0.1002	Rem/hr

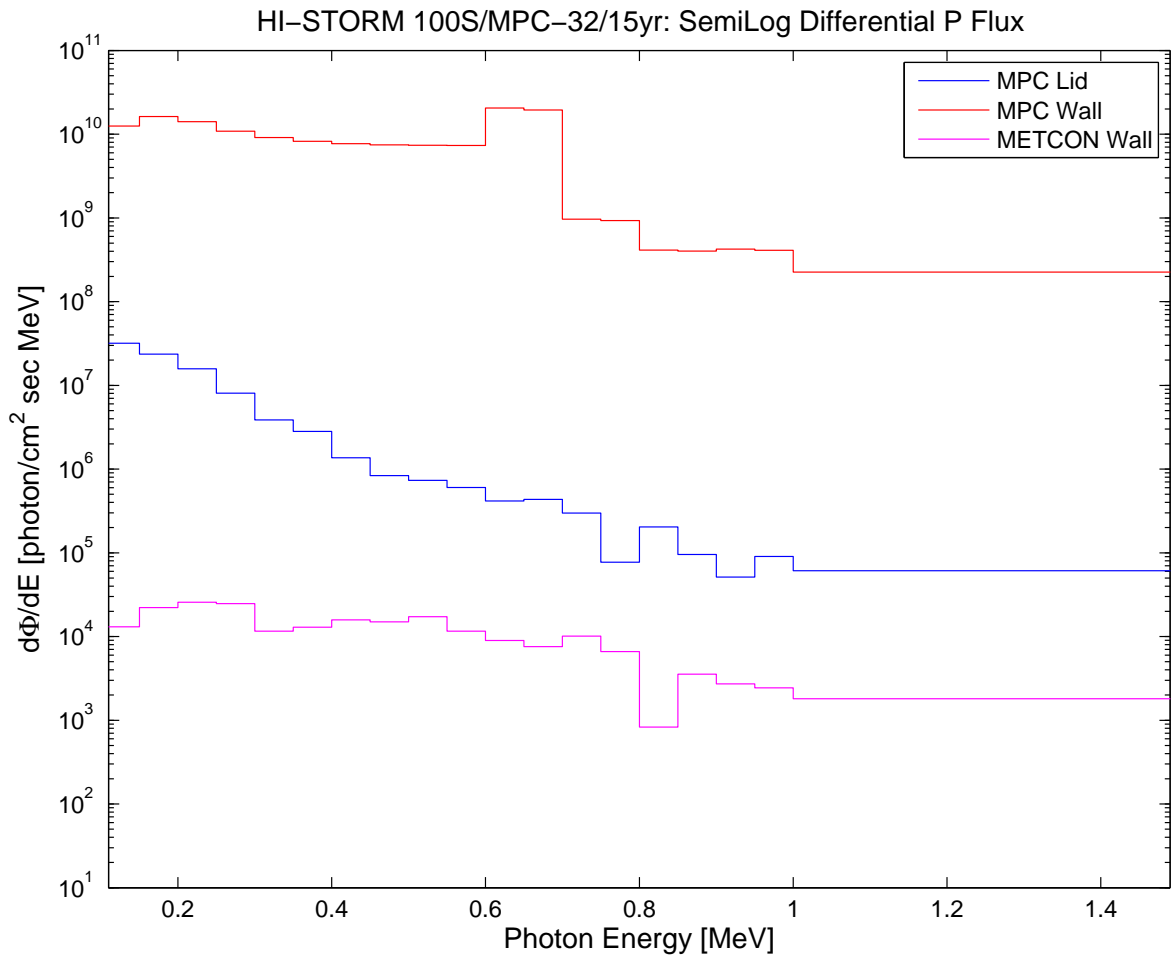


Figure 4.10: The transported photon spectra taken as a surface average for the MPC-32, housed in a 100S METCON, and cooled for 15 yr.

HI-STORM 100S/MPC-32/15yr: P Dose(θ,z), MPC shell in kiloRad(Si)/hr

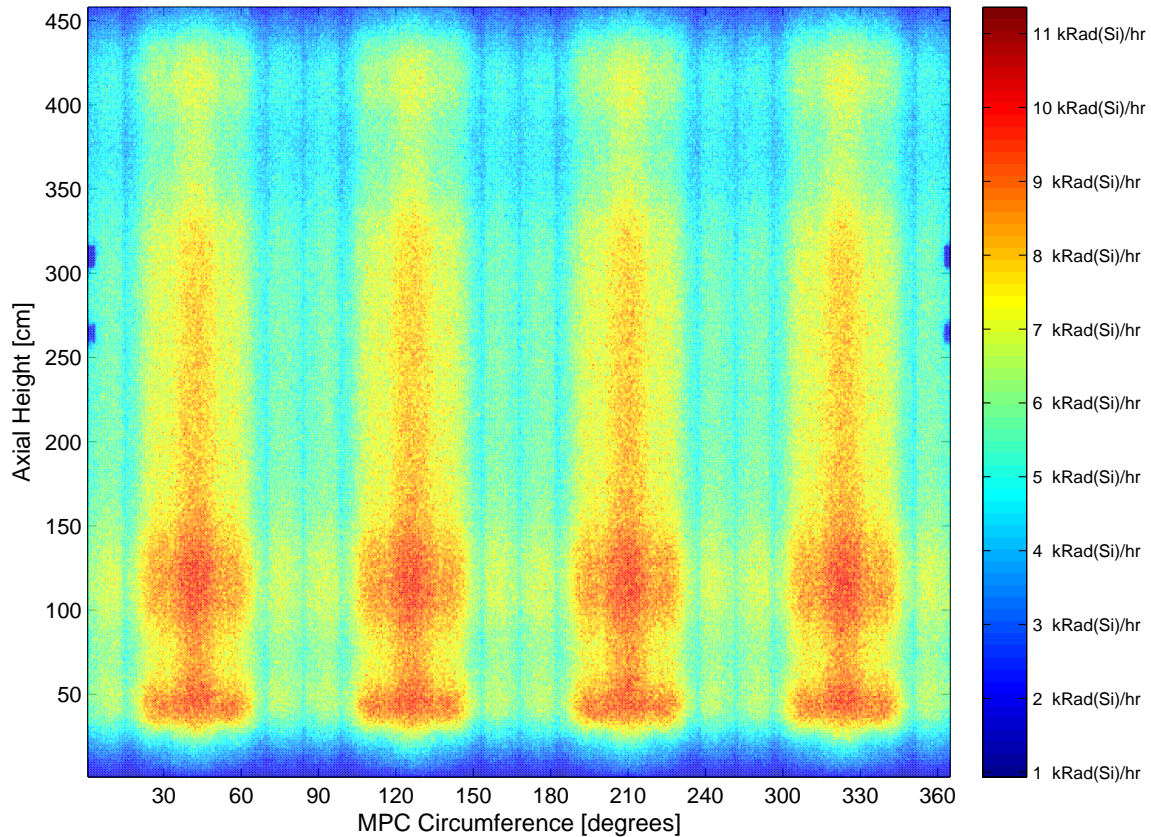


Figure 4.11: The MPC wall photon dose rate for a $6\text{cm} \cdot 6\text{cm}$ coaxial FMESH wrapped around the outside of a MPC-32, housed in a 100S METCON, and cooled for 15 yr. The y-axis spans the bottom to the top of the MPC and the x-axis spans 0 to 2π . This details a V.C. Summer cycle of a Westinghouse 17×17 assembly burned to $57.535 \frac{\text{MWd}}{\text{kg}}$ and includes an ORIGAMI 28 zone axial emission profile.

HI-STORM 100S/MPC-32/15yr: P Dose(x,y), MPC Lid in Rad(Si)/hr

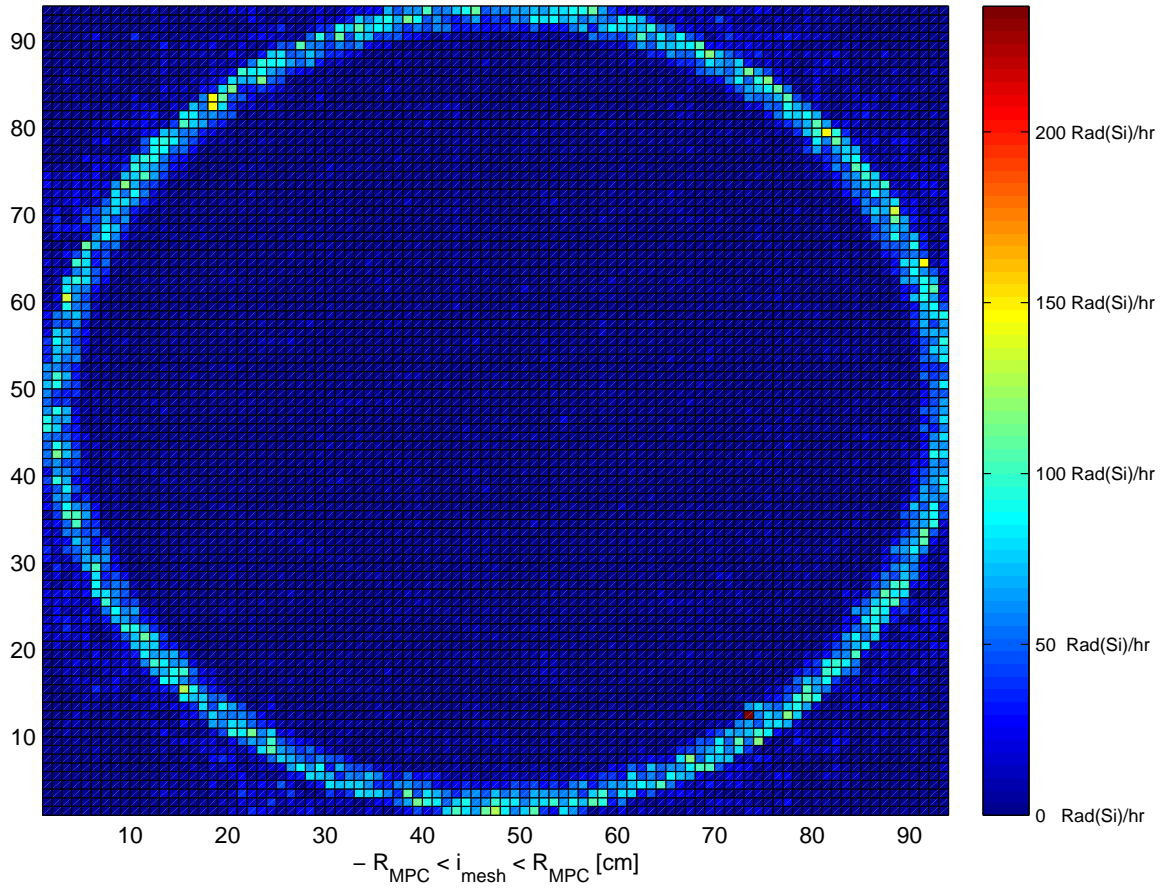


Figure 4.12: The MPC lid photon dose rate for a 45·45 FMESH in a plane at the lid surface for a MPC-32, housed in a 100S METCON, and cooled for 15 yr. Dose is in $\frac{mRad(Si)}{hr}$ for the matrix of 4 cm cells. This is the proposed deployment surface for the delivery system of the robotic instrumentation.

Table 4.5: The photon transport data for the HI-STORM 100S and MPC-32, populated with Westinghouse 17x17 assemblies enriched to 3.5%, with an ORIGAMI axial emission profile, a discharge burnup of $57.535 \frac{MWd}{kg}$, and cooled for 25yr.

Tally	Out	RE	Units
P: Si Dose, MPC Wall	3.4940E+03	0.0002	Rad(Si)/hr
P: Si Dose, MPC Wall, DF	3.9598E+03	0.0002	Rad(Si)/hr
P: Flux, MPC Wall	5.4987E+09	0.0002	photon/cm ² .sec
P: Flux, METCON Wall	6.8241E+03	0.0895	photon/cm ² .sec
P: Dose, outlet vent	1.4083E-02	0.2815	Rem/hr
P: Dose, inlet vent	1.2283E-02	0.4396	Rem/hr
P: Dose, METCON Wall	6.7790E-03	0.0920	Rem/hr
P: Dose, MPC Lid	1.3701E+00	0.0383	Rad(Si)/hr
P: Flux, MPC Lid	3.7116E+06	0.0406	photon/cm ² .sec
P: Dose, left outlet	8.5217E-05	0.4334	Rem/hr
P: Dose, right outlet	7.5090E-05	0.3364	Rem/hr
P: Dose, bottom outlet	1.6083E-03	0.9422	Rem/hr
P: Dose, left inlet	3.8947E-03	0.9333	Rem/hr
P: Dose, right inlet	5.6053E-04	0.5317	Rem/hr
P: Dose, above inlet	2.8357E-03	0.8307	Rem/hr
P: Dose, w/o Pb shield	3.8120E+03	0.0111	Rad(Si)/hr
P: Dose, 4-side Pb shield	1.7072E+03	0.0145	Rad(Si)/hr
P: Dose, 6-side Pb Shield	1.2543E+03	0.0168	Rad(Si)/hr
P: Dose, METCON ext. 15cm	1.5009E-02	0.6973	Rem/hr
P: Dose, METCON ext. 45cm	4.8478E-03	0.1504	Rem/hr
P: Dose, METCON ext. 75cm	3.6021E-03	0.1141	Rem/hr
P: Dose, METCON ext. 105cm	3.0167E-03	0.1000	Rem/hr

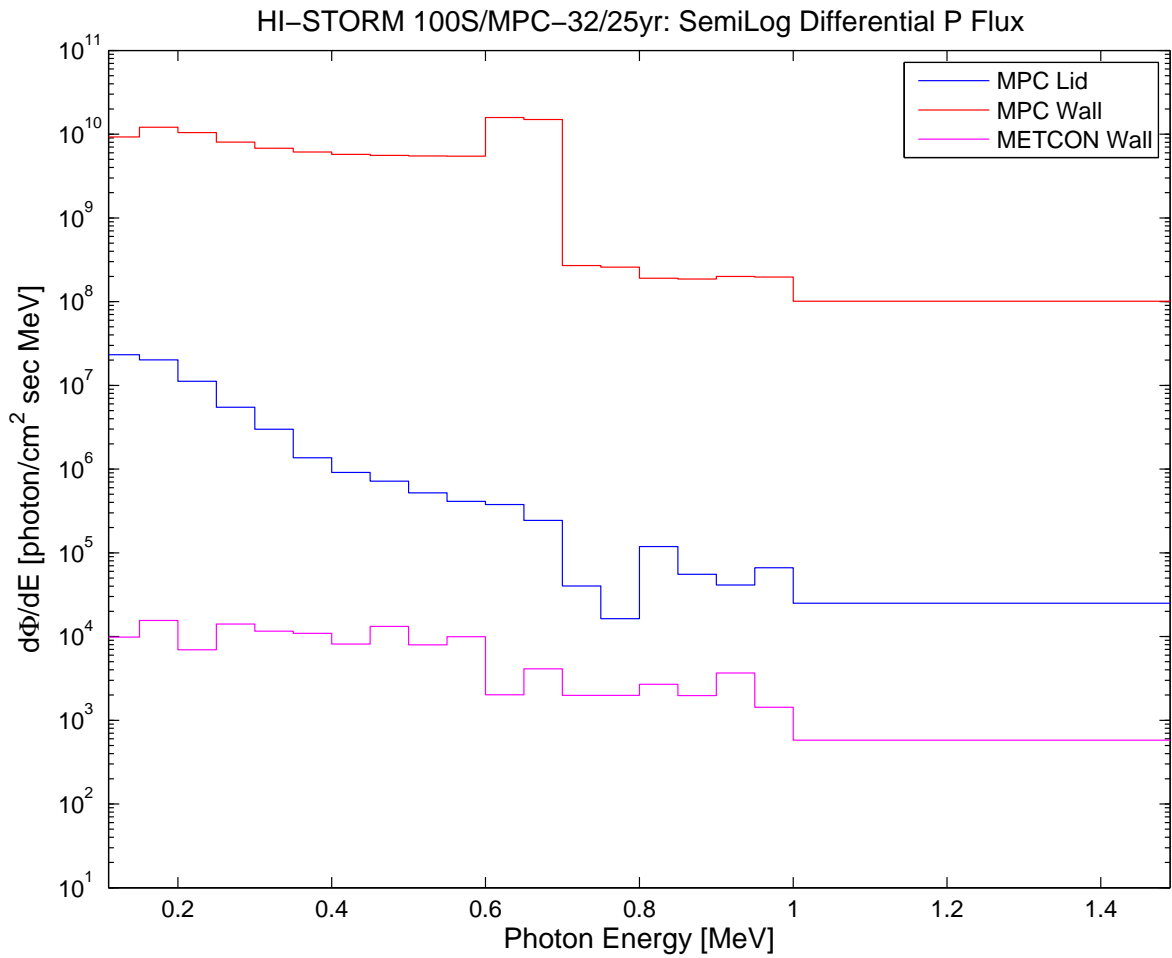


Figure 4.13: The transported photon spectra taken as a surface average for the MPC-32, housed in a 100S METCON, and cooled for 25 yr.

HI-STORM 100S/MPC-32/25yr: P Dose(θ,z), MPC shell in kiloRad(Si)/hr

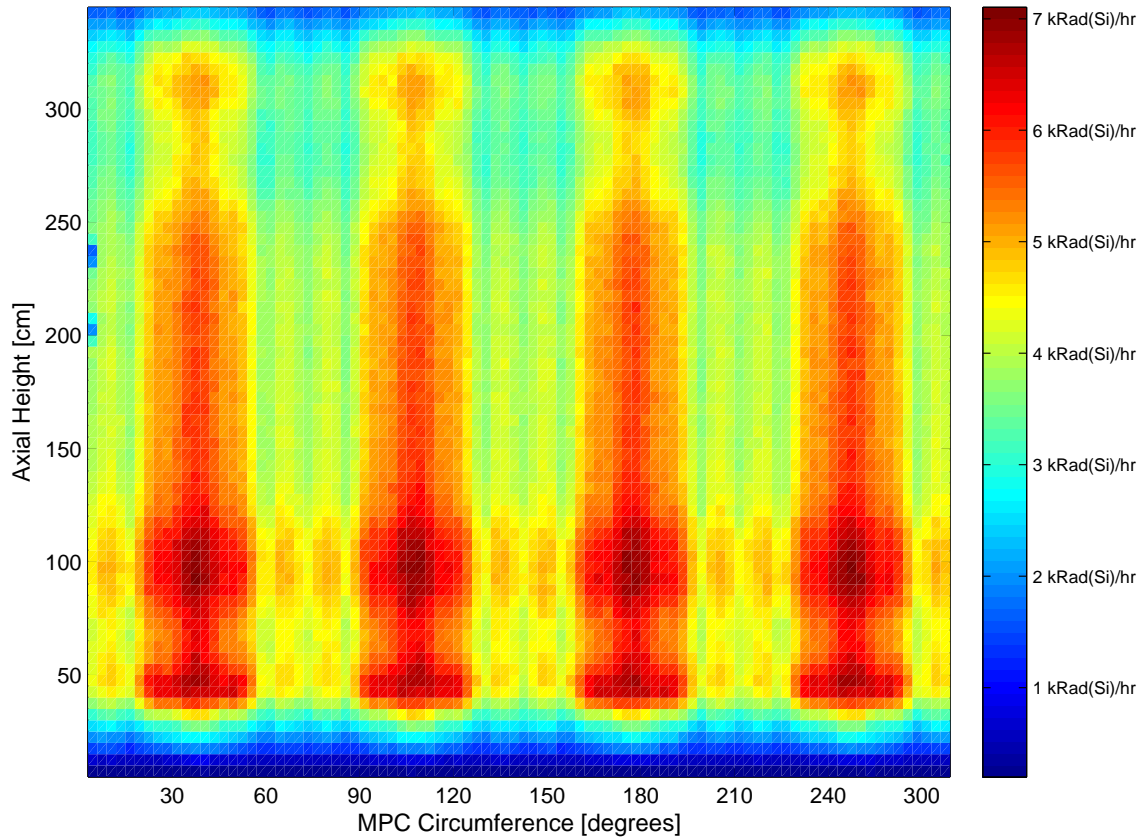


Figure 4.14: The MPC wall photon dose rate for a $6\text{cm} \cdot 6\text{cm}$ coaxial FMESH wrapped around the outside of a MPC-32, housed in a 100S METCON, and cooled for 25 yr. The y-axis spans the bottom to the top of the MPC and the x-axis spans 0 to 2π . This details a V.C. Summer cycle of a Westinghouse 17×17 assembly burned to $57.535 \frac{\text{MWd}}{\text{kg}}$ and includes an ORIGAMI 28 zone axial emission profile.

HI-STORM 100S/MPC-32/25yr: P Dose(x,y), MPC Lid in Rad(Si)/hr

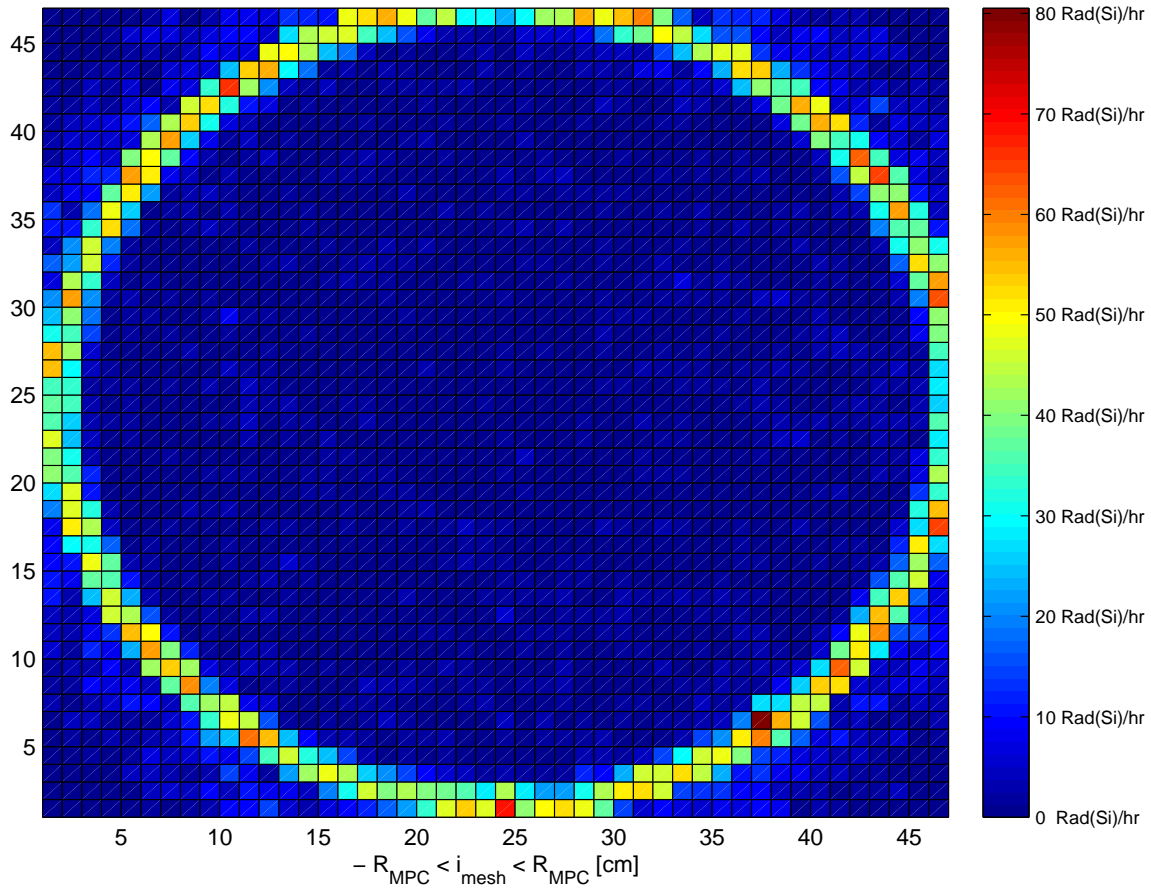


Figure 4.15: The MPC lid photon dose rate for a 45·45 FMESH in a plane at the lid surface for a MPC-32, housed in a 100S METCON, and cooled for 25 yr. Dose is in $\frac{mRad(Si)}{hr}$ for the matrix of 4 cm cells. This is the proposed deployment surface for the delivery system of the robotic instrumentation.

Table 4.6: The photon transport data is given for the HI-STORM 100S and MPC-68, populated with General Electric assemblies, enriched to 3.5%, burned in ORIGEN-ARP to $25.344 \frac{MWd}{kg}$, and cooled for 5yr.

Tally	Out	RE	Units
P: Si Dose, MPC Wall	2.9984E+03	0.0002	Rad(Si)/hr
P: Si Dose, MPC Wall, DF	3.3963E+03	0.0002	Rad(Si)/hr
P: Flux, MPC Wall	4.6477E+09	0.0002	photon/cm ² ·sec
P: Flux, METCON Wall	9.2621E+03	0.0610	photon/cm ² ·sec
P: Dose, outlet vent	4.5381E-02	0.1499	Rem/hr
P: Dose, inlet vent	9.7708E-03	0.3206	Rem/hr
P: Dose, METCON Wall	1.0916E-02	0.0625	Rem/hr
P: Dose, MPC Lid	3.9559E+00	0.0192	Rad(Si)/hr
P: Flux, MPC Lid	1.0368E+07	0.0196	photon/cm ² ·sec
P: Dose, left outlet	6.8506E-04	0.3848	Rem/hr
P: Dose, right outlet	5.5307E-03	0.8677	Rem/hr
P: Dose, bottom outlet	1.2244E-03	0.2596	Rem/hr
P: Dose, left inlet	1.6933E-04	0.2109	Rem/hr
P: Dose, right inlet	1.6878E-04	0.2532	Rem/hr
P: Dose, above inlet	4.9898E-04	0.1928	Rem/hr
P: Dose, w/o Pb shield	3.3510E+03	0.0097	Rad(Si)/hr
P: Dose, 4-side Pb shield	1.6430E+03	0.0133	Rad(Si)/hr
P: Dose, 6-side Pb Shield	1.2150E+03	0.0138	Rad(Si)/hr
P: Dose, METCON ext. 15cm	5.1287E-03	0.2124	Rem/hr
P: Dose, METCON ext. 45cm	3.3861E-03	0.1113	Rem/hr
P: Dose, METCON ext. 75cm	3.3863E-03	0.0905	Rem/hr
P: Dose, METCON ext. 105cm	3.3237E-03	0.0937	Rem/hr

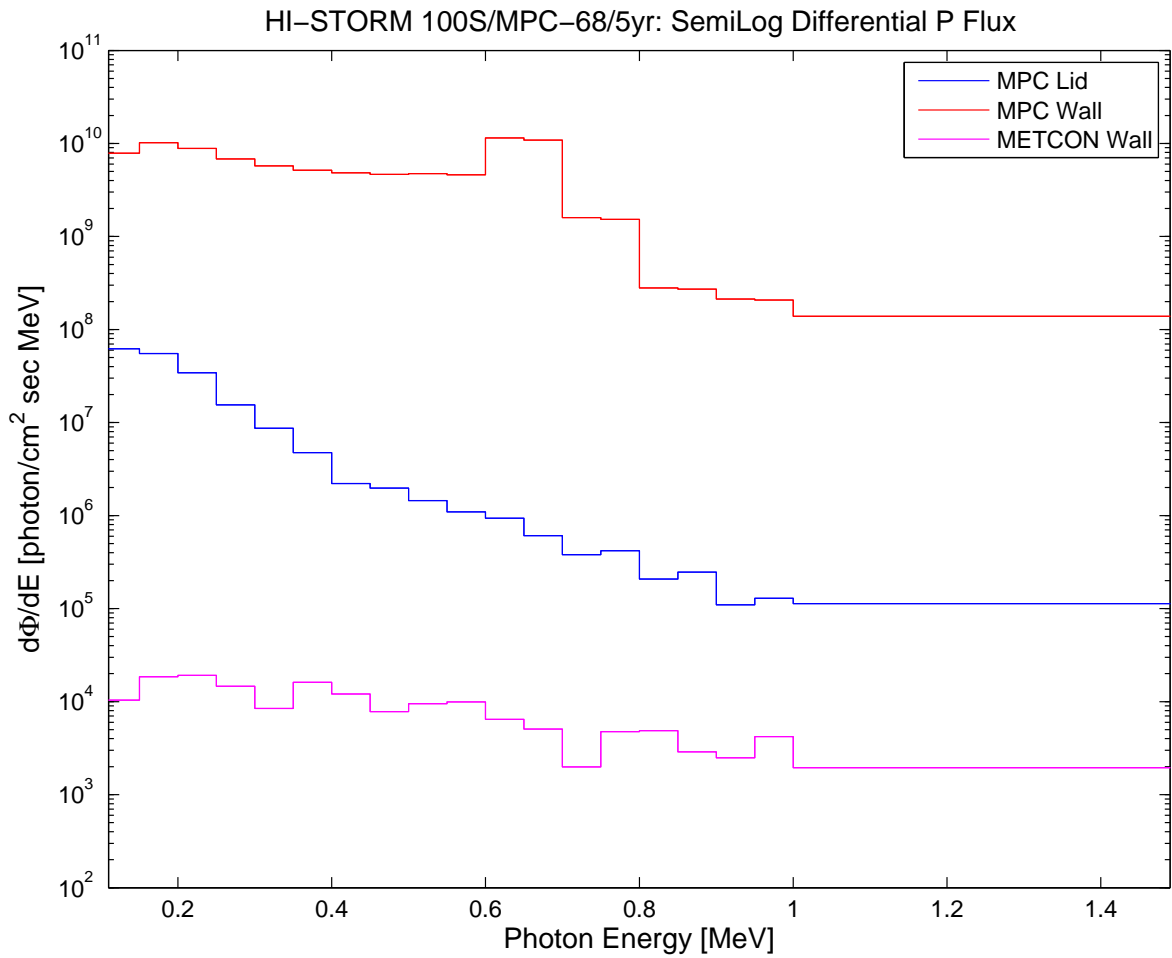


Figure 4.16: The transported photon spectra taken as a surface average for the MPC-68, housed in a 100S METCON, and cooled for 5 yr.

HI-STORM 100S/MPC-68/5yr: P Dose(θ,z), MPC shell in Rad(Si)/hr

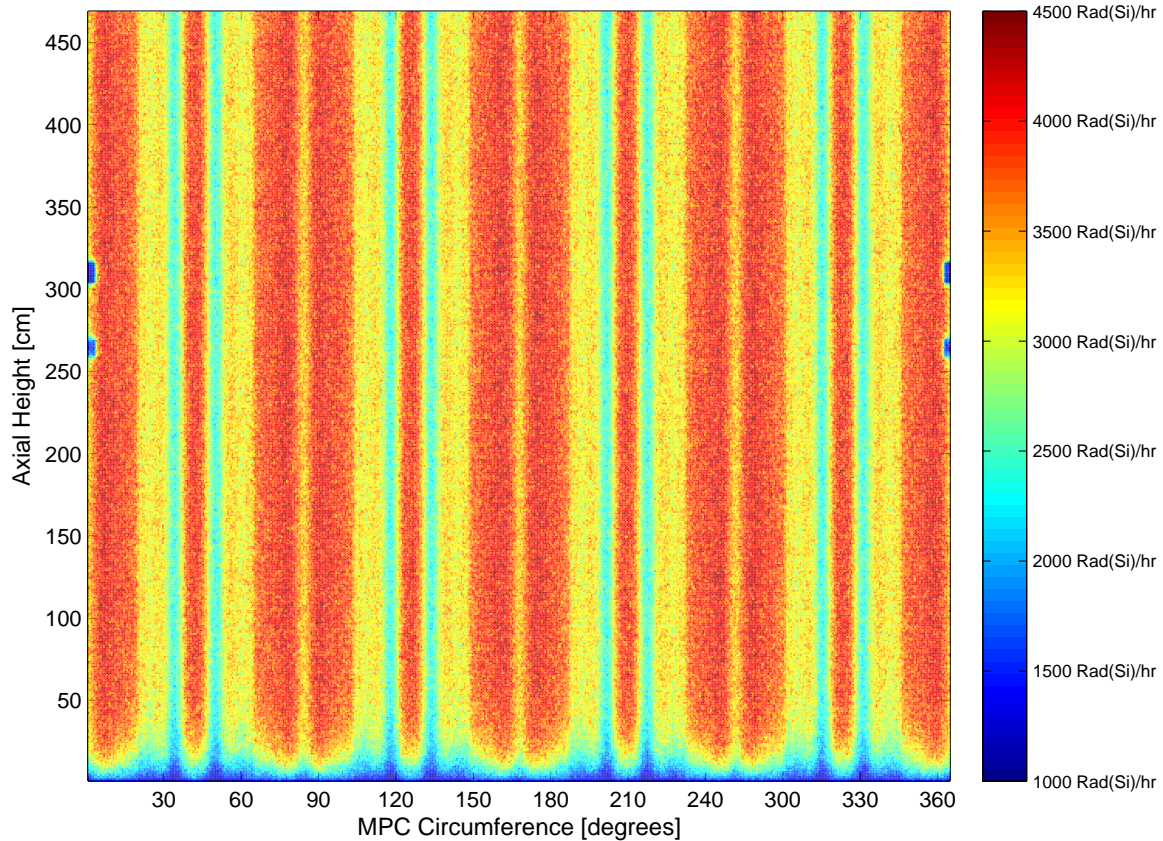


Figure 4.17: The MPC wall photon dose rate for a $6\text{cm} \cdot 6\text{cm}$ coaxial FMESH wrapped around the outside of a MPC-68, housed in a 100S METCON, and cooled for 5 yr. The y-axis spans the bottom to the top of the MPC and the x-axis spans 0 to 2π . This details a Cooper Nuclear Station cycle of a of a General Electric 8×8 assembly burned to $25.344 \frac{\text{MWd}}{\text{kg}}$ and includes an ORIGEN-ARP source term.

HI-STORM 100S/MPC-68/5yr: P Dose(x,y), MPC Lid in Rad(Si)/hr

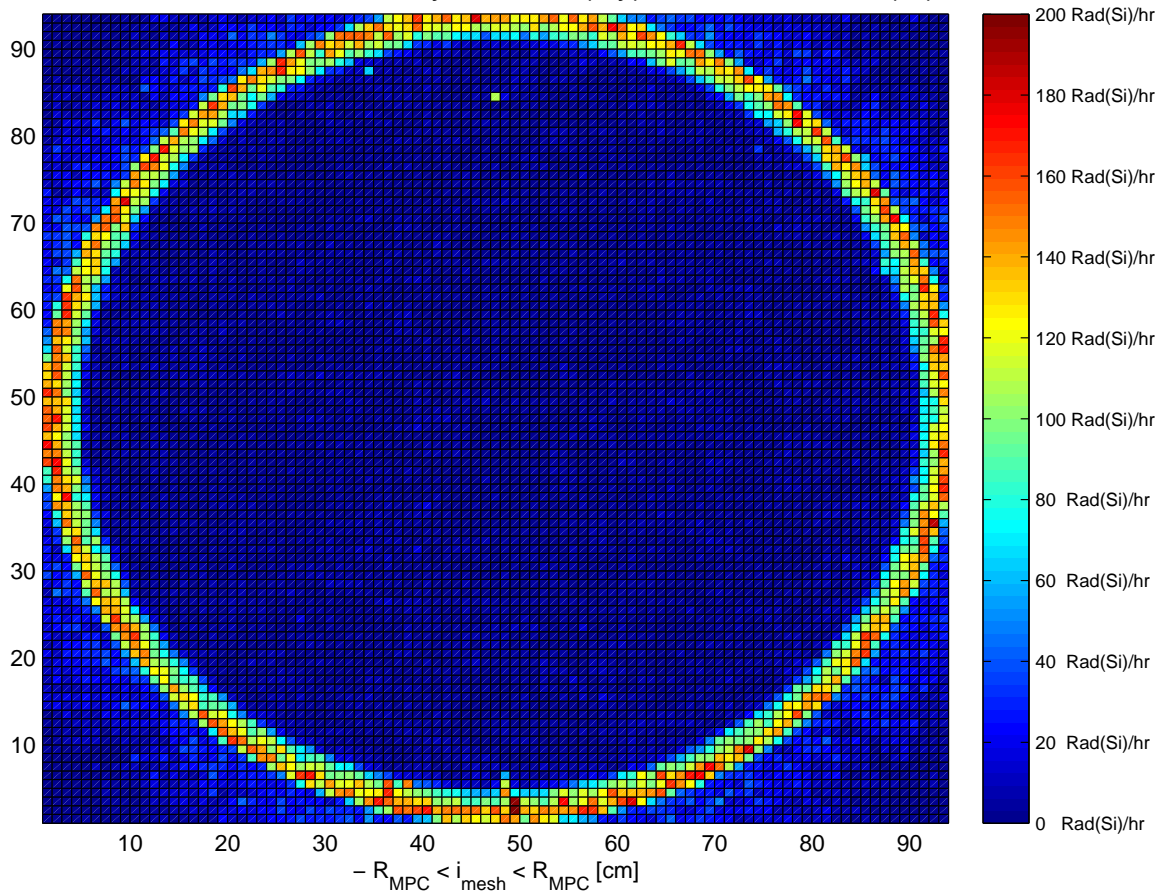


Figure 4.18: The MPC lid photon dose rate for a 45·45 FMESH in a plane at the lid surface for a MPC-68, housed in a 100S METCON, and cooled for 5 yr. Dose is in $\frac{mRad(Si)}{hr}$ for the matrix of 4 cm cells. This is the proposed deployment surface for the delivery system of the robotic instrumentation.

Table 4.7: The photon transport data is given for the HI-STORM 100S and MPC-68, populated with General Electric assemblies, enriched to 3.5%, burned in ORIGEN-ARP to 25.344 $\frac{MWd}{kg}$, and cooled for 15yr.

Tally	Out	RE	Units
P: Si Dose, MPC Wall	1.7648E+03	0.0003	Rad(Si)/hr
P: Si Dose, MPC Wall, DF	2.0002E+03	0.0002	Rad(Si)/hr
P: Flux, MPC Wall	2.8009E+09	0.0003	photon/cm ² ·sec
P: Flux, METCON Wall	2.8587E+03	0.1017	photon/cm ² ·sec
P: Dose, outlet vent	2.9980E-02	0.3406	Rem/hr
P: Dose, inlet vent	7.0808E-03	0.4908	Rem/hr
P: Dose, METCON Wall	2.6855E-03	0.1085	Rem/hr
P: Dose, MPC Lid	2.2601E+00	0.0311	Rad(Si)/hr
P: Flux, MPC Lid	5.9569E+06	0.0250	photon/cm ² ·sec
P: Dose, left outlet	2.9643E-04	0.4274	Rem/hr
P: Dose, right outlet	5.5881E-04	0.7483	Rem/hr
P: Dose, bottom outlet	1.7781E-04	0.2705	Rem/hr
P: Dose, left inlet	1.4207E-04	0.3099	Rem/hr
P: Dose, right inlet	1.2586E-04	0.3014	Rem/hr
P: Dose, above inlet	1.1433E-04	0.2451	Rem/hr
P: Dose, w/o Pb shield	1.9671E+03	0.0121	Rad(Si)/hr
P: Dose, 4-side Pb shield	9.2830E+02	0.0155	Rad(Si)/hr
P: Dose, 6-side Pb Shield	6.9335E+02	0.0180	Rad(Si)/hr
P: Dose, METCON ext. 15cm	2.3336E-03	0.1718	Rem/hr
P: Dose, METCON ext. 45cm	1.7299E-03	0.1349	Rem/hr
P: Dose, METCON ext. 75cm	1.5710E-03	0.1063	Rem/hr
P: Dose, METCON ext. 105cm	1.3460E-03	0.0936	Rem/hr

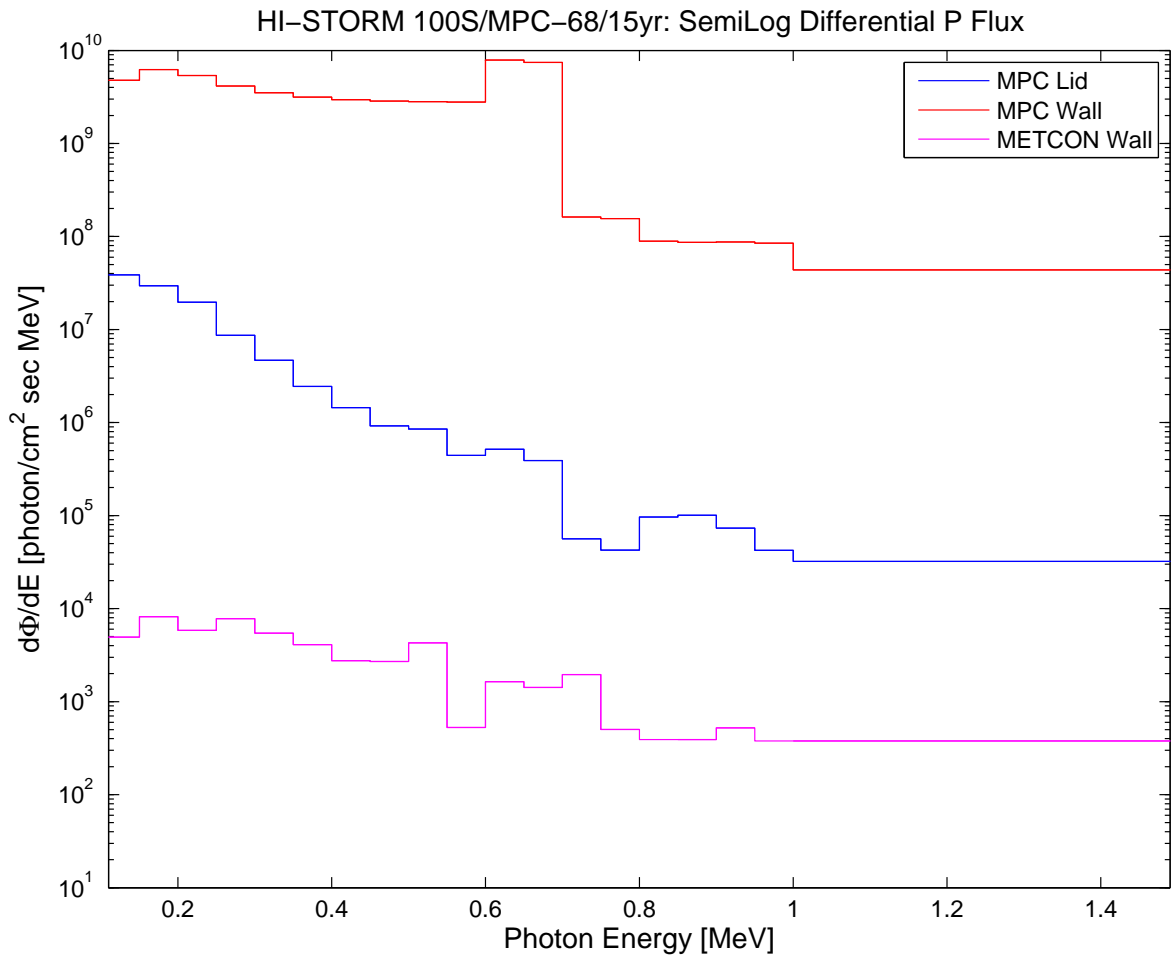


Figure 4.19: The transported photon spectra taken as a surface average for the MPC-68, housed in a 100S METCON, and cooled for 15 yr.

HI-STORM 100S/MPC-68/15yr: P Dose(θ,z), MPC shell in Rad(Si)/hr

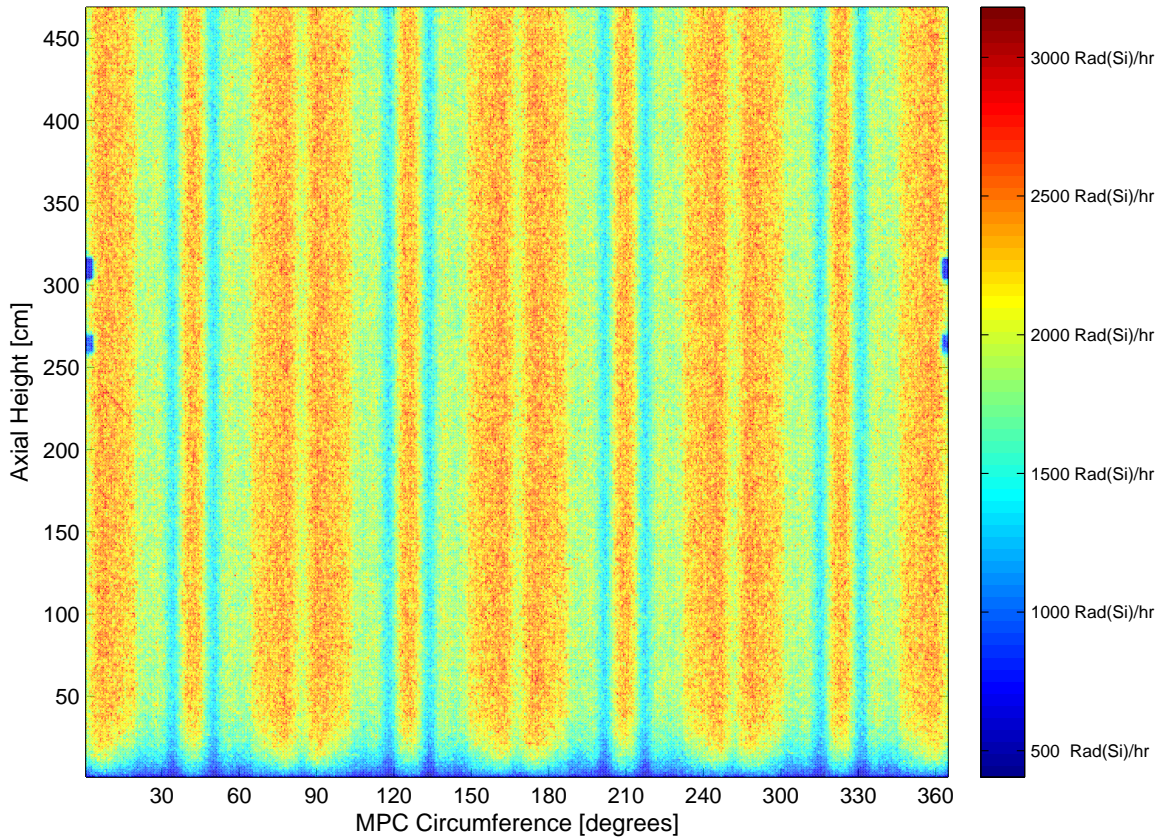


Figure 4.20: The MPC wall photon dose rate for a $6\text{cm} \cdot 6\text{cm}$ coaxial FMESH wrapped around the outside of a MPC-68, housed in a 100S METCON, and cooled for 15 yr. The y-axis spans the bottom to the top of the MPC and the x-axis spans 0 to 2π . This details a Cooper Nuclear Station cycle of a of a General Electric 8×8 assembly burned to $25.344 \frac{\text{MWd}}{\text{kg}}$ and includes an ORIGEN-ARP source term.

HI-STORM 100S/MPC-68/15yr: P Dose(x,y), MPC Lid in Rad(Si)/hr

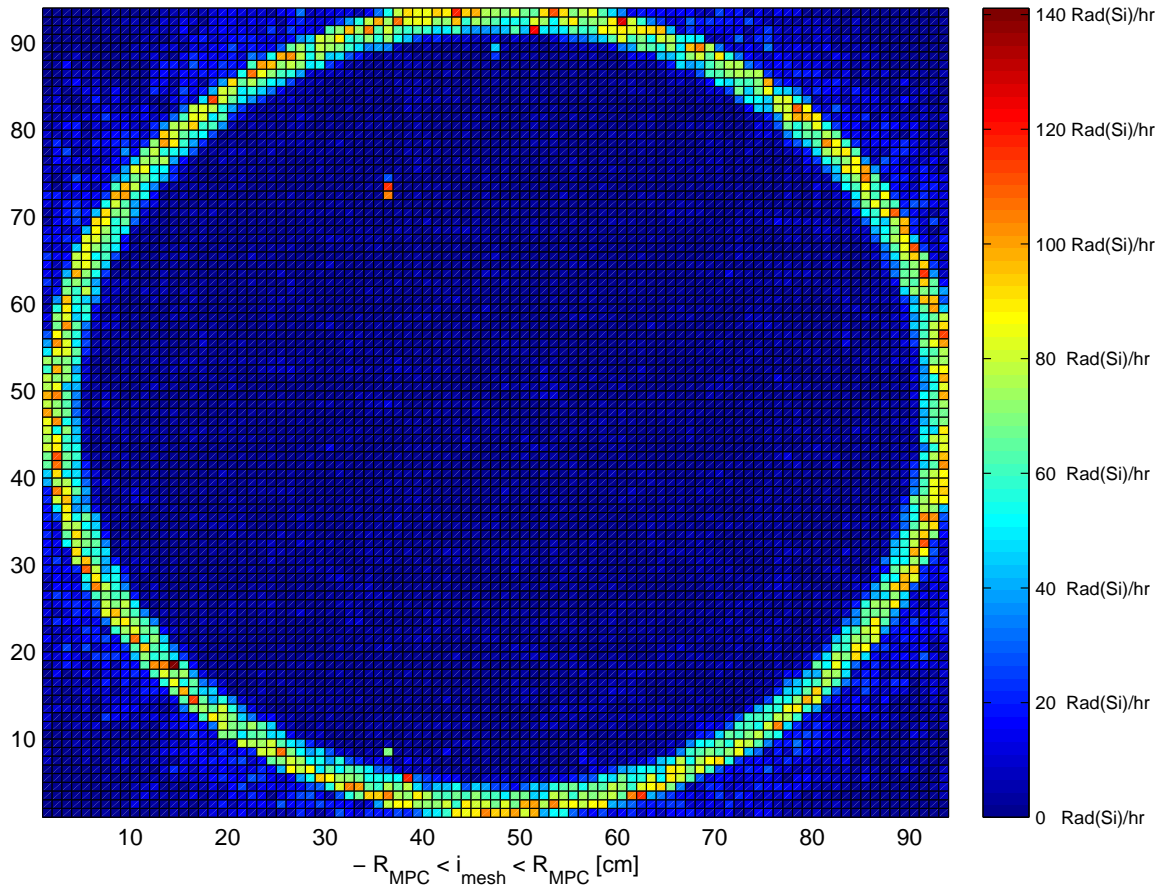


Figure 4.21: The MPC lid photon dose rate for a 45·45 FMESH in a plane at the lid surface for a MPC-68, housed in a 100S METCON, and cooled for 15 yr. Dose is in $\frac{mRad(Si)}{hr}$ for the matrix of 4 cm cells. This is the proposed deployment surface for the delivery system of the robotic instrumentation.

Table 4.8: The photon transport data is given for the HI-STORM 100S and MPC-68, populated with General Electric assemblies, enriched to 3.5%, burned in ORIGEN-ARP to 25.344 $\frac{MWd}{kg}$, and cooled for 25yr.

Tally	Out	RE	Units
P: Si Dose, MPC Wall	1.3542E+03	0.0005	Rad(Si)/hr
P: Si Dose, MPC Wall, DF	1.5350E+03	0.0004	Rad(Si)/hr
P: Flux, MPC Wall	2.1622E+09	0.0005	photon/cm ² ·sec
P: Flux, METCON Wall	1.7117E+03	0.1998	photon/cm ² ·sec
P: Dose, outlet vent	2.0430E-02	0.1916	Rem/hr
P: Dose, inlet vent	1.8290E-03	0.2379	Rem/hr
P: Dose, METCON Wall	1.6406E-03	0.2058	Rem/hr
P: Dose, MPC Lid	1.6157E+00	0.0429	Rad(Si)/hr
P: Flux, MPC Lid	4.4471E+06	0.0455	photon/cm ² ·sec
P: Dose, left outlet	3.5784E-04	0.8260	Rem/hr
P: Dose, right outlet	1.5736E-04	0.5936	Rem/hr
P: Dose, bottom outlet	2.6978E-04	0.7756	Rem/hr
P: Dose, left inlet	7.0244E-05	0.5031	Rem/hr
P: Dose, right inlet	8.7687E-05	0.4999	Rem/hr
P: Dose, above inlet	3.6391E-05	0.0975	Rem/hr
P: Dose, w/o Pb shield	1.5138E+03	0.0212	Rad(Si)/hr
P: Dose, 4-side Pb shield	7.5418E+02	0.0432	Rad(Si)/hr
P: Dose, 6-side Pb Shield	5.4833E+02	0.0412	Rad(Si)/hr
P: Dose, METCON ext. 15cm	1.8340E-03	0.3449	Rem/hr
P: Dose, METCON ext. 45cm	1.3900E-03	0.2168	Rem/hr
P: Dose, METCON ext. 75cm	1.1870E-03	0.1629	Rem/hr
P: Dose, METCON ext. 105cm	9.0909E-04	0.1429	Rem/hr

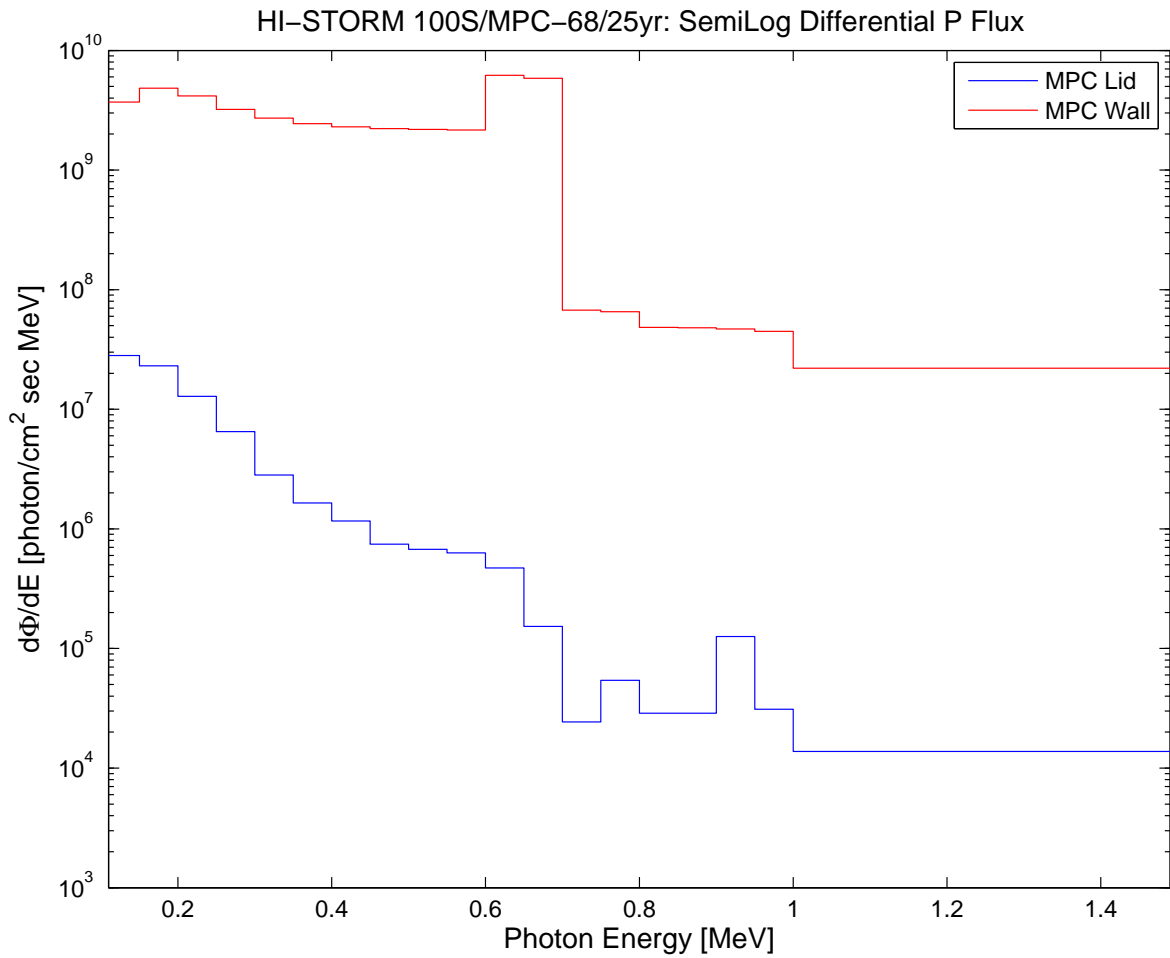


Figure 4.22: The transported photon spectra taken as a surface average for the MPC-68, housed in a 100S METCON, and cooled for 25 yr.

HI-STORM 100S/MPC-68/25yr: P Dose(θ,z), MPC shell in kiloRad(Si)/hr

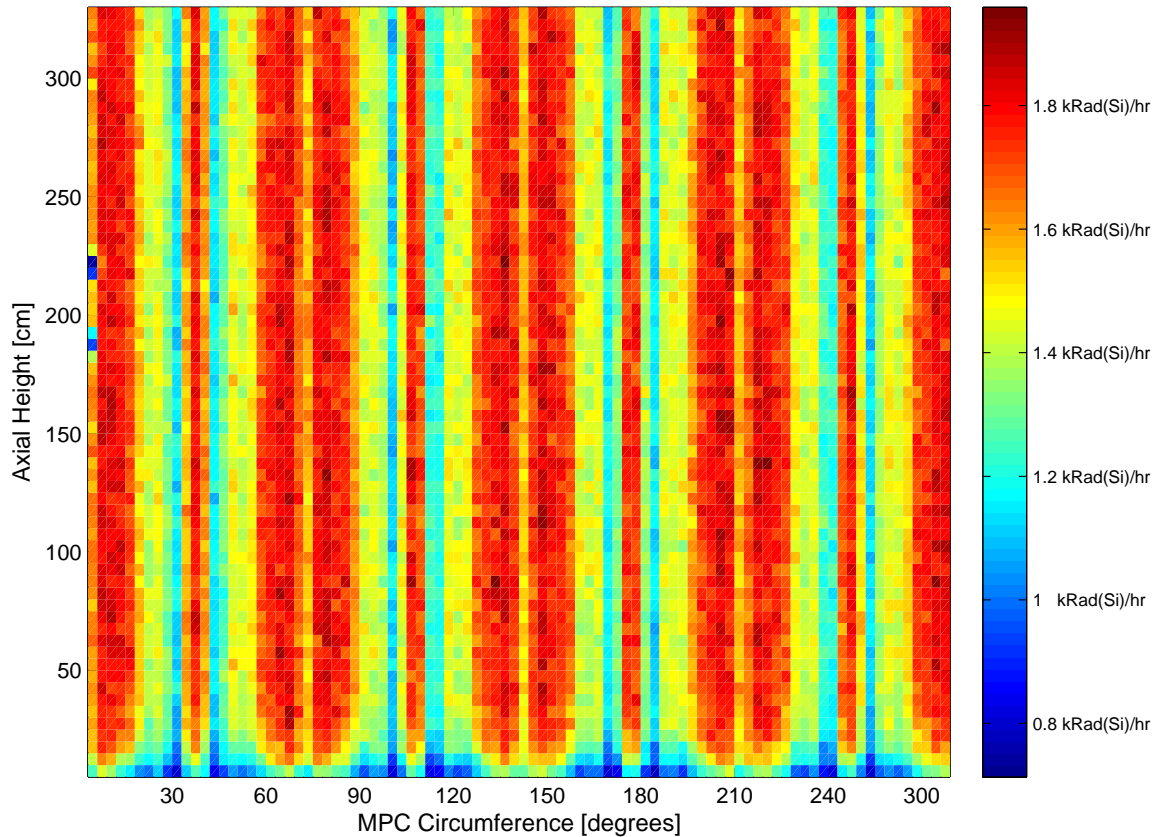


Figure 4.23: The MPC wall photon dose rate for a $6\text{cm} \cdot 6\text{cm}$ coaxial FMESH wrapped around the outside of a MPC-68, housed in a 100S METCON, and cooled for 25 yr. The y-axis spans the bottom to the top of the MPC and the x-axis spans 0 to 2π . This details a Cooper Nuclear Station cycle of a of a General Electric 8×8 assembly burned to $25.344 \frac{\text{MWd}}{\text{kg}}$ and includes an ORIGEN-ARP source term.

HI-STORM 100S/MPC-68/25yr: P Dose(x,y), MPC Lid in Rad(Si)/hr

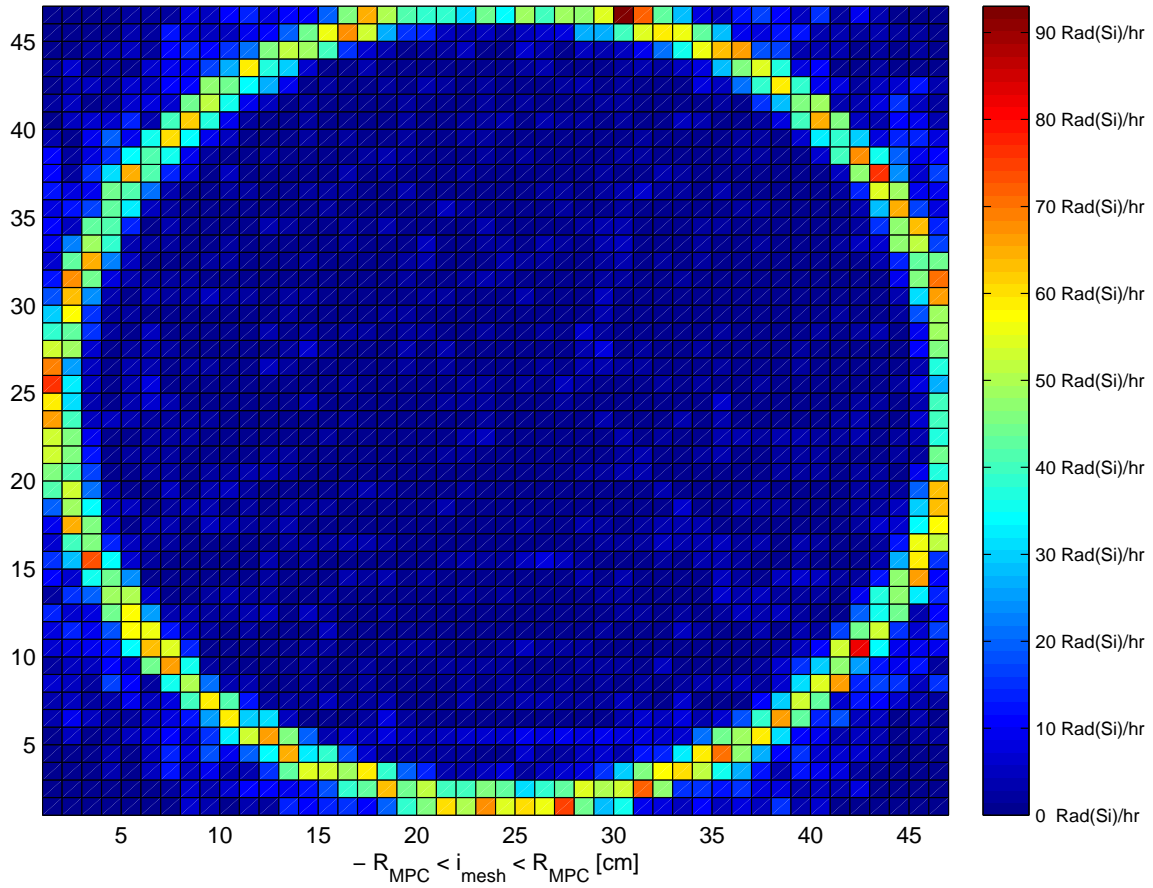


Figure 4.24: The MPC lid photon dose rate for a 45·45 FMESH in a plane at the lid surface for a MPC-68, housed in a 100S METCON, and cooled for 25 yr. Dose is in $\frac{mRad(Si)}{hr}$ for the matrix of 4 cm cells. This is the proposed deployment surface for the delivery system of the robotic instrumentation.

Table 4.9: The neutron transport data for the HI-STORM 100S and MPC-24, populated with Westinghouse 17x17 assemblies enriched to 3.5%, with an ORIGAMI axial emission profile, a discharge burnup of $57.535 \frac{MWd}{kg}$, and cooled for 5yr.

Tally	Out	RE	Units
N: Co-60 Activation	1.5807E-01	0.0025	Bq/gm (per hr exp.)
N: Si Dose, MPC Wall, DF	1.6766E-02	0.0006	Rad(Si)/hr
N: Dose, outlet vent	3.0885E-02	0.0457	Rem/hr
N: Dose, inlet vent	3.8157E-03	0.0515	Rem/hr
N: Dose, METCON Wall	3.2683E-03	0.0141	Rem/hr
N: Flux, MPC Wall	5.1607E+05	0.0003	neutron/cm ² .sec
N: Flux, METCON Wall	1.8308E+02	0.0053	neutron/cm ² .sec
N: Flux, MPC Lid	5.1719E+04	0.0032	neutron/cm ² .sec
N: Dose, MPC Lid	8.5350E-04	0.005	Rad(Si)/hr
N: Dose, left outlet	1.6364E-03	0.1088	Rem/hr
N: Dose, right outlet	1.4944E-03	0.0781	Rem/hr
N: Dose, bottom outlet	5.2911E-04	0.1804	Rem/hr
N: Dose, left inlet	2.7933E-04	0.1714	Rem/hr
N: Dose, right inlet	1.9388E-04	0.114	Rem/hr
N: Dose, above inlet	5.4134E-04	0.3388	Rem/hr
N: Dose, w/o Pb shield	2.1419E-02	0.0256	Rad(Si)/hr
N: Dose, 4-side Pb shield	1.8955E-02	0.0221	Rad(Si)/hr
N: Dose, 6-side Pb Shield	1.7710E-02	0.0218	Rad(Si)/hr
N: Dose, METCON ext. 15cm	2.1071E-03	0.0869	Rem/hr
N: Dose, METCON ext. 45cm	1.1682E-03	0.0337	Rem/hr
N: Dose, METCON ext. 75cm	9.8295E-04	0.0288	Rem/hr
N: Dose, METCON ext. 105cm	8.8350E-04	0.026	Rem/hr

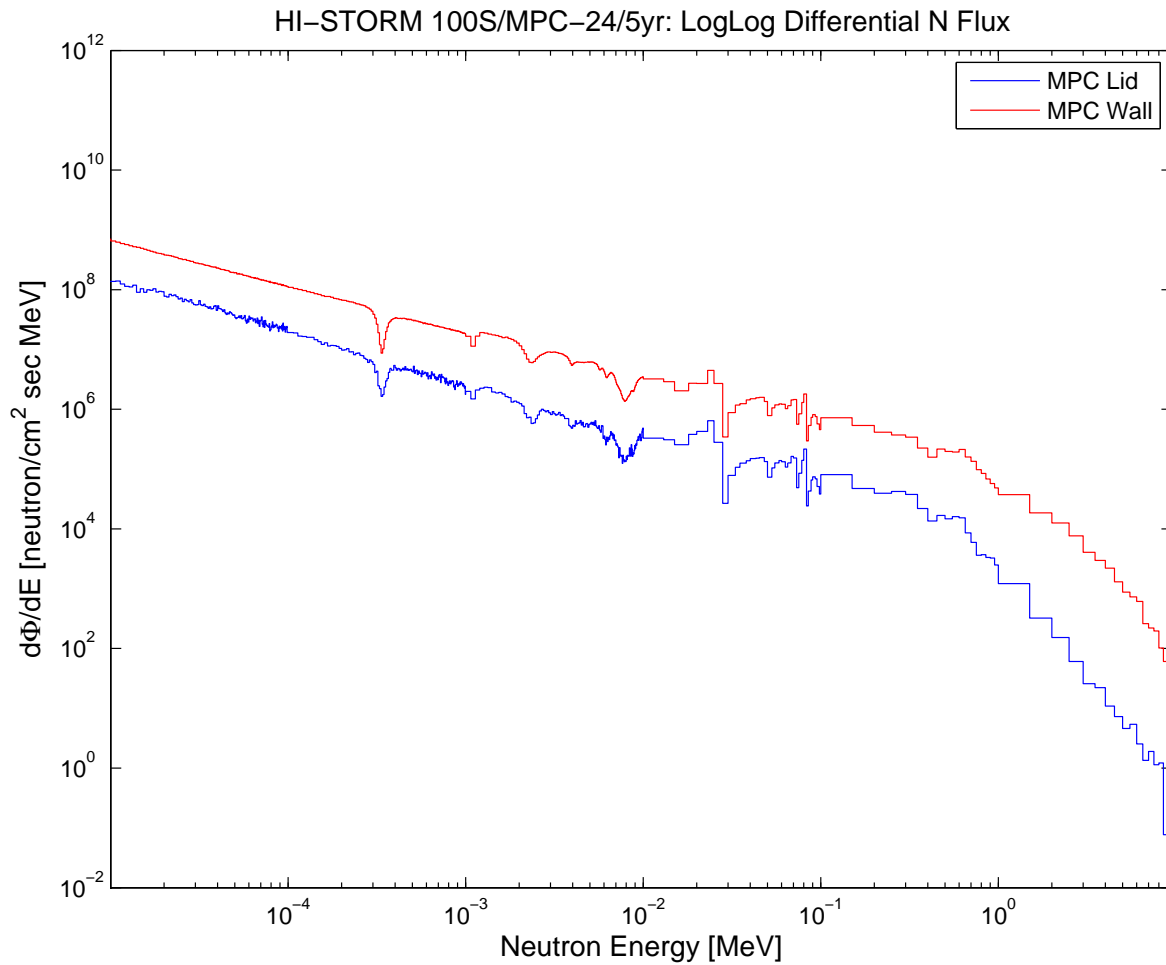


Figure 4.25: The transported neutron spectra taken as a surface average for the MPC-24, housed within a 100S METCON, and cooled for 5 yr.

HI-STORM 100S/MPC-24/5yr: N Dose(x,y), MPC Lid in mRad(Si)/hr

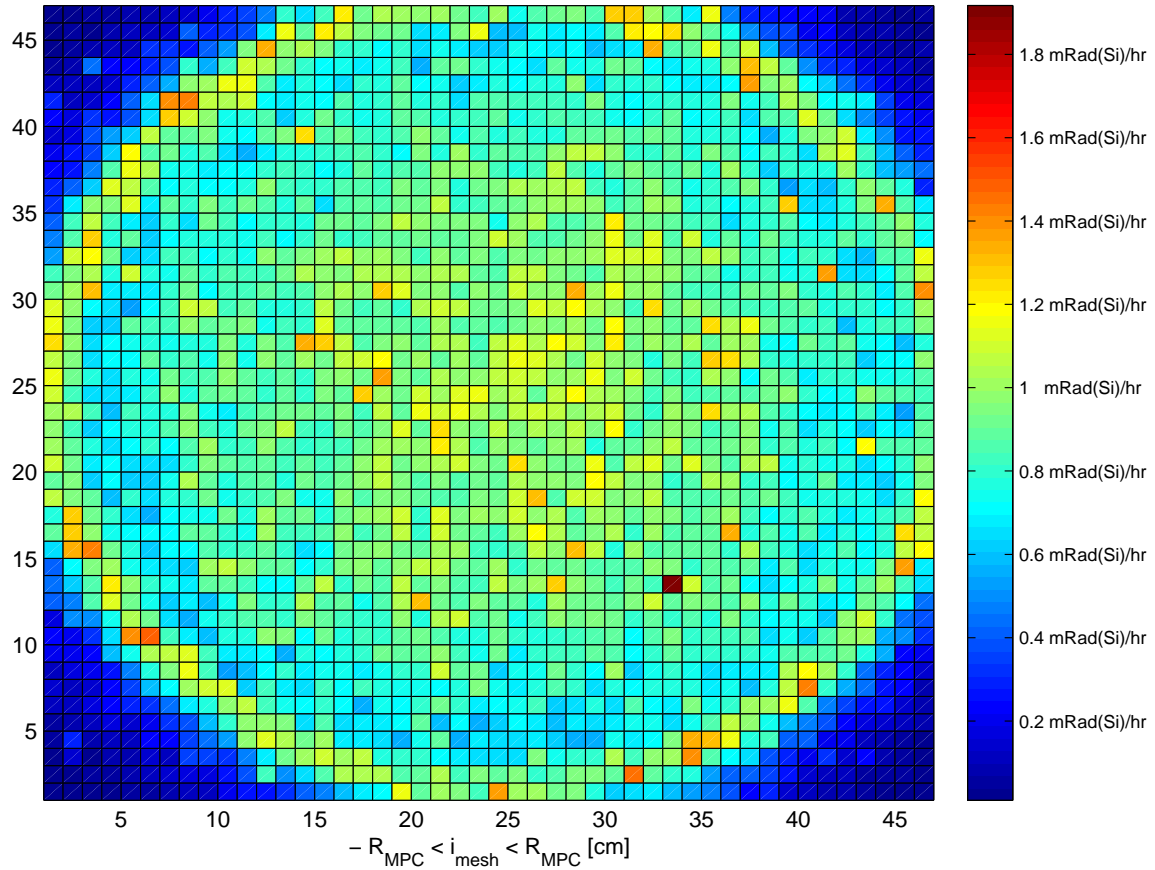


Figure 4.26: The MPC lid neutron dose rate for a 45·45 FMESH in a plane at the lid surface for a MPC-24, housed in a 100S METCON, and cooled for 5 yr. Dose is in $\frac{mRad(Si)}{hr}$ for the matrix of 4 cm cells. This is the proposed deployment surface for the delivery system of the robotic instrumentation.

HI-STORM 100S/MPC-24/5yr: N Dose(θ,z), MPC shell in mRad(Si)/hr

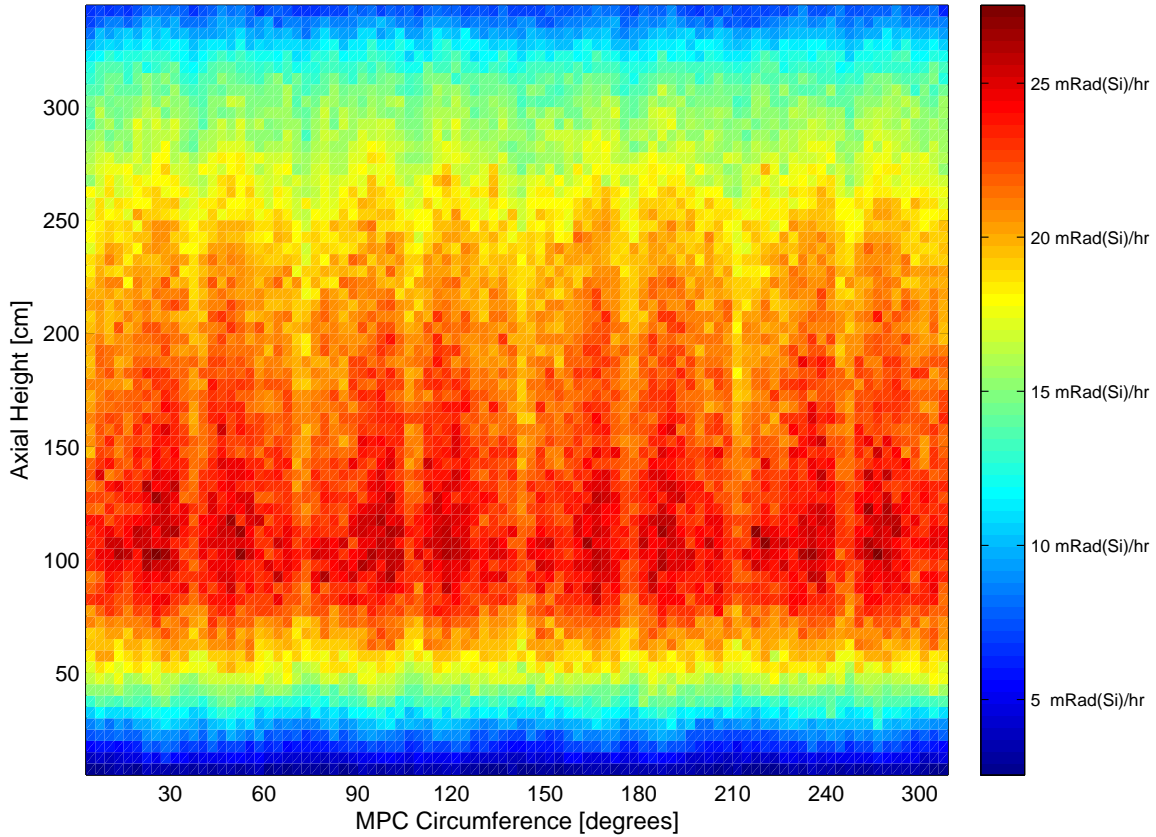


Figure 4.27: The MPC wall neutron dose rate for a $6\text{ cm} \cdot 6\text{ cm}$ coaxial FMESH wrapped around the outside of a MPC-24, housed in a 100S METCON, and cooled for 5 yr. The y-axis spans the bottom to the top of the MPC and the x-axis spans 0 to 2π . This details a V.C. Summer cycle of a Westinghouse 17×17 assembly burned to $57.535 \frac{\text{MWd}}{\text{kg}}$ and includes an ORIGAMI 28 zone axial emission profile.

Table 4.10: The neutron transport data for the HI-STORM 100S and MPC-24, populated with Westinghouse 17x17 assemblies enriched to 3.5%, with an ORIGAMI axial emission profile, a discharge burnup of $57.535 \frac{MWd}{kg}$, and cooled for 25yr.

Tally	Out	RE	Units
N: Co-60 Activation	7.5197E-02	0.0026	Bq/gm (per hr exp.)
N: Si Dose, MPC Wall, DF	7.9268E-03	0.0006	Rad(Si)/hr
N: Dose, outlet vent	1.4379E-02	0.0348	Rem/hr
N: Dose, inlet vent	1.7753E-03	0.0704	Rem/hr
N: Dose, METCON Wall	1.5357E-03	0.0141	Rem/hr
N: Flux, MPC Wall	2.4440E+05	0.0003	neutron/cm ² .sec
N: Flux, METCON Wall	8.6748E+01	0.0052	neutron/cm ² .sec
N: Flux, MPC Lid	2.4484E+04	0.0032	neutron/cm ² .sec
N: Dose, MPC Lid	4.0511E-04	0.0049	Rad(Si)/hr
N: Dose, left outlet	8.2648E-04	0.1186	Rem/hr
N: Dose, right outlet	7.4287E-04	0.0902	Rem/hr
N: Dose, bottom outlet	3.0215E-04	0.1766	Rem/hr
N: Dose, left inlet	2.0701E-04	0.3429	Rem/hr
N: Dose, right inlet	7.5245E-05	0.1298	Rem/hr
N: Dose, above inlet	2.8096E-04	0.3369	Rem/hr
N: Dose, w/o Pb shield	1.0112E-02	0.0257	Rad(Si)/hr
N: Dose, 4-side Pb shield	8.7780E-03	0.022	Rad(Si)/hr
N: Dose, 6-side Pb Shield	8.6961E-03	0.0213	Rad(Si)/hr
N: Dose, METCON ext. 15cm	9.7147E-04	0.0642	Rem/hr
N: Dose, METCON ext. 45cm	5.9631E-04	0.0404	Rem/hr
N: Dose, METCON ext. 75cm	5.0288E-04	0.0339	Rem/hr
N: Dose, METCON ext. 105cm	4.4110E-04	0.0302	Rem/hr

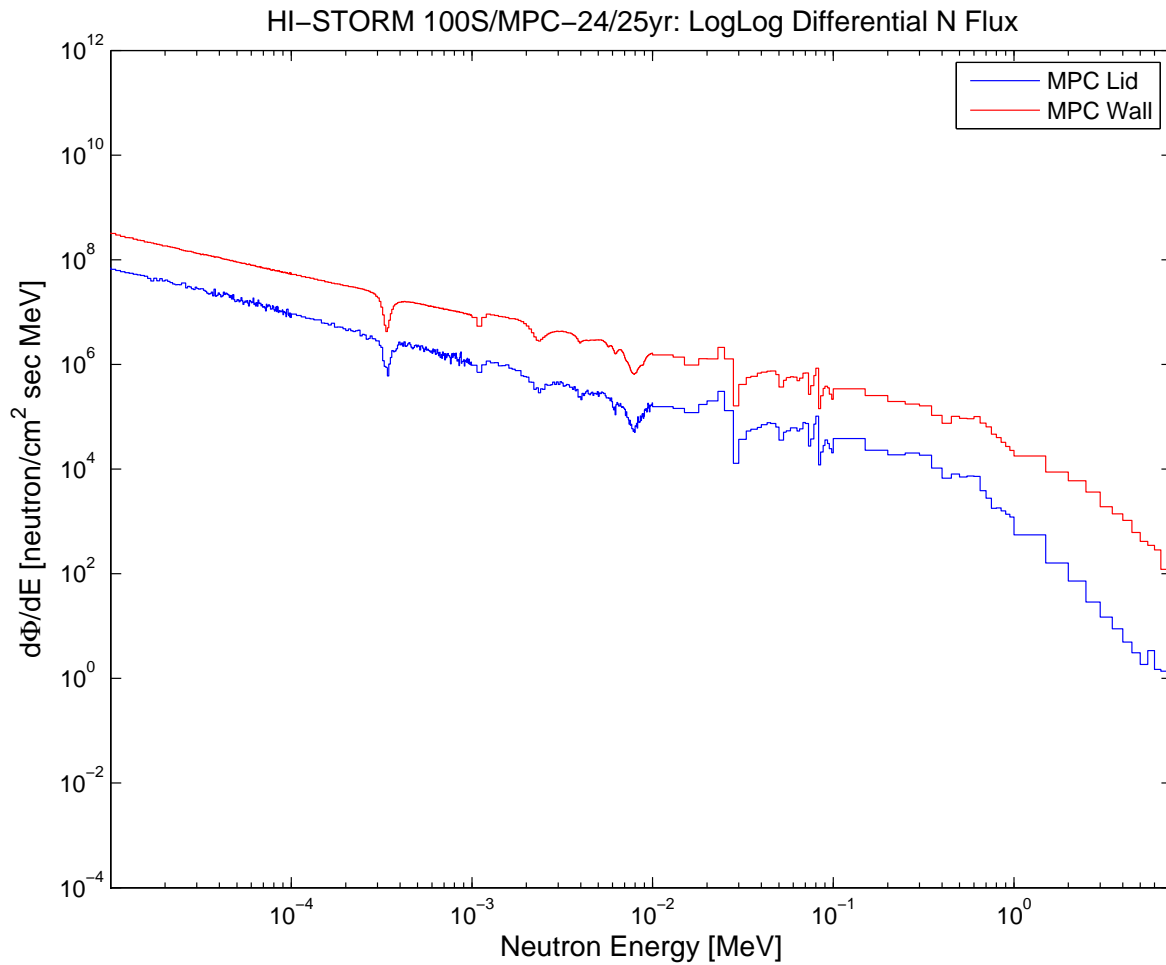


Figure 4.28: The transported neutron spectra taken as a surface average for the MPC-24, housed in a 100S METCON, and cooled for 25 yr.

HI-STORM 100S/MPC-24/25yr: N Dose(x,y), MPC Lid in mRad(Si)/hr

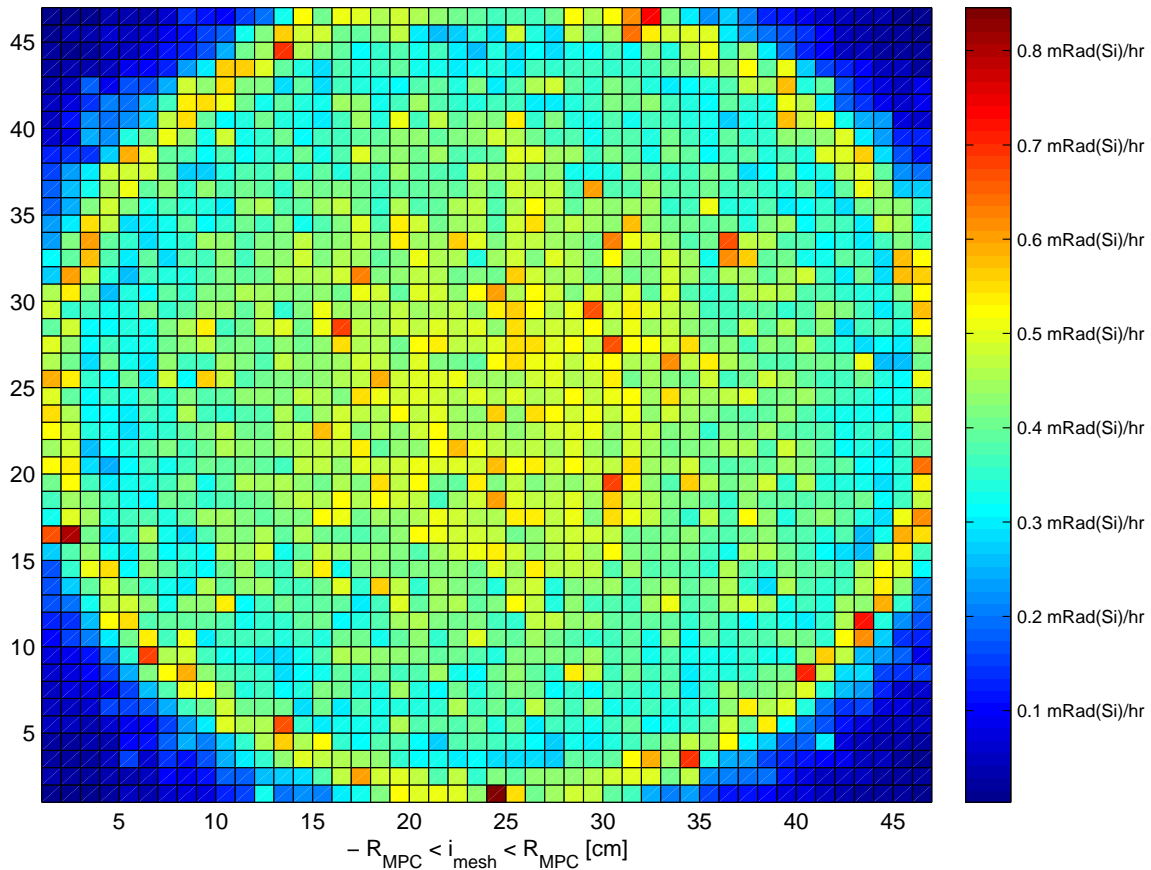


Figure 4.29: The MPC lid neutron dose rate for a 45·45 FMESH in a plane at the lid surface for a MPC-24, housed in a 100S METCON, and cooled for 25 yr. Dose is in $\frac{mRad(Si)}{hr}$ for the matrix of 4 cm cells. This is the proposed deployment surface for the delivery system of the robotic instrumentation.

HI-STORM 100S/MPC-24/25yr: N Dose(θ,z), MPC shell in mRad(Si)/hr

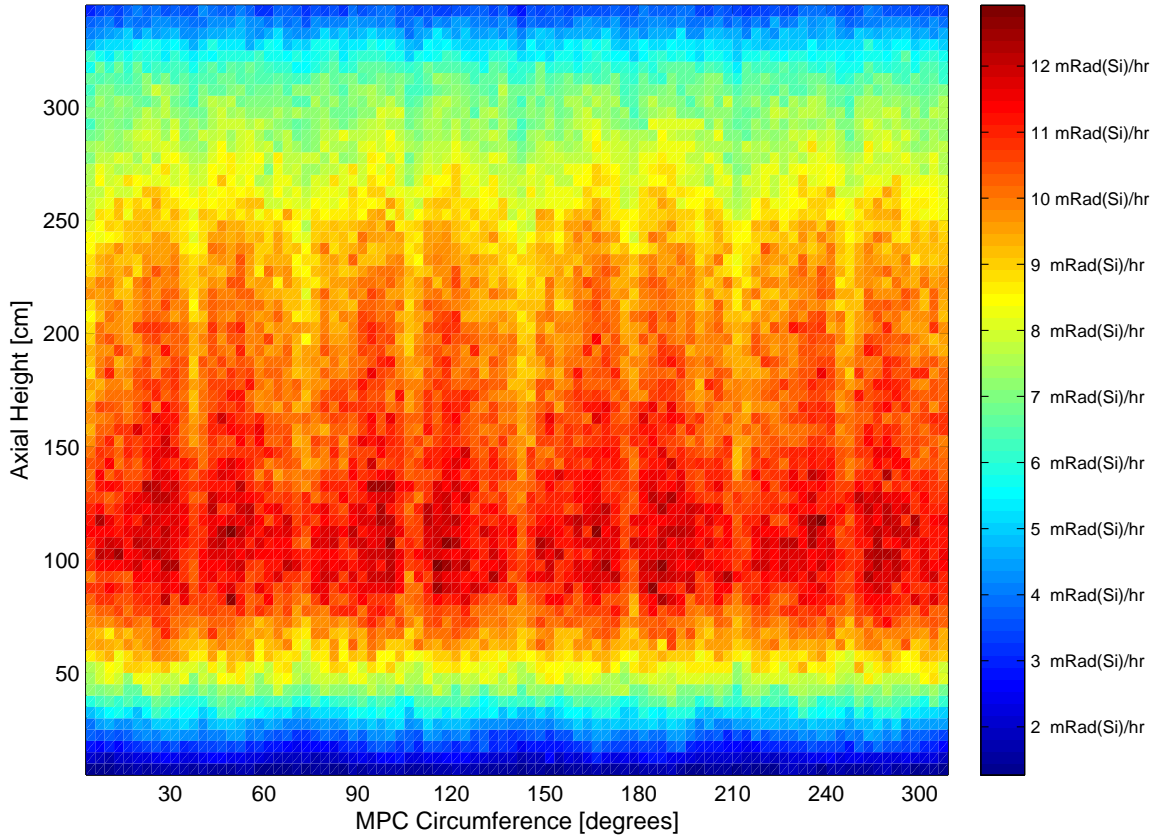


Figure 4.30: The MPC wall neutron dose rate for a $6\text{ cm} \cdot 6\text{ cm}$ coaxial FMESH wrapped around the outside of a MPC-24, housed in a 100S METCON, and cooled for 25 yr. The y-axis spans the bottom to the top of the MPC and the x-axis spans 0 to 2π . This details a V.C. Summer cycle of a Westinghouse 17×17 assembly burned to $57.535 \frac{\text{MWd}}{\text{kg}}$ and includes an ORIGAMI 28 zone axial emission profile.

Table 4.11: The neutron transport data for the HI-STORM 100S and MPC-32, populated with Westinghouse 17x17 assemblies enriched to 3.5%, with an ORIGAMI axial emission profile, a discharge burnup of $57.535 \frac{MWd}{kg}$, and cooled for 5yr.

Tally	Out	RE	Units
N: Co-60 Activation	2.1773E-01	0.0014	Bq/gm (per hr exp.)
N: Si Dose, MPC Wall, DF	2.4491E-02	0.0004	Rad(Si)/hr
N: Dose, outlet vent	5.1187E-02	0.0211	Rem/hr
N: Dose, inlet vent	6.3433E-03	0.0413	Rem/hr
N: Dose, METCON Wall	5.4323E-03	0.0072	Rem/hr
N: Flux, MPC Wall	7.1801E+05	0.0002	neutron/cm ² .sec
N: Flux, METCON Wall	2.7162E+02	0.0028	neutron/cm ² .sec
N: Flux, MPC Lid	7.8803E+04	0.0017	neutron/cm ² .sec
N: Dose, MPC Lid	1.4229E-03	0.0028	Rad(Si)/hr
N: Dose, left outlet	2.4414E-03	0.0365	Rem/hr
N: Dose, right outlet	2.6109E-03	0.0684	Rem/hr
N: Dose, bottom outlet	9.5776E-04	0.1177	Rem/hr
N: Dose, left inlet	5.0084E-04	0.1919	Rem/hr
N: Dose, right inlet	3.5727E-04	0.1218	Rem/hr
N: Dose, above inlet	1.0432E-03	0.1891	Rem/hr
N: Dose, w/o Pb shield	3.2223E-02	0.0144	Rad(Si)/hr
N: Dose, 4-side Pb shield	2.9209E-02	0.0127	Rad(Si)/hr
N: Dose, 6-side Pb Shield	2.6727E-02	0.0124	Rad(Si)/hr
N: Dose, METCON ext. 15cm	3.5146E-03	0.0676	Rem/hr
N: Dose, METCON ext. 45cm	1.9643E-03	0.0314	Rem/hr
N: Dose, METCON ext. 75cm	1.6267E-03	0.0178	Rem/hr
N: Dose, METCON ext. 105cm	1.4380E-03	0.0152	Rem/hr

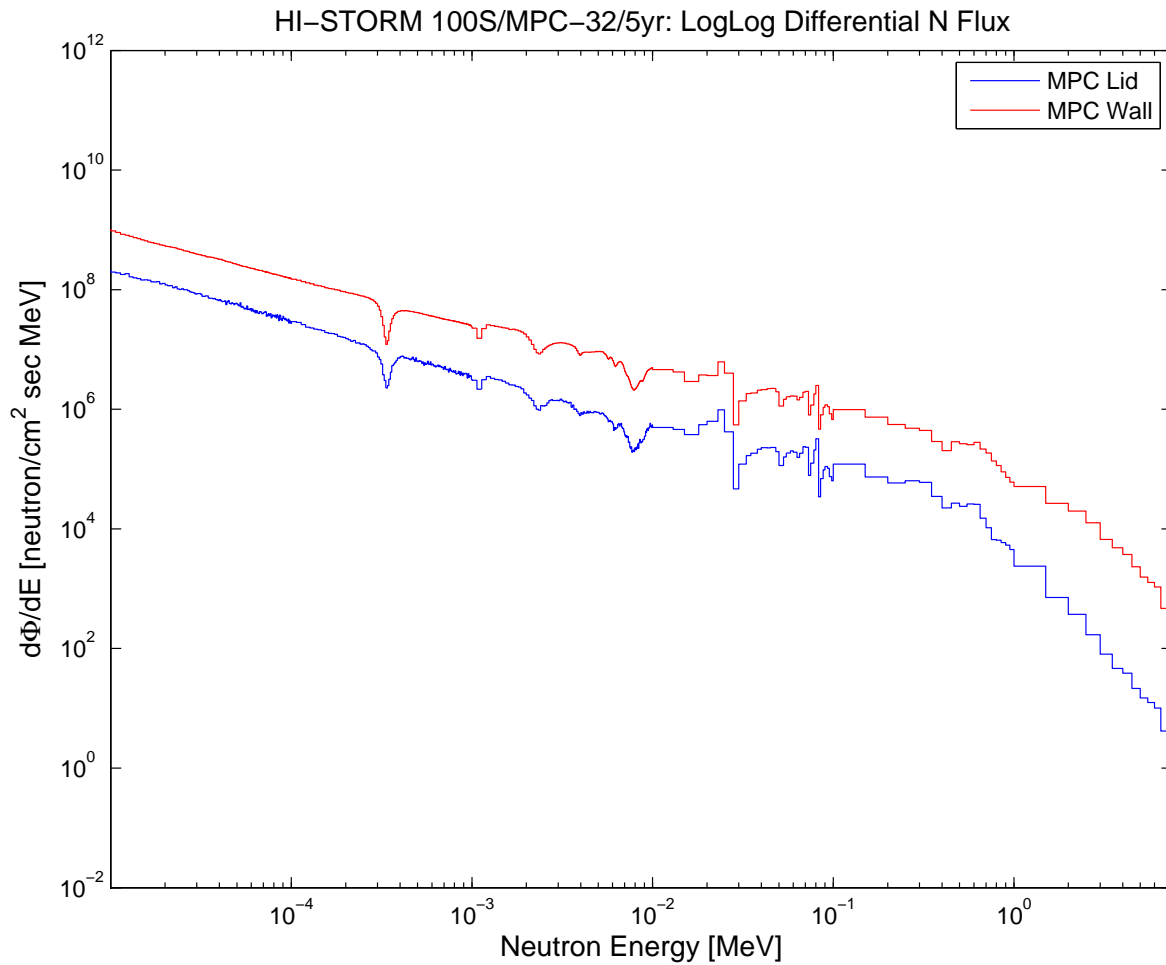


Figure 4.31: The transported neutron spectra taken as a surface average for the MPC-32, housed in a 100S METCON, and cooled for 5 yr.

HI-STORM 100S/MPC-32/5yr: N Dose(x,y), MPC Lid in mRad(Si)/hr

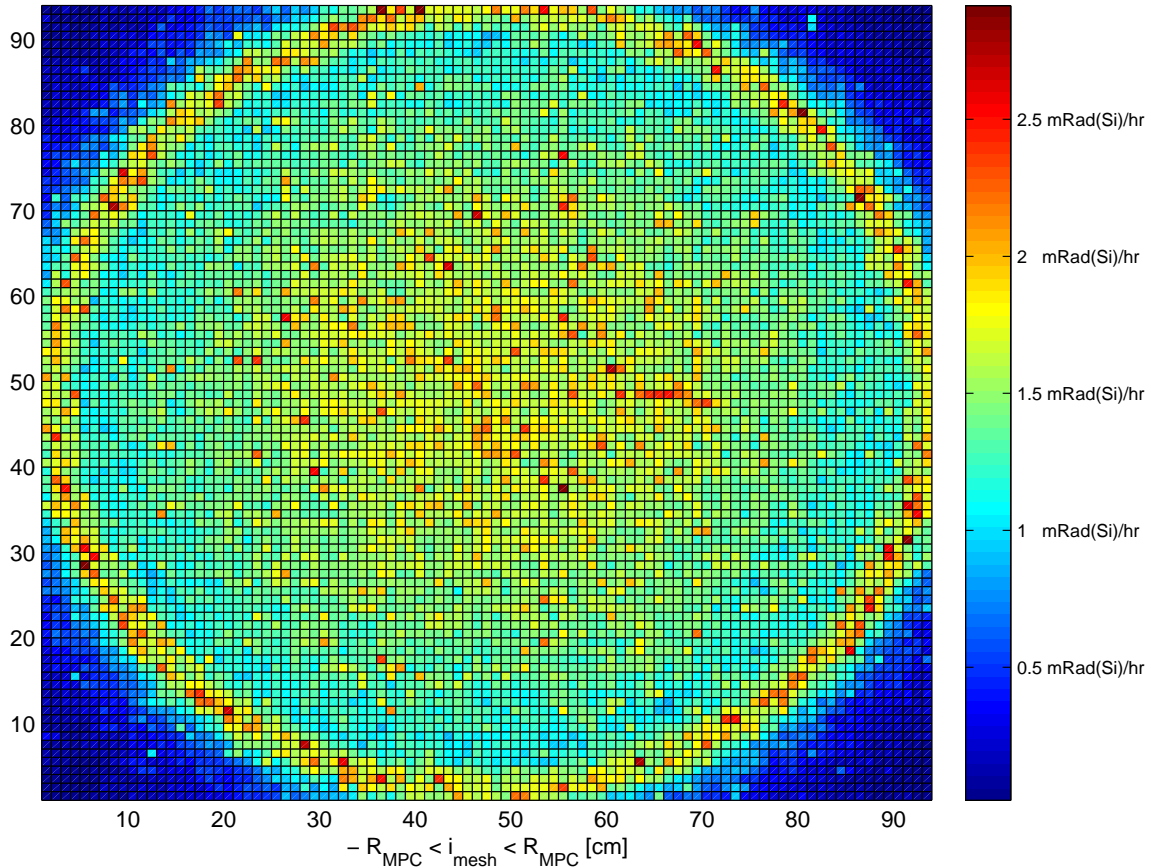


Figure 4.32: The MPC lid neutron dose rate for a 45·45 FMESH in a plane at the lid surface for a MPC-32, housed in a 100S METCON, and cooled for 5 yr. Dose is in $\frac{mRad(Si)}{hr}$ for the matrix of 4 cm cells. This is the proposed deployment surface for the delivery system of the robotic instrumentation.

Table 4.12: The neutron transport data for the HI-STORM 100S and MPC-32, populated with Westinghouse 17x17 assemblies enriched to 3.5%, with an ORIGAMI axial emission profile, a discharge burnup of $57.535 \frac{MWd}{kg}$, and cooled for 15yr.

Tally	Out	RE	Units
N: Co-60 Activation	1.4953E-01	0.0014	Bq/gm (per hr exp.)
N: Si Dose, MPC Wall, DF	1.6702E-02	0.0004	Rad(Si)/hr
N: Dose, outlet vent	3.3993E-02	0.0198	Rem/hr
N: Dose, inlet vent	4.4055E-03	0.0383	Rem/hr
N: Dose, METCON Wall	3.7062E-03	0.0071	Rem/hr
N: Flux, MPC Wall	4.9017E+05	0.0002	neutron/cm ² .sec
N: Flux, METCON Wall	1.8450E+02	0.0028	neutron/cm ² .sec
N: Flux, MPC Lid	5.4023E+04	0.0016	neutron/cm ² .sec
N: Dose, MPC Lid	9.7467E-04	0.0027	Rad(Si)/hr
N: Dose, left outlet	1.7789E-03	0.0624	Rem/hr
N: Dose, right outlet	1.9742E-03	0.0682	Rem/hr
N: Dose, bottom outlet	7.9687E-04	0.1402	Rem/hr
N: Dose, left inlet	3.1596E-04	0.1463	Rem/hr
N: Dose, right inlet	3.9308E-04	0.2045	Rem/hr
N: Dose, above inlet	7.2774E-04	0.2293	Rem/hr
N: Dose, w/o Pb shield	2.1331E-02	0.0138	Rad(Si)/hr
N: Dose, 4-side Pb shield	2.0187E-02	0.0128	Rad(Si)/hr
N: Dose, 6-side Pb Shield	1.8508E-02	0.0129	Rad(Si)/hr
N: Dose, METCON ext. 15cm	2.5276E-03	0.0603	Rem/hr
N: Dose, METCON ext. 45cm	1.3203E-03	0.0231	Rem/hr
N: Dose, METCON ext. 75cm	1.0973E-03	0.0176	Rem/hr
N: Dose, METCON ext. 105cm	9.7400E-04	0.015	Rem/hr

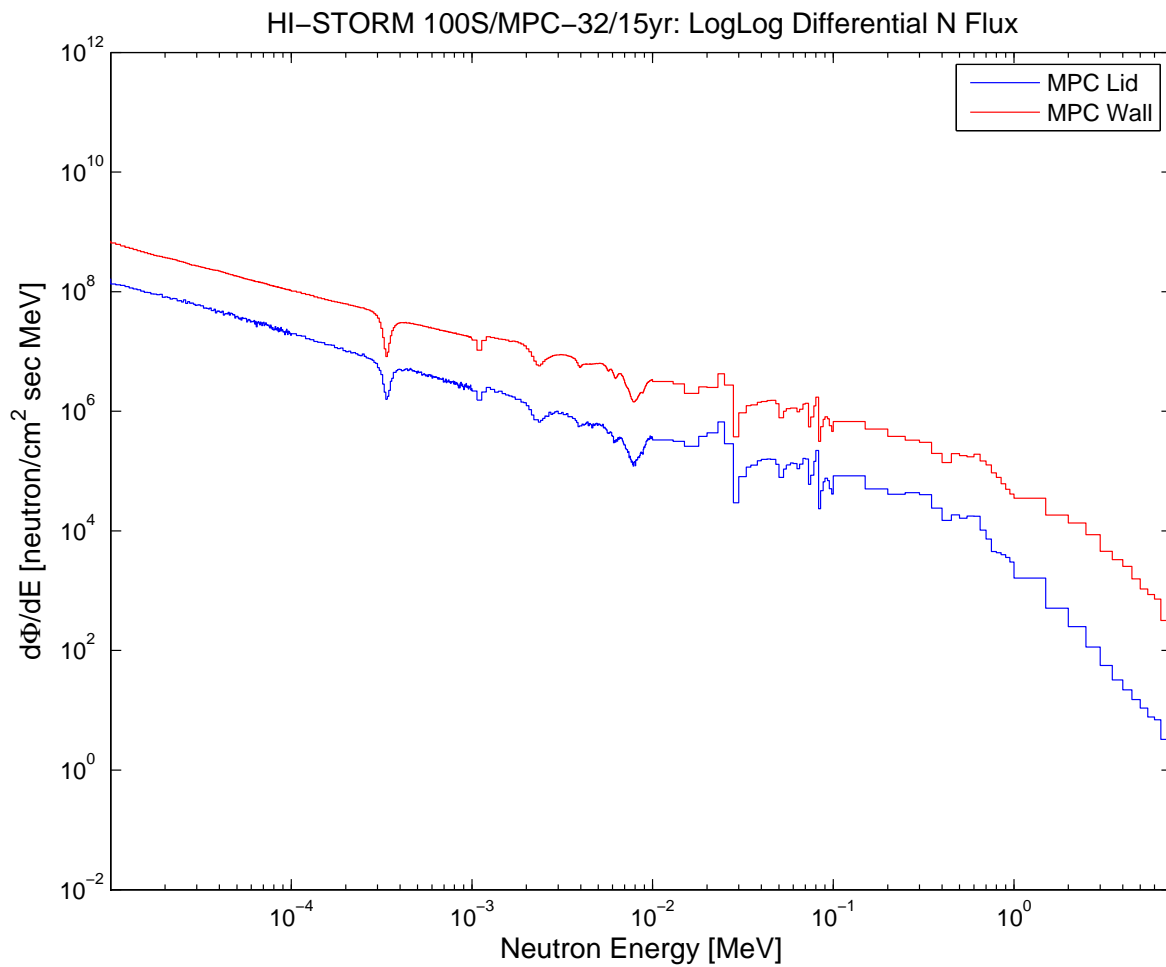


Figure 4.33: The transported neutron spectra taken as a surface average for the MPC-32, housed in a 100S METCON, and cooled for 15 yr.

HI-STORM 100S/MPC-32/15yr: N Dose(x,y), MPC Lid in mRad(Si)/hr

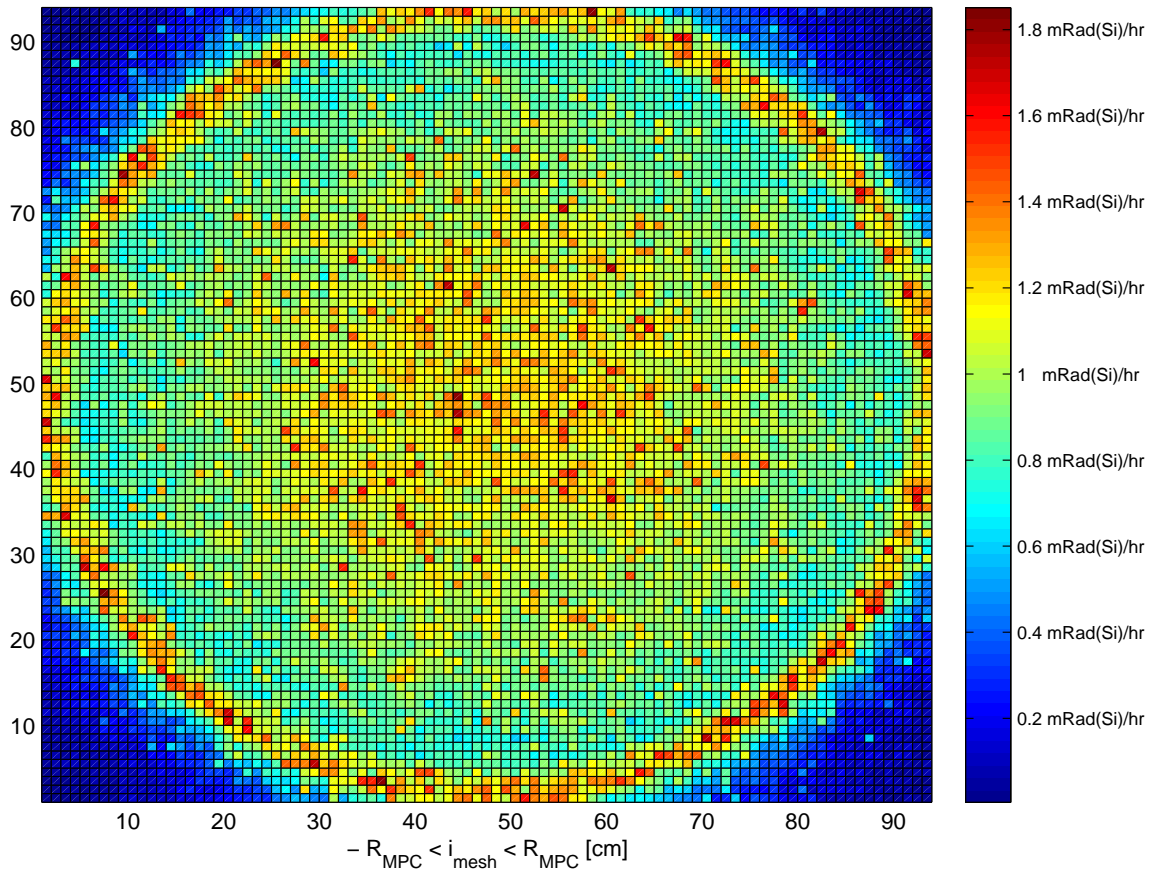


Figure 4.34: The MPC lid neutron dose rate for a 45·45 FMESH in a plane at the lid surface for a MPC-32, housed in a 100S METCON, and cooled for 15 yr. Dose is in $\frac{mRad(Si)}{hr}$ for the matrix of 4 cm cells. This is the proposed deployment surface for the delivery system of the robotic instrumentation.

Table 4.13: The neutron transport data for the HI-STORM 100S and MPC-32, populated with Westinghouse 17x17 assemblies enriched to 3.5%, with an ORIGAMI axial emission profile, a discharge burnup of $57.535 \frac{MWd}{kg}$, and cooled for 25yr.

Tally	Out	RE	Units
N: Co-60 Activation	1.0356E-01	0.0019	Bq/gm (per hr exp.)
N: Si Dose, MPC Wall, DF	1.1581E-02	0.0005	Rad(Si)/hr
N: Dose, outlet vent	2.3267E-02	0.0263	Rem/hr
N: Dose, inlet vent	3.1331E-03	0.0561	Rem/hr
N: Dose, METCON Wall	2.5524E-03	0.0102	Rem/hr
N: Flux, MPC Wall	3.4017E+05	0.0003	neutron/cm ² .sec
N: Flux, METCON Wall	1.2872E+02	0.004	neutron/cm ² .sec
N: Flux, MPC Lid	3.7419E+04	0.0024	neutron/cm ² .sec
N: Dose, MPC Lid	6.7950E-04	0.0039	Rad(Si)/hr
N: Dose, left outlet	1.3103E-03	0.0692	Rem/hr
N: Dose, right outlet	1.3061E-03	0.0799	Rem/hr
N: Dose, bottom outlet	5.0906E-04	0.125	Rem/hr
N: Dose, left inlet	1.4270E-04	0.0826	Rem/hr
N: Dose, right inlet	2.5295E-04	0.2786	Rem/hr
N: Dose, above inlet	3.9167E-04	0.1754	Rem/hr
N: Dose, w/o Pb shield	1.4783E-02	0.0206	Rad(Si)/hr
N: Dose, 4-side Pb shield	1.3772E-02	0.0174	Rad(Si)/hr
N: Dose, 6-side Pb Shield	1.3034E-02	0.0187	Rad(Si)/hr
N: Dose, METCON ext. 15cm	1.7083E-03	0.0675	Rem/hr
N: Dose, METCON ext. 45cm	9.1530E-04	0.0293	Rem/hr
N: Dose, METCON ext. 75cm	7.8151E-04	0.0279	Rem/hr
N: Dose, METCON ext. 105cm	7.0492E-04	0.0325	Rem/hr

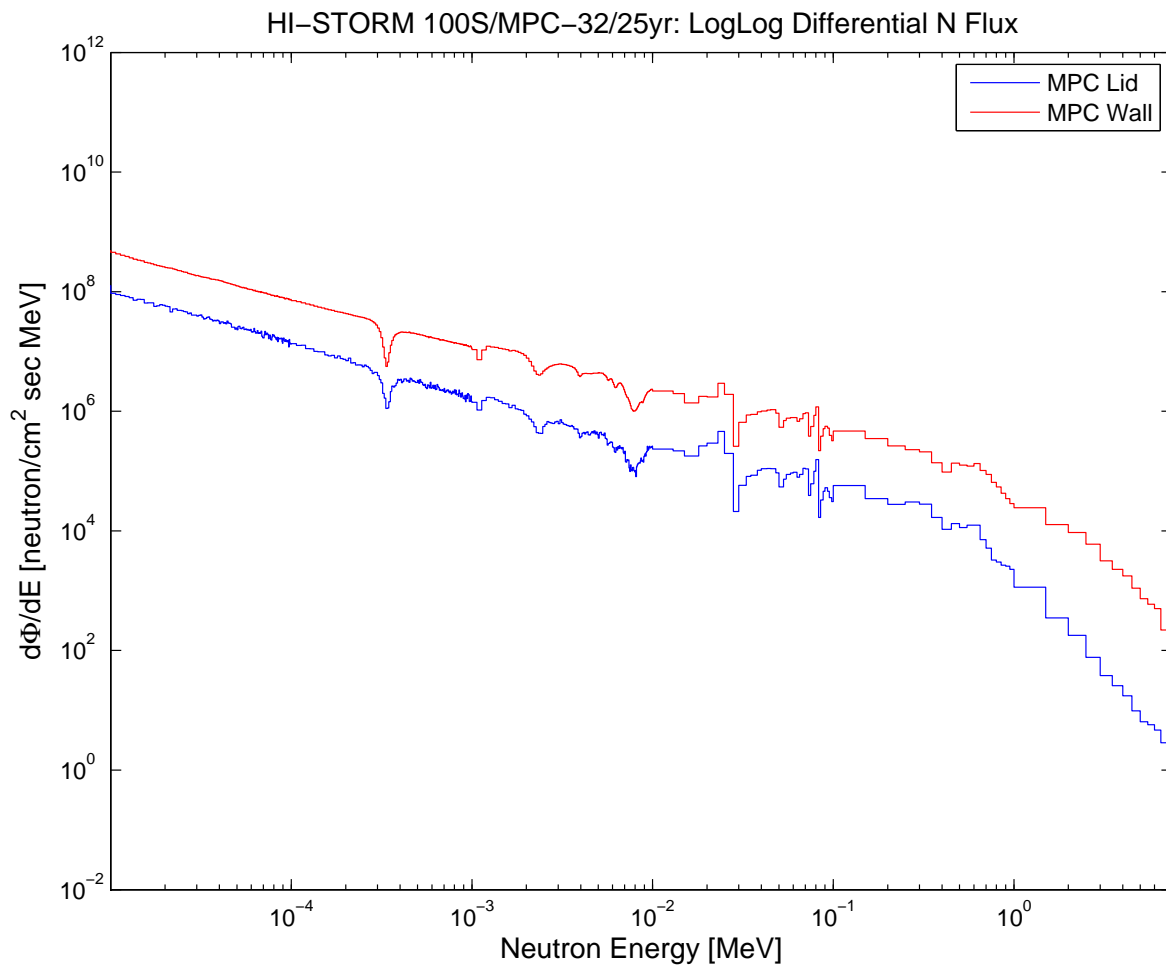


Figure 4.35: The transported neutron spectra taken as a surface average for the MPC-32, housed in a 100S METCON, and cooled for 25 yr.

HI-STORM 100S/MPC-32/25yr: N Dose(x,y), MPC Lid in mRad(Si)/hr

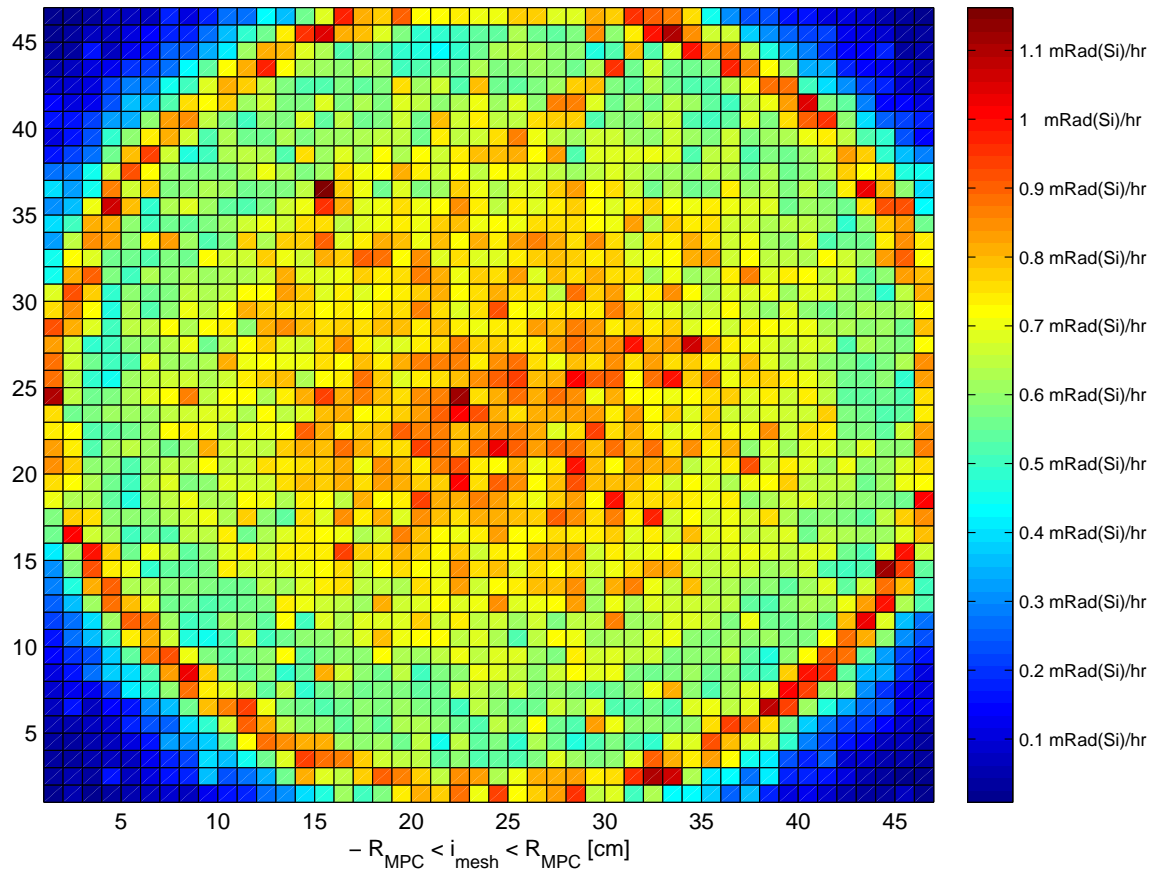


Figure 4.36: The MPC lid neutron dose rate for a 45·45 FMESH in a plane at the lid surface for a MPC-32, housed in a 100S METCON, and cooled for 25 yr. Dose is in $\frac{mRad(Si)}{hr}$ for the matrix of 4 cm cells. This is the proposed deployment surface for the delivery system of the robotic instrumentation.

HI-STORM 100S/MPC-32/25yr: N Dose(θ,z), MPC shell in mRad(Si)/hr

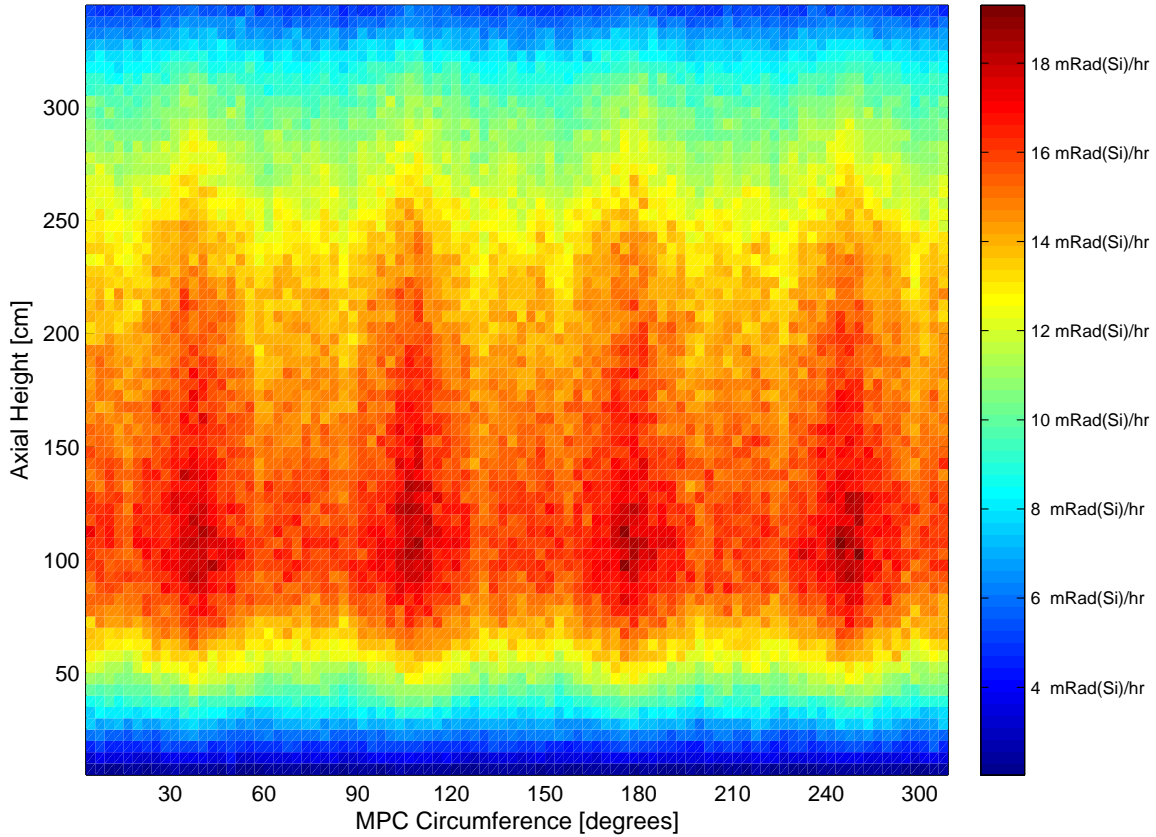


Figure 4.37: The MPC wall neutron dose rate for a $6\text{ cm} \cdot 6\text{ cm}$ coaxial FMESH wrapped around the outside of a MPC-32, housed in a 100S METCON, and cooled for 25 yr. The y-axis spans the bottom to the top of the MPC and the x-axis spans 0 to 2π . This details a V.C. Summer cycle of a Westinghouse 17×17 assembly burned to $57.535 \frac{\text{MWd}}{\text{kg}}$ and includes an ORIGAMI 28 zone axial emission profile.

Table 4.14: The neutron transport data is given for the HI-STORM 100S and MPC-68, populated with General Electric assemblies, enriched to 3.5%, burned in ORIGEN-ARP to 25.344 $\frac{MWd}{kg}$, and cooled for 5yr.

Tally	Out	RE	Units
N: Co-60 Activation	2.7851E-03	0.0013	Bq/gm (per hr exp.)
N: Si Dose, MPC Wall, DF	3.2813E-04	0.0003	Rad(Si)/hr
N: Dose, outlet vent	1.6331E-03	0.0132	Rem/hr
N: Dose, inlet vent	9.6000E-05	0.032	Rem/hr
N: Dose, METCON Wall	7.4433E-05	0.0067	Rem/hr
N: Flux, MPC Wall	9.4000E+03	0.0002	neutron/cm ² .sec
N: Flux, METCON Wall	3.7221E+00	0.0026	neutron/cm ² .sec
N: Flux, MPC Lid	2.3602E+03	0.001	neutron/cm ² .sec
N: Dose, MPC Lid	4.6332E-05	0.0017	Rad(Si)/hr
N: Dose, left outlet	8.3955E-05	0.0319	Rem/hr
N: Dose, right outlet	8.6298E-05	0.0298	Rem/hr
N: Dose, bottom outlet	3.9653E-05	0.0863	Rem/hr
N: Dose, left inlet	6.4913E-06	0.1434	Rem/hr
N: Dose, right inlet	6.6806E-06	0.1833	Rem/hr
N: Dose, above inlet	1.6919E-05	0.2682	Rem/hr
N: Dose, w/o Pb shield	3.4609E-04	0.0154	Rad(Si)/hr
N: Dose, 4-side Pb shield	3.4041E-04	0.0121	Rad(Si)/hr
N: Dose, 6-side Pb Shield	3.4589E-04	0.0123	Rad(Si)/hr
N: Dose, METCON ext. 15cm	5.0437E-05	0.0353	Rem/hr
N: Dose, METCON ext. 45cm	2.8124E-05	0.0202	Rem/hr
N: Dose, METCON ext. 75cm	2.2811E-05	0.0162	Rem/hr
N: Dose, METCON ext. 105cm	1.9643E-05	0.0142	Rem/hr

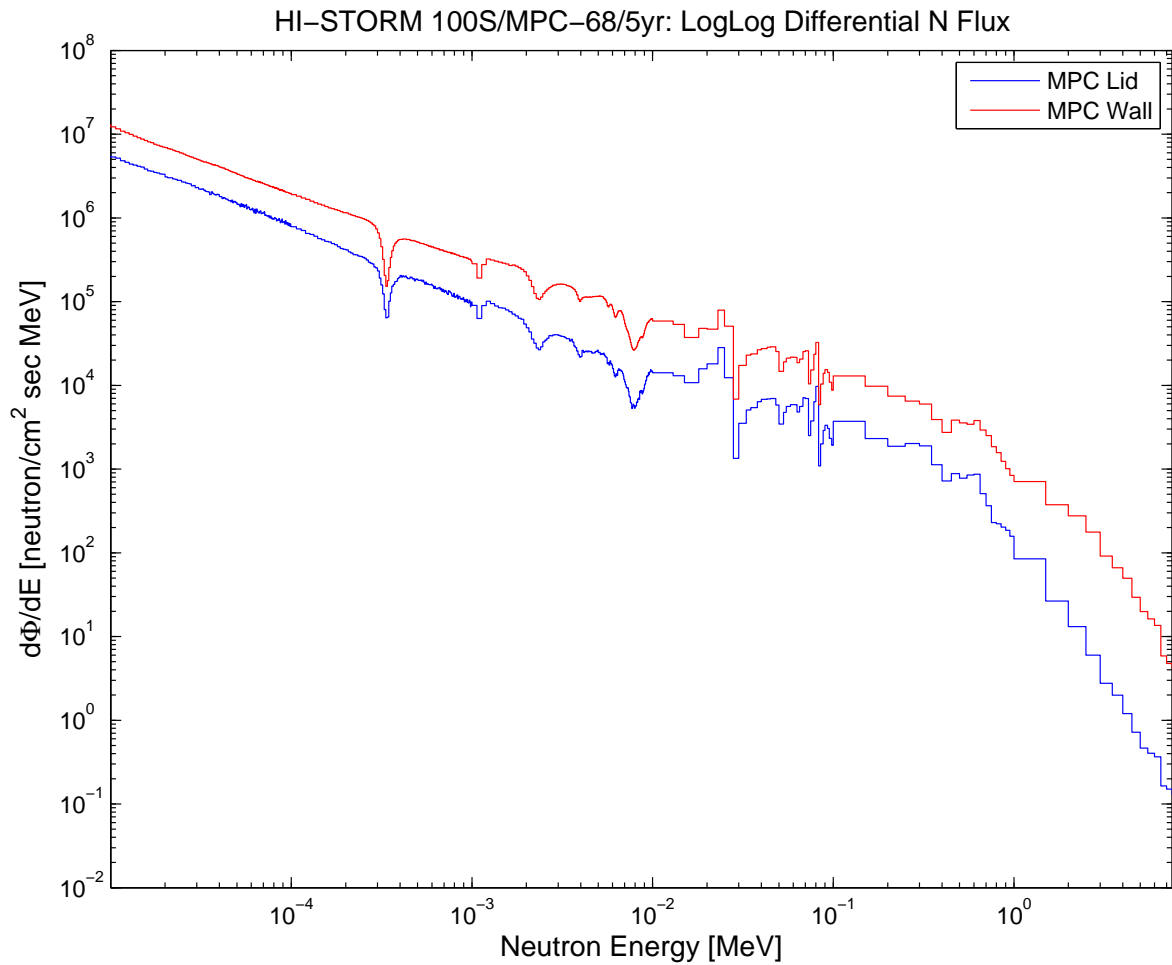


Figure 4.38: The transported neutron spectra taken as a surface average for the MPC-68, housed in a 100S METCON, and cooled for 5 yr.

HI-STORM 100S/MPC-68/5yr: N Dose(x,y), MPC Lid in mRad(Si)/hr

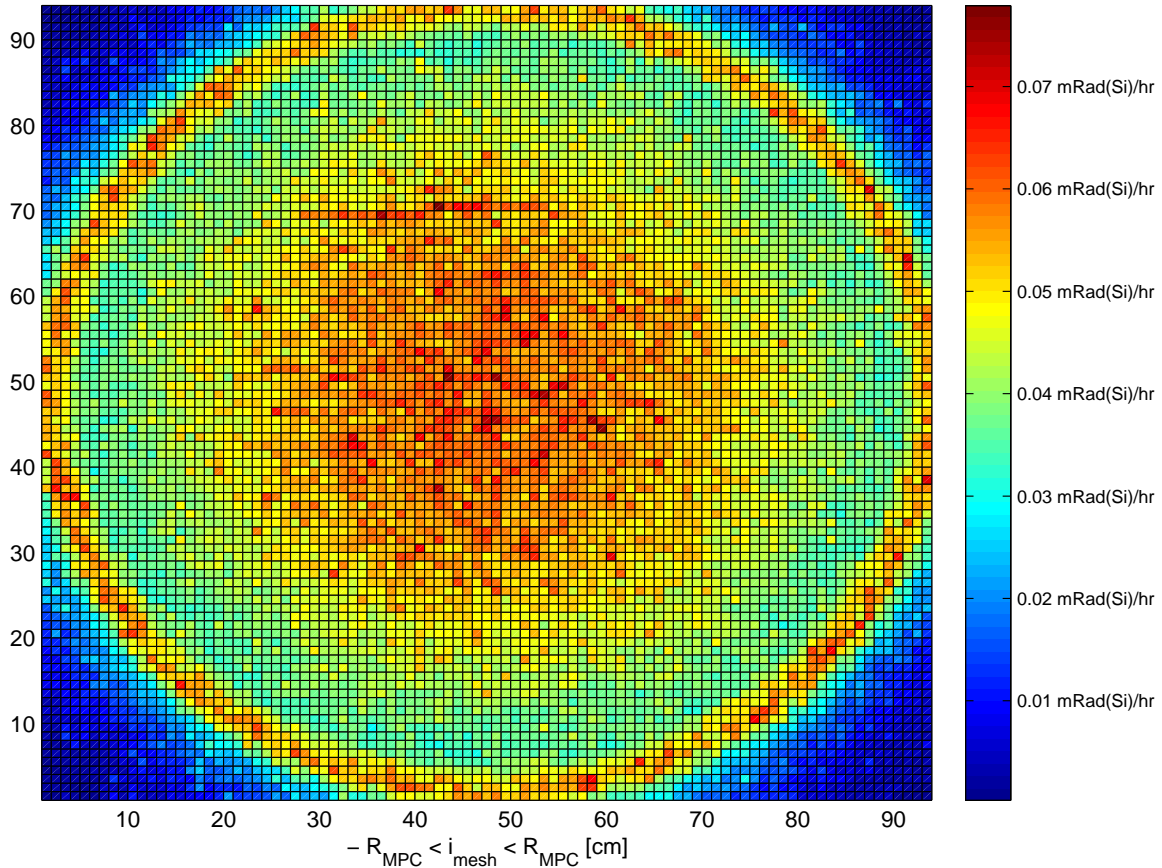


Figure 4.39: The MPC lid neutron dose rate for a 45·45 FMESH in a plane at the lid surface for a MPC-68, housed in a 100S METCON, and cooled for 5 yr. Dose is in $\frac{mRad(Si)}{hr}$ for the matrix of 4 cm cells. This is the proposed deployment surface for the delivery system of the robotic instrumentation.

Table 4.15: The neutron transport data is given for the HI-STORM 100S and MPC-68, populated with General Electric assemblies, enriched to 3.5%, burned in ORIGEN-ARP to 25.344 $\frac{MWd}{kg}$, and cooled for 15yr.

Tally	Out	RE	Units
N: Co-60 Activation	2.0344E-03	0.0013	Bq/gm (per hr exp.)
N: Si Dose, MPC Wall, DF	2.3870E-04	0.0003	Rad(Si)/hr
N: Dose, outlet vent	1.1962E-03	0.0122	Rem/hr
N: Dose, inlet vent	7.1288E-05	0.0322	Rem/hr
N: Dose, METCON Wall	5.4270E-05	0.0067	Rem/hr
N: Flux, MPC Wall	6.8546E+03	0.0002	neutron/cm ² .sec
N: Flux, METCON Wall	2.7244E+00	0.0026	neutron/cm ² .sec
N: Flux, MPC Lid	1.7206E+03	0.001	neutron/cm ² .sec
N: Dose, MPC Lid	3.3662E-05	0.0016	Rad(Si)/hr
N: Dose, left outlet	6.3329E-05	0.0324	Rem/hr
N: Dose, right outlet	6.5630E-05	0.0391	Rem/hr
N: Dose, bottom outlet	4.4656E-05	0.1488	Rem/hr
N: Dose, left inlet	8.3157E-06	0.4158	Rem/hr
N: Dose, right inlet	4.5289E-06	0.1199	Rem/hr
N: Dose, above inlet	1.0312E-05	0.1661	Rem/hr
N: Dose, w/o Pb shield	2.5415E-04	0.0162	Rad(Si)/hr
N: Dose, 4-side Pb shield	2.4904E-04	0.0126	Rad(Si)/hr
N: Dose, 6-side Pb Shield	2.5136E-04	0.0125	Rad(Si)/hr
N: Dose, METCON ext. 15cm	3.6278E-05	0.0328	Rem/hr
N: Dose, METCON ext. 45cm	2.0064E-05	0.0188	Rem/hr
N: Dose, METCON ext. 75cm	1.6354E-05	0.016	Rem/hr
N: Dose, METCON ext. 105cm	1.4081E-05	0.0144	Rem/hr

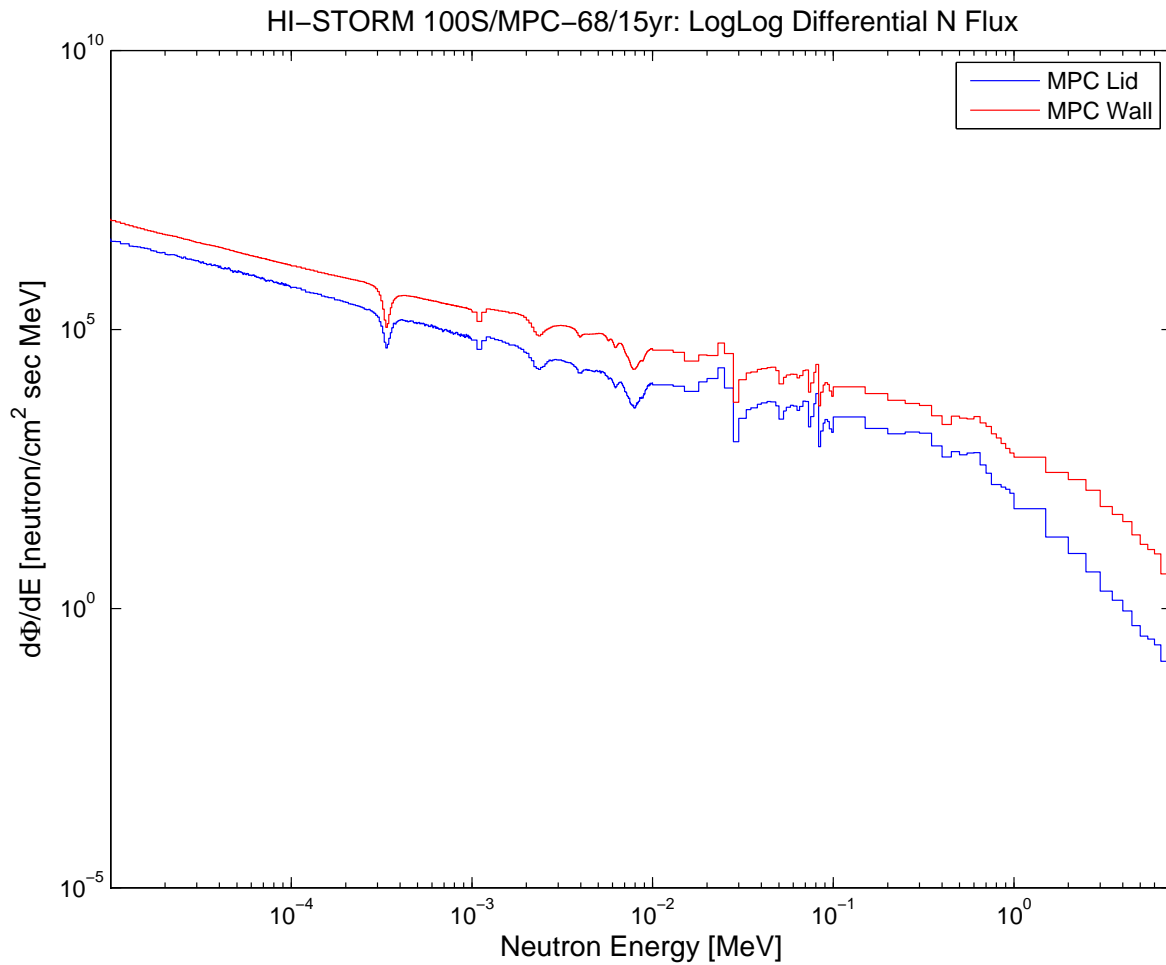


Figure 4.40: The transported neutron spectra taken as a surface average for the MPC-68, housed in a 100S METCON, and cooled for 15 yr.

HI-STORM 100S/MPC-68/15yr: N Dose(x,y), MPC Lid in mRad(Si)/hr

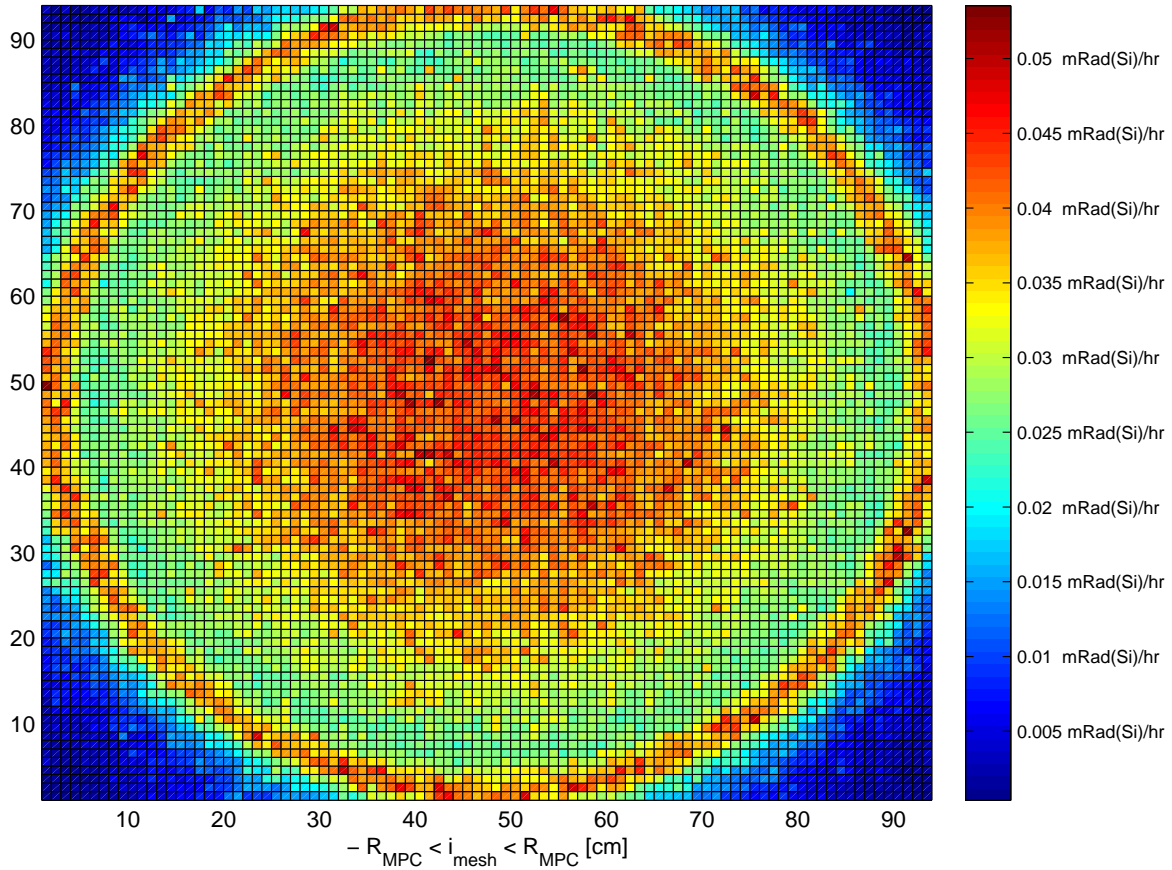


Figure 4.41: The MPC lid neutron dose rate for a 45·45 FMESH in a plane at the lid surface for a MPC-68, housed in a 100S METCON, and cooled for 15 yr. Dose is in $\frac{mRad(Si)}{hr}$ for the matrix of 4 cm cells. This is the proposed deployment surface for the delivery system of the robotic instrumentation.

Table 4.16: The neutron transport data is given for the HI-STORM 100S and MPC-68, populated with General Electric assemblies, enriched to 3.5%, burned in ORIGEN-ARP to $25.344 \frac{MWd}{kg}$, and cooled for 25yr.

Tally	Out	RE	Units
N: Co-60 Activation	1.5141E-03	0.0019	Bq/gm (per hr exp.)
N: Si Dose, MPC Wall, DF	1.7737E-04	0.0005	Rad(Si)/hr
N: Dose, outlet vent	8.7725E-04	0.0185	Rem/hr
N: Dose, inlet vent	5.0879E-05	0.0471	Rem/hr
N: Dose, METCON Wall	4.0421E-05	0.0094	Rem/hr
N: Flux, MPC Wall	5.1112E+03	0.0002	neutron/cm ² .sec
N: Flux, METCON Wall	2.0434E+00	0.0037	neutron/cm ² .sec
N: Flux, MPC Lid	1.2816E+03	0.0015	neutron/cm ² .sec
N: Dose, MPC Lid	2.5157E-05	0.0024	Rad(Si)/hr
N: Dose, left outlet	4.8229E-05	0.0739	Rem/hr
N: Dose, right outlet	4.3966E-05	0.0432	Rem/hr
N: Dose, bottom outlet	2.1831E-05	0.1363	Rem/hr
N: Dose, left inlet	2.3157E-06	0.0935	Rem/hr
N: Dose, right inlet	4.6253E-06	0.3653	Rem/hr
N: Dose, above inlet	9.6855E-06	0.2206	Rem/hr
N: Dose, w/o Pb shield	1.9303E-04	0.024	Rad(Si)/hr
N: Dose, 4-side Pb shield	1.8897E-04	0.0167	Rad(Si)/hr
N: Dose, 6-side Pb Shield	1.8447E-04	0.0177	Rad(Si)/hr
N: Dose, METCON ext. 15cm	2.5334E-05	0.0531	Rem/hr
N: Dose, METCON ext. 45cm	1.4902E-05	0.0305	Rem/hr
N: Dose, METCON ext. 75cm	1.2552E-05	0.0362	Rem/hr
N: Dose, METCON ext. 105cm	1.0574E-05	0.0222	Rem/hr

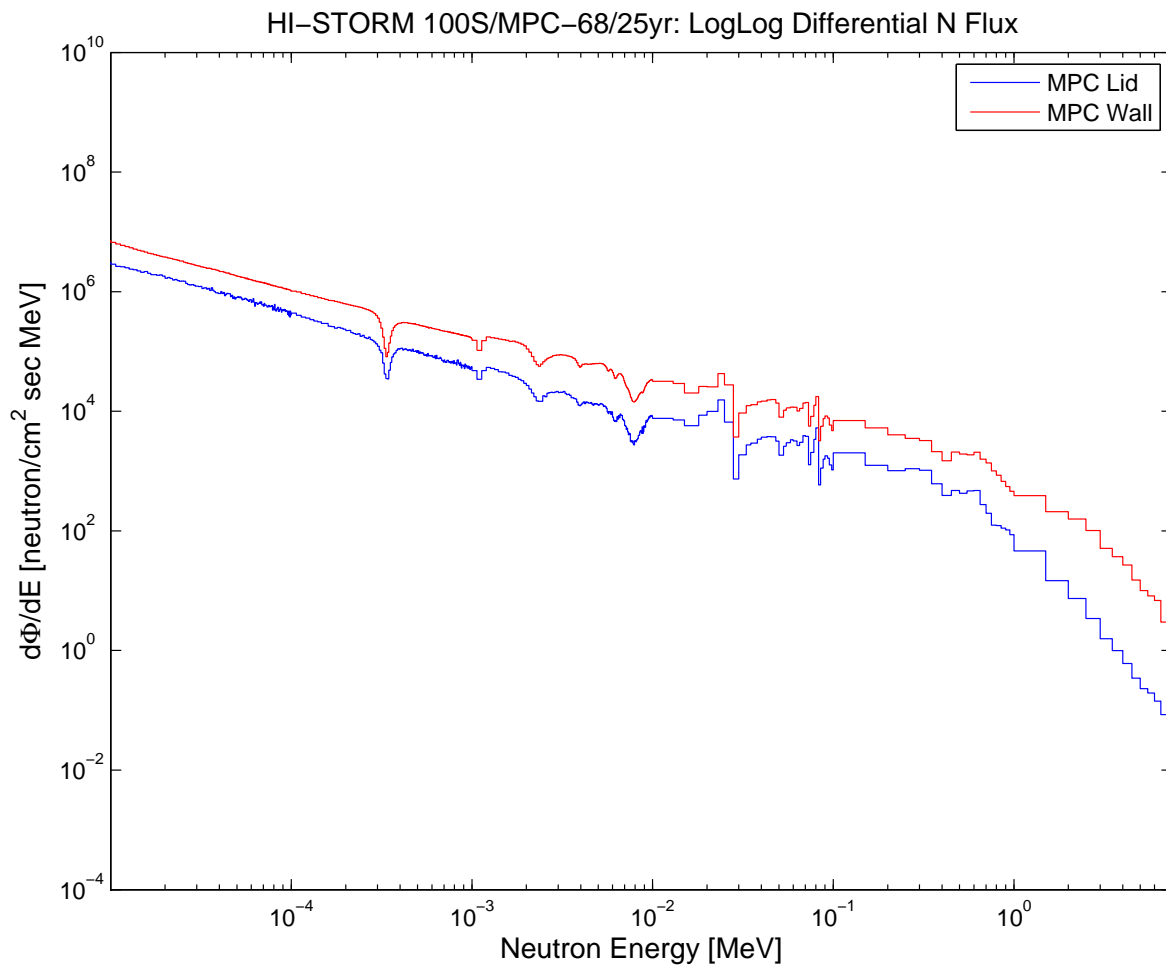


Figure 4.42: The transported neutron spectra taken as a surface average for the MPC-68, housed in a 100S METCON, and cooled for 25 yr.

HI-STORM 100S/MPC-68/25yr: N Dose(x,y), MPC Lid in mRad(Si)/hr

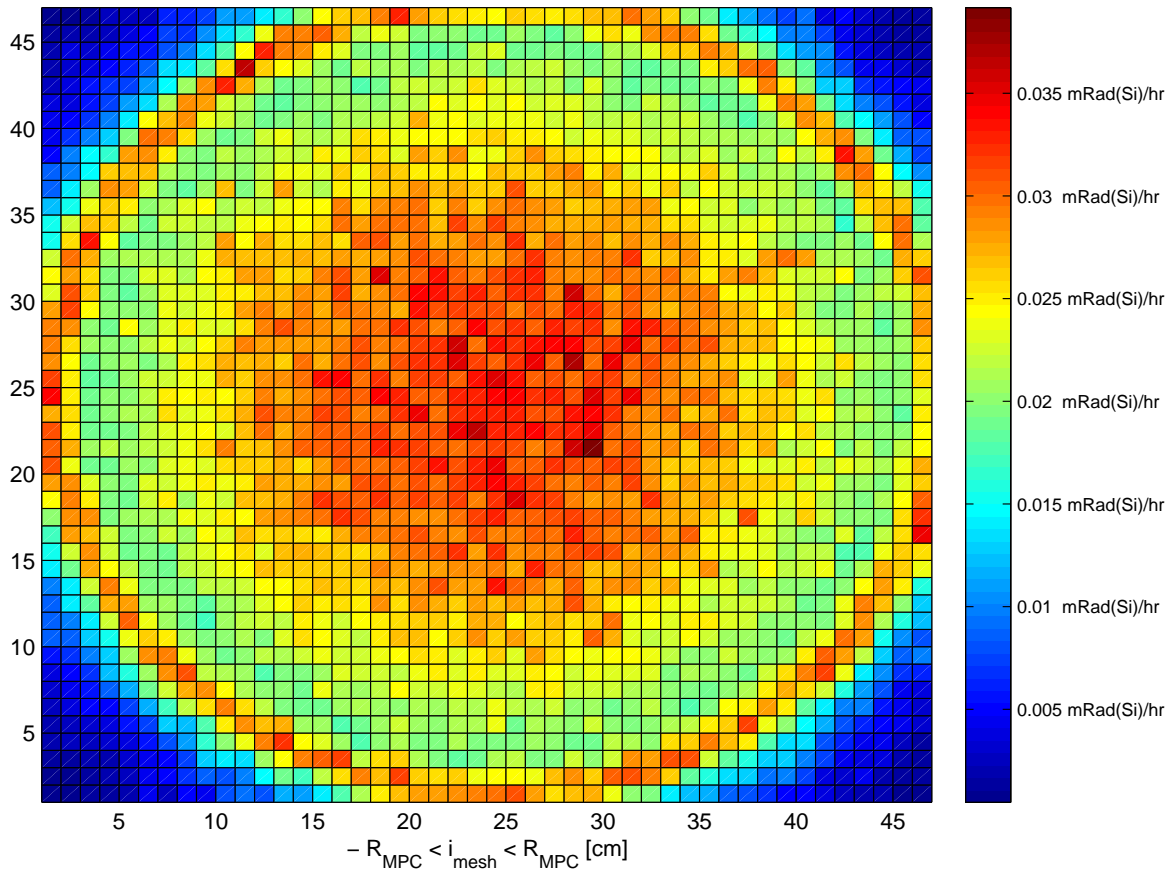


Figure 4.43: The MPC lid neutron dose rate for a 45·45 FMESH in a plane at the lid surface for a MPC-68, housed in a 100S METCON, and cooled for 25 yr. Dose is in $\frac{mRad(Si)}{hr}$ for the matrix of 4 cm cells. This is the proposed deployment surface for the delivery system of the robotic instrumentation.

HI-STORM 100S/MPC-68/25yr: N Dose(θ, z), MPC shell in mRad(Si)/hr

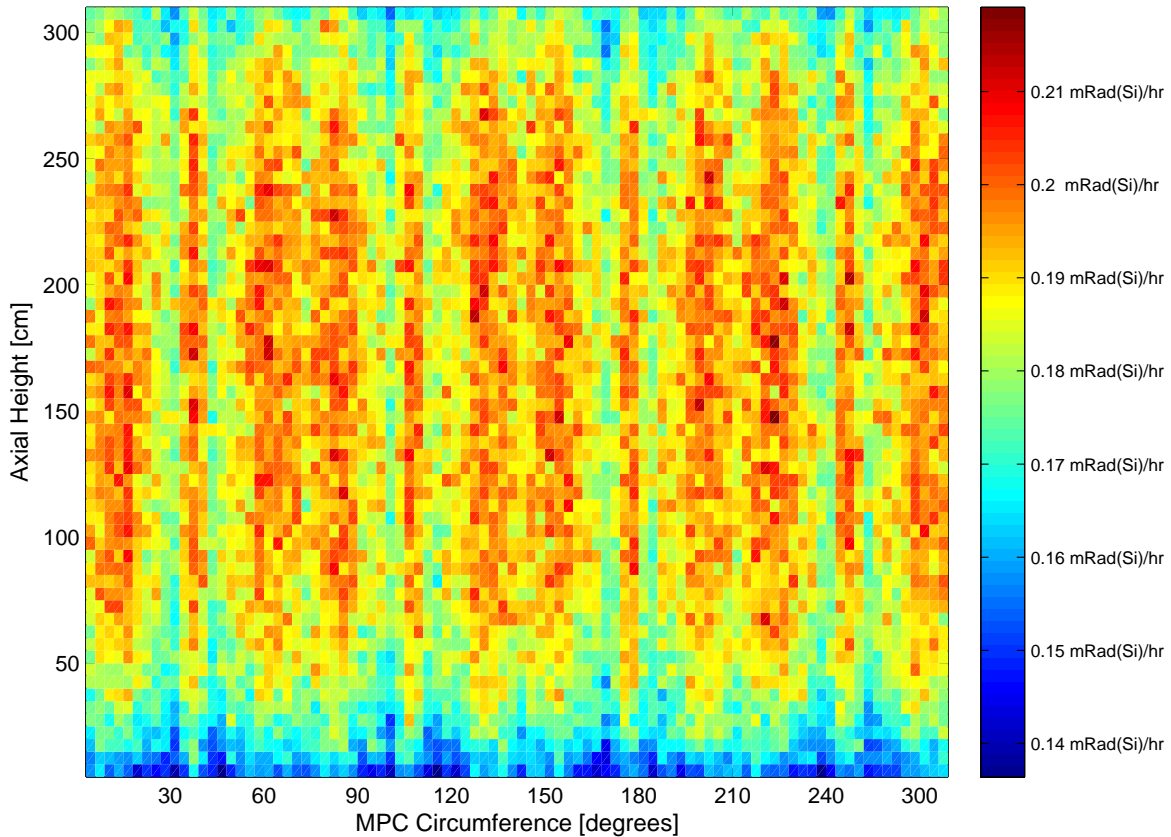


Figure 4.44: The MPC wall neutron dose rate for a $6\text{ cm} \cdot 6\text{ cm}$ coaxial FMESH wrapped around the outside of a MPC-68, housed in a 100S METCON, and cooled for 25 yr. The y-axis spans the bottom to the top of the MPC and the x-axis spans 0 to 2π . This details a Cooper Nuclear Station cycle of a of a General Electric 8×8 assembly burned to $25.344 \frac{\text{MWd}}{\text{kg}}$ and includes an ORIGEN-ARP source term.

CHAPTER 5

DISCUSSION

As mentioned, the cask will likely be accessed via interaction with one of the four outlet vents located at the top of the cask. As such, a composite of dose rates from both neutron and photon flux is useful for dosimetric concerns in regards to estimating dose received during an inspection period. It is known that the vents of the HI-STORM 100 design will likely require the removal of both an intermediate screen as well as γ -ray cross plates in order to load the robotic assembly into the vent. With this requirement for vent interaction, dose rates at both the outlet and inlet are shown in figures 5.1 and 5.2 respectively. These values consider the scenario where any small gauge wire screen specified by the design is removed, and the gamma cross plates are installed in both the inlet and outlet vents. It is well known that neutron source strength is proportional to burnup raised to the fourth power.[4] As burnup increases, neutron source strength will strongly respond in proportion to increasing power density. In the case of a tripling of burnup, neutron source would be expected to increase several magnitudes along with neutron dose rate. In this manner, we expect neutron dose rate contributions to be most noticeable when considering high burnup spent fuel storage. Furthermore, transport through a scattering pathway such as that as designed in the outlet vent of the HI-STORM will increase the contribution of neutron flux to dose outside of the canister. With regards to external photon dose, it is expected that ^{137m}Ba γ -rays, a daughter of ^{137}Cs , will dominate the photon dose rate outside of the METCON.[2]

HI-STORM 100S: N and P Dose, Outlet Vent for All Variants

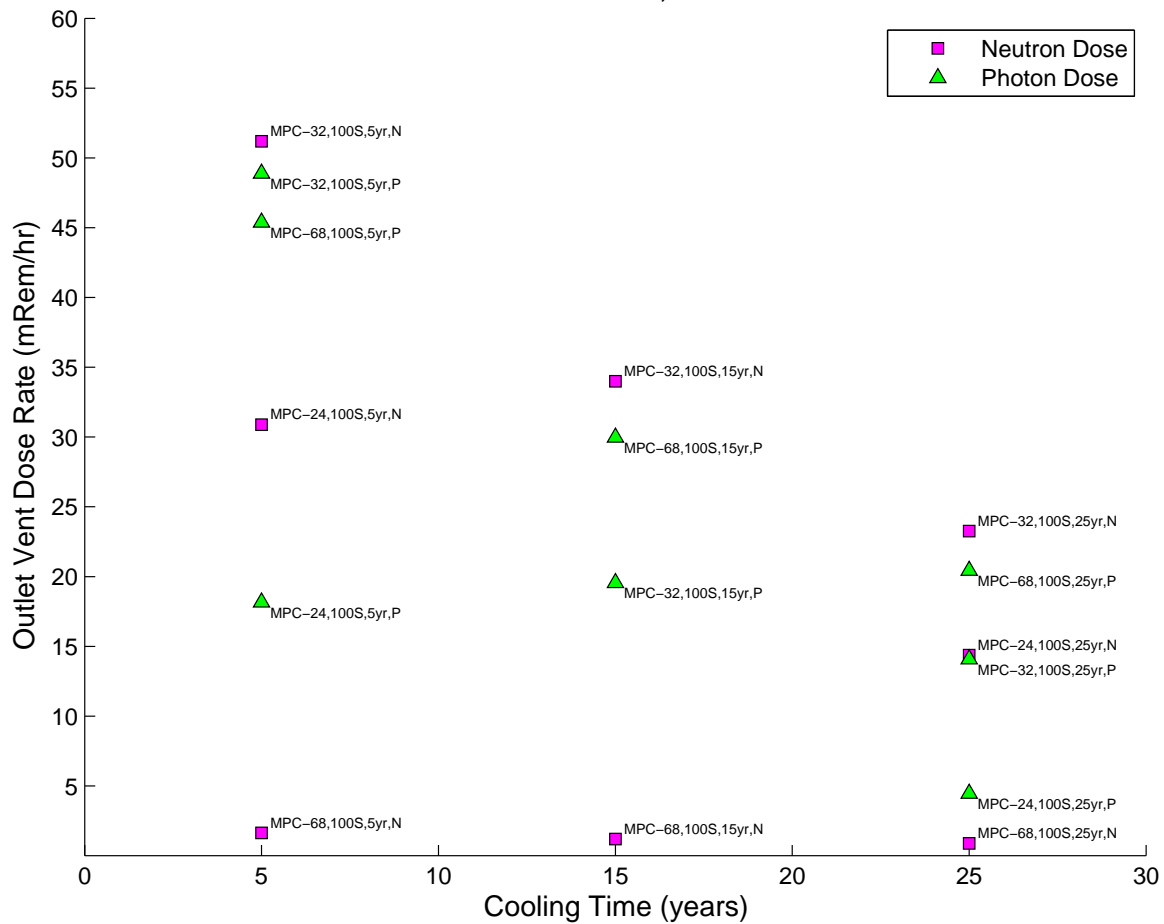


Figure 5.1: The composite of both neutron and photon dose rates taken for a 3 cm F5 Tally positioned within the upper, outlet vent.

However, the characterization spent fuel radioisotopes with ORIGEN-ARP and ORIGAMI allows us to consider the impact of other contributors to photon dose. The combined neutron and photon dose rate for an MPC-32, loaded with 32 PWR assemblies homogeneously burned to $57.535 \frac{MWd}{kg}$, housed within the 100S METCON, and cooled for 5 years is approximately $98 \frac{mRem}{hr}$. Available literature detailing storage pad dose rates agrees strongly with a dose rate of $100 \frac{mRem}{hr}$ at a generic vent opening for the HI-STORM design.[24] In this case, we note that the outlet vent dose rate is comparable to a slightly elevated midplane dose rate of a transport cask.[34]. Similarly, this research predicts an averaged METCON dose rate of $42 \frac{mRem}{hr}$, and again agrees strongly with a reported dose rate of $37 \frac{mRem}{hr}$ contact.[24] Of strongest note to this

HI-STORM 100S: N and P Dose, Inlet Vent for All Variants

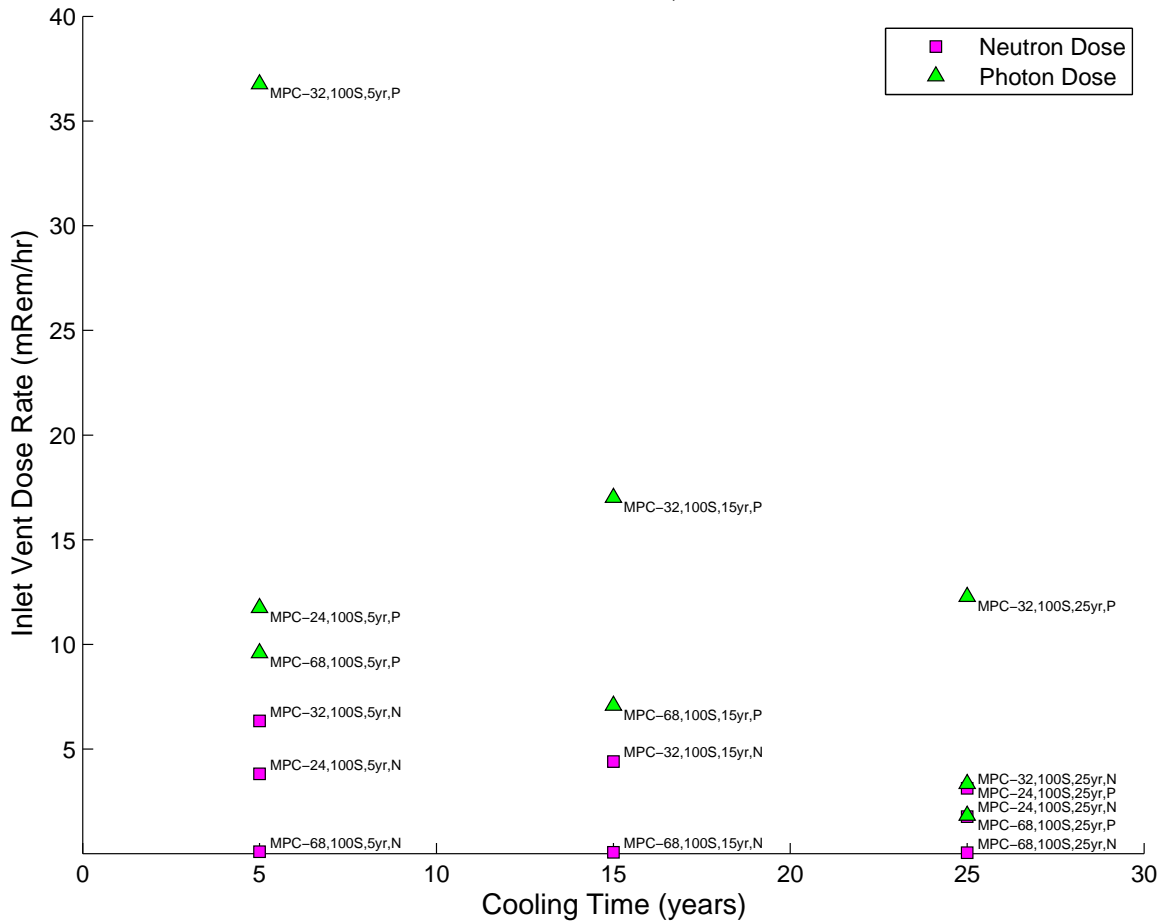


Figure 5.2: The composite of both neutron and photon dose rates taken for a 3 cm F5 Tally positioned within the lower, inlet vent.

research, is the axial profile of dose rate in $\frac{Rad(Si)}{hr}$ within the annular space corresponding to each multi-purpose canister, and that predicted behavior over time. While the target time frame for inspection is a combined cooling period of 25 years, the behavior of photon dose rate over that time span is considered within figures 5.3, 5.4, and 5.5.

In the case of figure 5.6, the variation of neutron dose rate within the annulus of the HI-STORM spent fuel storage cask is shown at both 5 and 25 years cooling. Spent fuel assemblies are loaded bottom down, and axial neutron emission is expected to be strongest towards the bottom half of the spent fuel storage design.[5] The profiles displayed within figure 5.6 display a dose rate correlated with the bottom peaked

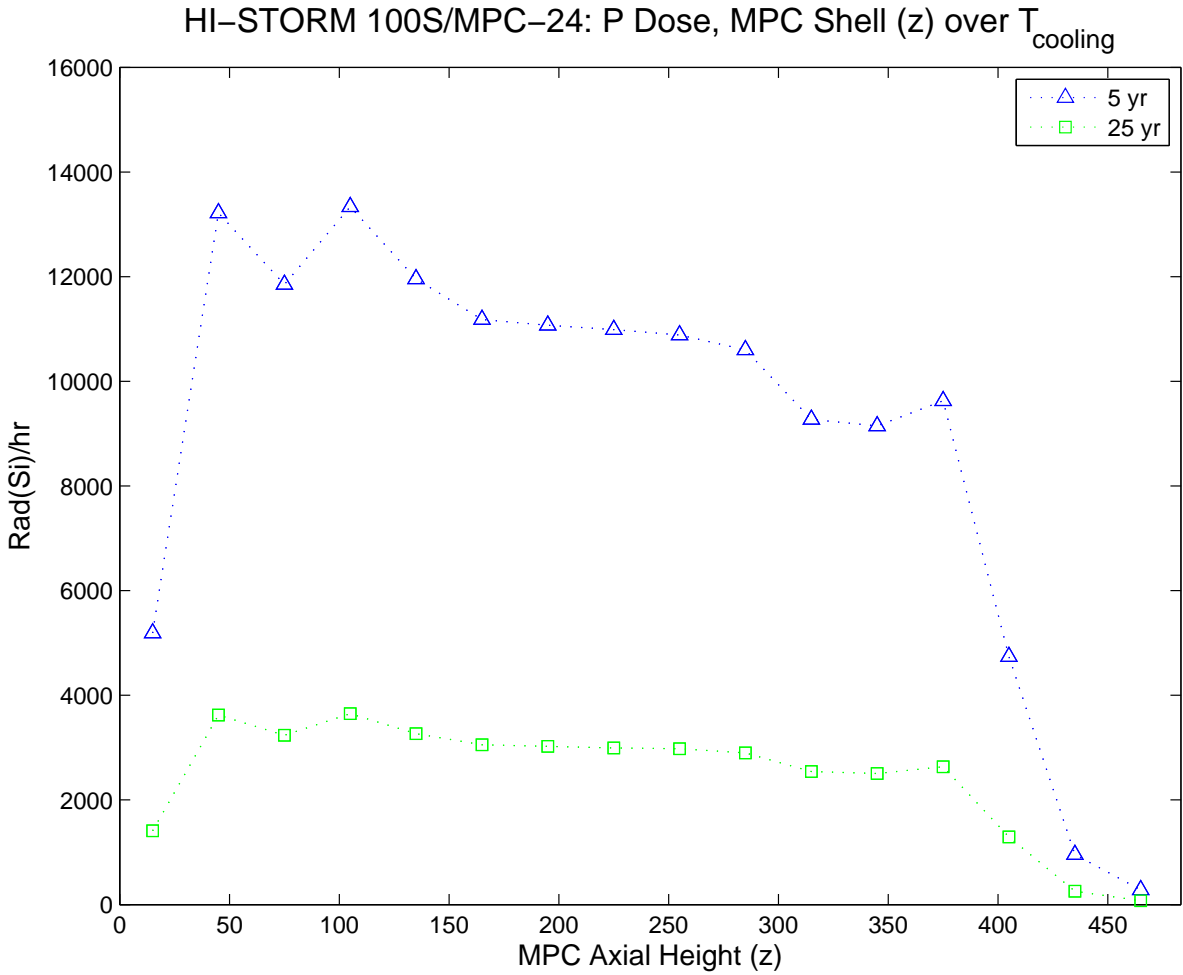


Figure 5.3: Time variant, segmented, photon tallies modified by a dose response function and divided into axial increments of 30 cm on the outer shell of the MPC-24.

burnup of the spent fuel assemblies housed within the multi-purpose canister. This coincides with a higher predicted neutron emission and dose rate towards the bottom of the HI-STORM design. When considering the generic METCON contact neutron dose rate, this research predicts $2.5 \frac{mRem}{hr}$ for an MPC-32, loaded with 32 PWR assemblies homogeneously burned to $57.535 \frac{MWd}{kg}$, housed within the 100S METCON, and cooled for 25 years. This compares favorably with an unexplicated literature value of $8.68 \pm 0.24 \frac{mRem}{hr}$ in association with a Holtec canister at Farley Unit 1.[17]

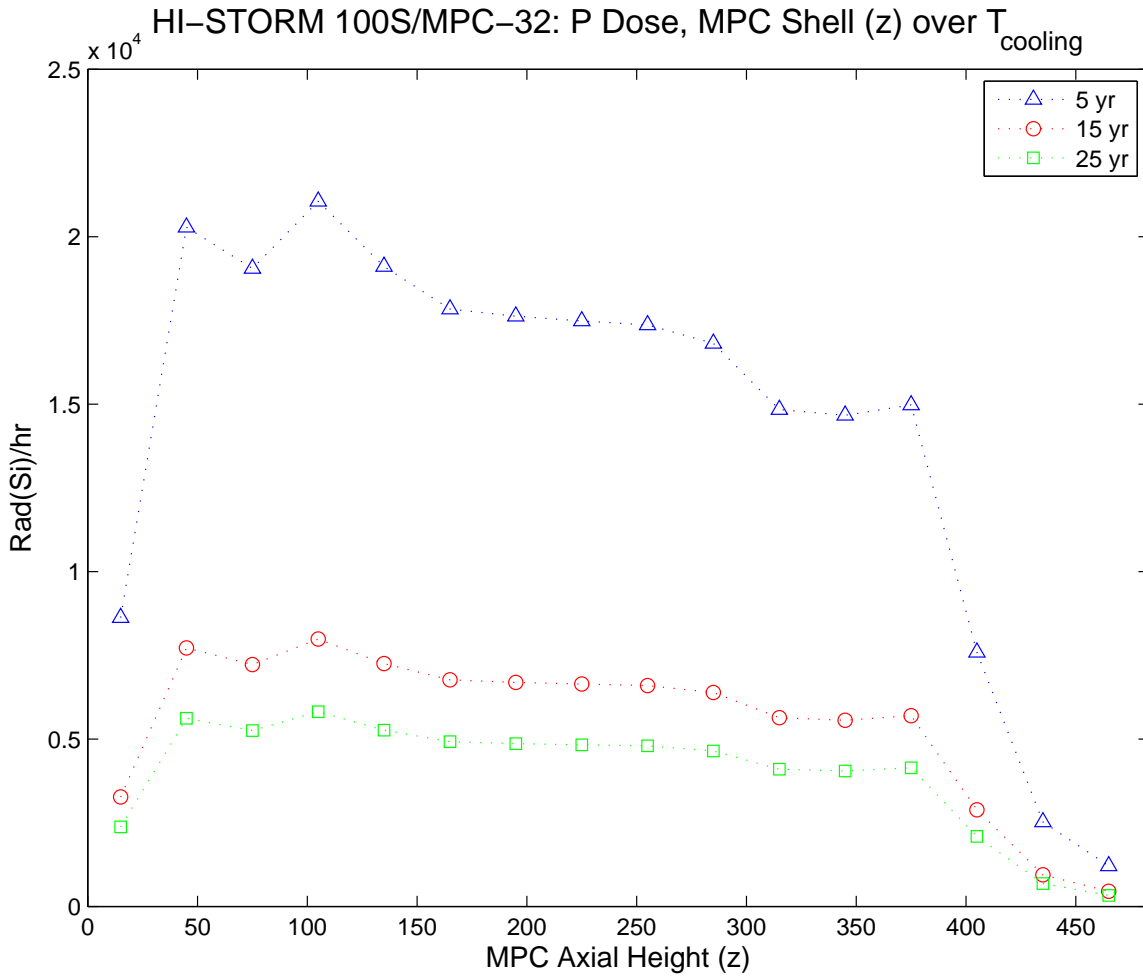


Figure 5.4: Time variant, segmented, photon tallies modified by a dose response function and divided into axial increments of 30 cm on the outer shell of the MPC-32. Note the y-axis has a multiplicative factor of 10^4 .

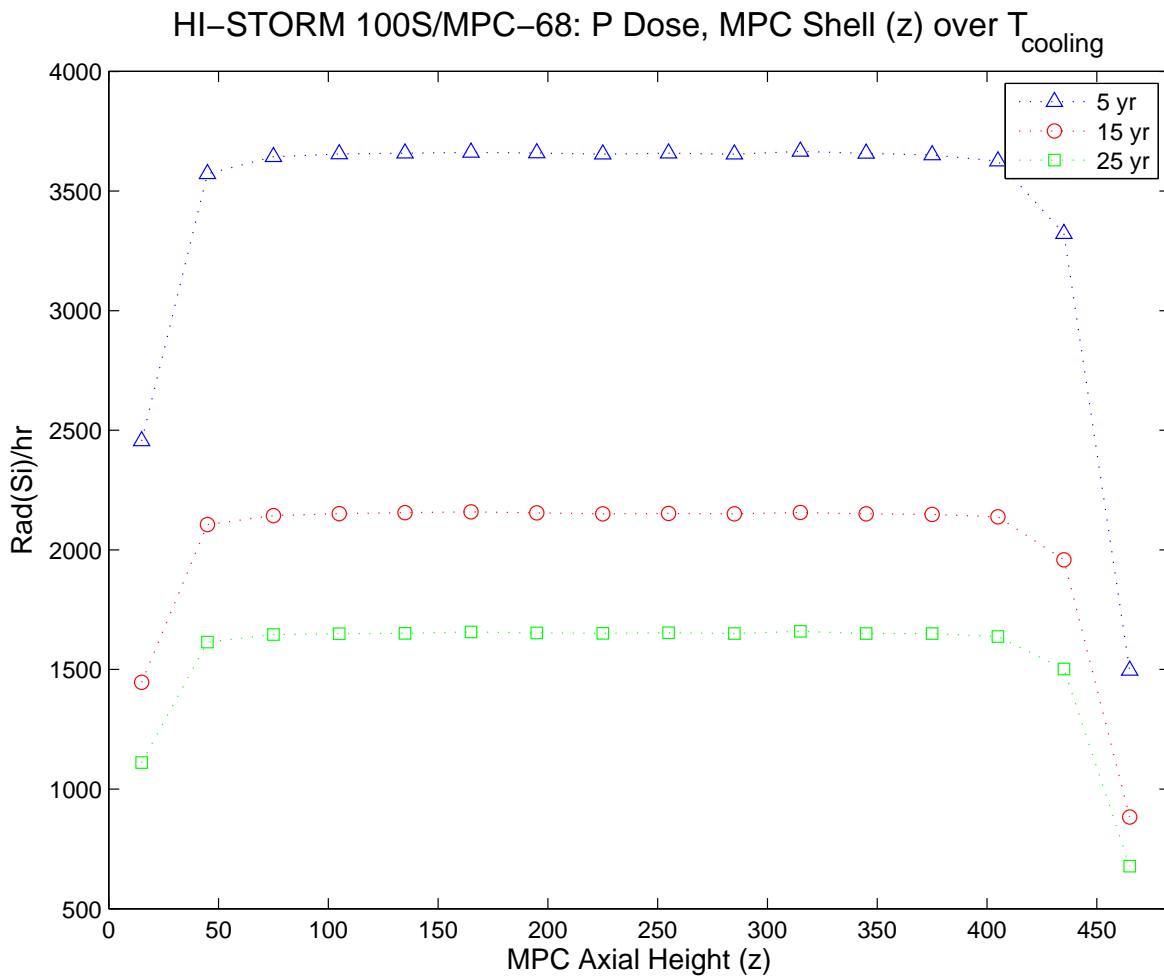


Figure 5.5: Time variant, segmented, photon tallies modified by a dose response function and divided into axial increments of 30 cm on the outer shell of the MPC-68.

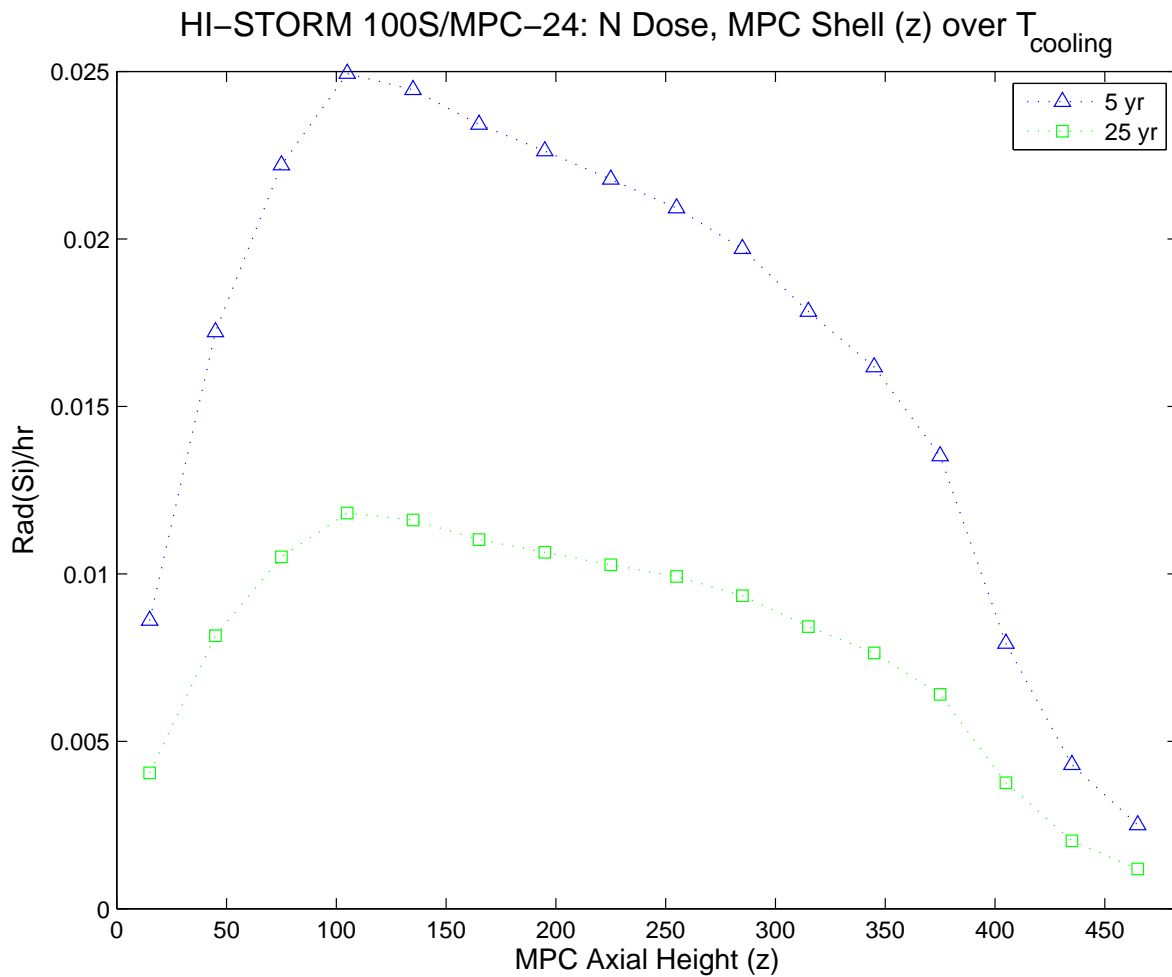


Figure 5.6: Time variant, segmented, neutron tallies modified by a dose response function and divided into axial increments of 30 cm on the outer shell of the MPC-24.

CHAPTER 6

CONCLUSIONS

It may be observed within the mesh maps of dose rate, photon dose is at a maximum where effective thickness of steel is reduced due to spatial position. Consistently, photon dose rates are proportional to the fuel burnup. They decrease with cooling period, reflecting the prominent γ -ray emission of multiple short lived fission products. Over longer time periods, concordant with its half life of 30.17 years, we expect to see ^{137}Cs to become the predominate contributors to photon dose. The loading of high burnup assemblies within non central positions in the MPC are anticipated to elevate photon dose rates on both the shell and lid of the MPC. In this manner, the homogeneous loading of assemblies within this research is conservative in nature. Traditionally, inward loading of high burnup assemblies will lower dose rate via mechanism of spent fuel assembly shielding of photon flux.

In the case of dose rate mapping of the multi-purpose canister lid, it is pertinent to observe that the overwhelming majority of dose will likely be absorbed while in the vicinity of the MPC edge. This is a result of vertical photon scatter along the annulus of the cask. Since photon dose corresponds to the vast majority of the dose rate inside of the METCON, careful consideration of loiter time on the MPC lid edge will be required.

The calculations performed for the limiting case of a MPC-32 burned to $57.535 \frac{\text{MWd}}{\text{kg}}$ and cooled for 5 years are described within table 4.3. This simulation predicts a photon dose rate found of $1.4349 \cdot 10^4 \frac{\text{Rad}(Si)}{\text{hr}}$. Similarly, literature sources for annular

dose rate for an MPC-32 burned to $62 \frac{MWd}{kg}$ and cooled for 5 years predicts a dose rate of $2.71 \cdot 10^4 \frac{Rad}{hr}$. [21] Considering the novel implementation of axially variant radiation emission and moderator density, a custom ORIGAMI depletion routine applied to unique and independently generated MCNP geometry, and legacy Silicon based flux to dose response functions originally applied to spacecraft, these results correlate well.

A hardened specialty camera capable of 50 MRad has been described as a potential candidate, and would have a loiter time of approximately 164.3 days given the limiting MPC-32, 100S, 5 year, photon dose rate found of $1.2678 \cdot 10^4 \frac{Rad(Si)}{hr}$ calculated within table 4.3. A typical radiation hardened component is expected to perform up to 1 MRad. [18] This would provide 3.3 days of in annulus time given the same scenario. For the case of the simulated 4-sided camera car, a 5mm Lead shield would approximately halve the dose rate to $6.6186 \cdot 10^3 \frac{Rad(Si)}{hr}$. This doubles annulus loiter time to 6.3 days for a 1 MRad hardened electronic component. In the case of amorphous α -Si, values of 10 MRad are quoted as threshold dose, where low temperature annealing of displacement damage is possible. [27]

6.1 FUTURE WORK

The current state of the MCNP input decks of this research is such that the system is well characterized. Notably, the earlier MPC-24 design was omitted in favor of the MPC-24EF and the HI-STORM 100S v.B was omitted due to mission incompatibility. The next step for the MCNP input deck could be informed implementation of an assembly loading pattern as opposed to a homogeneous loading. The multi-purpose canister should be loaded with higher dose rate assemblies shuffled inwardly into the basket.

The implementation of a varied burnup loading pattern would add value to the project in terms of the cask source strength, but also in regards to lowering the photon flux on the MPC. In terms of source characterization, the reference BWR assembly could be readily characterized within ORIGAMI providing detailed axial discharge burnup and cycle averaged moderator density. Lacking this information, it is currently well characterized in ORIGEN-ARP in a volume smear. This further work might allow higher fidelity evaluation of dose rates at the extrema of the multi-purpose canister height. However, it would not likely have a strong impact on the midplane dose rate. However, it would be of merit considering the interest in inspecting transverse weld lines in the area.

REFERENCES

- [1] CW Alexander. “A Review of Spent-Fuel Photon and Neutron Source Spectra”. In: (1986).
- [2] Markku Anttila and Posiva Oy. *Gamma and neutron dose rates on the outer surface of the nuclear waste disposal canisters*. Posiva, 1996.
- [3] SM Bowman and LC Leal. “ORIGEN-ARP: Automatic rapid process for spent fuel depletion, decay, and source term analysis”. In: *Vol. I, Sect. D1 of SCALE: A Modular Code System for Performing Standardized Computer Analyses for Licensing Evaluation, NUREG/CR-0200, Rev 6* (2000).
- [4] BL Broadhead. *Recommendations for Shielding Evaluations for Transport and Storage Packages*. Tech. rep. NUREG/CR-6802 (ORNL/TM-2002/31), US Nuclear Regulatory Commission, Oak Ridge National Laboratory, 2003.
- [5] Bryan L Broadhead et al. “Evaluation of shielding analysis methods in spent-fuel cask environments”. In: *Nuclear technology* 117.2 (1997), pp. 206–222.
- [6] L Caseres, Todd S Mintz, et al. *Atmospheric Stress Corrosion Cracking Susceptibility of Welded and Unwelded 304, 304L, and 316L Austenitic Stainless Steels Commonly Used for Dry Cask Storage Containers Exposed to Marine Environments*. Southwest Research Institute, 2010.
- [7] Holtec Center. “Holtec International Final Safety Analysis Report for the HISTORM 100 Cask System”. In: ().
- [8] “Certificate of Compliance 9261”. In: *United States Nuclear Regulatory Commission* 1 (2003). Form 335.
- [9] PT Choong. “Secondary radiation considerations in spent fuel storage cask design”. In: *Trans. Am. Nucl. Soc.:(United States)* 49.CONF-850610- (1985).
- [10] JR Coleman and TW Knight. “Evaluation of multiple, self-recycling of reprocessed uranium in LWR”. In: *Nuclear Engineering and Design* 240.5 (2010), pp. 1028–1032.

- [11] Judith M Cuta, Urban P Jenquin, and Mikal A McKinnon. *Evaluation of Effect of Fuel Assembly Loading Patterns on Thermal and Shielding Performance of a Spent Fuel Storage/Transportation Cask*. Tech. rep. Pacific Northwest National Laboratory, 2001.
- [12] O Delaire et al. *Study of alloying elements in the ZR matrix of Zircaloy-4 and ZIRLO using the Advanced Photon Source at Argonne*. Tech. rep. Argonne National Lab., IL (US), 2000.
- [13] Capital Energy. *Principal Design Features of LWR Fuel Assemblies*. 2015. URL: <http://capitalenergy.biz/?p=20563> (visited on 2016).
- [14] Ian Gauld and Matthew Francis. “Investigation of passive gamma spectroscopy to verify spent nuclear fuel content”. In: *51st Annual Meeting of the Institute of Nuclear Materials Management*. 2010.
- [15] SR Greene, JS Medford, and SA Macy. “Storage and Transport Cask Data for Used Commercial Nuclear Fuel 2013 US Edition”. In: *Group 2.13hq0903022* (2013), p. 20.
- [16] James F. Harrison. *GNF3 Introduction Meeting Presentation, Basic Fuel Assembly Licensing Elements*. Tech. rep. General Electric, Global Nuclear Fuel, 2014.
- [17] NE Hertel et al. “Dose equivalent factor for adjusting dosimeter readings in vicinity of the holtec MPC during drying in the plant farley unit i spent fuel room”. In: *Transactions of the American Nuclear Society* 96 (2007), pp. 442–443.
- [18] Andrew Holmes-Siedle and Len Adams. “Handbook of Radiation Effects”. In: (1993).
- [19] Jae-Hun Ko et al. “SHIELDING ANALYSIS OF DUAL PURPOSE CASKS FOR SPENT NUCLEAR FUEL UNDER NORMAL STORAGE CONDITIONS”. In: *Nuclear Engineering and Technology* 46.4 (2014), pp. 547–556.
- [20] K. Lindquist. *Handbook of Neutron Absorber Materials for Spent Nuclear Fuel Transportation and Storage Applications*. Tech. rep. Electric Power Research Institute, Palo Alto, CA (US), 2009.
- [21] Ryan M Meyer et al. *NDE to Manage Atmospheric SCC in Canisters for Dry Storage of Spent Fuel: An Assessment*. Tech. rep. Pacific Northwest National Laboratory (PNNL), Richland, WA (US), 2013.
- [22] Kevin G Mon. “Office of Civilian Radioactive Waste Management”. In: (2007).

- [23] CW Pennington. “HI-STAR: Holtec International’s MPC (multi-purpose canister) system”. In: *Nuclear Engineering International* 40.492 (1995), pp. 36–38.
- [24] EL Redmond. “Methodology for calculating dose rates from storage cask arrays using MCNP”. In: *Transactions of the American Nuclear Society* 77.CONF-971125– (1997).
- [25] Annette Rolle et al. “Verification of activity release compliance with regulatory limits within spent fuel transport cask”. In: *Proc. 16th Int. Symp. on Packaging and Transportation of Radioactive Materials (PATRAM 2010)*. 2010.
- [26] J Kenneth Shultis and Richard E Faw. “Radiation Shielding. American Nuclear Society”. In: *Inc., La Grand Park, Illinois USA* (2000).
- [27] JR Srour et al. “Damage mechanisms in radiation-tolerant amorphous silicon solar cells”. In: *Nuclear Science, IEEE Transactions on* 45.6 (1998), pp. 2624–2631.
- [28] National Institute of Standards and Technology. *X-ray Mass Attenuation Coefficients*. 2016. URL: <http://physics.nist.gov/PhysRefData/XrayMassCoef/ElemTab/z14.html> (visited on 2016).
- [29] Alan G Stanley, KE Martin, and WE Price. “Voyager electronic parts radiation program. Volume 2: Test requirements and procedures”. In: (1978).
- [30] S. Su et al. *Subsurface Shielding Specific Source Term Evaluation*. Tech. rep. Office of Civilian Radioactive Waste Management (US), 1999.
- [31] M.P. Unterweger et al. *Radionuclide Half-Life Measurements*. 2010. URL: <http://www.nist.gov/pml/data/halflife-html.cfm> (visited on 2016).
- [32] RG Williams III, Christopher J Gesh, Richard T Pagh, et al. “Compendium of material composition data for radiation transport modeling”. In: *Pacific Northwest National Laboratory* (2006), pp. 14–18.
- [33] Saishun Yamazaki, Katsumi Yoshida, and Toyohiko Yano. “Recovery of neutron-induced damage of Si analyzed by thermal expansion measurement”. In: *Journal of Nuclear Materials* 386 (2009), pp. 328–332.
- [34] D Zappe et al. “Evaluation of the radiation situation near a spent fuel element shipping cask”. In: (1989).

APPENDIX A

NPS DATA

Table A.1: The number of histories, NPS, for each given MCNP run.

Run	NPS
MPC-24/100S/5yr/N	1.70E+07
MPC-24/100S/5yr/P	1.49E+09
MPC-24/100S/25yr/N	1.70E+07
MPC-24/100S/25yr/P	1.69E+09
MPC-32/100S/5yr/N	5.40E+07
MPC-32/100S/5yr/P	4.90E+09
MPC-32/100S/15yr/N	5.50E+07
MPC-32/100S/15yr/P	5.00E+09
MPC-32/100S/25yr/N	2.70E+07
MPC-32/100S/25yr/P	4.94E+09
MPC-68/100S/5yr/N	6.10E+07
MPC-68/100S/5yr/P	7.00E+09
MPC-68/100S/15yr/N	6.10E+07
MPC-68/100S/15yr/P	3.90E+09
MPC-68/100S/25yr/N	3.00E+07
MPC-68/100S/25yr/P	1.28E+09
MPC-24/100S/25yr/NP	1.50E+07

APPENDIX B

ORIGEN-ARP BWR DATA

Table B.1: ORIGEN-ARP photon results for a GE 8×8 BWR assembly burned to 25.344 $\frac{MWd}{kg}$ and cooled for a combined time period of 5yr.

E [MeV]	$\frac{dS}{dE} [\frac{p}{MeVsec}]$	dE	dS [$\frac{p}{sec}$]
1.00E-02	6.85E+16	1.00E-02	6.845E+14
2.00E-02	3.83E+16	1.00E-02	3.830E+14
3.00E-02	3.12E+16	1.50E-02	4.673E+14
4.50E-02	1.49E+16	1.50E-02	2.234E+14
6.00E-02	9.82E+15	1.00E-02	9.820E+13
7.00E-02	8.40E+15	5.00E-03	4.199E+13
7.50E-02	6.90E+15	2.50E-02	1.726E+14
1.00E-01	4.11E+15	5.00E-02	2.055E+14
1.50E-01	2.23E+15	5.00E-02	1.115E+14
2.00E-01	1.06E+15	6.00E-02	6.330E+13
2.60E-01	6.93E+14	4.00E-02	2.772E+13
3.00E-01	6.23E+14	1.00E-01	6.230E+13
4.00E-01	5.56E+14	5.00E-02	2.780E+13
4.50E-01	4.11E+14	6.00E-02	2.464E+13
5.10E-01	1.32E+16	2.00E-03	2.642E+13
5.12E-01	8.48E+14	8.80E-02	7.460E+13
6.00E-01	2.41E+16	1.00E-01	2.414E+15
7.00E-01	2.57E+15	1.00E-01	2.571E+14
8.00E-01	2.43E+14	1.00E-01	2.431E+13
9.00E-01	1.61E+14	1.00E-01	1.614E+13
1.00E+00	9.48E+13	2.00E-01	1.897E+13
1.20E+00	1.75E+14	1.30E-01	2.272E+13
1.33E+00	7.40E+13	1.10E-01	8.140E+12
1.44E+00	1.60E+13	6.00E-02	9.570E+11
1.50E+00	6.53E+12	7.00E-02	4.572E+11
1.57E+00	1.43E+13	9.00E-02	1.291E+12
1.66E+00	2.00E+12	1.40E-01	2.803E+11
1.80E+00	1.18E+12	2.00E-01	2.366E+11

Continued on following page

E [MeV]	$\frac{dS}{dE} \left[\frac{p}{MeV \cdot sec} \right]$	dE	dS $\left[\frac{p}{sec} \right]$
2.00E+00	6.17E+11	1.50E-01	9.247E+10
2.15E+00	3.75E+12	2.00E-01	7.504E+11
2.35E+00	7.76E+11	1.50E-01	1.163E+11
2.50E+00	6.13E+10	2.50E-01	1.532E+10
2.75E+00	5.31E+10	2.50E-01	1.328E+10
3.00E+00	5.63E+09	5.00E-01	2.815E+09
3.50E+00	6.19E+06	5.00E-01	3.095E+06
4.00E+00	1.62E+06	5.00E-01	8.090E+05
4.50E+00	9.38E+05	5.00E-01	4.688E+05
5.00E+00	5.43E+05	5.00E-01	2.717E+05
5.50E+00	3.15E+05	5.00E-01	1.575E+05
6.00E+00	1.83E+05	5.00E-01	9.125E+04
6.50E+00	1.06E+05	5.00E-01	5.290E+04
7.00E+00	6.13E+04	5.00E-01	3.067E+04
7.50E+00	3.56E+04	5.00E-01	1.778E+04
8.00E+00	1.05E+04	2.00E+00	2.100E+04
1.00E+01			

Table B.2: ORIGEN-ARP neutron results for a GE 8×8 BWR assembly burned to 25.344 $\frac{MWd}{kg}$ and cooled for a combined time period of 5yr.

E [MeV]	$\frac{dS}{dE} \left[\frac{n}{MeV \cdot sec} \right]$	dE	dS $\left[\frac{n}{sec} \right]$
1.00E-11	1.165E+02	9.00E-11	1.049E-08
1.00E-10	4.749E+01	4.00E-10	1.900E-08
5.00E-10	3.098E+01	2.50E-10	7.745E-09
7.50E-10	2.703E+01	2.50E-10	6.758E-09
1.00E-09	2.347E+01	2.00E-10	4.694E-09
1.20E-09	2.202E+01	3.00E-10	6.606E-09
1.50E-09	1.937E+01	5.00E-10	9.685E-09
2.00E-09	1.749E+01	5.00E-10	8.745E-09
2.50E-09	1.593E+01	5.00E-10	7.965E-09
3.00E-09	1.458E+01	1.00E-09	1.458E-08
4.00E-09	1.317E+01	1.00E-09	1.317E-08
5.00E-09	1.190E+01	2.50E-09	2.975E-08
7.50E-09	1.077E+01	2.50E-09	2.693E-08
1.00E-08	9.657E+00	1.53E-08	1.478E-07
2.53E-08	9.314E+00	4.70E-09	4.378E-08
3.00E-08	9.436E+00	1.00E-08	9.436E-08
4.00E-08	9.628E+00	1.00E-08	9.628E-08
5.00E-08	9.945E+00	1.00E-08	9.945E-08

Continued on following page

E [MeV]	$\frac{dS}{dE} \left[\frac{n}{MeV \cdot sec} \right]$	dE	dS $\left[\frac{n}{sec} \right]$
6.00E-08	1.022E+01	1.00E-08	1.022E-07
7.00E-08	1.055E+01	1.00E-08	1.055E-07
8.00E-08	1.086E+01	1.00E-08	1.086E-07
9.00E-08	1.117E+01	1.00E-08	1.117E-07
1.00E-07	1.176E+01	2.50E-08	2.940E-07
1.25E-07	1.251E+01	2.50E-08	3.128E-07
1.50E-07	3.230E+02	2.50E-08	8.075E-06
1.75E-07	3.778E+02	2.50E-08	9.445E-06
2.00E-07	3.784E+02	2.50E-08	9.460E-06
2.25E-07	3.791E+02	2.50E-08	9.478E-06
2.50E-07	3.797E+02	2.50E-08	9.493E-06
2.75E-07	3.803E+02	2.50E-08	9.507E-06
3.00E-07	3.809E+02	2.50E-08	9.523E-06
3.25E-07	3.815E+02	2.50E-08	9.537E-06
3.50E-07	3.820E+02	2.50E-08	9.550E-06
3.75E-07	3.865E+02	2.50E-08	9.662E-06
4.00E-07	3.873E+02	5.00E-08	1.937E-05
4.50E-07	3.883E+02	5.00E-08	1.942E-05
5.00E-07	3.893E+02	5.00E-08	1.947E-05
5.50E-07	3.902E+02	5.00E-08	1.951E-05
6.00E-07	3.908E+02	2.50E-08	9.770E-06
6.25E-07	3.912E+02	2.50E-08	9.780E-06
6.50E-07	3.918E+02	5.00E-08	1.959E-05
7.00E-07	3.926E+02	5.00E-08	1.963E-05
7.50E-07	3.934E+02	5.00E-08	1.967E-05
8.00E-07	3.942E+02	5.00E-08	1.971E-05
8.50E-07	3.948E+02	5.00E-08	1.974E-05
9.00E-07	3.955E+02	2.50E-08	9.888E-06
9.25E-07	3.956E+02	2.50E-08	9.890E-06
9.50E-07	3.962E+02	2.50E-08	9.905E-06
9.75E-07	3.964E+02	2.50E-08	9.910E-06
1.00E-06	3.969E+02	1.00E-08	3.969E-06
1.01E-06	3.965E+02	1.00E-08	3.965E-06
1.02E-06	3.972E+02	1.00E-08	3.972E-06
1.03E-06	3.968E+02	1.00E-08	3.968E-06
1.04E-06	3.977E+02	1.00E-08	3.977E-06
1.05E-06	3.970E+02	1.00E-08	3.970E-06
1.06E-06	3.976E+02	1.00E-08	3.976E-06
1.07E-06	3.977E+02	1.00E-08	3.977E-06
1.08E-06	3.978E+02	1.00E-08	3.978E-06
1.09E-06	3.981E+02	1.00E-08	3.981E-06
1.10E-06	3.980E+02	1.00E-08	3.980E-06

Continued on following page

E [MeV]	$\frac{dS}{dE} \left[\frac{n}{MeV \cdot sec} \right]$	dE	dS $\left[\frac{n}{sec} \right]$
1.11E-06	3.983E+02	1.00E-08	3.983E-06
1.12E-06	6.428E+02	1.00E-08	6.428E-06
1.13E-06	6.452E+02	1.00E-08	6.452E-06
1.14E-06	6.504E+02	1.00E-08	6.504E-06
1.15E-06	2.021E+03	2.50E-08	5.052E-05
1.18E-06	2.310E+04	2.50E-08	5.775E-04
1.20E-06	2.211E+04	2.50E-08	5.527E-04
1.23E-06	2.119E+04	2.50E-08	5.298E-04
1.25E-06	3.581E+04	5.00E-08	1.791E-03
1.30E-06	2.345E+04	5.00E-08	1.173E-03
1.35E-06	2.397E+04	5.00E-08	1.199E-03
1.40E-06	1.058E+04	5.00E-08	5.290E-04
1.45E-06	2.462E+04	5.00E-08	1.231E-03
1.50E-06	2.509E+04	9.00E-08	2.258E-03
1.59E-06	3.401E+04	9.00E-08	3.061E-03
1.68E-06	2.681E+04	9.00E-08	2.413E-03
1.77E-06	1.912E+04	9.00E-08	1.721E-03
1.86E-06	3.684E+04	8.00E-08	2.947E-03
1.94E-06	2.917E+04	6.00E-08	1.750E-03
2.00E-06	2.883E+04	1.20E-07	3.460E-03
2.12E-06	2.992E+04	9.00E-08	2.693E-03
2.21E-06	2.168E+04	9.00E-08	1.951E-03
2.30E-06	3.088E+04	8.00E-08	2.470E-03
2.38E-06	4.093E+04	9.00E-08	3.684E-03
2.47E-06	2.302E+04	1.00E-07	2.302E-03
2.57E-06	4.155E+04	1.00E-07	4.155E-03
2.67E-06	3.350E+04	1.00E-07	3.350E-03
2.77E-06	3.437E+04	1.00E-07	3.437E-03
2.87E-06	3.423E+04	1.00E-07	3.423E-03
2.97E-06	3.720E+03	3.00E-08	1.116E-04
3.00E-06	5.378E+04	5.00E-08	2.689E-03
3.05E-06	2.613E+04	1.00E-07	2.613E-03
3.15E-06	3.963E+04	3.50E-07	1.387E-02
3.50E-06	3.412E+04	2.30E-07	7.848E-03
3.73E-06	4.360E+04	2.70E-07	1.177E-02
4.00E-06	4.068E+04	7.50E-07	3.051E-02
4.75E-06	4.424E+04	2.50E-07	1.106E-02
5.00E-06	4.908E+04	4.00E-07	1.963E-02
5.40E-06	4.827E+04	6.00E-07	2.896E-02
6.00E-06	4.444E+04	2.50E-07	1.111E-02
6.25E-06	5.635E+04	2.50E-07	1.409E-02
6.50E-06	5.186E+04	2.50E-07	1.297E-02

Continued on following page

E [MeV]	$\frac{dS}{dE} \left[\frac{n}{MeV \cdot sec} \right]$	dE	dS $\left[\frac{n}{sec} \right]$
6.75E-06	5.258E+04	2.50E-07	1.315E-02
7.00E-06	5.412E+04	1.50E-07	8.118E-03
7.15E-06	5.565E+04	9.50E-07	5.287E-02
8.10E-06	5.740E+04	1.00E-06	5.740E-02
9.10E-06	6.402E+04	9.00E-07	5.762E-02
1.00E-05	6.596E+04	1.50E-06	9.894E-02
1.15E-05	6.884E+04	4.00E-07	2.754E-02
1.19E-05	7.083E+04	1.00E-06	7.083E-02
1.29E-05	7.330E+04	8.50E-07	6.231E-02
1.38E-05	7.226E+04	6.50E-07	4.697E-02
1.44E-05	8.031E+04	7.00E-07	5.622E-02
1.51E-05	7.689E+04	9.00E-07	6.920E-02
1.60E-05	8.161E+04	1.00E-06	8.161E-02
1.70E-05	8.456E+04	1.50E-06	1.268E-01
1.85E-05	8.709E+04	5.00E-07	4.355E-02
1.90E-05	8.871E+04	1.00E-06	8.871E-02
2.00E-05	9.331E+04	1.00E-06	9.331E-02
2.10E-05	9.367E+04	1.50E-06	1.405E-01
2.25E-05	9.713E+04	2.50E-06	2.428E-01
2.50E-05	1.044E+05	2.50E-06	2.610E-01
2.75E-05	1.081E+05	2.50E-06	2.703E-01
3.00E-05	1.092E+05	1.25E-06	1.365E-01
3.13E-05	1.193E+05	5.00E-07	5.965E-02
3.18E-05	1.149E+05	1.50E-06	1.724E-01
3.33E-05	1.164E+05	5.00E-07	5.820E-02
3.38E-05	1.178E+05	8.50E-07	1.001E-01
3.46E-05	1.159E+05	9.00E-07	1.043E-01
3.55E-05	1.213E+05	1.50E-06	1.820E-01
3.70E-05	1.232E+05	1.00E-06	1.232E-01
3.80E-05	1.251E+05	1.10E-06	1.376E-01
3.91E-05	1.330E+05	5.00E-07	6.650E-02
3.96E-05	1.283E+05	1.40E-06	1.796E-01
4.10E-05	1.325E+05	1.40E-06	1.855E-01
4.24E-05	1.349E+05	1.60E-06	2.158E-01
4.40E-05	1.340E+05	1.20E-06	1.608E-01
4.52E-05	1.392E+05	1.80E-06	2.506E-01
4.70E-05	1.421E+05	1.30E-06	1.847E-01
4.83E-05	1.439E+05	9.00E-07	1.295E-01
4.92E-05	1.481E+05	1.40E-06	2.073E-01
5.06E-05	1.444E+05	1.40E-06	2.022E-01
5.20E-05	1.493E+05	1.40E-06	2.090E-01
5.34E-05	1.540E+05	5.60E-06	8.624E-01

Continued on following page

E [MeV]	$\frac{dS}{dE} \left[\frac{n}{MeV \cdot sec} \right]$	dE	dS $\left[\frac{n}{sec} \right]$
5.90E-05	1.591E+05	2.00E-06	3.182E-01
6.10E-05	1.640E+05	4.00E-06	6.560E-01
6.50E-05	1.652E+05	2.50E-06	4.130E-01
6.75E-05	1.724E+05	4.50E-06	7.758E-01
7.20E-05	1.752E+05	4.00E-06	7.008E-01
7.60E-05	1.810E+05	4.00E-06	7.240E-01
8.00E-05	1.849E+05	2.00E-06	3.698E-01
8.20E-05	1.905E+05	8.00E-06	1.524E+00
9.00E-05	2.000E+05	1.00E-05	2.000E+00
1.00E-04	2.090E+05	8.00E-06	1.672E+00
1.08E-04	2.165E+05	7.00E-06	1.516E+00
1.15E-04	2.217E+05	4.00E-06	8.868E-01
1.19E-04	2.267E+05	3.00E-06	6.801E-01
1.22E-04	2.532E+05	6.40E-05	1.620E+01
1.86E-04	2.795E+05	6.50E-06	1.817E+00
1.93E-04	2.889E+05	1.50E-05	4.334E+00
2.08E-04	2.918E+05	2.50E-06	7.295E-01
2.10E-04	3.060E+05	3.00E-05	9.180E+00
2.40E-04	3.313E+05	4.50E-05	1.491E+01
2.85E-04	3.520E+05	2.00E-05	7.040E+00
3.05E-04	4.214E+05	2.45E-04	1.032E+02
5.50E-04	5.039E+05	1.20E-04	6.047E+01
6.70E-04	5.295E+05	1.30E-05	6.884E+00
6.83E-04	5.817E+05	2.67E-04	1.553E+02
9.50E-04	6.629E+05	2.00E-04	1.326E+02
1.15E-03	7.442E+05	3.50E-04	2.605E+02
1.50E-03	7.993E+05	5.00E-05	3.996E+01
1.55E-03	8.369E+05	2.50E-04	2.092E+02
1.80E-03	9.126E+05	4.00E-04	3.650E+02
2.20E-03	9.664E+05	9.00E-05	8.698E+01
2.29E-03	1.007E+06	2.90E-04	2.920E+02
2.58E-03	1.078E+06	4.20E-04	4.528E+02
3.00E-03	1.185E+06	7.40E-04	8.769E+02
3.74E-03	1.262E+06	1.60E-04	2.019E+02
3.90E-03	1.435E+06	2.10E-03	3.014E+03
6.00E-03	1.708E+06	2.03E-03	3.467E+03
8.03E-03	1.910E+06	1.47E-03	2.808E+03
9.50E-03	2.161E+06	3.50E-03	7.564E+03
1.30E-02	2.495E+06	4.00E-03	9.980E+03
1.70E-02	2.943E+06	8.00E-03	2.354E+04
2.50E-02	3.362E+06	5.00E-03	1.681E+04
3.00E-02	3.899E+06	1.50E-02	5.849E+04

Continued on following page

E [MeV]	$\frac{dS}{dE} \left[\frac{n}{MeV \cdot sec} \right]$	dE	dS $\left[\frac{n}{sec} \right]$
4.50E-02	4.370E+06	5.00E-03	2.185E+04
5.00E-02	4.519E+06	2.00E-03	9.038E+03
5.20E-02	4.720E+06	8.00E-03	3.776E+04
6.00E-02	5.112E+06	1.30E-02	6.646E+04
7.30E-02	5.374E+06	2.00E-03	1.075E+04
7.50E-02	5.521E+06	7.00E-03	3.865E+04
8.20E-02	5.682E+06	3.00E-03	1.705E+04
8.50E-02	5.952E+06	1.50E-02	8.928E+04
1.00E-01	6.539E+06	2.83E-02	1.851E+05
1.28E-01	7.134E+06	2.17E-02	1.548E+05
1.50E-01	7.843E+06	5.00E-02	3.922E+05
2.00E-01	8.786E+06	7.00E-02	6.150E+05
2.70E-01	9.584E+06	6.00E-02	5.750E+05
3.30E-01	1.020E+07	7.00E-02	7.140E+05
4.00E-01	1.057E+07	2.00E-02	2.114E+05
4.20E-01	1.071E+07	2.00E-02	2.142E+05
4.40E-01	1.086E+07	3.00E-02	3.258E+05
4.70E-01	1.103E+07	2.95E-02	3.254E+05
5.00E-01	1.121E+07	5.05E-02	5.661E+05
5.50E-01	1.136E+07	2.30E-02	2.613E+05
5.73E-01	1.145E+07	2.70E-02	3.092E+05
6.00E-01	1.158E+07	7.00E-02	8.106E+05
6.70E-01	1.167E+07	9.00E-03	1.050E+05
6.79E-01	1.174E+07	7.10E-02	8.335E+05
7.50E-01	1.182E+07	7.00E-02	8.274E+05
8.20E-01	1.184E+07	4.11E-02	4.866E+05
8.61E-01	1.184E+07	1.39E-02	1.646E+05
8.75E-01	1.184E+07	2.50E-02	2.960E+05
9.00E-01	1.183E+07	2.00E-02	2.366E+05
9.20E-01	1.180E+07	9.00E-02	1.062E+06
1.01E+00	1.171E+07	9.00E-02	1.054E+06
1.10E+00	1.156E+07	1.00E-01	1.156E+06
1.20E+00	1.142E+07	5.00E-02	5.710E+05
1.25E+00	1.130E+07	6.70E-02	7.571E+05
1.32E+00	1.117E+07	3.90E-02	4.356E+05
1.36E+00	1.108E+07	4.40E-02	4.875E+05
1.40E+00	1.090E+07	1.00E-01	1.090E+06
1.50E+00	1.029E+07	3.50E-01	3.602E+06
1.85E+00	9.066E+06	5.04E-01	4.569E+06
2.35E+00	8.101E+06	1.25E-01	1.013E+06
2.48E+00	6.993E+06	5.21E-01	3.643E+06
3.00E+00	4.050E+06	1.30E+00	5.281E+06

Continued on following page

E [MeV]	$\frac{dS}{dE} \left[\frac{n}{MeV \cdot sec} \right]$	dE	dS $\left[\frac{n}{sec} \right]$
4.30E+00	2.045E+06	4.96E-01	1.014E+06
4.80E+00	1.024E+06	1.63E+00	1.673E+06
6.43E+00	3.010E+05	1.75E+00	5.277E+05
8.19E+00	7.664E+04	1.81E+00	1.389E+05
1.00E+01			

Table B.3: ORIGEN-ARP photon results for a GE 8×8 BWR assembly burned to 25.344 $\frac{MWd}{kg}$ and cooled for a combined time period of 15yr.

E [MeV]	$\frac{dS}{dE} \left[\frac{p}{MeV \cdot sec} \right]$	dE	dS $\left[\frac{p}{sec} \right]$
1.00E-02	4.77E+16	1.00E-02	4.767E+14
2.00E-02	2.49E+16	1.00E-02	2.485E+14
3.00E-02	2.12E+16	1.50E-02	3.180E+14
4.50E-02	1.09E+16	1.50E-02	1.628E+14
6.00E-02	6.64E+15	1.00E-02	6.639E+13
7.00E-02	5.69E+15	5.00E-03	2.844E+13
7.50E-02	4.49E+15	2.50E-02	1.122E+14
1.00E-01	2.44E+15	5.00E-02	1.222E+14
1.50E-01	1.46E+15	5.00E-02	7.295E+13
2.00E-01	6.79E+14	6.00E-02	4.072E+13
2.60E-01	4.57E+14	4.00E-02	1.827E+13
3.00E-01	4.01E+14	1.00E-01	4.009E+13
4.00E-01	2.53E+14	5.00E-02	1.266E+13
4.50E-01	1.97E+14	6.00E-02	1.183E+13
5.10E-01	1.18E+14	2.00E-03	2.354E+11
5.12E-01	1.04E+14	8.80E-02	9.187E+12
6.00E-01	1.73E+16	1.00E-01	1.727E+15
7.00E-01	1.93E+14	1.00E-01	1.927E+13
8.00E-01	7.22E+13	1.00E-01	7.219E+12
9.00E-01	7.72E+13	1.00E-01	7.718E+12
1.00E+00	2.48E+13	2.00E-01	4.962E+12
1.20E+00	7.90E+13	1.30E-01	1.027E+13
1.33E+00	5.91E+12	1.10E-01	6.495E+11
1.44E+00	4.65E+12	6.00E-02	2.790E+11
1.50E+00	1.51E+12	7.00E-02	1.057E+11
1.57E+00	6.32E+12	9.00E-02	5.684E+11
1.66E+00	5.19E+11	1.40E-01	7.259E+10
1.80E+00	1.64E+11	2.00E-01	3.274E+10
2.00E+00	3.78E+10	1.50E-01	5.676E+09
2.15E+00	7.79E+08	2.00E-01	1.558E+08

Continued on following page

E [MeV]	$\frac{dS}{dE} \left[\frac{p}{MeV \cdot sec} \right]$	dE	dS $\left[\frac{p}{sec} \right]$
2.35E+00	9.38E+08	1.50E-01	1.408E+08
2.50E+00	4.91E+08	2.50E-01	1.227E+08
2.75E+00	6.22E+07	2.50E-01	1.556E+07
3.00E+00	9.62E+06	5.00E-01	4.811E+06
3.50E+00	1.99E+06	5.00E-01	9.945E+05
4.00E+00	1.15E+06	5.00E-01	5.725E+05
4.50E+00	6.64E+05	5.00E-01	3.318E+05
5.00E+00	3.85E+05	5.00E-01	1.923E+05
5.50E+00	2.23E+05	5.00E-01	1.114E+05
6.00E+00	1.29E+05	5.00E-01	6.455E+04
6.50E+00	7.48E+04	5.00E-01	3.742E+04
7.00E+00	4.34E+04	5.00E-01	2.169E+04
7.50E+00	2.51E+04	5.00E-01	1.257E+04
8.00E+00	7.42E+03	2.00E+00	1.484E+04
1.00E+01			

Table B.4: ORIGEN-ARP neutron results for a GE 8×8 BWR assembly burned to 25.344 $\frac{MWd}{kg}$ and cooled for a combined time period of 15yr.

E [MeV]	$\frac{dS}{dE} \left[\frac{n}{MeV \cdot sec} \right]$	dE	dS $\left[\frac{n}{sec} \right]$
1.00E-11	1.163E+02	9.00E-11	1.047E-08
1.00E-10	4.742E+01	4.00E-10	1.897E-08
5.00E-10	3.094E+01	2.50E-10	7.735E-09
7.50E-10	2.699E+01	2.50E-10	6.748E-09
1.00E-09	2.343E+01	2.00E-10	4.686E-09
1.20E-09	2.199E+01	3.00E-10	6.597E-09
1.50E-09	1.934E+01	5.00E-10	9.670E-09
2.00E-09	1.746E+01	5.00E-10	8.730E-09
2.50E-09	1.590E+01	5.00E-10	7.950E-09
3.00E-09	1.456E+01	1.00E-09	1.456E-08
4.00E-09	1.315E+01	1.00E-09	1.315E-08
5.00E-09	1.188E+01	2.50E-09	2.970E-08
7.50E-09	1.075E+01	2.50E-09	2.688E-08
1.00E-08	9.646E+00	1.53E-08	1.476E-07
2.53E-08	9.305E+00	4.70E-09	4.373E-08
3.00E-08	9.426E+00	1.00E-08	9.426E-08
4.00E-08	9.618E+00	1.00E-08	9.618E-08
5.00E-08	9.934E+00	1.00E-08	9.934E-08
6.00E-08	1.021E+01	1.00E-08	1.021E-07
7.00E-08	1.053E+01	1.00E-08	1.053E-07

Continued on following page

E [MeV]	$\frac{dS}{dE} [\frac{n}{MeVsec}]$	dE	dS [$\frac{n}{sec}$]
8.00E-08	1.085E+01	1.00E-08	1.085E-07
9.00E-08	1.116E+01	1.00E-08	1.116E-07
1.00E-07	1.175E+01	2.50E-08	2.938E-07
1.25E-07	1.250E+01	2.50E-08	3.125E-07
1.50E-07	3.229E+02	2.50E-08	8.073E-06
1.75E-07	3.777E+02	2.50E-08	9.443E-06
2.00E-07	3.783E+02	2.50E-08	9.458E-06
2.25E-07	3.790E+02	2.50E-08	9.475E-06
2.50E-07	3.796E+02	2.50E-08	9.490E-06
2.75E-07	3.802E+02	2.50E-08	9.505E-06
3.00E-07	3.808E+02	2.50E-08	9.520E-06
3.25E-07	3.814E+02	2.50E-08	9.535E-06
3.50E-07	3.819E+02	2.50E-08	9.548E-06
3.75E-07	3.843E+02	2.50E-08	9.607E-06
4.00E-07	3.851E+02	5.00E-08	1.926E-05
4.50E-07	3.861E+02	5.00E-08	1.931E-05
5.00E-07	3.870E+02	5.00E-08	1.935E-05
5.50E-07	3.880E+02	5.00E-08	1.940E-05
6.00E-07	3.886E+02	2.50E-08	9.715E-06
6.25E-07	3.890E+02	2.50E-08	9.725E-06
6.50E-07	3.896E+02	5.00E-08	1.948E-05
7.00E-07	3.904E+02	5.00E-08	1.952E-05
7.50E-07	3.912E+02	5.00E-08	1.956E-05
8.00E-07	3.919E+02	5.00E-08	1.960E-05
8.50E-07	3.926E+02	5.00E-08	1.963E-05
9.00E-07	3.933E+02	2.50E-08	9.833E-06
9.25E-07	3.934E+02	2.50E-08	9.835E-06
9.50E-07	3.940E+02	2.50E-08	9.850E-06
9.75E-07	3.942E+02	2.50E-08	9.855E-06
1.00E-06	3.947E+02	1.00E-08	3.947E-06
1.01E-06	3.943E+02	1.00E-08	3.943E-06
1.02E-06	3.949E+02	1.00E-08	3.949E-06
1.03E-06	3.945E+02	1.00E-08	3.945E-06
1.04E-06	3.955E+02	1.00E-08	3.955E-06
1.05E-06	3.948E+02	1.00E-08	3.948E-06
1.06E-06	3.954E+02	1.00E-08	3.954E-06
1.07E-06	3.953E+02	1.00E-08	3.953E-06
1.08E-06	3.956E+02	1.00E-08	3.956E-06
1.09E-06	3.959E+02	1.00E-08	3.959E-06
1.10E-06	3.958E+02	1.00E-08	3.958E-06
1.11E-06	3.961E+02	1.00E-08	3.961E-06
1.12E-06	6.405E+02	1.00E-08	6.405E-06

Continued on following page

E [MeV]	$\frac{dS}{dE} \left[\frac{n}{MeV \cdot sec} \right]$	dE	dS $\left[\frac{n}{sec} \right]$
1.13E-06	6.430E+02	1.00E-08	6.430E-06
1.14E-06	6.482E+02	1.00E-08	6.482E-06
1.15E-06	2.000E+03	2.50E-08	5.000E-05
1.18E-06	1.671E+04	2.50E-08	4.178E-04
1.20E-06	1.569E+04	2.50E-08	3.923E-04
1.23E-06	1.469E+04	2.50E-08	3.673E-04
1.25E-06	2.521E+04	5.00E-08	1.261E-03
1.30E-06	1.658E+04	5.00E-08	8.290E-04
1.35E-06	1.697E+04	5.00E-08	8.485E-04
1.40E-06	7.658E+03	5.00E-08	3.829E-04
1.45E-06	1.742E+04	5.00E-08	8.710E-04
1.50E-06	1.776E+04	9.00E-08	1.598E-03
1.59E-06	2.398E+04	9.00E-08	2.158E-03
1.68E-06	1.897E+04	9.00E-08	1.707E-03
1.77E-06	1.374E+04	9.00E-08	1.237E-03
1.86E-06	2.570E+04	8.00E-08	2.056E-03
1.94E-06	2.080E+04	6.00E-08	1.248E-03
2.00E-06	2.030E+04	1.20E-07	2.436E-03
2.12E-06	2.117E+04	9.00E-08	1.905E-03
2.21E-06	1.565E+04	9.00E-08	1.409E-03
2.30E-06	2.184E+04	8.00E-08	1.747E-03
2.38E-06	2.870E+04	9.00E-08	2.583E-03
2.47E-06	1.637E+04	1.00E-07	1.637E-03
2.57E-06	2.916E+04	1.00E-07	2.916E-03
2.67E-06	2.366E+04	1.00E-07	2.366E-03
2.77E-06	2.442E+04	1.00E-07	2.442E-03
2.87E-06	2.405E+04	1.00E-07	2.405E-03
2.97E-06	3.404E+03	3.00E-08	1.021E-04
3.00E-06	3.753E+04	5.00E-08	1.877E-03
3.05E-06	1.869E+04	1.00E-07	1.869E-03
3.15E-06	2.793E+04	3.50E-07	9.776E-03
3.50E-06	2.427E+04	2.30E-07	5.582E-03
3.73E-06	3.069E+04	2.70E-07	8.286E-03
4.00E-06	2.876E+04	7.50E-07	2.157E-02
4.75E-06	3.118E+04	2.50E-07	7.795E-03
5.00E-06	3.457E+04	4.00E-07	1.383E-02
5.40E-06	3.409E+04	6.00E-07	2.045E-02
6.00E-06	3.149E+04	2.50E-07	7.873E-03
6.25E-06	3.964E+04	2.50E-07	9.910E-03
6.50E-06	3.659E+04	2.50E-07	9.148E-03
6.75E-06	3.701E+04	2.50E-07	9.253E-03
7.00E-06	3.832E+04	1.50E-07	5.748E-03

Continued on following page

E [MeV]	$\frac{dS}{dE} \left[\frac{n}{MeV \cdot sec} \right]$	dE	dS $\left[\frac{n}{sec} \right]$
7.15E-06	3.926E+04	9.50E-07	3.730E-02
8.10E-06	4.052E+04	1.00E-06	4.052E-02
9.10E-06	4.511E+04	9.00E-07	4.060E-02
1.00E-05	4.651E+04	1.50E-06	6.977E-02
1.15E-05	4.855E+04	4.00E-07	1.942E-02
1.19E-05	4.994E+04	1.00E-06	4.994E-02
1.29E-05	5.164E+04	8.50E-07	4.389E-02
1.38E-05	5.101E+04	6.50E-07	3.316E-02
1.44E-05	5.658E+04	7.00E-07	3.961E-02
1.51E-05	5.425E+04	9.00E-07	4.883E-02
1.60E-05	5.752E+04	1.00E-06	5.752E-02
1.70E-05	5.958E+04	1.50E-06	8.937E-02
1.85E-05	6.144E+04	5.00E-07	3.072E-02
1.90E-05	6.252E+04	1.00E-06	6.252E-02
2.00E-05	6.566E+04	1.00E-06	6.566E-02
2.10E-05	6.600E+04	1.50E-06	9.900E-02
2.25E-05	6.847E+04	2.50E-06	1.712E-01
2.50E-05	7.354E+04	2.50E-06	1.839E-01
2.75E-05	7.613E+04	2.50E-06	1.903E-01
3.00E-05	7.700E+04	1.25E-06	9.625E-02
3.13E-05	8.392E+04	5.00E-07	4.196E-02
3.18E-05	8.092E+04	1.50E-06	1.214E-01
3.33E-05	8.189E+04	5.00E-07	4.094E-02
3.38E-05	8.298E+04	8.50E-07	7.053E-02
3.46E-05	8.176E+04	9.00E-07	7.358E-02
3.55E-05	8.540E+04	1.50E-06	1.281E-01
3.70E-05	8.670E+04	1.00E-06	8.670E-02
3.80E-05	8.815E+04	1.10E-06	9.697E-02
3.91E-05	9.341E+04	5.00E-07	4.670E-02
3.96E-05	9.081E+04	1.40E-06	1.271E-01
4.10E-05	9.504E+04	1.40E-06	1.331E-01
4.24E-05	9.675E+04	1.60E-06	1.548E-01
4.40E-05	9.617E+04	1.20E-06	1.154E-01
4.52E-05	9.989E+04	1.80E-06	1.798E-01
4.70E-05	1.026E+05	1.30E-06	1.334E-01
4.83E-05	1.039E+05	9.00E-07	9.351E-02
4.92E-05	1.068E+05	1.40E-06	1.495E-01
5.06E-05	1.042E+05	1.40E-06	1.459E-01
5.20E-05	1.077E+05	1.40E-06	1.508E-01
5.34E-05	1.110E+05	5.60E-06	6.216E-01
5.90E-05	1.146E+05	2.00E-06	2.292E-01
6.10E-05	1.179E+05	4.00E-06	4.716E-01

Continued on following page

E [MeV]	$\frac{dS}{dE} \left[\frac{n}{MeV \cdot sec} \right]$	dE	dS $\left[\frac{n}{sec} \right]$
6.50E-05	1.189E+05	2.50E-06	2.973E-01
6.75E-05	1.239E+05	4.50E-06	5.576E-01
7.20E-05	1.259E+05	4.00E-06	5.036E-01
7.60E-05	1.300E+05	4.00E-06	5.200E-01
8.00E-05	1.329E+05	2.00E-06	2.658E-01
8.20E-05	1.368E+05	8.00E-06	1.094E+00
9.00E-05	1.436E+05	1.00E-05	1.436E+00
1.00E-04	1.500E+05	8.00E-06	1.200E+00
1.08E-04	1.553E+05	7.00E-06	1.087E+00
1.15E-04	1.591E+05	4.00E-06	6.364E-01
1.19E-04	1.625E+05	3.00E-06	4.875E-01
1.22E-04	1.813E+05	6.40E-05	1.160E+01
1.86E-04	1.998E+05	6.50E-06	1.299E+00
1.93E-04	2.064E+05	1.50E-05	3.096E+00
2.08E-04	2.089E+05	2.50E-06	5.223E-01
2.10E-04	2.189E+05	3.00E-05	6.567E+00
2.40E-04	2.370E+05	4.50E-05	1.067E+01
2.85E-04	2.518E+05	2.00E-05	5.036E+00
3.05E-04	3.008E+05	2.45E-04	7.370E+01
5.50E-04	3.590E+05	1.20E-04	4.308E+01
6.70E-04	3.771E+05	1.30E-05	4.902E+00
6.83E-04	4.141E+05	2.67E-04	1.106E+02
9.50E-04	4.731E+05	2.00E-04	9.462E+01
1.15E-03	5.317E+05	3.50E-04	1.861E+02
1.50E-03	5.710E+05	5.00E-05	2.855E+01
1.55E-03	5.976E+05	2.50E-04	1.494E+02
1.80E-03	6.510E+05	4.00E-04	2.604E+02
2.20E-03	6.890E+05	9.00E-05	6.201E+01
2.29E-03	7.176E+05	2.90E-04	2.081E+02
2.58E-03	7.681E+05	4.20E-04	3.226E+02
3.00E-03	8.450E+05	7.40E-04	6.253E+02
3.74E-03	8.997E+05	1.60E-04	1.440E+02
3.90E-03	1.025E+06	2.10E-03	2.153E+03
6.00E-03	1.220E+06	2.03E-03	2.477E+03
8.03E-03	1.364E+06	1.47E-03	2.005E+03
9.50E-03	1.545E+06	3.50E-03	5.408E+03
1.30E-02	1.784E+06	4.00E-03	7.136E+03
1.70E-02	2.106E+06	8.00E-03	1.685E+04
2.50E-02	2.405E+06	5.00E-03	1.203E+04
3.00E-02	2.789E+06	1.50E-02	4.184E+04
4.50E-02	3.124E+06	5.00E-03	1.562E+04
5.00E-02	3.230E+06	2.00E-03	6.460E+03

Continued on following page

E [MeV]	$\frac{dS}{dE} \left[\frac{n}{MeV \cdot sec} \right]$	dE	dS $\left[\frac{n}{sec} \right]$
5.20E-02	3.373E+06	8.00E-03	2.698E+04
6.00E-02	3.651E+06	1.30E-02	4.746E+04
7.30E-02	3.837E+06	2.00E-03	7.674E+03
7.50E-02	3.943E+06	7.00E-03	2.760E+04
8.20E-02	4.058E+06	3.00E-03	1.217E+04
8.50E-02	4.250E+06	1.50E-02	6.375E+04
1.00E-01	4.670E+06	2.83E-02	1.322E+05
1.28E-01	5.096E+06	2.17E-02	1.106E+05
1.50E-01	5.599E+06	5.00E-02	2.800E+05
2.00E-01	6.263E+06	7.00E-02	4.384E+05
2.70E-01	6.825E+06	6.00E-02	4.095E+05
3.30E-01	7.262E+06	7.00E-02	5.083E+05
4.00E-01	7.525E+06	2.00E-02	1.505E+05
4.20E-01	7.625E+06	2.00E-02	1.525E+05
4.40E-01	7.736E+06	3.00E-02	2.321E+05
4.70E-01	7.852E+06	2.95E-02	2.316E+05
5.00E-01	7.985E+06	5.05E-02	4.032E+05
5.50E-01	8.089E+06	2.30E-02	1.860E+05
5.73E-01	8.150E+06	2.70E-02	2.201E+05
6.00E-01	8.239E+06	7.00E-02	5.767E+05
6.70E-01	8.303E+06	9.00E-03	7.473E+04
6.79E-01	8.352E+06	7.10E-02	5.930E+05
7.50E-01	8.411E+06	7.00E-02	5.888E+05
8.20E-01	8.428E+06	4.11E-02	3.464E+05
8.61E-01	8.430E+06	1.39E-02	1.172E+05
8.75E-01	8.427E+06	2.50E-02	2.107E+05
9.00E-01	8.421E+06	2.00E-02	1.684E+05
9.20E-01	8.404E+06	9.00E-02	7.564E+05
1.01E+00	8.346E+06	9.00E-02	7.511E+05
1.10E+00	8.255E+06	1.00E-01	8.255E+05
1.20E+00	8.172E+06	5.00E-02	4.086E+05
1.25E+00	8.095E+06	6.70E-02	5.424E+05
1.32E+00	8.008E+06	3.90E-02	3.123E+05
1.36E+00	7.954E+06	4.40E-02	3.500E+05
1.40E+00	7.850E+06	1.00E-01	7.850E+05
1.50E+00	7.479E+06	3.50E-01	2.618E+06
1.85E+00	6.750E+06	5.04E-01	3.402E+06
2.35E+00	6.139E+06	1.25E-01	7.674E+05
2.48E+00	5.339E+06	5.21E-01	2.782E+06
3.00E+00	3.014E+06	1.30E+00	3.930E+06
4.30E+00	1.436E+06	4.96E-01	7.123E+05
4.80E+00	7.154E+05	1.63E+00	1.169E+06

Continued on following page

E [MeV]	$\frac{dS}{dE} \left[\frac{n}{MeVsec} \right]$	dE	dS $\left[\frac{n}{sec} \right]$
6.43E+00	2.092E+05	1.75E+00	3.667E+05
8.19E+00	5.311E+04	1.81E+00	9.629E+04
1.00E+01			

Table B.5: ORIGEN-ARP photon results for a GE 8×8 BWR assembly burned to 25.344 $\frac{MWd}{kg}$ and cooled for a combined time period of 25yr.

E [MeV]	$\frac{dS}{dE} \left[\frac{p}{MeVsec} \right]$	dE	dS $\left[\frac{p}{sec} \right]$
1.00E-02	3.80E+16	1.00E-02	3.802E+14
2.00E-02	1.93E+16	1.00E-02	1.929E+14
3.00E-02	1.64E+16	1.50E-02	2.463E+14
4.50E-02	9.07E+15	1.50E-02	1.361E+14
6.00E-02	5.17E+15	1.00E-02	5.171E+13
7.00E-02	4.44E+15	5.00E-03	2.219E+13
7.50E-02	3.46E+15	2.50E-02	8.648E+13
1.00E-01	1.83E+15	5.00E-02	9.125E+13
1.50E-01	1.14E+15	5.00E-02	5.675E+13
2.00E-01	5.18E+14	6.00E-02	3.110E+13
2.60E-01	3.57E+14	4.00E-02	1.426E+13
3.00E-01	3.12E+14	1.00E-01	3.122E+13
4.00E-01	1.87E+14	5.00E-02	9.330E+12
4.50E-01	1.49E+14	6.00E-02	8.958E+12
5.10E-01	5.42E+13	2.00E-03	1.083E+11
5.12E-01	5.50E+13	8.80E-02	4.843E+12
6.00E-01	1.36E+16	1.00E-01	1.364E+15
7.00E-01	6.83E+13	1.00E-01	6.829E+12
8.00E-01	4.12E+13	1.00E-01	4.116E+12
9.00E-01	4.14E+13	1.00E-01	4.140E+12
1.00E+00	1.44E+13	2.00E-01	2.876E+12
1.20E+00	3.74E+13	1.30E-01	4.861E+12
1.33E+00	2.70E+12	1.10E-01	2.969E+11
1.44E+00	2.59E+12	6.00E-02	1.554E+11
1.50E+00	1.09E+12	7.00E-02	7.651E+10
1.57E+00	3.21E+12	9.00E-02	2.885E+11
1.66E+00	4.02E+11	1.40E-01	5.627E+10
1.80E+00	1.27E+11	2.00E-01	2.544E+10
2.00E+00	2.91E+10	1.50E-01	4.371E+09
2.15E+00	1.00E+08	2.00E-01	2.006E+07
2.35E+00	1.11E+08	1.50E-01	1.671E+07
2.50E+00	3.93E+08	2.50E-01	9.820E+07

Continued on following page

E [MeV]	$\frac{dS}{dE} \left[\frac{p}{MeVsec} \right]$	dE	dS $\left[\frac{p}{sec} \right]$
2.75E+00	4.13E+06	2.50E-01	1.033E+06
3.00E+00	2.48E+06	5.00E-01	1.240E+06
3.50E+00	1.43E+06	5.00E-01	7.160E+05
4.00E+00	8.25E+05	5.00E-01	4.126E+05
4.50E+00	4.78E+05	5.00E-01	2.390E+05
5.00E+00	2.77E+05	5.00E-01	1.384E+05
5.50E+00	1.60E+05	5.00E-01	8.015E+04
6.00E+00	9.29E+04	5.00E-01	4.645E+04
6.50E+00	5.38E+04	5.00E-01	2.691E+04
7.00E+00	3.12E+04	5.00E-01	1.560E+04
7.50E+00	1.81E+04	5.00E-01	9.035E+03
8.00E+00	5.33E+03	2.00E+00	1.067E+04
1.00E+01			

Table B.6: ORIGEN-ARP neutron results for a GE 8 × 8 BWR assembly burned to 25.344 $\frac{MWd}{kg}$ and cooled for a combined time period of 25yr.

E [MeV]	$\frac{dS}{dE} \left[\frac{n}{MeVsec} \right]$	dE	dS $\left[\frac{n}{sec} \right]$
1.00E-11	1.162E+02	9.00E-11	1.046E-08
1.00E-10	4.735E+01	4.00E-10	1.894E-08
5.00E-10	3.089E+01	2.50E-10	7.723E-09
7.50E-10	2.695E+01	2.50E-10	6.738E-09
1.00E-09	2.340E+01	2.00E-10	4.680E-09
1.20E-09	2.195E+01	3.00E-10	6.585E-09
1.50E-09	1.932E+01	5.00E-10	9.660E-09
2.00E-09	1.743E+01	5.00E-10	8.715E-09
2.50E-09	1.588E+01	5.00E-10	7.940E-09
3.00E-09	1.454E+01	1.00E-09	1.454E-08
4.00E-09	1.313E+01	1.00E-09	1.313E-08
5.00E-09	1.186E+01	2.50E-09	2.965E-08
7.50E-09	1.074E+01	2.50E-09	2.685E-08
1.00E-08	9.634E+00	1.53E-08	1.474E-07
2.53E-08	9.294E+00	4.70E-09	4.368E-08
3.00E-08	9.416E+00	1.00E-08	9.416E-08
4.00E-08	9.607E+00	1.00E-08	9.607E-08
5.00E-08	9.923E+00	1.00E-08	9.923E-08
6.00E-08	1.020E+01	1.00E-08	1.020E-07
7.00E-08	1.052E+01	1.00E-08	1.052E-07
8.00E-08	1.084E+01	1.00E-08	1.084E-07
9.00E-08	1.115E+01	1.00E-08	1.115E-07

Continued on following page

E [MeV]	$\frac{dS}{dE} \left[\frac{n}{MeV \cdot sec} \right]$	dE	dS $\left[\frac{n}{sec} \right]$
1.00E-07	1.173E+01	2.50E-08	2.933E-07
1.25E-07	1.248E+01	2.50E-08	3.120E-07
1.50E-07	3.228E+02	2.50E-08	8.070E-06
1.75E-07	3.776E+02	2.50E-08	9.440E-06
2.00E-07	3.782E+02	2.50E-08	9.455E-06
2.25E-07	3.789E+02	2.50E-08	9.473E-06
2.50E-07	3.795E+02	2.50E-08	9.488E-06
2.75E-07	3.801E+02	2.50E-08	9.502E-06
3.00E-07	3.806E+02	2.50E-08	9.515E-06
3.25E-07	3.812E+02	2.50E-08	9.530E-06
3.50E-07	3.818E+02	2.50E-08	9.545E-06
3.75E-07	3.841E+02	2.50E-08	9.602E-06
4.00E-07	3.849E+02	5.00E-08	1.925E-05
4.50E-07	3.859E+02	5.00E-08	1.930E-05
5.00E-07	3.868E+02	5.00E-08	1.934E-05
5.50E-07	3.877E+02	5.00E-08	1.939E-05
6.00E-07	3.884E+02	2.50E-08	9.710E-06
6.25E-07	3.887E+02	2.50E-08	9.717E-06
6.50E-07	3.894E+02	5.00E-08	1.947E-05
7.00E-07	3.901E+02	5.00E-08	1.951E-05
7.50E-07	3.910E+02	5.00E-08	1.955E-05
8.00E-07	3.917E+02	5.00E-08	1.959E-05
8.50E-07	3.924E+02	5.00E-08	1.962E-05
9.00E-07	3.930E+02	2.50E-08	9.825E-06
9.25E-07	3.932E+02	2.50E-08	9.830E-06
9.50E-07	3.938E+02	2.50E-08	9.845E-06
9.75E-07	3.940E+02	2.50E-08	9.850E-06
1.00E-06	3.945E+02	1.00E-08	3.945E-06
1.01E-06	3.941E+02	1.00E-08	3.941E-06
1.02E-06	3.947E+02	1.00E-08	3.947E-06
1.03E-06	3.943E+02	1.00E-08	3.943E-06
1.04E-06	3.953E+02	1.00E-08	3.953E-06
1.05E-06	3.945E+02	1.00E-08	3.945E-06
1.06E-06	3.951E+02	1.00E-08	3.951E-06
1.07E-06	3.951E+02	1.00E-08	3.951E-06
1.08E-06	3.953E+02	1.00E-08	3.953E-06
1.09E-06	3.956E+02	1.00E-08	3.956E-06
1.10E-06	3.955E+02	1.00E-08	3.955E-06
1.11E-06	3.958E+02	1.00E-08	3.958E-06
1.12E-06	6.403E+02	1.00E-08	6.403E-06
1.13E-06	6.427E+02	1.00E-08	6.427E-06
1.14E-06	6.480E+02	1.00E-08	6.480E-06

Continued on following page

E [MeV]	$\frac{dS}{dE} \left[\frac{n}{MeV \cdot sec} \right]$	dE	dS $\left[\frac{n}{sec} \right]$
1.15E-06	1.982E+03	2.50E-08	4.955E-05
1.18E-06	1.235E+04	2.50E-08	3.088E-04
1.20E-06	1.130E+04	2.50E-08	2.825E-04
1.23E-06	1.026E+04	2.50E-08	2.565E-04
1.25E-06	1.801E+04	5.00E-08	9.005E-04
1.30E-06	1.194E+04	5.00E-08	5.970E-04
1.35E-06	1.223E+04	5.00E-08	6.115E-04
1.40E-06	5.678E+03	5.00E-08	2.839E-04
1.45E-06	1.255E+04	5.00E-08	6.275E-04
1.50E-06	1.279E+04	9.00E-08	1.151E-03
1.59E-06	1.717E+04	9.00E-08	1.545E-03
1.68E-06	1.367E+04	9.00E-08	1.230E-03
1.77E-06	1.010E+04	9.00E-08	9.090E-04
1.86E-06	1.813E+04	8.00E-08	1.450E-03
1.94E-06	1.513E+04	6.00E-08	9.078E-04
2.00E-06	1.451E+04	1.20E-07	1.741E-03
2.12E-06	1.525E+04	9.00E-08	1.373E-03
2.21E-06	1.158E+04	9.00E-08	1.042E-03
2.30E-06	1.570E+04	8.00E-08	1.256E-03
2.38E-06	2.042E+04	9.00E-08	1.838E-03
2.47E-06	1.186E+04	1.00E-07	1.186E-03
2.57E-06	2.075E+04	1.00E-07	2.075E-03
2.67E-06	1.701E+04	1.00E-07	1.701E-03
2.77E-06	1.767E+04	1.00E-07	1.767E-03
2.87E-06	1.716E+04	1.00E-07	1.716E-03
2.97E-06	3.231E+03	3.00E-08	9.693E-05
3.00E-06	2.646E+04	5.00E-08	1.323E-03
3.05E-06	1.367E+04	1.00E-07	1.367E-03
3.15E-06	2.000E+04	3.50E-07	7.000E-03
3.50E-06	1.760E+04	2.30E-07	4.048E-03
3.73E-06	2.194E+04	2.70E-07	5.924E-03
4.00E-06	2.068E+04	7.50E-07	1.551E-02
4.75E-06	2.231E+04	2.50E-07	5.578E-03
5.00E-06	2.473E+04	4.00E-07	9.892E-03
5.40E-06	2.449E+04	6.00E-07	1.469E-02
6.00E-06	2.272E+04	2.50E-07	5.680E-03
6.25E-06	2.830E+04	2.50E-07	7.075E-03
6.50E-06	2.624E+04	2.50E-07	6.560E-03
6.75E-06	2.646E+04	2.50E-07	6.615E-03
7.00E-06	2.762E+04	1.50E-07	4.143E-03
7.15E-06	2.814E+04	9.50E-07	2.673E-02
8.10E-06	2.909E+04	1.00E-06	2.909E-02

Continued on following page

E [MeV]	$\frac{dS}{dE} \left[\frac{n}{MeV \cdot sec} \right]$	dE	dS $\left[\frac{n}{sec} \right]$
9.10E-06	3.229E+04	9.00E-07	2.906E-02
1.00E-05	3.333E+04	1.50E-06	5.000E-02
1.15E-05	3.478E+04	4.00E-07	1.391E-02
1.19E-05	3.577E+04	1.00E-06	3.577E-02
1.29E-05	3.696E+04	8.50E-07	3.142E-02
1.38E-05	3.661E+04	6.50E-07	2.380E-02
1.44E-05	4.049E+04	7.00E-07	2.834E-02
1.51E-05	3.891E+04	9.00E-07	3.502E-02
1.60E-05	4.120E+04	1.00E-06	4.120E-02
1.70E-05	4.264E+04	1.50E-06	6.396E-02
1.85E-05	4.405E+04	5.00E-07	2.203E-02
1.90E-05	4.476E+04	1.00E-06	4.476E-02
2.00E-05	4.692E+04	1.00E-06	4.692E-02
2.10E-05	4.724E+04	1.50E-06	7.086E-02
2.25E-05	4.904E+04	2.50E-06	1.226E-01
2.50E-05	5.260E+04	2.50E-06	1.315E-01
2.75E-05	5.446E+04	2.50E-06	1.362E-01
3.00E-05	5.518E+04	1.25E-06	6.898E-02
3.13E-05	5.991E+04	5.00E-07	2.995E-02
3.18E-05	5.789E+04	1.50E-06	8.684E-02
3.33E-05	5.851E+04	5.00E-07	2.925E-02
3.38E-05	5.937E+04	8.50E-07	5.046E-02
3.46E-05	5.862E+04	9.00E-07	5.276E-02
3.55E-05	6.110E+04	1.50E-06	9.165E-02
3.70E-05	6.198E+04	1.00E-06	6.198E-02
3.80E-05	6.310E+04	1.10E-06	6.941E-02
3.91E-05	6.658E+04	5.00E-07	3.329E-02
3.96E-05	6.535E+04	1.40E-06	9.149E-02
4.10E-05	6.953E+04	1.40E-06	9.734E-02
4.24E-05	7.078E+04	1.60E-06	1.132E-01
4.40E-05	7.040E+04	1.20E-06	8.448E-02
4.52E-05	7.313E+04	1.80E-06	1.316E-01
4.70E-05	7.567E+04	1.30E-06	9.837E-02
4.83E-05	7.667E+04	9.00E-07	6.900E-02
4.92E-05	7.859E+04	1.40E-06	1.100E-01
5.06E-05	7.685E+04	1.40E-06	1.076E-01
5.20E-05	7.928E+04	1.40E-06	1.110E-01
5.34E-05	8.163E+04	5.60E-06	4.571E-01
5.90E-05	8.425E+04	2.00E-06	1.685E-01
6.10E-05	8.660E+04	4.00E-06	3.464E-01
6.50E-05	8.732E+04	2.50E-06	2.183E-01
6.75E-05	9.093E+04	4.50E-06	4.092E-01

Continued on following page

E [MeV]	$\frac{dS}{dE} [\frac{n}{MeVsec}]$	dE	dS [$\frac{n}{sec}$]
7.20E-05	9.236E+04	4.00E-06	3.694E-01
7.60E-05	9.528E+04	4.00E-06	3.811E-01
8.00E-05	9.751E+04	2.00E-06	1.950E-01
8.20E-05	1.003E+05	8.00E-06	8.024E-01
9.00E-05	1.052E+05	1.00E-05	1.052E+00
1.00E-04	1.098E+05	8.00E-06	8.784E-01
1.08E-04	1.137E+05	7.00E-06	7.959E-01
1.15E-04	1.164E+05	4.00E-06	4.656E-01
1.19E-04	1.187E+05	3.00E-06	3.561E-01
1.22E-04	1.323E+05	6.40E-05	8.467E+00
1.86E-04	1.456E+05	6.50E-06	9.464E-01
1.93E-04	1.503E+05	1.50E-05	2.255E+00
2.08E-04	1.525E+05	2.50E-06	3.813E-01
2.10E-04	1.596E+05	3.00E-05	4.788E+00
2.40E-04	1.728E+05	4.50E-05	7.776E+00
2.85E-04	1.836E+05	2.00E-05	3.672E+00
3.05E-04	2.188E+05	2.45E-04	5.361E+01
5.50E-04	2.605E+05	1.20E-04	3.126E+01
6.70E-04	2.735E+05	1.30E-05	3.556E+00
6.83E-04	3.002E+05	2.67E-04	8.015E+01
9.50E-04	3.441E+05	2.00E-04	6.882E+01
1.15E-03	3.872E+05	3.50E-04	1.355E+02
1.50E-03	4.158E+05	5.00E-05	2.079E+01
1.55E-03	4.349E+05	2.50E-04	1.087E+02
1.80E-03	4.731E+05	4.00E-04	1.892E+02
2.20E-03	5.005E+05	9.00E-05	4.504E+01
2.29E-03	5.211E+05	2.90E-04	1.511E+02
2.58E-03	5.577E+05	4.20E-04	2.342E+02
3.00E-03	6.138E+05	7.40E-04	4.542E+02
3.74E-03	6.538E+05	1.60E-04	1.046E+02
3.90E-03	7.467E+05	2.10E-03	1.568E+03
6.00E-03	8.885E+05	2.03E-03	1.804E+03
8.03E-03	9.927E+05	1.47E-03	1.459E+03
9.50E-03	1.126E+06	3.50E-03	3.941E+03
1.30E-02	1.300E+06	4.00E-03	5.200E+03
1.70E-02	1.536E+06	8.00E-03	1.229E+04
2.50E-02	1.755E+06	5.00E-03	8.775E+03
3.00E-02	2.034E+06	1.50E-02	3.051E+04
4.50E-02	2.277E+06	5.00E-03	1.139E+04
5.00E-02	2.353E+06	2.00E-03	4.706E+03
5.20E-02	2.456E+06	8.00E-03	1.965E+04
6.00E-02	2.657E+06	1.30E-02	3.454E+04

Continued on following page

E [MeV]	$\frac{dS}{dE} \left[\frac{n}{MeV \cdot sec} \right]$	dE	dS $\left[\frac{n}{sec} \right]$
7.30E-02	2.792E+06	2.00E-03	5.584E+03
7.50E-02	2.869E+06	7.00E-03	2.008E+04
8.20E-02	2.953E+06	3.00E-03	8.859E+03
8.50E-02	3.094E+06	1.50E-02	4.641E+04
1.00E-01	3.400E+06	2.83E-02	9.622E+04
1.28E-01	3.710E+06	2.17E-02	8.051E+04
1.50E-01	4.074E+06	5.00E-02	2.037E+05
2.00E-01	4.549E+06	7.00E-02	3.184E+05
2.70E-01	4.950E+06	6.00E-02	2.970E+05
3.30E-01	5.264E+06	7.00E-02	3.685E+05
4.00E-01	5.458E+06	2.00E-02	1.092E+05
4.20E-01	5.531E+06	2.00E-02	1.106E+05
4.40E-01	5.612E+06	3.00E-02	1.684E+05
4.70E-01	5.696E+06	2.95E-02	1.680E+05
5.00E-01	5.790E+06	5.05E-02	2.924E+05
5.50E-01	5.865E+06	2.30E-02	1.349E+05
5.73E-01	5.908E+06	2.70E-02	1.595E+05
6.00E-01	5.970E+06	7.00E-02	4.179E+05
6.70E-01	6.015E+06	9.00E-03	5.414E+04
6.79E-01	6.051E+06	7.10E-02	4.296E+05
7.50E-01	6.095E+06	7.00E-02	4.267E+05
8.20E-01	6.108E+06	4.11E-02	2.510E+05
8.61E-01	6.111E+06	1.39E-02	8.494E+04
8.75E-01	6.108E+06	2.50E-02	1.527E+05
9.00E-01	6.104E+06	2.00E-02	1.221E+05
9.20E-01	6.097E+06	9.00E-02	5.487E+05
1.01E+00	6.063E+06	9.00E-02	5.457E+05
1.10E+00	6.007E+06	1.00E-01	6.007E+05
1.20E+00	5.959E+06	5.00E-02	2.980E+05
1.25E+00	5.914E+06	6.70E-02	3.962E+05
1.32E+00	5.856E+06	3.90E-02	2.284E+05
1.36E+00	5.828E+06	4.40E-02	2.564E+05
1.40E+00	5.770E+06	1.00E-01	5.770E+05
1.50E+00	5.559E+06	3.50E-01	1.946E+06
1.85E+00	5.160E+06	5.04E-01	2.601E+06
2.35E+00	4.786E+06	1.25E-01	5.983E+05
2.48E+00	4.195E+06	5.21E-01	2.186E+06
3.00E+00	2.302E+06	1.30E+00	3.002E+06
4.30E+00	1.023E+06	4.96E-01	5.074E+05
4.80E+00	5.059E+05	1.63E+00	8.266E+05
6.43E+00	1.470E+05	1.75E+00	2.577E+05
8.19E+00	3.715E+04	1.81E+00	6.735E+04

Continued on following page

E [MeV]	$\frac{dS}{dE} \left[\frac{n}{MeVsec} \right]$	dE	dS $\left[\frac{n}{sec} \right]$
1.00E+01			

Table B.7: ORIGEN-ARP photon results for a GE 8×8 BWR assembly burned to 25.344 $\frac{MWd}{kg}$ and cooled for a combined time period of 35yr.

E [MeV]	$\frac{dS}{dE} \left[\frac{p}{MeVsec} \right]$	dE	dS $\left[\frac{p}{sec} \right]$
1.00E-02	3.05E+16	1.00E-02	3.052E+14
2.00E-02	1.51E+16	1.00E-02	1.511E+14
3.00E-02	1.28E+16	1.50E-02	1.926E+14
4.50E-02	7.65E+15	1.50E-02	1.148E+14
6.00E-02	4.04E+15	1.00E-02	4.039E+13
7.00E-02	3.47E+15	5.00E-03	1.737E+13
7.50E-02	2.69E+15	2.50E-02	6.735E+13
1.00E-01	1.39E+15	5.00E-02	6.965E+13
1.50E-01	8.86E+14	5.00E-02	4.431E+13
2.00E-01	4.00E+14	6.00E-02	2.401E+13
2.60E-01	2.79E+14	4.00E-02	1.114E+13
3.00E-01	2.44E+14	1.00E-01	2.437E+13
4.00E-01	1.45E+14	5.00E-02	7.225E+12
4.50E-01	1.16E+14	6.00E-02	6.972E+12
5.10E-01	2.84E+13	2.00E-03	5.674E+10
5.12E-01	3.90E+13	8.80E-02	3.435E+12
6.00E-01	1.08E+16	1.00E-01	1.082E+15
7.00E-01	4.18E+13	1.00E-01	4.176E+12
8.00E-01	2.64E+13	1.00E-01	2.644E+12
9.00E-01	2.39E+13	1.00E-01	2.390E+12
1.00E+00	9.37E+12	2.00E-01	1.874E+12
1.20E+00	1.84E+13	1.30E-01	2.386E+12
1.33E+00	1.95E+12	1.10E-01	2.140E+11
1.44E+00	1.56E+12	6.00E-02	9.348E+10
1.50E+00	8.16E+11	7.00E-02	5.713E+10
1.57E+00	1.73E+12	9.00E-02	1.560E+11
1.66E+00	3.13E+11	1.40E-01	4.383E+10
1.80E+00	9.95E+10	2.00E-01	1.990E+10
2.00E+00	2.28E+10	1.50E-01	3.417E+09
2.15E+00	7.75E+07	2.00E-01	1.549E+07
2.35E+00	8.64E+07	1.50E-01	1.297E+07
2.50E+00	3.54E+08	2.50E-01	8.853E+07
2.75E+00	3.00E+06	2.50E-01	7.495E+05
3.00E+00	1.82E+06	5.00E-01	9.110E+05

Continued on following page

E [MeV]	$\frac{dS}{dE} \left[\frac{p}{MeVsec} \right]$	dE	dS $\left[\frac{p}{sec} \right]$
3.50E+00	1.05E+06	5.00E-01	5.270E+05
4.00E+00	6.06E+05	5.00E-01	3.032E+05
4.50E+00	3.51E+05	5.00E-01	1.755E+05
5.00E+00	2.03E+05	5.00E-01	1.016E+05
5.50E+00	1.18E+05	5.00E-01	5.885E+04
6.00E+00	6.81E+04	5.00E-01	3.407E+04
6.50E+00	3.95E+04	5.00E-01	1.974E+04
7.00E+00	2.29E+04	5.00E-01	1.144E+04
7.50E+00	1.33E+04	5.00E-01	6.625E+03
8.00E+00	3.91E+03	2.00E+00	7.816E+03
1.00E+01			

Table B.8: ORIGEN-ARP neutron results for a GE 8×8 BWR assembly burned to 25.344 $\frac{MWd}{kg}$ and cooled for a combined time period of 35yr.

E [MeV]	$\frac{dS}{dE} \left[\frac{n}{MeVsec} \right]$	dE	dS $\left[\frac{n}{sec} \right]$
1.00E-11	1.160E+02	9.00E-11	1.044E-08
1.00E-10	4.728E+01	4.00E-10	1.891E-08
5.00E-10	3.085E+01	2.50E-10	7.713E-09
7.50E-10	2.691E+01	2.50E-10	6.728E-09
1.00E-09	2.336E+01	2.00E-10	4.672E-09
1.20E-09	2.192E+01	3.00E-10	6.576E-09
1.50E-09	1.929E+01	5.00E-10	9.645E-09
2.00E-09	1.741E+01	5.00E-10	8.705E-09
2.50E-09	1.586E+01	5.00E-10	7.930E-09
3.00E-09	1.452E+01	1.00E-09	1.452E-08
4.00E-09	1.311E+01	1.00E-09	1.311E-08
5.00E-09	1.185E+01	2.50E-09	2.963E-08
7.50E-09	1.072E+01	2.50E-09	2.680E-08
1.00E-08	9.622E+00	1.53E-08	1.472E-07
2.53E-08	9.284E+00	4.70E-09	4.363E-08
3.00E-08	9.406E+00	1.00E-08	9.406E-08
4.00E-08	9.596E+00	1.00E-08	9.596E-08
5.00E-08	9.911E+00	1.00E-08	9.911E-08
6.00E-08	1.018E+01	1.00E-08	1.018E-07
7.00E-08	1.051E+01	1.00E-08	1.051E-07
8.00E-08	1.083E+01	1.00E-08	1.083E-07
9.00E-08	1.113E+01	1.00E-08	1.113E-07
1.00E-07	1.172E+01	2.50E-08	2.930E-07
1.25E-07	1.247E+01	2.50E-08	3.118E-07

Continued on following page

E [MeV]	$\frac{dS}{dE} \left[\frac{n}{MeV \cdot sec} \right]$	dE	dS $\left[\frac{n}{sec} \right]$
1.50E-07	3.227E+02	2.50E-08	8.068E-06
1.75E-07	3.775E+02	2.50E-08	9.438E-06
2.00E-07	3.781E+02	2.50E-08	9.453E-06
2.25E-07	3.788E+02	2.50E-08	9.470E-06
2.50E-07	3.794E+02	2.50E-08	9.485E-06
2.75E-07	3.799E+02	2.50E-08	9.497E-06
3.00E-07	3.805E+02	2.50E-08	9.513E-06
3.25E-07	3.811E+02	2.50E-08	9.527E-06
3.50E-07	3.816E+02	2.50E-08	9.540E-06
3.75E-07	3.839E+02	2.50E-08	9.597E-06
4.00E-07	3.847E+02	5.00E-08	1.924E-05
4.50E-07	3.857E+02	5.00E-08	1.929E-05
5.00E-07	3.866E+02	5.00E-08	1.933E-05
5.50E-07	3.875E+02	5.00E-08	1.938E-05
6.00E-07	3.881E+02	2.50E-08	9.703E-06
6.25E-07	3.885E+02	2.50E-08	9.712E-06
6.50E-07	3.892E+02	5.00E-08	1.946E-05
7.00E-07	3.899E+02	5.00E-08	1.950E-05
7.50E-07	3.908E+02	5.00E-08	1.954E-05
8.00E-07	3.915E+02	5.00E-08	1.958E-05
8.50E-07	3.922E+02	5.00E-08	1.961E-05
9.00E-07	3.928E+02	2.50E-08	9.820E-06
9.25E-07	3.929E+02	2.50E-08	9.822E-06
9.50E-07	3.935E+02	2.50E-08	9.837E-06
9.75E-07	3.937E+02	2.50E-08	9.842E-06
1.00E-06	3.942E+02	1.00E-08	3.942E-06
1.01E-06	3.939E+02	1.00E-08	3.939E-06
1.02E-06	3.945E+02	1.00E-08	3.945E-06
1.03E-06	3.941E+02	1.00E-08	3.941E-06
1.04E-06	3.950E+02	1.00E-08	3.950E-06
1.05E-06	3.943E+02	1.00E-08	3.943E-06
1.06E-06	3.949E+02	1.00E-08	3.949E-06
1.07E-06	3.948E+02	1.00E-08	3.948E-06
1.08E-06	3.951E+02	1.00E-08	3.951E-06
1.09E-06	3.954E+02	1.00E-08	3.954E-06
1.10E-06	3.953E+02	1.00E-08	3.953E-06
1.11E-06	3.956E+02	1.00E-08	3.956E-06
1.12E-06	6.401E+02	1.00E-08	6.401E-06
1.13E-06	6.425E+02	1.00E-08	6.425E-06
1.14E-06	6.477E+02	1.00E-08	6.477E-06
1.15E-06	1.965E+03	2.50E-08	4.912E-05
1.18E-06	9.376E+03	2.50E-08	2.344E-04

Continued on following page

E [MeV]	$\frac{dS}{dE} \left[\frac{n}{MeV \cdot sec} \right]$	dE	dS $\left[\frac{n}{sec} \right]$
1.20E-06	8.307E+03	2.50E-08	2.077E-04
1.23E-06	7.237E+03	2.50E-08	1.809E-04
1.25E-06	1.309E+04	5.00E-08	6.545E-04
1.30E-06	8.773E+03	5.00E-08	4.387E-04
1.35E-06	8.992E+03	5.00E-08	4.496E-04
1.40E-06	4.325E+03	5.00E-08	2.163E-04
1.45E-06	9.233E+03	5.00E-08	4.616E-04
1.50E-06	9.398E+03	9.00E-08	8.458E-04
1.59E-06	1.251E+04	9.00E-08	1.126E-03
1.68E-06	1.005E+04	9.00E-08	9.045E-04
1.77E-06	7.606E+03	9.00E-08	6.845E-04
1.86E-06	1.296E+04	8.00E-08	1.037E-03
1.94E-06	1.126E+04	6.00E-08	6.756E-04
2.00E-06	1.056E+04	1.20E-07	1.267E-03
2.12E-06	1.120E+04	9.00E-08	1.008E-03
2.21E-06	8.798E+03	9.00E-08	7.918E-04
2.30E-06	1.152E+04	8.00E-08	9.216E-04
2.38E-06	1.476E+04	9.00E-08	1.328E-03
2.47E-06	8.780E+03	1.00E-07	8.780E-04
2.57E-06	1.500E+04	1.00E-07	1.500E-03
2.67E-06	1.247E+04	1.00E-07	1.247E-03
2.77E-06	1.306E+04	1.00E-07	1.306E-03
2.87E-06	1.246E+04	1.00E-07	1.246E-03
2.97E-06	3.108E+03	3.00E-08	9.324E-05
3.00E-06	1.891E+04	5.00E-08	9.455E-04
3.05E-06	1.024E+04	1.00E-07	1.024E-03
3.15E-06	1.458E+04	3.50E-07	5.103E-03
3.50E-06	1.305E+04	2.30E-07	3.002E-03
3.73E-06	1.596E+04	2.70E-07	4.309E-03
4.00E-06	1.517E+04	7.50E-07	1.138E-02
4.75E-06	1.626E+04	2.50E-07	4.065E-03
5.00E-06	1.801E+04	4.00E-07	7.204E-03
5.40E-06	1.793E+04	6.00E-07	1.076E-02
6.00E-06	1.672E+04	2.50E-07	4.180E-03
6.25E-06	2.056E+04	2.50E-07	5.140E-03
6.50E-06	1.918E+04	2.50E-07	4.795E-03
6.75E-06	1.926E+04	2.50E-07	4.815E-03
7.00E-06	2.031E+04	1.50E-07	3.047E-03
7.15E-06	2.056E+04	9.50E-07	1.953E-02
8.10E-06	2.128E+04	1.00E-06	2.128E-02
9.10E-06	2.353E+04	9.00E-07	2.118E-02
1.00E-05	2.432E+04	1.50E-06	3.648E-02

Continued on following page

E [MeV]	$\frac{dS}{dE} \left[\frac{n}{MeV \cdot sec} \right]$	dE	dS $\left[\frac{n}{sec} \right]$
1.15E-05	2.538E+04	4.00E-07	1.015E-02
1.19E-05	2.611E+04	1.00E-06	2.611E-02
1.29E-05	2.693E+04	8.50E-07	2.289E-02
1.38E-05	2.678E+04	6.50E-07	1.741E-02
1.44E-05	2.951E+04	7.00E-07	2.066E-02
1.51E-05	2.843E+04	9.00E-07	2.559E-02
1.60E-05	3.005E+04	1.00E-06	3.005E-02
1.70E-05	3.108E+04	1.50E-06	4.662E-02
1.85E-05	3.217E+04	5.00E-07	1.609E-02
1.90E-05	3.264E+04	1.00E-06	3.264E-02
2.00E-05	3.412E+04	1.00E-06	3.412E-02
2.10E-05	3.444E+04	1.50E-06	5.166E-02
2.25E-05	3.578E+04	2.50E-06	8.945E-02
2.50E-05	3.830E+04	2.50E-06	9.575E-02
2.75E-05	3.966E+04	2.50E-06	9.915E-02
3.00E-05	4.028E+04	1.25E-06	5.035E-02
3.13E-05	4.351E+04	5.00E-07	2.175E-02
3.18E-05	4.218E+04	1.50E-06	6.327E-02
3.33E-05	4.254E+04	5.00E-07	2.127E-02
3.38E-05	4.324E+04	8.50E-07	3.675E-02
3.46E-05	4.283E+04	9.00E-07	3.855E-02
3.55E-05	4.450E+04	1.50E-06	6.675E-02
3.70E-05	4.511E+04	1.00E-06	4.511E-02
3.80E-05	4.600E+04	1.10E-06	5.060E-02
3.91E-05	4.827E+04	5.00E-07	2.413E-02
3.96E-05	4.795E+04	1.40E-06	6.713E-02
4.10E-05	5.202E+04	1.40E-06	7.283E-02
4.24E-05	5.296E+04	1.60E-06	8.474E-02
4.40E-05	5.273E+04	1.20E-06	6.328E-02
4.52E-05	5.476E+04	1.80E-06	9.857E-02
4.70E-05	5.715E+04	1.30E-06	7.430E-02
4.83E-05	5.793E+04	9.00E-07	5.214E-02
4.92E-05	5.921E+04	1.40E-06	8.289E-02
5.06E-05	5.803E+04	1.40E-06	8.124E-02
5.20E-05	5.978E+04	1.40E-06	8.369E-02
5.34E-05	6.148E+04	5.60E-06	3.443E-01
5.90E-05	6.342E+04	2.00E-06	1.268E-01
6.10E-05	6.507E+04	4.00E-06	2.603E-01
6.50E-05	6.566E+04	2.50E-06	1.642E-01
6.75E-05	6.828E+04	4.50E-06	3.073E-01
7.20E-05	6.933E+04	4.00E-06	2.773E-01
7.60E-05	7.146E+04	4.00E-06	2.858E-01

Continued on following page

E [MeV]	$\frac{dS}{dE} \left[\frac{n}{MeV \cdot sec} \right]$	dE	dS $\left[\frac{n}{sec} \right]$
8.00E-05	7.320E+04	2.00E-06	1.464E-01
8.20E-05	7.524E+04	8.00E-06	6.019E-01
9.00E-05	7.885E+04	1.00E-05	7.885E-01
1.00E-04	8.222E+04	8.00E-06	6.578E-01
1.08E-04	8.512E+04	7.00E-06	5.958E-01
1.15E-04	8.712E+04	4.00E-06	3.485E-01
1.19E-04	8.874E+04	3.00E-06	2.662E-01
1.22E-04	9.872E+04	6.40E-05	6.318E+00
1.86E-04	1.084E+05	6.50E-06	7.046E-01
1.93E-04	1.118E+05	1.50E-05	1.677E+00
2.08E-04	1.138E+05	2.50E-06	2.845E-01
2.10E-04	1.190E+05	3.00E-05	3.570E+00
2.40E-04	1.288E+05	4.50E-05	5.796E+00
2.85E-04	1.368E+05	2.00E-05	2.736E+00
3.05E-04	1.626E+05	2.45E-04	3.984E+01
5.50E-04	1.930E+05	1.20E-04	2.316E+01
6.70E-04	2.026E+05	1.30E-05	2.634E+00
6.83E-04	2.222E+05	2.67E-04	5.933E+01
9.50E-04	2.556E+05	2.00E-04	5.112E+01
1.15E-03	2.881E+05	3.50E-04	1.008E+02
1.50E-03	3.093E+05	5.00E-05	1.547E+01
1.55E-03	3.234E+05	2.50E-04	8.085E+01
1.80E-03	3.513E+05	4.00E-04	1.405E+02
2.20E-03	3.714E+05	9.00E-05	3.343E+01
2.29E-03	3.865E+05	2.90E-04	1.121E+02
2.58E-03	4.136E+05	4.20E-04	1.737E+02
3.00E-03	4.554E+05	7.40E-04	3.370E+02
3.74E-03	4.853E+05	1.60E-04	7.765E+01
3.90E-03	5.558E+05	2.10E-03	1.167E+03
6.00E-03	6.611E+05	2.03E-03	1.342E+03
8.03E-03	7.384E+05	1.47E-03	1.085E+03
9.50E-03	8.390E+05	3.50E-03	2.937E+03
1.30E-02	9.689E+05	4.00E-03	3.876E+03
1.70E-02	1.146E+06	8.00E-03	9.168E+03
2.50E-02	1.309E+06	5.00E-03	6.545E+03
3.00E-02	1.516E+06	1.50E-02	2.274E+04
4.50E-02	1.696E+06	5.00E-03	8.480E+03
5.00E-02	1.752E+06	2.00E-03	3.504E+03
5.20E-02	1.828E+06	8.00E-03	1.462E+04
6.00E-02	1.976E+06	1.30E-02	2.569E+04
7.30E-02	2.076E+06	2.00E-03	4.152E+03
7.50E-02	2.134E+06	7.00E-03	1.494E+04

Continued on following page

E [MeV]	$\frac{dS}{dE} [\frac{n}{MeVsec}]$	dE	dS [$\frac{n}{sec}$]
8.20E-02	2.196E+06	3.00E-03	6.588E+03
8.50E-02	2.301E+06	1.50E-02	3.452E+04
1.00E-01	2.529E+06	2.83E-02	7.157E+04
1.28E-01	2.760E+06	2.17E-02	5.989E+04
1.50E-01	3.029E+06	5.00E-02	1.515E+05
2.00E-01	3.374E+06	7.00E-02	2.362E+05
2.70E-01	3.667E+06	6.00E-02	2.200E+05
3.30E-01	3.896E+06	7.00E-02	2.727E+05
4.00E-01	4.043E+06	2.00E-02	8.086E+04
4.20E-01	4.098E+06	2.00E-02	8.196E+04
4.40E-01	4.157E+06	3.00E-02	1.247E+05
4.70E-01	4.219E+06	2.95E-02	1.245E+05
5.00E-01	4.287E+06	5.05E-02	2.165E+05
5.50E-01	4.342E+06	2.30E-02	9.987E+04
5.73E-01	4.373E+06	2.70E-02	1.181E+05
6.00E-01	4.416E+06	7.00E-02	3.091E+05
6.70E-01	4.449E+06	9.00E-03	4.004E+04
6.79E-01	4.475E+06	7.10E-02	3.177E+05
7.50E-01	4.509E+06	7.00E-02	3.156E+05
8.20E-01	4.520E+06	4.11E-02	1.858E+05
8.61E-01	4.523E+06	1.39E-02	6.287E+04
8.75E-01	4.521E+06	2.50E-02	1.130E+05
9.00E-01	4.518E+06	2.00E-02	9.036E+04
9.20E-01	4.517E+06	9.00E-02	4.065E+05
1.01E+00	4.498E+06	9.00E-02	4.048E+05
1.10E+00	4.466E+06	1.00E-01	4.466E+05
1.20E+00	4.442E+06	5.00E-02	2.221E+05
1.25E+00	4.417E+06	6.70E-02	2.959E+05
1.32E+00	4.380E+06	3.90E-02	1.708E+05
1.36E+00	4.368E+06	4.40E-02	1.922E+05
1.40E+00	4.342E+06	1.00E-01	4.342E+05
1.50E+00	4.237E+06	3.50E-01	1.483E+06
1.85E+00	4.056E+06	5.04E-01	2.044E+06
2.35E+00	3.841E+06	1.25E-01	4.801E+05
2.48E+00	3.394E+06	5.21E-01	1.768E+06
3.00E+00	1.808E+06	1.30E+00	2.358E+06
4.30E+00	7.409E+05	4.96E-01	3.675E+05
4.80E+00	3.628E+05	1.63E+00	5.928E+05
6.43E+00	1.045E+05	1.75E+00	1.832E+05
8.19E+00	2.626E+04	1.81E+00	4.761E+04
1.00E+01			

Table B.9: ORIGEN-ARP photon results for a GE 8×8 BWR assembly burned to 25.344 $\frac{MWd}{kg}$ and cooled for a combined time period of 45yr.

E [MeV]	$\frac{dS}{dE} [\frac{p}{MeV \cdot sec}]$	dE	dS [$\frac{p}{sec}$]
1.00E-02	2.46E+16	1.00E-02	2.463E+14
2.00E-02	1.19E+16	1.00E-02	1.187E+14
3.00E-02	1.01E+16	1.50E-02	1.511E+14
4.50E-02	6.51E+15	1.50E-02	9.768E+13
6.00E-02	3.16E+15	1.00E-02	3.158E+13
7.00E-02	2.72E+15	5.00E-03	1.361E+13
7.50E-02	2.11E+15	2.50E-02	5.263E+13
1.00E-01	1.08E+15	5.00E-02	5.375E+13
1.50E-01	6.93E+14	5.00E-02	3.463E+13
2.00E-01	3.11E+14	6.00E-02	1.864E+13
2.60E-01	2.18E+14	4.00E-02	8.716E+12
3.00E-01	1.90E+14	1.00E-01	1.904E+13
4.00E-01	1.13E+14	5.00E-02	5.635E+12
4.50E-01	9.07E+13	6.00E-02	5.444E+12
5.10E-01	1.49E+13	2.00E-03	2.972E+10
5.12E-01	2.90E+13	8.80E-02	2.553E+12
6.00E-01	8.59E+15	1.00E-01	8.591E+14
7.00E-01	2.83E+13	1.00E-01	2.832E+12
8.00E-01	1.81E+13	1.00E-01	1.814E+12
9.00E-01	1.49E+13	1.00E-01	1.489E+12
1.00E+00	6.49E+12	2.00E-01	1.298E+12
1.20E+00	9.48E+12	1.30E-01	1.233E+12
1.33E+00	1.46E+12	1.10E-01	1.605E+11
1.44E+00	1.01E+12	6.00E-02	6.054E+10
1.50E+00	6.21E+11	7.00E-02	4.346E+10
1.57E+00	1.01E+12	9.00E-02	9.081E+10
1.66E+00	2.44E+11	1.40E-01	3.420E+10
1.80E+00	7.78E+10	2.00E-01	1.556E+10
2.00E+00	1.78E+10	1.50E-01	2.672E+09
2.15E+00	6.03E+07	2.00E-01	1.205E+07
2.35E+00	6.76E+07	1.50E-01	1.014E+07
2.50E+00	3.20E+08	2.50E-01	8.005E+07
2.75E+00	2.26E+06	2.50E-01	5.660E+05
3.00E+00	1.38E+06	5.00E-01	6.880E+05
3.50E+00	7.96E+05	5.00E-01	3.979E+05
4.00E+00	4.57E+05	5.00E-01	2.284E+05
4.50E+00	2.64E+05	5.00E-01	1.322E+05
5.00E+00	1.53E+05	5.00E-01	7.645E+04
5.50E+00	8.85E+04	5.00E-01	4.425E+04

Continued on following page

E [MeV]	$\frac{dS}{dE} [\frac{p}{MeVsec}]$	dE	dS [$\frac{p}{sec}$]
6.00E+00	5.12E+04	5.00E-01	2.562E+04
6.50E+00	2.97E+04	5.00E-01	1.484E+04
7.00E+00	1.72E+04	5.00E-01	8.590E+03
7.50E+00	9.95E+03	5.00E-01	4.977E+03
8.00E+00	2.94E+03	2.00E+00	5.870E+03
1.00E+01			

Table B.10: ORIGEN-ARP neutron results for a GE 8×8 BWR assembly burned to 25.344 $\frac{MWd}{kg}$ and cooled for a combined time period of 45yr.

E [MeV]	$\frac{dS}{dE} [\frac{n}{MeVsec}]$	dE	dS [$\frac{n}{sec}$]
1.00E-11	1.158E+02	9.00E-11	1.042E-08
1.00E-10	4.721E+01	4.00E-10	1.888E-08
5.00E-10	3.080E+01	2.50E-10	7.700E-09
7.50E-10	2.687E+01	2.50E-10	6.718E-09
1.00E-09	2.333E+01	2.00E-10	4.666E-09
1.20E-09	2.189E+01	3.00E-10	6.567E-09
1.50E-09	1.926E+01	5.00E-10	9.630E-09
2.00E-09	1.738E+01	5.00E-10	8.690E-09
2.50E-09	1.583E+01	5.00E-10	7.915E-09
3.00E-09	1.449E+01	1.00E-09	1.449E-08
4.00E-09	1.310E+01	1.00E-09	1.310E-08
5.00E-09	1.183E+01	2.50E-09	2.958E-08
7.50E-09	1.071E+01	2.50E-09	2.678E-08
1.00E-08	9.610E+00	1.53E-08	1.470E-07
2.53E-08	9.274E+00	4.70E-09	4.359E-08
3.00E-08	9.395E+00	1.00E-08	9.395E-08
4.00E-08	9.585E+00	1.00E-08	9.585E-08
5.00E-08	9.900E+00	1.00E-08	9.900E-08
6.00E-08	1.017E+01	1.00E-08	1.017E-07
7.00E-08	1.050E+01	1.00E-08	1.050E-07
8.00E-08	1.081E+01	1.00E-08	1.081E-07
9.00E-08	1.112E+01	1.00E-08	1.112E-07
1.00E-07	1.170E+01	2.50E-08	2.925E-07
1.25E-07	1.245E+01	2.50E-08	3.113E-07
1.50E-07	3.226E+02	2.50E-08	8.065E-06
1.75E-07	3.773E+02	2.50E-08	9.433E-06
2.00E-07	3.780E+02	2.50E-08	9.450E-06
2.25E-07	3.787E+02	2.50E-08	9.468E-06
2.50E-07	3.793E+02	2.50E-08	9.483E-06

Continued on following page

E [MeV]	$\frac{dS}{dE} \left[\frac{n}{MeV \cdot sec} \right]$	dE	dS $\left[\frac{n}{sec} \right]$
2.75E-07	3.798E+02	2.50E-08	9.495E-06
3.00E-07	3.804E+02	2.50E-08	9.510E-06
3.25E-07	3.810E+02	2.50E-08	9.525E-06
3.50E-07	3.815E+02	2.50E-08	9.538E-06
3.75E-07	3.837E+02	2.50E-08	9.592E-06
4.00E-07	3.845E+02	5.00E-08	1.923E-05
4.50E-07	3.855E+02	5.00E-08	1.928E-05
5.00E-07	3.864E+02	5.00E-08	1.932E-05
5.50E-07	3.873E+02	5.00E-08	1.937E-05
6.00E-07	3.879E+02	2.50E-08	9.698E-06
6.25E-07	3.883E+02	2.50E-08	9.707E-06
6.50E-07	3.889E+02	5.00E-08	1.945E-05
7.00E-07	3.897E+02	5.00E-08	1.949E-05
7.50E-07	3.905E+02	5.00E-08	1.953E-05
8.00E-07	3.913E+02	5.00E-08	1.957E-05
8.50E-07	3.919E+02	5.00E-08	1.960E-05
9.00E-07	3.926E+02	2.50E-08	9.815E-06
9.25E-07	3.927E+02	2.50E-08	9.817E-06
9.50E-07	3.933E+02	2.50E-08	9.832E-06
9.75E-07	3.935E+02	2.50E-08	9.837E-06
1.00E-06	3.940E+02	1.00E-08	3.940E-06
1.01E-06	3.936E+02	1.00E-08	3.936E-06
1.02E-06	3.942E+02	1.00E-08	3.942E-06
1.03E-06	3.939E+02	1.00E-08	3.939E-06
1.04E-06	3.948E+02	1.00E-08	3.948E-06
1.05E-06	3.941E+02	1.00E-08	3.941E-06
1.06E-06	3.947E+02	1.00E-08	3.947E-06
1.07E-06	3.946E+02	1.00E-08	3.946E-06
1.08E-06	3.949E+02	1.00E-08	3.949E-06
1.09E-06	3.952E+02	1.00E-08	3.952E-06
1.10E-06	3.951E+02	1.00E-08	3.951E-06
1.11E-06	3.954E+02	1.00E-08	3.954E-06
1.12E-06	6.399E+02	1.00E-08	6.399E-06
1.13E-06	6.423E+02	1.00E-08	6.423E-06
1.14E-06	6.475E+02	1.00E-08	6.475E-06
1.15E-06	1.949E+03	2.50E-08	4.872E-05
1.18E-06	7.344E+03	2.50E-08	1.836E-04
1.20E-06	6.263E+03	2.50E-08	1.566E-04
1.23E-06	5.173E+03	2.50E-08	1.293E-04
1.25E-06	9.739E+03	5.00E-08	4.869E-04
1.30E-06	6.611E+03	5.00E-08	3.306E-04
1.35E-06	6.781E+03	5.00E-08	3.391E-04

Continued on following page

E [MeV]	$\frac{dS}{dE} \left[\frac{n}{MeV \cdot sec} \right]$	dE	dS $\left[\frac{n}{sec} \right]$
1.40E-06	3.400E+03	5.00E-08	1.700E-04
1.45E-06	6.965E+03	5.00E-08	3.483E-04
1.50E-06	7.082E+03	9.00E-08	6.374E-04
1.59E-06	9.337E+03	9.00E-08	8.403E-04
1.68E-06	7.571E+03	9.00E-08	6.814E-04
1.77E-06	5.904E+03	9.00E-08	5.314E-04
1.86E-06	9.439E+03	8.00E-08	7.551E-04
1.94E-06	8.619E+03	6.00E-08	5.171E-04
2.00E-06	7.866E+03	1.20E-07	9.439E-04
2.12E-06	8.436E+03	9.00E-08	7.592E-04
2.21E-06	6.896E+03	9.00E-08	6.206E-04
2.30E-06	8.660E+03	8.00E-08	6.928E-04
2.38E-06	1.089E+04	9.00E-08	9.801E-04
2.47E-06	6.677E+03	1.00E-07	6.677E-04
2.57E-06	1.108E+04	1.00E-07	1.108E-03
2.67E-06	9.363E+03	1.00E-07	9.363E-04
2.77E-06	9.906E+03	1.00E-07	9.906E-04
2.87E-06	9.245E+03	1.00E-07	9.245E-04
2.97E-06	3.020E+03	3.00E-08	9.060E-05
3.00E-06	1.376E+04	5.00E-08	6.880E-04
3.05E-06	7.897E+03	1.00E-07	7.897E-04
3.15E-06	1.088E+04	3.50E-07	3.808E-03
3.50E-06	9.938E+03	2.30E-07	2.286E-03
3.73E-06	1.188E+04	2.70E-07	3.208E-03
4.00E-06	1.140E+04	7.50E-07	8.550E-03
4.75E-06	1.213E+04	2.50E-07	3.033E-03
5.00E-06	1.343E+04	4.00E-07	5.372E-03
5.40E-06	1.345E+04	6.00E-07	8.070E-03
6.00E-06	1.263E+04	2.50E-07	3.158E-03
6.25E-06	1.527E+04	2.50E-07	3.817E-03
6.50E-06	1.435E+04	2.50E-07	3.588E-03
6.75E-06	1.434E+04	2.50E-07	3.585E-03
7.00E-06	1.531E+04	1.50E-07	2.297E-03
7.15E-06	1.538E+04	9.50E-07	1.461E-02
8.10E-06	1.594E+04	1.00E-06	1.594E-02
9.10E-06	1.755E+04	9.00E-07	1.580E-02
1.00E-05	1.818E+04	1.50E-06	2.727E-02
1.15E-05	1.897E+04	4.00E-07	7.588E-03
1.19E-05	1.950E+04	1.00E-06	1.950E-02
1.29E-05	2.009E+04	8.50E-07	1.708E-02
1.38E-05	2.006E+04	6.50E-07	1.304E-02
1.44E-05	2.201E+04	7.00E-07	1.541E-02

Continued on following page

E [MeV]	$\frac{dS}{dE} \left[\frac{n}{MeV \cdot sec} \right]$	dE	dS $\left[\frac{n}{sec} \right]$
1.51E-05	2.128E+04	9.00E-07	1.915E-02
1.60E-05	2.243E+04	1.00E-06	2.243E-02
1.70E-05	2.318E+04	1.50E-06	3.477E-02
1.85E-05	2.406E+04	5.00E-07	1.203E-02
1.90E-05	2.436E+04	1.00E-06	2.436E-02
2.00E-05	2.538E+04	1.00E-06	2.538E-02
2.10E-05	2.569E+04	1.50E-06	3.854E-02
2.25E-05	2.672E+04	2.50E-06	6.680E-02
2.50E-05	2.854E+04	2.50E-06	7.135E-02
2.75E-05	2.956E+04	2.50E-06	7.390E-02
3.00E-05	3.011E+04	1.25E-06	3.764E-02
3.13E-05	3.232E+04	5.00E-07	1.616E-02
3.18E-05	3.144E+04	1.50E-06	4.716E-02
3.33E-05	3.164E+04	5.00E-07	1.582E-02
3.38E-05	3.223E+04	8.50E-07	2.740E-02
3.46E-05	3.204E+04	9.00E-07	2.884E-02
3.55E-05	3.317E+04	1.50E-06	4.975E-02
3.70E-05	3.358E+04	1.00E-06	3.358E-02
3.80E-05	3.432E+04	1.10E-06	3.775E-02
3.91E-05	3.576E+04	5.00E-07	1.788E-02
3.96E-05	3.605E+04	1.40E-06	5.047E-02
4.10E-05	4.000E+04	1.40E-06	5.600E-02
4.24E-05	4.072E+04	1.60E-06	6.515E-02
4.40E-05	4.059E+04	1.20E-06	4.871E-02
4.52E-05	4.214E+04	1.80E-06	7.585E-02
4.70E-05	4.440E+04	1.30E-06	5.772E-02
4.83E-05	4.504E+04	9.00E-07	4.054E-02
4.92E-05	4.588E+04	1.40E-06	6.423E-02
5.06E-05	4.509E+04	1.40E-06	6.313E-02
5.20E-05	4.637E+04	1.40E-06	6.492E-02
5.34E-05	4.763E+04	5.60E-06	2.667E-01
5.90E-05	4.909E+04	2.00E-06	9.818E-02
6.10E-05	5.028E+04	4.00E-06	2.011E-01
6.50E-05	5.077E+04	2.50E-06	1.269E-01
6.75E-05	5.272E+04	4.50E-06	2.372E-01
7.20E-05	5.352E+04	4.00E-06	2.141E-01
7.60E-05	5.510E+04	4.00E-06	2.204E-01
8.00E-05	5.650E+04	2.00E-06	1.130E-01
8.20E-05	5.800E+04	8.00E-06	4.640E-01
9.00E-05	6.074E+04	1.00E-05	6.074E-01
1.00E-04	6.327E+04	8.00E-06	5.062E-01
1.08E-04	6.549E+04	7.00E-06	4.584E-01

Continued on following page

E [MeV]	$\frac{dS}{dE} \left[\frac{n}{MeV \cdot sec} \right]$	dE	dS $\left[\frac{n}{sec} \right]$
1.15E-04	6.702E+04	4.00E-06	2.681E-01
1.19E-04	6.814E+04	3.00E-06	2.044E-01
1.22E-04	7.567E+04	6.40E-05	4.843E+00
1.86E-04	8.294E+04	6.50E-06	5.391E-01
1.93E-04	8.539E+04	1.50E-05	1.281E+00
2.08E-04	8.726E+04	2.50E-06	2.182E-01
2.10E-04	9.111E+04	3.00E-05	2.733E+00
2.40E-04	9.860E+04	4.50E-05	4.437E+00
2.85E-04	1.047E+05	2.00E-05	2.094E+00
3.05E-04	1.241E+05	2.45E-04	3.040E+01
5.50E-04	1.468E+05	1.20E-04	1.762E+01
6.70E-04	1.540E+05	1.30E-05	2.002E+00
6.83E-04	1.687E+05	2.67E-04	4.504E+01
9.50E-04	1.950E+05	2.00E-04	3.900E+01
1.15E-03	2.202E+05	3.50E-04	7.707E+01
1.50E-03	2.363E+05	5.00E-05	1.182E+01
1.55E-03	2.469E+05	2.50E-04	6.173E+01
1.80E-03	2.677E+05	4.00E-04	1.071E+02
2.20E-03	2.828E+05	9.00E-05	2.545E+01
2.29E-03	2.942E+05	2.90E-04	8.532E+01
2.58E-03	3.148E+05	4.20E-04	1.322E+02
3.00E-03	3.468E+05	7.40E-04	2.566E+02
3.74E-03	3.698E+05	1.60E-04	5.917E+01
3.90E-03	4.249E+05	2.10E-03	8.923E+02
6.00E-03	5.051E+05	2.03E-03	1.025E+03
8.03E-03	5.639E+05	1.47E-03	8.289E+02
9.50E-03	6.419E+05	3.50E-03	2.247E+03
1.30E-02	7.414E+05	4.00E-03	2.966E+03
1.70E-02	8.781E+05	8.00E-03	7.025E+03
2.50E-02	1.003E+06	5.00E-03	5.015E+03
3.00E-02	1.161E+06	1.50E-02	1.742E+04
4.50E-02	1.297E+06	5.00E-03	6.485E+03
5.00E-02	1.340E+06	2.00E-03	2.680E+03
5.20E-02	1.397E+06	8.00E-03	1.118E+04
6.00E-02	1.509E+06	1.30E-02	1.962E+04
7.30E-02	1.585E+06	2.00E-03	3.170E+03
7.50E-02	1.630E+06	7.00E-03	1.141E+04
8.20E-02	1.677E+06	3.00E-03	5.031E+03
8.50E-02	1.757E+06	1.50E-02	2.636E+04
1.00E-01	1.932E+06	2.83E-02	5.468E+04
1.28E-01	2.109E+06	2.17E-02	4.577E+04
1.50E-01	2.313E+06	5.00E-02	1.157E+05

Continued on following page

E [MeV]	$\frac{dS}{dE} [\frac{n}{MeVsec}]$	dE	dS [$\frac{n}{sec}$]
2.00E-01	2.569E+06	7.00E-02	1.798E+05
2.70E-01	2.787E+06	6.00E-02	1.672E+05
3.30E-01	2.959E+06	7.00E-02	2.071E+05
4.00E-01	3.073E+06	2.00E-02	6.146E+04
4.20E-01	3.115E+06	2.00E-02	6.230E+04
4.40E-01	3.160E+06	3.00E-02	9.480E+04
4.70E-01	3.206E+06	2.95E-02	9.458E+04
5.00E-01	3.257E+06	5.05E-02	1.645E+05
5.50E-01	3.298E+06	2.30E-02	7.585E+04
5.73E-01	3.321E+06	2.70E-02	8.967E+04
6.00E-01	3.351E+06	7.00E-02	2.346E+05
6.70E-01	3.375E+06	9.00E-03	3.038E+04
6.79E-01	3.395E+06	7.10E-02	2.410E+05
7.50E-01	3.423E+06	7.00E-02	2.396E+05
8.20E-01	3.431E+06	4.11E-02	1.410E+05
8.61E-01	3.434E+06	1.39E-02	4.773E+04
8.75E-01	3.433E+06	2.50E-02	8.583E+04
9.00E-01	3.431E+06	2.00E-02	6.862E+04
9.20E-01	3.434E+06	9.00E-02	3.091E+05
1.01E+00	3.425E+06	9.00E-02	3.083E+05
1.10E+00	3.409E+06	1.00E-01	3.409E+05
1.20E+00	3.401E+06	5.00E-02	1.701E+05
1.25E+00	3.390E+06	6.70E-02	2.271E+05
1.32E+00	3.366E+06	3.90E-02	1.313E+05
1.36E+00	3.365E+06	4.40E-02	1.481E+05
1.40E+00	3.359E+06	1.00E-01	3.359E+05
1.50E+00	3.325E+06	3.50E-01	1.164E+06
1.85E+00	3.288E+06	5.04E-01	1.657E+06
2.35E+00	3.178E+06	1.25E-01	3.973E+05
2.48E+00	2.830E+06	5.21E-01	1.474E+06
3.00E+00	1.463E+06	1.30E+00	1.908E+06
4.30E+00	5.478E+05	4.96E-01	2.717E+05
4.80E+00	2.650E+05	1.63E+00	4.330E+05
6.43E+00	7.548E+04	1.75E+00	1.323E+05
8.19E+00	1.883E+04	1.81E+00	3.414E+04
1.00E+01			

APPENDIX C

ORIGEN-ARP PWR DATA

Table C.1: ORIGEN-ARP photon results for a Westinghouse 17×17 PWR assembly burned to $57.535 \frac{MWd}{kg}$ and cooled for a combined time period of 5yr.

E [MeV]	$\frac{dS}{dE} [\frac{p}{MeVsec}]$	dE	dS [$\frac{p}{sec}$]
1.00E-02	1.65E+17	1.00E-02	1.652E+15
2.00E-02	9.26E+16	1.00E-02	9.257E+14
3.00E-02	7.82E+16	1.50E-02	1.172E+15
4.50E-02	3.52E+16	1.50E-02	5.277E+14
6.00E-02	2.28E+16	1.00E-02	2.281E+14
7.00E-02	1.99E+16	5.00E-03	9.940E+13
7.50E-02	1.66E+16	2.50E-02	4.148E+14
1.00E-01	1.15E+16	5.00E-02	5.735E+14
1.50E-01	5.31E+15	5.00E-02	2.654E+14
2.00E-01	2.74E+15	6.00E-02	1.642E+14
2.60E-01	1.65E+15	4.00E-02	6.588E+13
3.00E-01	1.50E+15	1.00E-01	1.496E+14
4.00E-01	1.70E+15	5.00E-02	8.515E+13
4.50E-01	1.43E+15	6.00E-02	8.562E+13
5.10E-01	7.78E+16	2.00E-03	1.557E+14
5.12E-01	6.00E+15	8.80E-02	5.283E+14
6.00E-01	7.07E+16	1.00E-01	7.065E+15
7.00E-01	1.97E+16	1.00E-01	1.969E+15
8.00E-01	1.45E+15	1.00E-01	1.450E+14
9.00E-01	7.99E+14	1.00E-01	7.987E+13
1.00E+00	5.57E+14	2.00E-01	1.114E+14
1.20E+00	9.48E+14	1.30E-01	1.232E+14
1.33E+00	5.52E+14	1.10E-01	6.073E+13
1.44E+00	6.90E+13	6.00E-02	4.141E+12
1.50E+00	3.24E+13	7.00E-02	2.265E+12
1.57E+00	7.43E+13	9.00E-02	6.687E+12
1.66E+00	8.58E+12	1.40E-01	1.202E+12
1.80E+00	5.76E+12	2.00E-01	1.152E+12

Continued on following page

E [MeV]	$\frac{dS}{dE} \left[\frac{p}{MeV \cdot sec} \right]$	dE	dS $\left[\frac{p}{sec} \right]$
2.00E+00	3.29E+12	1.50E-01	4.938E+11
2.15E+00	1.19E+13	2.00E-01	2.380E+12
2.35E+00	4.44E+12	1.50E-01	6.665E+11
2.50E+00	3.63E+11	2.50E-01	9.068E+10
2.75E+00	3.11E+11	2.50E-01	7.770E+10
3.00E+00	3.38E+10	5.00E-01	1.689E+10
3.50E+00	1.98E+08	5.00E-01	9.910E+07
4.00E+00	1.03E+08	5.00E-01	5.160E+07
4.50E+00	5.98E+07	5.00E-01	2.992E+07
5.00E+00	3.47E+07	5.00E-01	1.735E+07
5.50E+00	2.01E+07	5.00E-01	1.006E+07
6.00E+00	1.17E+07	5.00E-01	5.830E+06
6.50E+00	6.76E+06	5.00E-01	3.382E+06
7.00E+00	3.92E+06	5.00E-01	1.961E+06
7.50E+00	2.27E+06	5.00E-01	1.137E+06
8.00E+00	6.71E+05	2.00E+00	1.343E+06
1.00E+01			

Table C.2: ORIGEN-ARP photon results for a Westinghouse 17×17 PWR assembly burned to $57.535 \frac{MWd}{kg}$ and cooled for a combined time period of 5yr.

E [MeV]	$\frac{dS}{dE} \left[\frac{n}{MeV \cdot sec} \right]$	dE	dS $\left[\frac{n}{sec} \right]$
1.00E-11	5.902E+04	9.00E-11	5.312E-06
1.00E-10	2.406E+04	4.00E-10	9.624E-06
5.00E-10	1.570E+04	2.50E-10	3.925E-06
7.50E-10	1.369E+04	2.50E-10	3.423E-06
1.00E-09	1.189E+04	2.00E-10	2.378E-06
1.20E-09	1.115E+04	3.00E-10	3.345E-06
1.50E-09	9.814E+03	5.00E-10	4.907E-06
2.00E-09	8.858E+03	5.00E-10	4.429E-06
2.50E-09	8.068E+03	5.00E-10	4.034E-06
3.00E-09	7.386E+03	1.00E-09	7.386E-06
4.00E-09	6.673E+03	1.00E-09	6.673E-06
5.00E-09	6.028E+03	2.50E-09	1.507E-05
7.50E-09	5.456E+03	2.50E-09	1.364E-05
1.00E-08	4.839E+03	1.53E-08	7.404E-05
2.53E-08	4.641E+03	4.70E-09	2.181E-05
3.00E-08	4.703E+03	1.00E-08	4.703E-05
4.00E-08	4.800E+03	1.00E-08	4.800E-05
5.00E-08	4.961E+03	1.00E-08	4.961E-05

Continued on following page

E [MeV]	$\frac{dS}{dE} \left[\frac{n}{MeV \cdot sec} \right]$	dE	dS $\left[\frac{n}{sec} \right]$
6.00E-08	5.099E+03	1.00E-08	5.099E-05
7.00E-08	5.265E+03	1.00E-08	5.265E-05
8.00E-08	5.426E+03	1.00E-08	5.426E-05
9.00E-08	5.582E+03	1.00E-08	5.582E-05
1.00E-07	5.880E+03	2.50E-08	1.470E-04
1.25E-07	6.261E+03	2.50E-08	1.565E-04
1.50E-07	7.101E+03	2.50E-08	1.775E-04
1.75E-07	7.558E+03	2.50E-08	1.890E-04
2.00E-07	7.876E+03	2.50E-08	1.969E-04
2.25E-07	8.223E+03	2.50E-08	2.056E-04
2.50E-07	8.528E+03	2.50E-08	2.132E-04
2.75E-07	8.819E+03	2.50E-08	2.205E-04
3.00E-07	9.111E+03	2.50E-08	2.278E-04
3.25E-07	9.420E+03	2.50E-08	2.355E-04
3.50E-07	9.685E+03	2.50E-08	2.421E-04
3.75E-07	9.939E+03	2.50E-08	2.485E-04
4.00E-07	1.033E+04	5.00E-08	5.165E-04
4.50E-07	1.084E+04	5.00E-08	5.420E-04
5.00E-07	1.130E+04	5.00E-08	5.650E-04
5.50E-07	1.177E+04	5.00E-08	5.885E-04
6.00E-07	1.208E+04	2.50E-08	3.020E-04
6.25E-07	1.228E+04	2.50E-08	3.070E-04
6.50E-07	1.261E+04	5.00E-08	6.305E-04
7.00E-07	1.299E+04	5.00E-08	6.495E-04
7.50E-07	1.342E+04	5.00E-08	6.710E-04
8.00E-07	1.379E+04	5.00E-08	6.895E-04
8.50E-07	1.414E+04	5.00E-08	7.070E-04
9.00E-07	1.447E+04	2.50E-08	3.618E-04
9.25E-07	1.453E+04	2.50E-08	3.633E-04
9.50E-07	1.483E+04	2.50E-08	3.708E-04
9.75E-07	1.494E+04	2.50E-08	3.735E-04
1.00E-06	1.519E+04	1.00E-08	1.519E-04
1.01E-06	1.500E+04	1.00E-08	1.500E-04
1.02E-06	1.530E+04	1.00E-08	1.530E-04
1.03E-06	1.511E+04	1.00E-08	1.511E-04
1.04E-06	1.558E+04	1.00E-08	1.558E-04
1.05E-06	1.862E+04	1.00E-08	1.862E-04
1.06E-06	1.896E+04	1.00E-08	1.896E-04
1.07E-06	3.118E+04	1.00E-08	3.118E-04
1.08E-06	1.918E+04	1.00E-08	1.918E-04
1.09E-06	1.930E+04	1.00E-08	1.930E-04
1.10E-06	1.929E+04	1.00E-08	1.929E-04

Continued on following page

E [MeV]	$\frac{dS}{dE} \left[\frac{n}{MeV \cdot sec} \right]$	dE	dS $\left[\frac{n}{sec} \right]$
1.11E-06	1.941E+04	1.00E-08	1.941E-04
1.12E-06	2.097E+04	1.00E-08	2.097E-04
1.13E-06	2.114E+04	1.00E-08	2.114E-04
1.14E-06	2.134E+04	1.00E-08	2.134E-04
1.15E-06	2.517E+04	2.50E-08	6.292E-04
1.18E-06	1.409E+06	2.50E-08	3.523E-02
1.20E-06	1.415E+06	2.50E-08	3.538E-02
1.23E-06	1.428E+06	2.50E-08	3.570E-02
1.25E-06	2.311E+06	5.00E-08	1.156E-01
1.30E-06	1.498E+06	5.00E-08	7.490E-02
1.35E-06	1.529E+06	5.00E-08	7.645E-02
1.40E-06	6.518E+05	5.00E-08	3.259E-02
1.45E-06	1.569E+06	5.00E-08	7.845E-02
1.50E-06	1.602E+06	9.00E-08	1.442E-01
1.59E-06	2.192E+06	9.00E-08	1.973E-01
1.68E-06	1.709E+06	9.00E-08	1.538E-01
1.77E-06	1.185E+06	9.00E-08	1.067E-01
1.86E-06	2.430E+06	8.00E-08	1.944E-01
1.94E-06	1.830E+06	6.00E-08	1.098E-01
2.00E-06	1.865E+06	1.20E-07	2.238E-01
2.12E-06	1.911E+06	9.00E-08	1.720E-01
2.21E-06	1.326E+06	9.00E-08	1.193E-01
2.30E-06	1.977E+06	8.00E-08	1.582E-01
2.38E-06	2.662E+06	9.00E-08	2.396E-01
2.47E-06	1.462E+06	1.00E-07	1.462E-01
2.57E-06	2.705E+06	1.00E-07	2.705E-01
2.67E-06	2.146E+06	1.00E-07	2.146E-01
2.77E-06	2.179E+06	1.00E-07	2.179E-01
2.87E-06	2.220E+06	1.00E-07	2.220E-01
2.97E-06	8.879E+04	3.00E-08	2.664E-03
3.00E-06	3.551E+06	5.00E-08	1.776E-01
3.05E-06	1.628E+06	1.00E-07	1.628E-01
3.15E-06	2.557E+06	3.50E-07	8.950E-01
3.50E-06	2.156E+06	2.30E-07	4.959E-01
3.73E-06	2.819E+06	2.70E-07	7.611E-01
4.00E-06	2.606E+06	7.50E-07	1.955E+00
4.75E-06	2.857E+06	2.50E-07	7.143E-01
5.00E-06	3.169E+06	4.00E-07	1.268E+00
5.40E-06	3.098E+06	6.00E-07	1.859E+00
6.00E-06	2.836E+06	2.50E-07	7.090E-01
6.25E-06	3.651E+06	2.50E-07	9.127E-01
6.50E-06	3.337E+06	2.50E-07	8.343E-01

Continued on following page

E [MeV]	$\frac{dS}{dE} \left[\frac{n}{MeV \cdot sec} \right]$	dE	dS $\left[\frac{n}{sec} \right]$
6.75E-06	3.401E+06	2.50E-07	8.503E-01
7.00E-06	3.452E+06	1.50E-07	5.178E-01
7.15E-06	3.582E+06	9.50E-07	3.403E+00
8.10E-06	3.689E+06	1.00E-06	3.689E+00
9.10E-06	4.133E+06	9.00E-07	3.720E+00
1.00E-05	4.251E+06	1.50E-06	6.377E+00
1.15E-05	4.437E+06	4.00E-07	1.775E+00
1.19E-05	4.566E+06	1.00E-06	4.566E+00
1.29E-05	4.734E+06	8.50E-07	4.024E+00
1.38E-05	4.645E+06	6.50E-07	3.019E+00
1.44E-05	5.184E+06	7.00E-07	3.629E+00
1.51E-05	4.950E+06	9.00E-07	4.455E+00
1.60E-05	5.264E+06	1.00E-06	5.264E+00
1.70E-05	5.461E+06	1.50E-06	8.192E+00
1.85E-05	5.609E+06	5.00E-07	2.805E+00
1.90E-05	5.724E+06	1.00E-06	5.724E+00
2.00E-05	6.040E+06	1.00E-06	6.040E+00
2.10E-05	6.047E+06	1.50E-06	9.071E+00
2.25E-05	6.264E+06	2.50E-06	1.566E+01
2.50E-05	6.749E+06	2.50E-06	1.687E+01
2.75E-05	6.985E+06	2.50E-06	1.746E+01
3.00E-05	7.036E+06	1.25E-06	8.795E+00
3.13E-05	7.733E+06	5.00E-07	3.866E+00
3.18E-05	7.421E+06	1.50E-06	1.113E+01
3.33E-05	7.537E+06	5.00E-07	3.768E+00
3.38E-05	7.612E+06	8.50E-07	6.470E+00
3.46E-05	7.461E+06	9.00E-07	6.715E+00
3.55E-05	7.834E+06	1.50E-06	1.175E+01
3.70E-05	7.967E+06	1.00E-06	7.967E+00
3.80E-05	8.077E+06	1.10E-06	8.885E+00
3.91E-05	8.639E+06	5.00E-07	4.319E+00
3.96E-05	8.262E+06	1.40E-06	1.157E+01
4.10E-05	8.412E+06	1.40E-06	1.178E+01
4.24E-05	8.561E+06	1.60E-06	1.370E+01
4.40E-05	8.494E+06	1.20E-06	1.019E+01
4.52E-05	8.842E+06	1.80E-06	1.592E+01
4.70E-05	8.990E+06	1.30E-06	1.169E+01
4.83E-05	9.090E+06	9.00E-07	8.181E+00
4.92E-05	9.392E+06	1.40E-06	1.315E+01
5.06E-05	9.133E+06	1.40E-06	1.279E+01
5.20E-05	9.453E+06	1.40E-06	1.323E+01
5.34E-05	9.758E+06	5.60E-06	5.464E+01

Continued on following page

E [MeV]	$\frac{dS}{dE} \left[\frac{n}{MeV \cdot sec} \right]$	dE	dS $\left[\frac{n}{sec} \right]$
5.90E-05	1.008E+07	2.00E-06	2.016E+01
6.10E-05	1.041E+07	4.00E-06	4.164E+01
6.50E-05	1.047E+07	2.50E-06	2.618E+01
6.75E-05	1.094E+07	4.50E-06	4.923E+01
7.20E-05	1.112E+07	4.00E-06	4.448E+01
7.60E-05	1.149E+07	4.00E-06	4.596E+01
8.00E-05	1.171E+07	2.00E-06	2.342E+01
8.20E-05	1.207E+07	8.00E-06	9.656E+01
9.00E-05	1.268E+07	1.00E-05	1.268E+02
1.00E-04	1.327E+07	8.00E-06	1.062E+02
1.08E-04	1.374E+07	7.00E-06	9.618E+01
1.15E-04	1.407E+07	4.00E-06	5.628E+01
1.19E-04	1.441E+07	3.00E-06	4.323E+01
1.22E-04	1.611E+07	6.40E-05	1.031E+03
1.86E-04	1.781E+07	6.50E-06	1.158E+02
1.93E-04	1.842E+07	1.50E-05	2.763E+02
2.08E-04	1.858E+07	2.50E-06	4.645E+01
2.10E-04	1.950E+07	3.00E-05	5.850E+02
2.40E-04	2.106E+07	4.50E-05	9.477E+02
2.85E-04	2.234E+07	2.00E-05	4.468E+02
3.05E-04	2.679E+07	2.45E-04	6.564E+03
5.50E-04	3.210E+07	1.20E-04	3.852E+03
6.70E-04	3.374E+07	1.30E-05	4.386E+02
6.83E-04	3.710E+07	2.67E-04	9.906E+03
9.50E-04	4.210E+07	2.00E-04	8.420E+03
1.15E-03	4.726E+07	3.50E-04	1.654E+04
1.50E-03	5.080E+07	5.00E-05	2.540E+03
1.55E-03	5.319E+07	2.50E-04	1.330E+04
1.80E-03	5.808E+07	4.00E-04	2.323E+04
2.20E-03	6.153E+07	9.00E-05	5.538E+03
2.29E-03	6.408E+07	2.90E-04	1.858E+04
2.58E-03	6.857E+07	4.20E-04	2.880E+04
3.00E-03	7.532E+07	7.40E-04	5.574E+04
3.74E-03	8.020E+07	1.60E-04	1.283E+04
3.90E-03	9.112E+07	2.10E-03	1.914E+05
6.00E-03	1.085E+08	2.03E-03	2.203E+05
8.03E-03	1.212E+08	1.47E-03	1.782E+05
9.50E-03	1.371E+08	3.50E-03	4.799E+05
1.30E-02	1.581E+08	4.00E-03	6.324E+05
1.70E-02	1.864E+08	8.00E-03	1.491E+06
2.50E-02	2.129E+08	5.00E-03	1.065E+06
3.00E-02	2.470E+08	1.50E-02	3.705E+06

Continued on following page

E [MeV]	$\frac{dS}{dE} [\frac{n}{MeVsec}]$	dE	dS [$\frac{n}{sec}$]
4.50E-02	2.771E+08	5.00E-03	1.386E+06
5.00E-02	2.866E+08	2.00E-03	5.732E+05
5.20E-02	2.995E+08	8.00E-03	2.396E+06
6.00E-02	3.246E+08	1.30E-02	4.220E+06
7.30E-02	3.413E+08	2.00E-03	6.826E+05
7.50E-02	3.507E+08	7.00E-03	2.455E+06
8.20E-02	3.608E+08	3.00E-03	1.082E+06
8.50E-02	3.779E+08	1.50E-02	5.669E+06
1.00E-01	4.151E+08	2.83E-02	1.175E+07
1.28E-01	4.528E+08	2.17E-02	9.826E+06
1.50E-01	4.981E+08	5.00E-02	2.491E+07
2.00E-01	5.592E+08	7.00E-02	3.914E+07
2.70E-01	6.108E+08	6.00E-02	3.665E+07
3.30E-01	6.506E+08	7.00E-02	4.554E+07
4.00E-01	6.735E+08	2.00E-02	1.347E+07
4.20E-01	6.822E+08	2.00E-02	1.364E+07
4.40E-01	6.922E+08	3.00E-02	2.077E+07
4.70E-01	7.029E+08	2.95E-02	2.074E+07
5.00E-01	7.152E+08	5.05E-02	3.612E+07
5.50E-01	7.249E+08	2.30E-02	1.667E+07
5.73E-01	7.305E+08	2.70E-02	1.972E+07
6.00E-01	7.393E+08	7.00E-02	5.175E+07
6.70E-01	7.453E+08	9.00E-03	6.708E+06
6.79E-01	7.495E+08	7.10E-02	5.321E+07
7.50E-01	7.544E+08	7.00E-02	5.281E+07
8.20E-01	7.558E+08	4.11E-02	3.106E+07
8.61E-01	7.558E+08	1.39E-02	1.051E+07
8.75E-01	7.554E+08	2.50E-02	1.889E+07
9.00E-01	7.548E+08	2.00E-02	1.510E+07
9.20E-01	7.522E+08	9.00E-02	6.770E+07
1.01E+00	7.452E+08	9.00E-02	6.707E+07
1.10E+00	7.345E+08	1.00E-01	7.345E+07
1.20E+00	7.241E+08	5.00E-02	3.621E+07
1.25E+00	7.150E+08	6.70E-02	4.791E+07
1.32E+00	7.059E+08	3.90E-02	2.753E+07
1.36E+00	6.986E+08	4.40E-02	3.074E+07
1.40E+00	6.851E+08	1.00E-01	6.851E+07
1.50E+00	6.383E+08	3.50E-01	2.234E+08
1.85E+00	5.428E+08	5.04E-01	2.736E+08
2.35E+00	4.719E+08	1.25E-01	5.899E+07
2.48E+00	4.032E+08	5.21E-01	2.101E+08
3.00E+00	2.439E+08	1.30E+00	3.180E+08

Continued on following page

E [MeV]	$\frac{dS}{dE} \left[\frac{n}{MeV \cdot sec} \right]$	dE	dS $\left[\frac{n}{sec} \right]$
4.30E+00	1.336E+08	4.96E-01	6.627E+07
4.80E+00	6.761E+07	1.63E+00	1.105E+08
6.43E+00	2.006E+07	1.75E+00	3.517E+07
8.19E+00	5.142E+06	1.81E+00	9.322E+06
1.00E+01			

Table C.3: ORIGEN-ARP photon results for a Westinghouse 17×17 PWR assembly burned to $57.535 \frac{MWd}{kg}$ and cooled for a combined time period of 15yr.

E [MeV]	$\frac{dS}{dE} \left[\frac{p}{MeV \cdot sec} \right]$	dE	dS $\left[\frac{p}{sec} \right]$
1.00E-02	9.97E+16	1.00E-02	9.969E+14
2.00E-02	4.89E+16	1.00E-02	4.891E+14
3.00E-02	4.64E+16	1.50E-02	6.963E+14
4.50E-02	2.22E+16	1.50E-02	3.332E+14
6.00E-02	1.29E+16	1.00E-02	1.286E+14
7.00E-02	1.14E+16	5.00E-03	5.700E+13
7.50E-02	8.80E+15	2.50E-02	2.199E+14
1.00E-01	5.53E+15	5.00E-02	2.766E+14
1.50E-01	2.79E+15	5.00E-02	1.394E+14
2.00E-01	1.42E+15	6.00E-02	8.490E+13
2.60E-01	8.78E+14	4.00E-02	3.513E+13
3.00E-01	7.56E+14	1.00E-01	7.562E+13
4.00E-01	5.21E+14	5.00E-02	2.605E+13
4.50E-01	3.95E+14	6.00E-02	2.372E+13
5.10E-01	3.00E+14	2.00E-03	6.006E+11
5.12E-01	4.18E+14	8.80E-02	3.681E+13
6.00E-01	4.15E+16	1.00E-01	4.154E+15
7.00E-01	1.09E+15	1.00E-01	1.093E+14
8.00E-01	2.97E+14	1.00E-01	2.965E+13
9.00E-01	3.53E+14	1.00E-01	3.532E+13
1.00E+00	9.77E+13	2.00E-01	1.954E+13
1.20E+00	4.19E+14	1.30E-01	5.450E+13
1.33E+00	2.45E+13	1.10E-01	2.696E+12
1.44E+00	2.02E+13	6.00E-02	1.213E+12
1.50E+00	3.71E+12	7.00E-02	2.600E+11
1.57E+00	3.11E+13	9.00E-02	2.801E+12
1.66E+00	1.00E+12	1.40E-01	1.400E+11
1.80E+00	3.08E+11	2.00E-01	6.160E+10
2.00E+00	7.26E+10	1.50E-01	1.089E+10
2.15E+00	4.17E+09	2.00E-01	8.340E+08

Continued on following page

E [MeV]	$\frac{dS}{dE} [\frac{p}{MeVsec}]$	dE	dS [$\frac{p}{sec}$]
2.35E+00	4.98E+09	1.50E-01	7.472E+08
2.50E+00	3.34E+09	2.50E-01	8.350E+08
2.75E+00	6.83E+08	2.50E-01	1.707E+08
3.00E+00	2.47E+08	5.00E-01	1.236E+08
3.50E+00	1.22E+08	5.00E-01	6.100E+07
4.00E+00	7.07E+07	5.00E-01	3.535E+07
4.50E+00	4.10E+07	5.00E-01	2.049E+07
5.00E+00	2.38E+07	5.00E-01	1.188E+07
5.50E+00	1.38E+07	5.00E-01	6.890E+06
6.00E+00	7.99E+06	5.00E-01	3.994E+06
6.50E+00	4.63E+06	5.00E-01	2.316E+06
7.00E+00	2.69E+06	5.00E-01	1.343E+06
7.50E+00	1.56E+06	5.00E-01	7.785E+05
8.00E+00	4.60E+05	2.00E+00	9.196E+05
1.00E+01			

Table C.4: ORIGEN-ARP photon results for a Westinghouse 17×17 PWR assembly burned to $57.535 \frac{MWd}{kg}$ and cooled for a combined time period of 15yr.

E [MeV]	$\frac{dS}{dE} [\frac{n}{MeVsec}]$	dE	dS [$\frac{n}{sec}$]
1.00E-11	5.893E+04	9.00E-11	5.304E-06
1.00E-10	2.402E+04	4.00E-10	9.608E-06
5.00E-10	1.567E+04	2.50E-10	3.918E-06
7.50E-10	1.367E+04	2.50E-10	3.418E-06
1.00E-09	1.187E+04	2.00E-10	2.374E-06
1.20E-09	1.114E+04	3.00E-10	3.342E-06
1.50E-09	9.800E+03	5.00E-10	4.900E-06
2.00E-09	8.845E+03	5.00E-10	4.423E-06
2.50E-09	8.056E+03	5.00E-10	4.028E-06
3.00E-09	7.375E+03	1.00E-09	7.375E-06
4.00E-09	6.664E+03	1.00E-09	6.664E-06
5.00E-09	6.019E+03	2.50E-09	1.505E-05
7.50E-09	5.448E+03	2.50E-09	1.362E-05
1.00E-08	4.832E+03	1.53E-08	7.393E-05
2.53E-08	4.635E+03	4.70E-09	2.178E-05
3.00E-08	4.696E+03	1.00E-08	4.696E-05
4.00E-08	4.793E+03	1.00E-08	4.793E-05
5.00E-08	4.953E+03	1.00E-08	4.953E-05
6.00E-08	5.092E+03	1.00E-08	5.092E-05
7.00E-08	5.258E+03	1.00E-08	5.258E-05

Continued on following page

E [MeV]	$\frac{dS}{dE} [\frac{n}{MeV \cdot sec}]$	dE	dS [$\frac{n}{sec}$]
8.00E-08	5.419E+03	1.00E-08	5.419E-05
9.00E-08	5.574E+03	1.00E-08	5.574E-05
1.00E-07	5.871E+03	2.50E-08	1.468E-04
1.25E-07	6.252E+03	2.50E-08	1.563E-04
1.50E-07	7.092E+03	2.50E-08	1.773E-04
1.75E-07	7.548E+03	2.50E-08	1.887E-04
2.00E-07	7.865E+03	2.50E-08	1.966E-04
2.25E-07	8.212E+03	2.50E-08	2.053E-04
2.50E-07	8.516E+03	2.50E-08	2.129E-04
2.75E-07	8.807E+03	2.50E-08	2.202E-04
3.00E-07	9.099E+03	2.50E-08	2.275E-04
3.25E-07	9.407E+03	2.50E-08	2.352E-04
3.50E-07	9.671E+03	2.50E-08	2.418E-04
3.75E-07	9.919E+03	2.50E-08	2.480E-04
4.00E-07	1.031E+04	5.00E-08	5.155E-04
4.50E-07	1.082E+04	5.00E-08	5.410E-04
5.00E-07	1.128E+04	5.00E-08	5.640E-04
5.50E-07	1.174E+04	5.00E-08	5.870E-04
6.00E-07	1.206E+04	2.50E-08	3.015E-04
6.25E-07	1.226E+04	2.50E-08	3.065E-04
6.50E-07	1.259E+04	5.00E-08	6.295E-04
7.00E-07	1.297E+04	5.00E-08	6.485E-04
7.50E-07	1.339E+04	5.00E-08	6.695E-04
8.00E-07	1.376E+04	5.00E-08	6.880E-04
8.50E-07	1.411E+04	5.00E-08	7.055E-04
9.00E-07	1.444E+04	2.50E-08	3.610E-04
9.25E-07	1.451E+04	2.50E-08	3.628E-04
9.50E-07	1.480E+04	2.50E-08	3.700E-04
9.75E-07	1.491E+04	2.50E-08	3.728E-04
1.00E-06	1.516E+04	1.00E-08	1.516E-04
1.01E-06	1.497E+04	1.00E-08	1.497E-04
1.02E-06	1.528E+04	1.00E-08	1.528E-04
1.03E-06	1.508E+04	1.00E-08	1.508E-04
1.04E-06	1.556E+04	1.00E-08	1.556E-04
1.05E-06	1.543E+04	1.00E-08	1.543E-04
1.06E-06	1.574E+04	1.00E-08	1.574E-04
1.07E-06	1.660E+04	1.00E-08	1.660E-04
1.08E-06	1.585E+04	1.00E-08	1.585E-04
1.09E-06	1.598E+04	1.00E-08	1.598E-04
1.10E-06	1.594E+04	1.00E-08	1.594E-04
1.11E-06	1.608E+04	1.00E-08	1.608E-04
1.12E-06	1.760E+04	1.00E-08	1.760E-04

Continued on following page

E [MeV]	$\frac{dS}{dE} \left[\frac{n}{MeV \cdot sec} \right]$	dE	dS $\left[\frac{n}{sec} \right]$
1.13E-06	1.775E+04	1.00E-08	1.775E-04
1.14E-06	1.791E+04	1.00E-08	1.791E-04
1.15E-06	2.168E+04	2.50E-08	5.420E-04
1.18E-06	9.659E+05	2.50E-08	2.415E-02
1.20E-06	9.696E+05	2.50E-08	2.424E-02
1.23E-06	9.774E+05	2.50E-08	2.444E-02
1.25E-06	1.581E+06	5.00E-08	7.905E-02
1.30E-06	1.026E+06	5.00E-08	5.130E-02
1.35E-06	1.048E+06	5.00E-08	5.240E-02
1.40E-06	4.489E+05	5.00E-08	2.245E-02
1.45E-06	1.075E+06	5.00E-08	5.375E-02
1.50E-06	1.098E+06	9.00E-08	9.882E-02
1.59E-06	1.500E+06	9.00E-08	1.350E-01
1.68E-06	1.171E+06	9.00E-08	1.054E-01
1.77E-06	8.136E+05	9.00E-08	7.322E-02
1.86E-06	1.662E+06	8.00E-08	1.330E-01
1.94E-06	1.254E+06	6.00E-08	7.524E-02
2.00E-06	1.278E+06	1.20E-07	1.534E-01
2.12E-06	1.311E+06	9.00E-08	1.180E-01
2.21E-06	9.088E+05	9.00E-08	8.179E-02
2.30E-06	1.355E+06	8.00E-08	1.084E-01
2.38E-06	1.822E+06	9.00E-08	1.640E-01
2.47E-06	1.004E+06	1.00E-07	1.004E-01
2.57E-06	1.850E+06	1.00E-07	1.850E-01
2.67E-06	1.470E+06	1.00E-07	1.470E-01
2.77E-06	1.493E+06	1.00E-07	1.493E-01
2.87E-06	1.521E+06	1.00E-07	1.521E-01
2.97E-06	6.737E+04	3.00E-08	2.021E-03
3.00E-06	2.428E+06	5.00E-08	1.214E-01
3.05E-06	1.117E+06	1.00E-07	1.117E-01
3.15E-06	1.751E+06	3.50E-07	6.129E-01
3.50E-06	1.478E+06	2.30E-07	3.399E-01
3.73E-06	1.930E+06	2.70E-07	5.211E-01
4.00E-06	1.786E+06	7.50E-07	1.340E+00
4.75E-06	1.957E+06	2.50E-07	4.893E-01
5.00E-06	2.170E+06	4.00E-07	8.680E-01
5.40E-06	2.122E+06	6.00E-07	1.273E+00
6.00E-06	1.943E+06	2.50E-07	4.858E-01
6.25E-06	2.499E+06	2.50E-07	6.247E-01
6.50E-06	2.286E+06	2.50E-07	5.715E-01
6.75E-06	2.330E+06	2.50E-07	5.825E-01
7.00E-06	2.365E+06	1.50E-07	3.548E-01

Continued on following page

E [MeV]	$\frac{dS}{dE} \left[\frac{n}{MeV \cdot sec} \right]$	dE	dS $\left[\frac{n}{sec} \right]$
7.15E-06	2.454E+06	9.50E-07	2.331E+00
8.10E-06	2.528E+06	1.00E-06	2.528E+00
9.10E-06	2.831E+06	9.00E-07	2.548E+00
1.00E-05	2.912E+06	1.50E-06	4.368E+00
1.15E-05	3.039E+06	4.00E-07	1.216E+00
1.19E-05	3.127E+06	1.00E-06	3.127E+00
1.29E-05	3.243E+06	8.50E-07	2.757E+00
1.38E-05	3.183E+06	6.50E-07	2.069E+00
1.44E-05	3.551E+06	7.00E-07	2.486E+00
1.51E-05	3.390E+06	9.00E-07	3.051E+00
1.60E-05	3.606E+06	1.00E-06	3.606E+00
1.70E-05	3.740E+06	1.50E-06	5.610E+00
1.85E-05	3.842E+06	5.00E-07	1.921E+00
1.90E-05	3.921E+06	1.00E-06	3.921E+00
2.00E-05	4.136E+06	1.00E-06	4.136E+00
2.10E-05	4.142E+06	1.50E-06	6.213E+00
2.25E-05	4.291E+06	2.50E-06	1.073E+01
2.50E-05	4.622E+06	2.50E-06	1.156E+01
2.75E-05	4.784E+06	2.50E-06	1.196E+01
3.00E-05	4.820E+06	1.25E-06	6.025E+00
3.13E-05	5.296E+06	5.00E-07	2.648E+00
3.18E-05	5.083E+06	1.50E-06	7.625E+00
3.33E-05	5.162E+06	5.00E-07	2.581E+00
3.38E-05	5.214E+06	8.50E-07	4.432E+00
3.46E-05	5.111E+06	9.00E-07	4.600E+00
3.55E-05	5.366E+06	1.50E-06	8.049E+00
3.70E-05	5.457E+06	1.00E-06	5.457E+00
3.80E-05	5.532E+06	1.10E-06	6.085E+00
3.91E-05	5.916E+06	5.00E-07	2.958E+00
3.96E-05	5.660E+06	1.40E-06	7.924E+00
4.10E-05	5.768E+06	1.40E-06	8.075E+00
4.24E-05	5.870E+06	1.60E-06	9.392E+00
4.40E-05	5.825E+06	1.20E-06	6.990E+00
4.52E-05	6.062E+06	1.80E-06	1.091E+01
4.70E-05	6.166E+06	1.30E-06	8.016E+00
4.83E-05	6.235E+06	9.00E-07	5.612E+00
4.92E-05	6.440E+06	1.40E-06	9.016E+00
5.06E-05	6.264E+06	1.40E-06	8.770E+00
5.20E-05	6.483E+06	1.40E-06	9.076E+00
5.34E-05	6.692E+06	5.60E-06	3.748E+01
5.90E-05	6.914E+06	2.00E-06	1.383E+01
6.10E-05	7.135E+06	4.00E-06	2.854E+01

Continued on following page

E [MeV]	$\frac{dS}{dE} \left[\frac{n}{MeV \cdot sec} \right]$	dE	dS $\left[\frac{n}{sec} \right]$
6.50E-05	7.182E+06	2.50E-06	1.796E+01
6.75E-05	7.500E+06	4.50E-06	3.375E+01
7.20E-05	7.622E+06	4.00E-06	3.049E+01
7.60E-05	7.881E+06	4.00E-06	3.152E+01
8.00E-05	8.031E+06	2.00E-06	1.606E+01
8.20E-05	8.276E+06	8.00E-06	6.621E+01
9.00E-05	8.695E+06	1.00E-05	8.695E+01
1.00E-04	9.096E+06	8.00E-06	7.277E+01
1.08E-04	9.419E+06	7.00E-06	6.593E+01
1.15E-04	9.646E+06	4.00E-06	3.858E+01
1.19E-04	9.880E+06	3.00E-06	2.964E+01
1.22E-04	1.104E+07	6.40E-05	7.066E+02
1.86E-04	1.221E+07	6.50E-06	7.936E+01
1.93E-04	1.263E+07	1.50E-05	1.895E+02
2.08E-04	1.274E+07	2.50E-06	3.185E+01
2.10E-04	1.337E+07	3.00E-05	4.011E+02
2.40E-04	1.444E+07	4.50E-05	6.498E+02
2.85E-04	1.532E+07	2.00E-05	3.064E+02
3.05E-04	1.837E+07	2.45E-04	4.501E+03
5.50E-04	2.200E+07	1.20E-04	2.640E+03
6.70E-04	2.313E+07	1.30E-05	3.007E+02
6.83E-04	2.543E+07	2.67E-04	6.790E+03
9.50E-04	2.886E+07	2.00E-04	5.772E+03
1.15E-03	3.240E+07	3.50E-04	1.134E+04
1.50E-03	3.482E+07	5.00E-05	1.741E+03
1.55E-03	3.646E+07	2.50E-04	9.115E+03
1.80E-03	3.982E+07	4.00E-04	1.593E+04
2.20E-03	4.218E+07	9.00E-05	3.796E+03
2.29E-03	4.392E+07	2.90E-04	1.274E+04
2.58E-03	4.700E+07	4.20E-04	1.974E+04
3.00E-03	5.163E+07	7.40E-04	3.821E+04
3.74E-03	5.498E+07	1.60E-04	8.797E+03
3.90E-03	6.247E+07	2.10E-03	1.312E+05
6.00E-03	7.438E+07	2.03E-03	1.510E+05
8.03E-03	8.312E+07	1.47E-03	1.222E+05
9.50E-03	9.400E+07	3.50E-03	3.290E+05
1.30E-02	1.084E+08	4.00E-03	4.336E+05
1.70E-02	1.278E+08	8.00E-03	1.022E+06
2.50E-02	1.459E+08	5.00E-03	7.295E+05
3.00E-02	1.693E+08	1.50E-02	2.540E+06
4.50E-02	1.900E+08	5.00E-03	9.500E+05
5.00E-02	1.965E+08	2.00E-03	3.930E+05

Continued on following page

E [MeV]	$\frac{dS}{dE} \left[\frac{n}{MeV \cdot sec} \right]$	dE	dS $\left[\frac{n}{sec} \right]$
5.20E-02	2.053E+08	8.00E-03	1.642E+06
6.00E-02	2.225E+08	1.30E-02	2.893E+06
7.30E-02	2.340E+08	2.00E-03	4.680E+05
7.50E-02	2.404E+08	7.00E-03	1.683E+06
8.20E-02	2.473E+08	3.00E-03	7.419E+05
8.50E-02	2.591E+08	1.50E-02	3.887E+06
1.00E-01	2.846E+08	2.83E-02	8.054E+06
1.28E-01	3.104E+08	2.17E-02	6.736E+06
1.50E-01	3.414E+08	5.00E-02	1.707E+07
2.00E-01	3.833E+08	7.00E-02	2.683E+07
2.70E-01	4.186E+08	6.00E-02	2.512E+07
3.30E-01	4.459E+08	7.00E-02	3.121E+07
4.00E-01	4.616E+08	2.00E-02	9.232E+06
4.20E-01	4.676E+08	2.00E-02	9.352E+06
4.40E-01	4.745E+08	3.00E-02	1.424E+07
4.70E-01	4.818E+08	2.95E-02	1.421E+07
5.00E-01	4.902E+08	5.05E-02	2.476E+07
5.50E-01	4.968E+08	2.30E-02	1.143E+07
5.73E-01	5.007E+08	2.70E-02	1.352E+07
6.00E-01	5.067E+08	7.00E-02	3.547E+07
6.70E-01	5.108E+08	9.00E-03	4.597E+06
6.79E-01	5.137E+08	7.10E-02	3.647E+07
7.50E-01	5.170E+08	7.00E-02	3.619E+07
8.20E-01	5.180E+08	4.11E-02	2.129E+07
8.61E-01	5.180E+08	1.39E-02	7.200E+06
8.75E-01	5.177E+08	2.50E-02	1.294E+07
9.00E-01	5.173E+08	2.00E-02	1.035E+07
9.20E-01	5.155E+08	9.00E-02	4.640E+07
1.01E+00	5.108E+08	9.00E-02	4.597E+07
1.10E+00	5.035E+08	1.00E-01	5.035E+07
1.20E+00	4.964E+08	5.00E-02	2.482E+07
1.25E+00	4.902E+08	6.70E-02	3.284E+07
1.32E+00	4.840E+08	3.90E-02	1.888E+07
1.36E+00	4.790E+08	4.40E-02	2.108E+07
1.40E+00	4.698E+08	1.00E-01	4.698E+07
1.50E+00	4.380E+08	3.50E-01	1.533E+08
1.85E+00	3.730E+08	5.04E-01	1.880E+08
2.35E+00	3.247E+08	1.25E-01	4.059E+07
2.48E+00	2.775E+08	5.21E-01	1.446E+08
3.00E+00	1.676E+08	1.30E+00	2.186E+08
4.30E+00	9.144E+07	4.96E-01	4.535E+07
4.80E+00	4.623E+07	1.63E+00	7.554E+07

Continued on following page

E [MeV]	$\frac{dS}{dE} [\frac{n}{MeVsec}]$	dE	dS [$\frac{n}{sec}$]
6.43E+00	1.370E+07	1.75E+00	2.402E+07
8.19E+00	3.509E+06	1.81E+00	6.362E+06
1.00E+01			

Table C.5: ORIGEN-ARP photon results for a Westinghouse 17×17 PWR assembly burned to $57.535 \frac{MWd}{kg}$ and cooled for a combined time period of 25yr.

E [MeV]	$\frac{dS}{dE} [\frac{p}{MeVsec}]$	dE	dS [$\frac{p}{sec}$]
1.00E-02	7.98E+16	1.00E-02	7.977E+14
2.00E-02	3.76E+16	1.00E-02	3.762E+14
3.00E-02	3.53E+16	1.50E-02	5.300E+14
4.50E-02	1.89E+16	1.50E-02	2.835E+14
6.00E-02	9.98E+15	1.00E-02	9.976E+13
7.00E-02	8.95E+15	5.00E-03	4.477E+13
7.50E-02	6.69E+15	2.50E-02	1.672E+14
1.00E-01	3.88E+15	5.00E-02	1.939E+14
1.50E-01	2.16E+15	5.00E-02	1.078E+14
2.00E-01	1.04E+15	6.00E-02	6.246E+13
2.60E-01	6.86E+14	4.00E-02	2.744E+13
3.00E-01	5.86E+14	1.00E-01	5.864E+13
4.00E-01	3.57E+14	5.00E-02	1.786E+13
4.50E-01	2.82E+14	6.00E-02	1.691E+13
5.10E-01	1.13E+14	2.00E-03	2.252E+11
5.12E-01	1.41E+14	8.80E-02	1.242E+13
6.00E-01	3.25E+16	1.00E-01	3.247E+15
7.00E-01	2.50E+14	1.00E-01	2.497E+13
8.00E-01	1.40E+14	1.00E-01	1.401E+13
9.00E-01	1.71E+14	1.00E-01	1.705E+13
1.00E+00	4.66E+13	2.00E-01	9.314E+12
1.20E+00	1.91E+14	1.30E-01	2.484E+13
1.33E+00	5.09E+12	1.10E-01	5.600E+11
1.44E+00	9.97E+12	6.00E-02	5.984E+11
1.50E+00	2.43E+12	7.00E-02	1.698E+11
1.57E+00	1.46E+13	9.00E-02	1.315E+12
1.66E+00	7.62E+11	1.40E-01	1.067E+11
1.80E+00	2.37E+11	2.00E-01	4.730E+10
2.00E+00	5.42E+10	1.50E-01	8.126E+09
2.15E+00	1.23E+09	2.00E-01	2.458E+08
2.35E+00	2.11E+08	1.50E-01	3.159E+07
2.50E+00	2.70E+09	2.50E-01	6.743E+08

Continued on following page

E [MeV]	$\frac{dS}{dE} \left[\frac{p}{MeVsec} \right]$	dE	dS $\left[\frac{p}{sec} \right]$
2.75E+00	2.39E+08	2.50E-01	5.978E+07
3.00E+00	1.45E+08	5.00E-01	7.240E+07
3.50E+00	8.39E+07	5.00E-01	4.197E+07
4.00E+00	4.86E+07	5.00E-01	2.432E+07
4.50E+00	2.82E+07	5.00E-01	1.410E+07
5.00E+00	1.64E+07	5.00E-01	8.175E+06
5.50E+00	9.48E+06	5.00E-01	4.739E+06
6.00E+00	5.50E+06	5.00E-01	2.748E+06
6.50E+00	3.19E+06	5.00E-01	1.593E+06
7.00E+00	1.85E+06	5.00E-01	9.235E+05
7.50E+00	1.07E+06	5.00E-01	5.355E+05
8.00E+00	3.16E+05	2.00E+00	6.326E+05
1.00E+01			

Table C.6: ORIGEN-ARP photon results for a Westinghouse 17×17 PWR assembly burned to $57.535 \frac{MWd}{kg}$ and cooled for a combined time period of 25yr.

E [MeV]	$\frac{dS}{dE} \left[\frac{n}{MeVsec} \right]$	dE	dS $\left[\frac{n}{sec} \right]$
1.00E-11	5.885E+04	9.00E-11	5.297E-06
1.00E-10	2.399E+04	4.00E-10	9.596E-06
5.00E-10	1.565E+04	2.50E-10	3.913E-06
7.50E-10	1.365E+04	2.50E-10	3.413E-06
1.00E-09	1.185E+04	2.00E-10	2.370E-06
1.20E-09	1.112E+04	3.00E-10	3.336E-06
1.50E-09	9.785E+03	5.00E-10	4.893E-06
2.00E-09	8.832E+03	5.00E-10	4.416E-06
2.50E-09	8.045E+03	5.00E-10	4.023E-06
3.00E-09	7.365E+03	1.00E-09	7.365E-06
4.00E-09	6.654E+03	1.00E-09	6.654E-06
5.00E-09	6.010E+03	2.50E-09	1.503E-05
7.50E-09	5.440E+03	2.50E-09	1.360E-05
1.00E-08	4.825E+03	1.53E-08	7.382E-05
2.53E-08	4.628E+03	4.70E-09	2.175E-05
3.00E-08	4.690E+03	1.00E-08	4.690E-05
4.00E-08	4.786E+03	1.00E-08	4.786E-05
5.00E-08	4.946E+03	1.00E-08	4.946E-05
6.00E-08	5.085E+03	1.00E-08	5.085E-05
7.00E-08	5.250E+03	1.00E-08	5.250E-05
8.00E-08	5.411E+03	1.00E-08	5.411E-05
9.00E-08	5.566E+03	1.00E-08	5.566E-05

Continued on following page

E [MeV]	$\frac{dS}{dE} \left[\frac{n}{MeV \cdot sec} \right]$	dE	dS $\left[\frac{n}{sec} \right]$
1.00E-07	5.863E+03	2.50E-08	1.466E-04
1.25E-07	6.243E+03	2.50E-08	1.561E-04
1.50E-07	7.082E+03	2.50E-08	1.771E-04
1.75E-07	7.538E+03	2.50E-08	1.885E-04
2.00E-07	7.855E+03	2.50E-08	1.964E-04
2.25E-07	8.200E+03	2.50E-08	2.050E-04
2.50E-07	8.505E+03	2.50E-08	2.126E-04
2.75E-07	8.795E+03	2.50E-08	2.199E-04
3.00E-07	9.086E+03	2.50E-08	2.272E-04
3.25E-07	9.394E+03	2.50E-08	2.349E-04
3.50E-07	9.658E+03	2.50E-08	2.415E-04
3.75E-07	9.906E+03	2.50E-08	2.477E-04
4.00E-07	1.029E+04	5.00E-08	5.145E-04
4.50E-07	1.080E+04	5.00E-08	5.400E-04
5.00E-07	1.127E+04	5.00E-08	5.635E-04
5.50E-07	1.173E+04	5.00E-08	5.865E-04
6.00E-07	1.204E+04	2.50E-08	3.010E-04
6.25E-07	1.224E+04	2.50E-08	3.060E-04
6.50E-07	1.257E+04	5.00E-08	6.285E-04
7.00E-07	1.295E+04	5.00E-08	6.475E-04
7.50E-07	1.337E+04	5.00E-08	6.685E-04
8.00E-07	1.374E+04	5.00E-08	6.870E-04
8.50E-07	1.409E+04	5.00E-08	7.045E-04
9.00E-07	1.442E+04	2.50E-08	3.605E-04
9.25E-07	1.449E+04	2.50E-08	3.623E-04
9.50E-07	1.478E+04	2.50E-08	3.695E-04
9.75E-07	1.489E+04	2.50E-08	3.723E-04
1.00E-06	1.514E+04	1.00E-08	1.514E-04
1.01E-06	1.495E+04	1.00E-08	1.495E-04
1.02E-06	1.525E+04	1.00E-08	1.525E-04
1.03E-06	1.506E+04	1.00E-08	1.506E-04
1.04E-06	1.553E+04	1.00E-08	1.553E-04
1.05E-06	1.518E+04	1.00E-08	1.518E-04
1.06E-06	1.549E+04	1.00E-08	1.549E-04
1.07E-06	1.552E+04	1.00E-08	1.552E-04
1.08E-06	1.559E+04	1.00E-08	1.559E-04
1.09E-06	1.572E+04	1.00E-08	1.572E-04
1.10E-06	1.568E+04	1.00E-08	1.568E-04
1.11E-06	1.581E+04	1.00E-08	1.581E-04
1.12E-06	1.734E+04	1.00E-08	1.734E-04
1.13E-06	1.748E+04	1.00E-08	1.748E-04
1.14E-06	1.764E+04	1.00E-08	1.764E-04

Continued on following page

E [MeV]	$\frac{dS}{dE} \left[\frac{n}{MeV \cdot sec} \right]$	dE	dS $\left[\frac{n}{sec} \right]$
1.15E-06	2.133E+04	2.50E-08	5.332E-04
1.18E-06	6.660E+05	2.50E-08	1.665E-02
1.20E-06	6.678E+05	2.50E-08	1.670E-02
1.23E-06	6.725E+05	2.50E-08	1.681E-02
1.25E-06	1.085E+06	5.00E-08	5.425E-02
1.30E-06	7.064E+05	5.00E-08	3.532E-02
1.35E-06	7.216E+05	5.00E-08	3.608E-02
1.40E-06	3.128E+05	5.00E-08	1.564E-02
1.45E-06	7.401E+05	5.00E-08	3.701E-02
1.50E-06	7.560E+05	9.00E-08	6.804E-02
1.59E-06	1.031E+06	9.00E-08	9.279E-02
1.68E-06	8.065E+05	9.00E-08	7.259E-02
1.77E-06	5.628E+05	9.00E-08	5.065E-02
1.86E-06	1.142E+06	8.00E-08	9.136E-02
1.94E-06	8.638E+05	6.00E-08	5.183E-02
2.00E-06	8.795E+05	1.20E-07	1.055E-01
2.12E-06	9.028E+05	9.00E-08	8.125E-02
2.21E-06	6.286E+05	9.00E-08	5.657E-02
2.30E-06	9.329E+05	8.00E-08	7.463E-02
2.38E-06	1.252E+06	9.00E-08	1.127E-01
2.47E-06	6.937E+05	1.00E-07	6.937E-02
2.57E-06	1.271E+06	1.00E-07	1.271E-01
2.67E-06	1.012E+06	1.00E-07	1.012E-01
2.77E-06	1.029E+06	1.00E-07	1.029E-01
2.87E-06	1.047E+06	1.00E-07	1.047E-01
2.97E-06	5.613E+04	3.00E-08	1.684E-03
3.00E-06	1.666E+06	5.00E-08	8.330E-02
3.05E-06	7.722E+05	1.00E-07	7.722E-02
3.15E-06	1.205E+06	3.50E-07	4.218E-01
3.50E-06	1.019E+06	2.30E-07	2.344E-01
3.73E-06	1.328E+06	2.70E-07	3.586E-01
4.00E-06	1.230E+06	7.50E-07	9.225E-01
4.75E-06	1.348E+06	2.50E-07	3.370E-01
5.00E-06	1.493E+06	4.00E-07	5.972E-01
5.40E-06	1.461E+06	6.00E-07	8.766E-01
6.00E-06	1.340E+06	2.50E-07	3.350E-01
6.25E-06	1.719E+06	2.50E-07	4.297E-01
6.50E-06	1.574E+06	2.50E-07	3.935E-01
6.75E-06	1.604E+06	2.50E-07	4.010E-01
7.00E-06	1.629E+06	1.50E-07	2.444E-01
7.15E-06	1.690E+06	9.50E-07	1.606E+00
8.10E-06	1.741E+06	1.00E-06	1.741E+00

Continued on following page

E [MeV]	$\frac{dS}{dE} \left[\frac{n}{MeV \cdot sec} \right]$	dE	dS $\left[\frac{n}{sec} \right]$
9.10E-06	1.948E+06	9.00E-07	1.753E+00
1.00E-05	2.005E+06	1.50E-06	3.008E+00
1.15E-05	2.093E+06	4.00E-07	8.372E-01
1.19E-05	2.153E+06	1.00E-06	2.153E+00
1.29E-05	2.233E+06	8.50E-07	1.898E+00
1.38E-05	2.192E+06	6.50E-07	1.425E+00
1.44E-05	2.444E+06	7.00E-07	1.711E+00
1.51E-05	2.335E+06	9.00E-07	2.102E+00
1.60E-05	2.483E+06	1.00E-06	2.483E+00
1.70E-05	2.575E+06	1.50E-06	3.863E+00
1.85E-05	2.645E+06	5.00E-07	1.323E+00
1.90E-05	2.699E+06	1.00E-06	2.699E+00
2.00E-05	2.847E+06	1.00E-06	2.847E+00
2.10E-05	2.852E+06	1.50E-06	4.278E+00
2.25E-05	2.954E+06	2.50E-06	7.385E+00
2.50E-05	3.182E+06	2.50E-06	7.955E+00
2.75E-05	3.294E+06	2.50E-06	8.235E+00
3.00E-05	3.319E+06	1.25E-06	4.149E+00
3.13E-05	3.644E+06	5.00E-07	1.822E+00
3.18E-05	3.500E+06	1.50E-06	5.250E+00
3.33E-05	3.554E+06	5.00E-07	1.777E+00
3.38E-05	3.589E+06	8.50E-07	3.051E+00
3.46E-05	3.520E+06	9.00E-07	3.168E+00
3.55E-05	3.694E+06	1.50E-06	5.541E+00
3.70E-05	3.757E+06	1.00E-06	3.757E+00
3.80E-05	3.808E+06	1.10E-06	4.189E+00
3.91E-05	4.070E+06	5.00E-07	2.035E+00
3.96E-05	3.898E+06	1.40E-06	5.457E+00
4.10E-05	3.976E+06	1.40E-06	5.566E+00
4.24E-05	4.046E+06	1.60E-06	6.474E+00
4.40E-05	4.017E+06	1.20E-06	4.820E+00
4.52E-05	4.179E+06	1.80E-06	7.522E+00
4.70E-05	4.252E+06	1.30E-06	5.528E+00
4.83E-05	4.300E+06	9.00E-07	3.870E+00
4.92E-05	4.440E+06	1.40E-06	6.216E+00
5.06E-05	4.321E+06	1.40E-06	6.049E+00
5.20E-05	4.471E+06	1.40E-06	6.259E+00
5.34E-05	4.615E+06	5.60E-06	2.584E+01
5.90E-05	4.768E+06	2.00E-06	9.536E+00
6.10E-05	4.919E+06	4.00E-06	1.968E+01
6.50E-05	4.952E+06	2.50E-06	1.238E+01
6.75E-05	5.171E+06	4.50E-06	2.327E+01

Continued on following page

E [MeV]	$\frac{dS}{dE} \left[\frac{n}{MeV \cdot sec} \right]$	dE	dS $\left[\frac{n}{sec} \right]$
7.20E-05	5.255E+06	4.00E-06	2.102E+01
7.60E-05	5.433E+06	4.00E-06	2.173E+01
8.00E-05	5.538E+06	2.00E-06	1.108E+01
8.20E-05	5.706E+06	8.00E-06	4.565E+01
9.00E-05	5.995E+06	1.00E-05	5.995E+01
1.00E-04	6.271E+06	8.00E-06	5.017E+01
1.08E-04	6.494E+06	7.00E-06	4.546E+01
1.15E-04	6.650E+06	4.00E-06	2.660E+01
1.19E-04	6.810E+06	3.00E-06	2.043E+01
1.22E-04	7.613E+06	6.40E-05	4.872E+02
1.86E-04	8.414E+06	6.50E-06	5.469E+01
1.93E-04	8.704E+06	1.50E-05	1.306E+02
2.08E-04	8.780E+06	2.50E-06	2.195E+01
2.10E-04	9.212E+06	3.00E-05	2.764E+02
2.40E-04	9.952E+06	4.50E-05	4.478E+02
2.85E-04	1.056E+07	2.00E-05	2.112E+02
3.05E-04	1.266E+07	2.45E-04	3.102E+03
5.50E-04	1.516E+07	1.20E-04	1.819E+03
6.70E-04	1.594E+07	1.30E-05	2.072E+02
6.83E-04	1.752E+07	2.67E-04	4.678E+03
9.50E-04	1.989E+07	2.00E-04	3.978E+03
1.15E-03	2.233E+07	3.50E-04	7.816E+03
1.50E-03	2.400E+07	5.00E-05	1.200E+03
1.55E-03	2.513E+07	2.50E-04	6.283E+03
1.80E-03	2.744E+07	4.00E-04	1.098E+04
2.20E-03	2.907E+07	9.00E-05	2.616E+03
2.29E-03	3.027E+07	2.90E-04	8.778E+03
2.58E-03	3.239E+07	4.20E-04	1.360E+04
3.00E-03	3.559E+07	7.40E-04	2.634E+04
3.74E-03	3.789E+07	1.60E-04	6.062E+03
3.90E-03	4.306E+07	2.10E-03	9.043E+04
6.00E-03	5.127E+07	2.03E-03	1.041E+05
8.03E-03	5.729E+07	1.47E-03	8.422E+04
9.50E-03	6.479E+07	3.50E-03	2.268E+05
1.30E-02	7.471E+07	4.00E-03	2.988E+05
1.70E-02	8.809E+07	8.00E-03	7.047E+05
2.50E-02	1.006E+08	5.00E-03	5.030E+05
3.00E-02	1.167E+08	1.50E-02	1.751E+06
4.50E-02	1.309E+08	5.00E-03	6.545E+05
5.00E-02	1.354E+08	2.00E-03	2.708E+05
5.20E-02	1.415E+08	8.00E-03	1.132E+06
6.00E-02	1.534E+08	1.30E-02	1.994E+06

Continued on following page

E [MeV]	$\frac{dS}{dE} \left[\frac{n}{MeV \cdot sec} \right]$	dE	dS $\left[\frac{n}{sec} \right]$
7.30E-02	1.612E+08	2.00E-03	3.224E+05
7.50E-02	1.657E+08	7.00E-03	1.160E+06
8.20E-02	1.705E+08	3.00E-03	5.115E+05
8.50E-02	1.786E+08	1.50E-02	2.679E+06
1.00E-01	1.961E+08	2.83E-02	5.550E+06
1.28E-01	2.139E+08	2.17E-02	4.642E+06
1.50E-01	2.353E+08	5.00E-02	1.177E+07
2.00E-01	2.641E+08	7.00E-02	1.849E+07
2.70E-01	2.885E+08	6.00E-02	1.731E+07
3.30E-01	3.073E+08	7.00E-02	2.151E+07
4.00E-01	3.181E+08	2.00E-02	6.362E+06
4.20E-01	3.222E+08	2.00E-02	6.444E+06
4.40E-01	3.269E+08	3.00E-02	9.807E+06
4.70E-01	3.320E+08	2.95E-02	9.794E+06
5.00E-01	3.378E+08	5.05E-02	1.706E+07
5.50E-01	3.423E+08	2.30E-02	7.873E+06
5.73E-01	3.450E+08	2.70E-02	9.315E+06
6.00E-01	3.491E+08	7.00E-02	2.444E+07
6.70E-01	3.519E+08	9.00E-03	3.167E+06
6.79E-01	3.540E+08	7.10E-02	2.513E+07
7.50E-01	3.563E+08	7.00E-02	2.494E+07
8.20E-01	3.569E+08	4.11E-02	1.467E+07
8.61E-01	3.569E+08	1.39E-02	4.961E+06
8.75E-01	3.567E+08	2.50E-02	8.918E+06
9.00E-01	3.565E+08	2.00E-02	7.130E+06
9.20E-01	3.553E+08	9.00E-02	3.198E+07
1.01E+00	3.520E+08	9.00E-02	3.168E+07
1.10E+00	3.470E+08	1.00E-01	3.470E+07
1.20E+00	3.422E+08	5.00E-02	1.711E+07
1.25E+00	3.379E+08	6.70E-02	2.264E+07
1.32E+00	3.337E+08	3.90E-02	1.301E+07
1.36E+00	3.303E+08	4.40E-02	1.453E+07
1.40E+00	3.240E+08	1.00E-01	3.240E+07
1.50E+00	3.023E+08	3.50E-01	1.058E+08
1.85E+00	2.580E+08	5.04E-01	1.300E+08
2.35E+00	2.250E+08	1.25E-01	2.813E+07
2.48E+00	1.924E+08	5.21E-01	1.002E+08
3.00E+00	1.159E+08	1.30E+00	1.511E+08
4.30E+00	6.291E+07	4.96E-01	3.120E+07
4.80E+00	3.179E+07	1.63E+00	5.194E+07
6.43E+00	9.415E+06	1.75E+00	1.650E+07
8.19E+00	2.410E+06	1.81E+00	4.369E+06

Continued on following page

E [MeV]	$\frac{dS}{dE} \left[\frac{n}{MeVsec} \right]$	dE	dS $\left[\frac{n}{sec} \right]$
1.00E+01			

Table C.7: ORIGEN-ARP photon results for a Westinghouse 17×17 PWR assembly burned to $57.535 \frac{MWd}{kg}$ and cooled for a combined time period of 35yr.

E [MeV]	$\frac{dS}{dE} \left[\frac{p}{MeVsec} \right]$	dE	dS $\left[\frac{p}{sec} \right]$
1.00E-02	6.45E+16	1.00E-02	6.451E+14
2.00E-02	2.95E+16	1.00E-02	2.946E+14
3.00E-02	2.74E+16	1.50E-02	4.110E+14
4.50E-02	1.63E+16	1.50E-02	2.445E+14
6.00E-02	7.79E+15	1.00E-02	7.785E+13
7.00E-02	7.09E+15	5.00E-03	3.543E+13
7.50E-02	5.19E+15	2.50E-02	1.297E+14
1.00E-01	2.85E+15	5.00E-02	1.425E+14
1.50E-01	1.68E+15	5.00E-02	8.400E+13
2.00E-01	7.87E+14	6.00E-02	4.723E+13
2.60E-01	5.38E+14	4.00E-02	2.152E+13
3.00E-01	4.57E+14	1.00E-01	4.573E+13
4.00E-01	2.73E+14	5.00E-02	1.364E+13
4.50E-01	2.18E+14	6.00E-02	1.306E+13
5.10E-01	5.89E+13	2.00E-03	1.178E+11
5.12E-01	8.77E+13	8.80E-02	7.720E+12
6.00E-01	2.58E+16	1.00E-01	2.575E+15
7.00E-01	1.25E+14	1.00E-01	1.253E+13
8.00E-01	7.72E+13	1.00E-01	7.724E+12
9.00E-01	8.61E+13	1.00E-01	8.611E+12
1.00E+00	2.61E+13	2.00E-01	5.222E+12
1.20E+00	8.84E+13	1.30E-01	1.149E+13
1.33E+00	3.36E+12	1.10E-01	3.694E+11
1.44E+00	5.20E+12	6.00E-02	3.118E+11
1.50E+00	1.69E+12	7.00E-02	1.184E+11
1.57E+00	7.09E+12	9.00E-02	6.376E+11
1.66E+00	5.89E+11	1.40E-01	8.249E+10
1.80E+00	1.85E+11	2.00E-01	3.698E+10
2.00E+00	4.24E+10	1.50E-01	6.353E+09
2.15E+00	8.63E+08	2.00E-01	1.725E+08
2.35E+00	1.61E+08	1.50E-01	2.411E+07
2.50E+00	2.40E+09	2.50E-01	5.993E+08
2.75E+00	1.65E+08	2.50E-01	4.125E+07
3.00E+00	1.00E+08	5.00E-01	5.000E+07

Continued on following page

E [MeV]	$\frac{dS}{dE} [\frac{p}{MeVsec}]$	dE	dS [$\frac{p}{sec}$]
3.50E+00	5.80E+07	5.00E-01	2.900E+07
4.00E+00	3.36E+07	5.00E-01	1.680E+07
4.50E+00	1.95E+07	5.00E-01	9.740E+06
5.00E+00	1.13E+07	5.00E-01	5.645E+06
5.50E+00	6.55E+06	5.00E-01	3.274E+06
6.00E+00	3.80E+06	5.00E-01	1.898E+06
6.50E+00	2.20E+06	5.00E-01	1.101E+06
7.00E+00	1.28E+06	5.00E-01	6.380E+05
7.50E+00	7.40E+05	5.00E-01	3.700E+05
8.00E+00	2.19E+05	2.00E+00	4.370E+05
1.00E+01			

Table C.8: ORIGEN-ARP photon results for a Westinghouse 17×17 PWR assembly burned to $57.535 \frac{MWd}{kg}$ and cooled for a combined time period of 35yr.

E [MeV]	$\frac{dS}{dE} [\frac{n}{MeVsec}]$	dE	dS [$\frac{n}{sec}$]
1.00E-11	5.876E+04	9.00E-11	5.288E-06
1.00E-10	2.395E+04	4.00E-10	9.580E-06
5.00E-10	1.563E+04	2.50E-10	3.908E-06
7.50E-10	1.363E+04	2.50E-10	3.408E-06
1.00E-09	1.184E+04	2.00E-10	2.368E-06
1.20E-09	1.111E+04	3.00E-10	3.333E-06
1.50E-09	9.771E+03	5.00E-10	4.886E-06
2.00E-09	8.819E+03	5.00E-10	4.410E-06
2.50E-09	8.033E+03	5.00E-10	4.017E-06
3.00E-09	7.354E+03	1.00E-09	7.354E-06
4.00E-09	6.644E+03	1.00E-09	6.644E-06
5.00E-09	6.002E+03	2.50E-09	1.501E-05
7.50E-09	5.432E+03	2.50E-09	1.358E-05
1.00E-08	4.818E+03	1.53E-08	7.372E-05
2.53E-08	4.621E+03	4.70E-09	2.172E-05
3.00E-08	4.683E+03	1.00E-08	4.683E-05
4.00E-08	4.779E+03	1.00E-08	4.779E-05
5.00E-08	4.939E+03	1.00E-08	4.939E-05
6.00E-08	5.077E+03	1.00E-08	5.077E-05
7.00E-08	5.242E+03	1.00E-08	5.242E-05
8.00E-08	5.403E+03	1.00E-08	5.403E-05
9.00E-08	5.558E+03	1.00E-08	5.558E-05
1.00E-07	5.854E+03	2.50E-08	1.464E-04
1.25E-07	6.233E+03	2.50E-08	1.558E-04

Continued on following page

E [MeV]	$\frac{dS}{dE} \left[\frac{n}{MeV \cdot sec} \right]$	dE	dS $\left[\frac{n}{sec} \right]$
1.50E-07	7.072E+03	2.50E-08	1.768E-04
1.75E-07	7.527E+03	2.50E-08	1.882E-04
2.00E-07	7.844E+03	2.50E-08	1.961E-04
2.25E-07	8.189E+03	2.50E-08	2.047E-04
2.50E-07	8.493E+03	2.50E-08	2.123E-04
2.75E-07	8.783E+03	2.50E-08	2.196E-04
3.00E-07	9.074E+03	2.50E-08	2.269E-04
3.25E-07	9.381E+03	2.50E-08	2.345E-04
3.50E-07	9.644E+03	2.50E-08	2.411E-04
3.75E-07	9.892E+03	2.50E-08	2.473E-04
4.00E-07	1.028E+04	5.00E-08	5.140E-04
4.50E-07	1.079E+04	5.00E-08	5.395E-04
5.00E-07	1.125E+04	5.00E-08	5.625E-04
5.50E-07	1.171E+04	5.00E-08	5.855E-04
6.00E-07	1.203E+04	2.50E-08	3.008E-04
6.25E-07	1.222E+04	2.50E-08	3.055E-04
6.50E-07	1.255E+04	5.00E-08	6.275E-04
7.00E-07	1.293E+04	5.00E-08	6.465E-04
7.50E-07	1.335E+04	5.00E-08	6.675E-04
8.00E-07	1.372E+04	5.00E-08	6.860E-04
8.50E-07	1.407E+04	5.00E-08	7.035E-04
9.00E-07	1.440E+04	2.50E-08	3.600E-04
9.25E-07	1.446E+04	2.50E-08	3.615E-04
9.50E-07	1.476E+04	2.50E-08	3.690E-04
9.75E-07	1.487E+04	2.50E-08	3.718E-04
1.00E-06	1.512E+04	1.00E-08	1.512E-04
1.01E-06	1.493E+04	1.00E-08	1.493E-04
1.02E-06	1.523E+04	1.00E-08	1.523E-04
1.03E-06	1.504E+04	1.00E-08	1.504E-04
1.04E-06	1.551E+04	1.00E-08	1.551E-04
1.05E-06	1.514E+04	1.00E-08	1.514E-04
1.06E-06	1.545E+04	1.00E-08	1.545E-04
1.07E-06	1.542E+04	1.00E-08	1.542E-04
1.08E-06	1.555E+04	1.00E-08	1.555E-04
1.09E-06	1.568E+04	1.00E-08	1.568E-04
1.10E-06	1.564E+04	1.00E-08	1.564E-04
1.11E-06	1.577E+04	1.00E-08	1.577E-04
1.12E-06	1.730E+04	1.00E-08	1.730E-04
1.13E-06	1.744E+04	1.00E-08	1.744E-04
1.14E-06	1.760E+04	1.00E-08	1.760E-04
1.15E-06	2.121E+04	2.50E-08	5.302E-04
1.18E-06	4.617E+05	2.50E-08	1.154E-02

Continued on following page

E [MeV]	$\frac{dS}{dE} \left[\frac{n}{MeV \cdot sec} \right]$	dE	dS $\left[\frac{n}{sec} \right]$
1.20E-06	4.621E+05	2.50E-08	1.155E-02
1.23E-06	4.647E+05	2.50E-08	1.162E-02
1.25E-06	7.474E+05	5.00E-08	3.737E-02
1.30E-06	4.886E+05	5.00E-08	2.443E-02
1.35E-06	4.993E+05	5.00E-08	2.497E-02
1.40E-06	2.202E+05	5.00E-08	1.101E-02
1.45E-06	5.121E+05	5.00E-08	2.561E-02
1.50E-06	5.231E+05	9.00E-08	4.708E-02
1.59E-06	7.110E+05	9.00E-08	6.399E-02
1.68E-06	5.581E+05	9.00E-08	5.023E-02
1.77E-06	3.919E+05	9.00E-08	3.527E-02
1.86E-06	7.866E+05	8.00E-08	6.293E-02
1.94E-06	5.980E+05	6.00E-08	3.588E-02
2.00E-06	6.082E+05	1.20E-07	7.298E-02
2.12E-06	6.247E+05	9.00E-08	5.622E-02
2.21E-06	4.378E+05	9.00E-08	3.940E-02
2.30E-06	6.454E+05	8.00E-08	5.163E-02
2.38E-06	8.631E+05	9.00E-08	7.768E-02
2.47E-06	4.823E+05	1.00E-07	4.823E-02
2.57E-06	8.768E+05	1.00E-07	8.768E-02
2.67E-06	7.002E+05	1.00E-07	7.002E-02
2.77E-06	7.118E+05	1.00E-07	7.118E-02
2.87E-06	7.239E+05	1.00E-07	7.239E-02
2.97E-06	4.869E+04	3.00E-08	1.461E-03
3.00E-06	1.147E+06	5.00E-08	5.735E-02
3.05E-06	5.372E+05	1.00E-07	5.372E-02
3.15E-06	8.325E+05	3.50E-07	2.914E-01
3.50E-06	7.066E+05	2.30E-07	1.625E-01
3.73E-06	9.173E+05	2.70E-07	2.477E-01
4.00E-06	8.513E+05	7.50E-07	6.385E-01
4.75E-06	9.320E+05	2.50E-07	2.330E-01
5.00E-06	1.032E+06	4.00E-07	4.128E-01
5.40E-06	1.011E+06	6.00E-07	6.066E-01
6.00E-06	9.284E+05	2.50E-07	2.321E-01
6.25E-06	1.188E+06	2.50E-07	2.970E-01
6.50E-06	1.088E+06	2.50E-07	2.720E-01
6.75E-06	1.109E+06	2.50E-07	2.773E-01
7.00E-06	1.127E+06	1.50E-07	1.691E-01
7.15E-06	1.169E+06	9.50E-07	1.111E+00
8.10E-06	1.205E+06	1.00E-06	1.205E+00
9.10E-06	1.347E+06	9.00E-07	1.212E+00
1.00E-05	1.387E+06	1.50E-06	2.081E+00

Continued on following page

E [MeV]	$\frac{dS}{dE} \left[\frac{n}{MeV \cdot sec} \right]$	dE	dS $\left[\frac{n}{sec} \right]$
1.15E-05	1.447E+06	4.00E-07	5.788E-01
1.19E-05	1.489E+06	1.00E-06	1.489E+00
1.29E-05	1.544E+06	8.50E-07	1.312E+00
1.38E-05	1.517E+06	6.50E-07	9.860E-01
1.44E-05	1.690E+06	7.00E-07	1.183E+00
1.51E-05	1.616E+06	9.00E-07	1.454E+00
1.60E-05	1.717E+06	1.00E-06	1.717E+00
1.70E-05	1.781E+06	1.50E-06	2.672E+00
1.85E-05	1.830E+06	5.00E-07	9.150E-01
1.90E-05	1.867E+06	1.00E-06	1.867E+00
2.00E-05	1.968E+06	1.00E-06	1.968E+00
2.10E-05	1.972E+06	1.50E-06	2.958E+00
2.25E-05	2.044E+06	2.50E-06	5.110E+00
2.50E-05	2.200E+06	2.50E-06	5.500E+00
2.75E-05	2.278E+06	2.50E-06	5.695E+00
3.00E-05	2.296E+06	1.25E-06	2.870E+00
3.13E-05	2.518E+06	5.00E-07	1.259E+00
3.18E-05	2.420E+06	1.50E-06	3.630E+00
3.33E-05	2.457E+06	5.00E-07	1.229E+00
3.38E-05	2.482E+06	8.50E-07	2.110E+00
3.46E-05	2.435E+06	9.00E-07	2.192E+00
3.55E-05	2.555E+06	1.50E-06	3.832E+00
3.70E-05	2.598E+06	1.00E-06	2.598E+00
3.80E-05	2.634E+06	1.10E-06	2.897E+00
3.91E-05	2.813E+06	5.00E-07	1.407E+00
3.96E-05	2.697E+06	1.40E-06	3.776E+00
4.10E-05	2.755E+06	1.40E-06	3.857E+00
4.24E-05	2.803E+06	1.60E-06	4.485E+00
4.40E-05	2.784E+06	1.20E-06	3.341E+00
4.52E-05	2.896E+06	1.80E-06	5.213E+00
4.70E-05	2.948E+06	1.30E-06	3.832E+00
4.83E-05	2.981E+06	9.00E-07	2.683E+00
4.92E-05	3.077E+06	1.40E-06	4.308E+00
5.06E-05	2.996E+06	1.40E-06	4.194E+00
5.20E-05	3.099E+06	1.40E-06	4.339E+00
5.34E-05	3.198E+06	5.60E-06	1.791E+01
5.90E-05	3.304E+06	2.00E-06	6.608E+00
6.10E-05	3.409E+06	4.00E-06	1.364E+01
6.50E-05	3.432E+06	2.50E-06	8.580E+00
6.75E-05	3.583E+06	4.50E-06	1.612E+01
7.20E-05	3.642E+06	4.00E-06	1.457E+01
7.60E-05	3.764E+06	4.00E-06	1.506E+01

Continued on following page

E [MeV]	$\frac{dS}{dE} \left[\frac{n}{MeV \cdot sec} \right]$	dE	dS $\left[\frac{n}{sec} \right]$
8.00E-05	3.838E+06	2.00E-06	7.676E+00
8.20E-05	3.954E+06	8.00E-06	3.163E+01
9.00E-05	4.154E+06	1.00E-05	4.154E+01
1.00E-04	4.345E+06	8.00E-06	3.476E+01
1.08E-04	4.499E+06	7.00E-06	3.149E+01
1.15E-04	4.607E+06	4.00E-06	1.843E+01
1.19E-04	4.718E+06	3.00E-06	1.415E+01
1.22E-04	5.273E+06	6.40E-05	3.375E+02
1.86E-04	5.828E+06	6.50E-06	3.788E+01
1.93E-04	6.028E+06	1.50E-05	9.042E+01
2.08E-04	6.082E+06	2.50E-06	1.521E+01
2.10E-04	6.381E+06	3.00E-05	1.914E+02
2.40E-04	6.894E+06	4.50E-05	3.102E+02
2.85E-04	7.316E+06	2.00E-05	1.463E+02
3.05E-04	8.768E+06	2.45E-04	2.148E+03
5.50E-04	1.050E+07	1.20E-04	1.260E+03
6.70E-04	1.104E+07	1.30E-05	1.435E+02
6.83E-04	1.213E+07	2.67E-04	3.239E+03
9.50E-04	1.378E+07	2.00E-04	2.756E+03
1.15E-03	1.547E+07	3.50E-04	5.415E+03
1.50E-03	1.662E+07	5.00E-05	8.310E+02
1.55E-03	1.741E+07	2.50E-04	4.353E+03
1.80E-03	1.900E+07	4.00E-04	7.600E+03
2.20E-03	2.013E+07	9.00E-05	1.812E+03
2.29E-03	2.096E+07	2.90E-04	6.078E+03
2.58E-03	2.243E+07	4.20E-04	9.421E+03
3.00E-03	2.465E+07	7.40E-04	1.824E+04
3.74E-03	2.624E+07	1.60E-04	4.198E+03
3.90E-03	2.983E+07	2.10E-03	6.264E+04
6.00E-03	3.551E+07	2.03E-03	7.209E+04
8.03E-03	3.968E+07	1.47E-03	5.833E+04
9.50E-03	4.488E+07	3.50E-03	1.571E+05
1.30E-02	5.176E+07	4.00E-03	2.070E+05
1.70E-02	6.103E+07	8.00E-03	4.882E+05
2.50E-02	6.970E+07	5.00E-03	3.485E+05
3.00E-02	8.087E+07	1.50E-02	1.213E+06
4.50E-02	9.070E+07	5.00E-03	4.535E+05
5.00E-02	9.382E+07	2.00E-03	1.876E+05
5.20E-02	9.803E+07	8.00E-03	7.842E+05
6.00E-02	1.062E+08	1.30E-02	1.381E+06
7.30E-02	1.117E+08	2.00E-03	2.234E+05
7.50E-02	1.148E+08	7.00E-03	8.036E+05

Continued on following page

E [MeV]	$\frac{dS}{dE} \left[\frac{n}{MeV \cdot sec} \right]$	dE	dS $\left[\frac{n}{sec} \right]$
8.20E-02	1.181E+08	3.00E-03	3.543E+05
8.50E-02	1.237E+08	1.50E-02	1.856E+06
1.00E-01	1.359E+08	2.83E-02	3.846E+06
1.28E-01	1.482E+08	2.17E-02	3.216E+06
1.50E-01	1.630E+08	5.00E-02	8.150E+06
2.00E-01	1.829E+08	7.00E-02	1.280E+07
2.70E-01	1.997E+08	6.00E-02	1.198E+07
3.30E-01	2.127E+08	7.00E-02	1.489E+07
4.00E-01	2.202E+08	2.00E-02	4.404E+06
4.20E-01	2.231E+08	2.00E-02	4.462E+06
4.40E-01	2.264E+08	3.00E-02	6.792E+06
4.70E-01	2.299E+08	2.95E-02	6.782E+06
5.00E-01	2.339E+08	5.05E-02	1.181E+07
5.50E-01	2.370E+08	2.30E-02	5.451E+06
5.73E-01	2.389E+08	2.70E-02	6.450E+06
6.00E-01	2.417E+08	7.00E-02	1.692E+07
6.70E-01	2.437E+08	9.00E-03	2.193E+06
6.79E-01	2.451E+08	7.10E-02	1.740E+07
7.50E-01	2.467E+08	7.00E-02	1.727E+07
8.20E-01	2.471E+08	4.11E-02	1.016E+07
8.61E-01	2.471E+08	1.39E-02	3.435E+06
8.75E-01	2.470E+08	2.50E-02	6.175E+06
9.00E-01	2.468E+08	2.00E-02	4.936E+06
9.20E-01	2.460E+08	9.00E-02	2.214E+07
1.01E+00	2.437E+08	9.00E-02	2.193E+07
1.10E+00	2.403E+08	1.00E-01	2.403E+07
1.20E+00	2.370E+08	5.00E-02	1.185E+07
1.25E+00	2.341E+08	6.70E-02	1.568E+07
1.32E+00	2.312E+08	3.90E-02	9.017E+06
1.36E+00	2.289E+08	4.40E-02	1.007E+07
1.40E+00	2.246E+08	1.00E-01	2.246E+07
1.50E+00	2.097E+08	3.50E-01	7.340E+07
1.85E+00	1.795E+08	5.04E-01	9.047E+07
2.35E+00	1.569E+08	1.25E-01	1.961E+07
2.48E+00	1.343E+08	5.21E-01	6.997E+07
3.00E+00	8.061E+07	1.30E+00	1.051E+08
4.30E+00	4.347E+07	4.96E-01	2.156E+07
4.80E+00	2.195E+07	1.63E+00	3.587E+07
6.43E+00	6.495E+06	1.75E+00	1.139E+07
8.19E+00	1.662E+06	1.81E+00	3.013E+06
1.00E+01			

Table C.9: ORIGEN-ARP photon results for a Westinghouse 17×17 PWR assembly burned to $57.535 \frac{MWd}{kg}$ and cooled for a combined time period of 45yr.

E [MeV]	$\frac{dS}{dE} [\frac{p}{MeV \cdot sec}]$	dE	dS [$\frac{p}{sec}$]
1.00E-02	5.26E+16	1.00E-02	5.256E+14
2.00E-02	2.32E+16	1.00E-02	2.317E+14
3.00E-02	2.14E+16	1.50E-02	3.212E+14
4.50E-02	1.42E+16	1.50E-02	2.129E+14
6.00E-02	6.09E+15	1.00E-02	6.086E+13
7.00E-02	5.64E+15	5.00E-03	2.819E+13
7.50E-02	4.05E+15	2.50E-02	1.013E+14
1.00E-01	2.16E+15	5.00E-02	1.078E+14
1.50E-01	1.31E+15	5.00E-02	6.560E+13
2.00E-01	6.05E+14	6.00E-02	3.627E+13
2.60E-01	4.23E+14	4.00E-02	1.692E+13
3.00E-01	3.57E+14	1.00E-01	3.573E+13
4.00E-01	2.12E+14	5.00E-02	1.058E+13
4.50E-01	1.70E+14	6.00E-02	1.018E+13
5.10E-01	3.09E+13	2.00E-03	6.174E+10
5.12E-01	6.07E+13	8.80E-02	5.339E+12
6.00E-01	2.04E+16	1.00E-01	2.044E+15
7.00E-01	7.37E+13	1.00E-01	7.367E+12
8.00E-01	4.63E+13	1.00E-01	4.625E+12
9.00E-01	4.63E+13	1.00E-01	4.625E+12
1.00E+00	1.59E+13	2.00E-01	3.182E+12
1.20E+00	4.19E+13	1.30E-01	5.442E+12
1.33E+00	2.54E+12	1.10E-01	2.791E+11
1.44E+00	2.90E+12	6.00E-02	1.741E+11
1.50E+00	1.23E+12	7.00E-02	8.617E+10
1.57E+00	3.60E+12	9.00E-02	3.242E+11
1.66E+00	4.58E+11	1.40E-01	6.409E+10
1.80E+00	1.45E+11	2.00E-01	2.892E+10
2.00E+00	3.31E+10	1.50E-01	4.968E+09
2.15E+00	6.10E+08	2.00E-01	1.219E+08
2.35E+00	1.26E+08	1.50E-01	1.884E+07
2.50E+00	2.13E+09	2.50E-01	5.333E+08
2.75E+00	1.15E+08	2.50E-01	2.865E+07
3.00E+00	6.95E+07	5.00E-01	3.476E+07
3.50E+00	4.03E+07	5.00E-01	2.015E+07
4.00E+00	2.33E+07	5.00E-01	1.167E+07
4.50E+00	1.35E+07	5.00E-01	6.765E+06
5.00E+00	7.85E+06	5.00E-01	3.923E+06
5.50E+00	4.55E+06	5.00E-01	2.274E+06

Continued on following page

E [MeV]	$\frac{dS}{dE} [\frac{p}{MeVsec}]$	dE	dS [$\frac{p}{sec}$]
6.00E+00	2.64E+06	5.00E-01	1.319E+06
6.50E+00	1.53E+06	5.00E-01	7.645E+05
7.00E+00	8.86E+05	5.00E-01	4.432E+05
7.50E+00	5.14E+05	5.00E-01	2.570E+05
8.00E+00	1.52E+05	2.00E+00	3.034E+05
1.00E+01			

Table C.10: ORIGEN-ARP photon results for a Westinghouse 17×17 PWR assembly burned to $57.535 \frac{MWd}{kg}$ and cooled for a combined time period of 45yr.

E [MeV]	$\frac{dS}{dE} [\frac{n}{MeVsec}]$	dE	dS [$\frac{n}{sec}$]
1.00E-11	5.868E+04	9.00E-11	5.281E-06
1.00E-10	2.392E+04	4.00E-10	9.568E-06
5.00E-10	1.560E+04	2.50E-10	3.900E-06
7.50E-10	1.361E+04	2.50E-10	3.403E-06
1.00E-09	1.182E+04	2.00E-10	2.364E-06
1.20E-09	1.109E+04	3.00E-10	3.327E-06
1.50E-09	9.757E+03	5.00E-10	4.879E-06
2.00E-09	8.806E+03	5.00E-10	4.403E-06
2.50E-09	8.021E+03	5.00E-10	4.011E-06
3.00E-09	7.343E+03	1.00E-09	7.343E-06
4.00E-09	6.634E+03	1.00E-09	6.634E-06
5.00E-09	5.993E+03	2.50E-09	1.498E-05
7.50E-09	5.424E+03	2.50E-09	1.356E-05
1.00E-08	4.811E+03	1.53E-08	7.361E-05
2.53E-08	4.614E+03	4.70E-09	2.169E-05
3.00E-08	4.676E+03	1.00E-08	4.676E-05
4.00E-08	4.772E+03	1.00E-08	4.772E-05
5.00E-08	4.932E+03	1.00E-08	4.932E-05
6.00E-08	5.070E+03	1.00E-08	5.070E-05
7.00E-08	5.235E+03	1.00E-08	5.235E-05
8.00E-08	5.395E+03	1.00E-08	5.395E-05
9.00E-08	5.550E+03	1.00E-08	5.550E-05
1.00E-07	5.845E+03	2.50E-08	1.461E-04
1.25E-07	6.224E+03	2.50E-08	1.556E-04
1.50E-07	7.062E+03	2.50E-08	1.766E-04
1.75E-07	7.517E+03	2.50E-08	1.879E-04
2.00E-07	7.833E+03	2.50E-08	1.958E-04
2.25E-07	8.178E+03	2.50E-08	2.045E-04
2.50E-07	8.481E+03	2.50E-08	2.120E-04

Continued on following page

E [MeV]	$\frac{dS}{dE} \left[\frac{n}{MeV \cdot sec} \right]$	dE	dS $\left[\frac{n}{sec} \right]$
2.75E-07	8.771E+03	2.50E-08	2.193E-04
3.00E-07	9.061E+03	2.50E-08	2.265E-04
3.25E-07	9.368E+03	2.50E-08	2.342E-04
3.50E-07	9.631E+03	2.50E-08	2.408E-04
3.75E-07	9.878E+03	2.50E-08	2.470E-04
4.00E-07	1.026E+04	5.00E-08	5.130E-04
4.50E-07	1.077E+04	5.00E-08	5.385E-04
5.00E-07	1.123E+04	5.00E-08	5.615E-04
5.50E-07	1.169E+04	5.00E-08	5.845E-04
6.00E-07	1.201E+04	2.50E-08	3.003E-04
6.25E-07	1.221E+04	2.50E-08	3.053E-04
6.50E-07	1.253E+04	5.00E-08	6.265E-04
7.00E-07	1.291E+04	5.00E-08	6.455E-04
7.50E-07	1.333E+04	5.00E-08	6.665E-04
8.00E-07	1.370E+04	5.00E-08	6.850E-04
8.50E-07	1.405E+04	5.00E-08	7.025E-04
9.00E-07	1.438E+04	2.50E-08	3.595E-04
9.25E-07	1.444E+04	2.50E-08	3.610E-04
9.50E-07	1.474E+04	2.50E-08	3.685E-04
9.75E-07	1.485E+04	2.50E-08	3.713E-04
1.00E-06	1.510E+04	1.00E-08	1.510E-04
1.01E-06	1.491E+04	1.00E-08	1.491E-04
1.02E-06	1.521E+04	1.00E-08	1.521E-04
1.03E-06	1.502E+04	1.00E-08	1.502E-04
1.04E-06	1.549E+04	1.00E-08	1.549E-04
1.05E-06	1.512E+04	1.00E-08	1.512E-04
1.06E-06	1.542E+04	1.00E-08	1.542E-04
1.07E-06	1.539E+04	1.00E-08	1.539E-04
1.08E-06	1.552E+04	1.00E-08	1.552E-04
1.09E-06	1.566E+04	1.00E-08	1.566E-04
1.10E-06	1.561E+04	1.00E-08	1.561E-04
1.11E-06	1.575E+04	1.00E-08	1.575E-04
1.12E-06	1.727E+04	1.00E-08	1.727E-04
1.13E-06	1.742E+04	1.00E-08	1.742E-04
1.14E-06	1.758E+04	1.00E-08	1.758E-04
1.15E-06	2.110E+04	2.50E-08	5.275E-04
1.18E-06	3.222E+05	2.50E-08	8.055E-03
1.20E-06	3.219E+05	2.50E-08	8.047E-03
1.23E-06	3.229E+05	2.50E-08	8.073E-03
1.25E-06	5.170E+05	5.00E-08	2.585E-02
1.30E-06	3.401E+05	5.00E-08	1.701E-02
1.35E-06	3.476E+05	5.00E-08	1.738E-02

Continued on following page

E [MeV]	$\frac{dS}{dE} \left[\frac{n}{MeV \cdot sec} \right]$	dE	dS $\left[\frac{n}{sec} \right]$
1.40E-06	1.570E+05	5.00E-08	7.850E-03
1.45E-06	3.566E+05	5.00E-08	1.783E-02
1.50E-06	3.643E+05	9.00E-08	3.279E-02
1.59E-06	4.928E+05	9.00E-08	4.435E-02
1.68E-06	3.886E+05	9.00E-08	3.497E-02
1.77E-06	2.754E+05	9.00E-08	2.479E-02
1.86E-06	5.444E+05	8.00E-08	4.355E-02
1.94E-06	4.167E+05	6.00E-08	2.500E-02
2.00E-06	4.232E+05	1.20E-07	5.078E-02
2.12E-06	4.350E+05	9.00E-08	3.915E-02
2.21E-06	3.076E+05	9.00E-08	2.768E-02
2.30E-06	4.493E+05	8.00E-08	3.594E-02
2.38E-06	5.980E+05	9.00E-08	5.382E-02
2.47E-06	3.381E+05	1.00E-07	3.381E-02
2.57E-06	6.077E+05	1.00E-07	6.077E-02
2.67E-06	4.874E+05	1.00E-07	4.874E-02
2.77E-06	4.957E+05	1.00E-07	4.957E-02
2.87E-06	5.036E+05	1.00E-07	5.036E-02
2.97E-06	4.359E+04	3.00E-08	1.308E-03
3.00E-06	7.922E+05	5.00E-08	3.961E-02
3.05E-06	3.769E+05	1.00E-07	3.769E-02
3.15E-06	5.786E+05	3.50E-07	2.025E-01
3.50E-06	4.934E+05	2.30E-07	1.135E-01
3.73E-06	6.372E+05	2.70E-07	1.720E-01
4.00E-06	5.930E+05	7.50E-07	4.448E-01
4.75E-06	6.486E+05	2.50E-07	1.622E-01
5.00E-06	7.173E+05	4.00E-07	2.869E-01
5.40E-06	7.036E+05	6.00E-07	4.222E-01
6.00E-06	6.478E+05	2.50E-07	1.620E-01
6.25E-06	8.249E+05	2.50E-07	2.062E-01
6.50E-06	7.575E+05	2.50E-07	1.894E-01
6.75E-06	7.717E+05	2.50E-07	1.929E-01
7.00E-06	7.847E+05	1.50E-07	1.177E-01
7.15E-06	8.133E+05	9.50E-07	7.726E-01
8.10E-06	8.388E+05	1.00E-06	8.388E-01
9.10E-06	9.369E+05	9.00E-07	8.432E-01
1.00E-05	9.649E+05	1.50E-06	1.447E+00
1.15E-05	1.007E+06	4.00E-07	4.028E-01
1.19E-05	1.036E+06	1.00E-06	1.036E+00
1.29E-05	1.074E+06	8.50E-07	9.129E-01
1.38E-05	1.057E+06	6.50E-07	6.870E-01
1.44E-05	1.175E+06	7.00E-07	8.225E-01

Continued on following page

E [MeV]	$\frac{dS}{dE} \left[\frac{n}{MeV \cdot sec} \right]$	dE	dS $\left[\frac{n}{sec} \right]$
1.51E-05	1.125E+06	9.00E-07	1.013E+00
1.60E-05	1.195E+06	1.00E-06	1.195E+00
1.70E-05	1.239E+06	1.50E-06	1.859E+00
1.85E-05	1.273E+06	5.00E-07	6.365E-01
1.90E-05	1.299E+06	1.00E-06	1.299E+00
2.00E-05	1.369E+06	1.00E-06	1.369E+00
2.10E-05	1.372E+06	1.50E-06	2.058E+00
2.25E-05	1.422E+06	2.50E-06	3.555E+00
2.50E-05	1.530E+06	2.50E-06	3.825E+00
2.75E-05	1.585E+06	2.50E-06	3.963E+00
3.00E-05	1.598E+06	1.25E-06	1.998E+00
3.13E-05	1.750E+06	5.00E-07	8.750E-01
3.18E-05	1.684E+06	1.50E-06	2.526E+00
3.33E-05	1.710E+06	5.00E-07	8.550E-01
3.38E-05	1.727E+06	8.50E-07	1.468E+00
3.46E-05	1.696E+06	9.00E-07	1.526E+00
3.55E-05	1.778E+06	1.50E-06	2.667E+00
3.70E-05	1.808E+06	1.00E-06	1.808E+00
3.80E-05	1.833E+06	1.10E-06	2.016E+00
3.91E-05	1.955E+06	5.00E-07	9.775E-01
3.96E-05	1.877E+06	1.40E-06	2.628E+00
4.10E-05	1.922E+06	1.40E-06	2.691E+00
4.24E-05	1.955E+06	1.60E-06	3.128E+00
4.40E-05	1.943E+06	1.20E-06	2.332E+00
4.52E-05	2.020E+06	1.80E-06	3.636E+00
4.70E-05	2.058E+06	1.30E-06	2.675E+00
4.83E-05	2.081E+06	9.00E-07	1.873E+00
4.92E-05	2.147E+06	1.40E-06	3.006E+00
5.06E-05	2.092E+06	1.40E-06	2.929E+00
5.20E-05	2.163E+06	1.40E-06	3.028E+00
5.34E-05	2.232E+06	5.60E-06	1.250E+01
5.90E-05	2.306E+06	2.00E-06	4.612E+00
6.10E-05	2.378E+06	4.00E-06	9.512E+00
6.50E-05	2.395E+06	2.50E-06	5.988E+00
6.75E-05	2.499E+06	4.50E-06	1.125E+01
7.20E-05	2.541E+06	4.00E-06	1.016E+01
7.60E-05	2.626E+06	4.00E-06	1.050E+01
8.00E-05	2.678E+06	2.00E-06	5.356E+00
8.20E-05	2.759E+06	8.00E-06	2.207E+01
9.00E-05	2.898E+06	1.00E-05	2.898E+01
1.00E-04	3.031E+06	8.00E-06	2.425E+01
1.08E-04	3.138E+06	7.00E-06	2.197E+01

Continued on following page

E [MeV]	$\frac{dS}{dE} [\frac{n}{MeVsec}]$	dE	dS [$\frac{n}{sec}$]
1.15E-04	3.214E+06	4.00E-06	1.286E+01
1.19E-04	3.290E+06	3.00E-06	9.870E+00
1.22E-04	3.677E+06	6.40E-05	2.353E+02
1.86E-04	4.063E+06	6.50E-06	2.641E+01
1.93E-04	4.202E+06	1.50E-05	6.303E+01
2.08E-04	4.242E+06	2.50E-06	1.061E+01
2.10E-04	4.449E+06	3.00E-05	1.335E+02
2.40E-04	4.808E+06	4.50E-05	2.164E+02
2.85E-04	5.102E+06	2.00E-05	1.020E+02
3.05E-04	6.113E+06	2.45E-04	1.498E+03
5.50E-04	7.318E+06	1.20E-04	8.782E+02
6.70E-04	7.692E+06	1.30E-05	1.000E+02
6.83E-04	8.455E+06	2.67E-04	2.257E+03
9.50E-04	9.608E+06	2.00E-04	1.922E+03
1.15E-03	1.079E+07	3.50E-04	3.777E+03
1.50E-03	1.159E+07	5.00E-05	5.795E+02
1.55E-03	1.214E+07	2.50E-04	3.035E+03
1.80E-03	1.325E+07	4.00E-04	5.300E+03
2.20E-03	1.403E+07	9.00E-05	1.263E+03
2.29E-03	1.461E+07	2.90E-04	4.237E+03
2.58E-03	1.564E+07	4.20E-04	6.569E+03
3.00E-03	1.718E+07	7.40E-04	1.271E+04
3.74E-03	1.830E+07	1.60E-04	2.928E+03
3.90E-03	2.080E+07	2.10E-03	4.368E+04
6.00E-03	2.476E+07	2.03E-03	5.026E+04
8.03E-03	2.767E+07	1.47E-03	4.067E+04
9.50E-03	3.130E+07	3.50E-03	1.096E+05
1.30E-02	3.610E+07	4.00E-03	1.444E+05
1.70E-02	4.256E+07	8.00E-03	3.405E+05
2.50E-02	4.862E+07	5.00E-03	2.431E+05
3.00E-02	5.640E+07	1.50E-02	8.460E+05
4.50E-02	6.325E+07	5.00E-03	3.163E+05
5.00E-02	6.542E+07	2.00E-03	1.308E+05
5.20E-02	6.836E+07	8.00E-03	5.469E+05
6.00E-02	7.406E+07	1.30E-02	9.628E+05
7.30E-02	7.787E+07	2.00E-03	1.557E+05
7.50E-02	8.001E+07	7.00E-03	5.601E+05
8.20E-02	8.233E+07	3.00E-03	2.470E+05
8.50E-02	8.624E+07	1.50E-02	1.294E+06
1.00E-01	9.473E+07	2.83E-02	2.681E+06
1.28E-01	1.033E+08	2.17E-02	2.242E+06
1.50E-01	1.136E+08	5.00E-02	5.680E+06

Continued on following page

E [MeV]	$\frac{dS}{dE} [\frac{n}{MeVsec}]$	dE	dS [$\frac{n}{sec}$]
2.00E-01	1.275E+08	7.00E-02	8.925E+06
2.70E-01	1.392E+08	6.00E-02	8.352E+06
3.30E-01	1.483E+08	7.00E-02	1.038E+07
4.00E-01	1.535E+08	2.00E-02	3.070E+06
4.20E-01	1.555E+08	2.00E-02	3.110E+06
4.40E-01	1.578E+08	3.00E-02	4.734E+06
4.70E-01	1.602E+08	2.95E-02	4.726E+06
5.00E-01	1.630E+08	5.05E-02	8.232E+06
5.50E-01	1.652E+08	2.30E-02	3.800E+06
5.73E-01	1.665E+08	2.70E-02	4.496E+06
6.00E-01	1.684E+08	7.00E-02	1.179E+07
6.70E-01	1.698E+08	9.00E-03	1.528E+06
6.79E-01	1.708E+08	7.10E-02	1.213E+07
7.50E-01	1.719E+08	7.00E-02	1.203E+07
8.20E-01	1.722E+08	4.11E-02	7.077E+06
8.61E-01	1.722E+08	1.39E-02	2.394E+06
8.75E-01	1.721E+08	2.50E-02	4.303E+06
9.00E-01	1.720E+08	2.00E-02	3.440E+06
9.20E-01	1.714E+08	9.00E-02	1.543E+07
1.01E+00	1.699E+08	9.00E-02	1.529E+07
1.10E+00	1.675E+08	1.00E-01	1.675E+07
1.20E+00	1.653E+08	5.00E-02	8.265E+06
1.25E+00	1.633E+08	6.70E-02	1.094E+07
1.32E+00	1.613E+08	3.90E-02	6.291E+06
1.36E+00	1.597E+08	4.40E-02	7.027E+06
1.40E+00	1.568E+08	1.00E-01	1.568E+07
1.50E+00	1.466E+08	3.50E-01	5.131E+07
1.85E+00	1.259E+08	5.04E-01	6.345E+07
2.35E+00	1.104E+08	1.25E-01	1.380E+07
2.48E+00	9.463E+07	5.21E-01	4.930E+07
3.00E+00	5.653E+07	1.30E+00	7.372E+07
4.30E+00	3.020E+07	4.96E-01	1.498E+07
4.80E+00	1.523E+07	1.63E+00	2.489E+07
6.43E+00	4.504E+06	1.75E+00	7.896E+06
8.19E+00	1.151E+06	1.81E+00	2.087E+06
1.00E+01			

APPENDIX D

ORIGAMI PWR DATA

Table D.1: ORIGAMI photon results for a Westinghouse 17×17 PWR assembly burned to $57.535 \frac{MWd}{kg}$ and cooled for a combined time period of 5yr.

E [eV]	dS [$\frac{p}{sec}$]	dE [eV]	Bin Mid. E [MeV]	$\frac{dS}{dE}$ [$\frac{p}{MeV sec}$]
1.00E+04	1.125E+14	1.00E+04	1.50E-02	1.13E+16
2.00E+04	6.421E+13	1.00E+04	2.50E-02	6.42E+15
3.00E+04	8.020E+13	1.50E+04	3.75E-02	5.35E+15
4.50E+04	3.564E+13	1.50E+04	5.25E-02	2.38E+15
6.00E+04	1.535E+13	1.00E+04	6.50E-02	1.53E+15
7.00E+04	6.670E+12	5.00E+03	7.25E-02	1.33E+15
7.50E+04	2.868E+13	2.50E+04	8.75E-02	1.15E+15
1.00E+05	3.902E+13	5.00E+04	1.25E-01	7.80E+14
1.50E+05	1.793E+13	5.00E+04	1.75E-01	3.59E+14
2.00E+05	1.104E+13	6.00E+04	2.30E-01	1.84E+14
2.60E+05	4.422E+12	4.00E+04	2.80E-01	1.11E+14
3.00E+05	1.007E+13	1.00E+05	3.50E-01	1.01E+14
4.00E+05	6.201E+12	5.00E+04	4.25E-01	1.24E+14
4.50E+05	6.240E+12	6.00E+04	4.80E-01	1.04E+14
5.10E+05	1.105E+13	2.00E+03	5.11E-01	5.52E+15
5.12E+05	4.105E+13	8.80E+04	5.56E-01	4.66E+14
6.00E+05	5.001E+14	1.00E+05	6.50E-01	5.00E+15
7.00E+05	1.536E+14	1.00E+05	7.50E-01	1.54E+15
8.00E+05	1.068E+13	1.00E+05	8.50E-01	1.07E+14
9.00E+05	5.375E+12	1.00E+05	9.50E-01	5.37E+13
1.00E+06	8.181E+12	2.00E+05	1.10E+00	4.09E+13
1.20E+06	8.304E+12	1.30E+05	1.27E+00	6.39E+13
1.33E+06	4.741E+12	1.10E+05	1.39E+00	4.31E+13
1.44E+06	2.799E+11	6.00E+04	1.47E+00	4.67E+12
1.50E+06	1.577E+11	7.00E+04	1.54E+00	2.25E+12
1.57E+06	4.515E+11	9.00E+04	1.62E+00	5.02E+12
1.66E+06	8.394E+10	1.40E+05	1.73E+00	6.00E+11
1.80E+06	8.100E+10	2.00E+05	1.90E+00	4.05E+11

Continued on following page

E [eV]	dS [$\frac{p}{sec}$]	dE [eV]	Bin Mid. E [MeV]	$\frac{dS}{dE}$ [$\frac{p}{MeV sec}$]
2.00E+06	3.485E+10	1.50E+05	2.08E+00	2.32E+11
2.15E+06	1.604E+11	2.00E+05	2.25E+00	8.02E+11
2.35E+06	4.716E+10	1.50E+05	2.43E+00	3.14E+11
2.50E+06	6.466E+09	2.50E+05	2.63E+00	2.59E+10
2.75E+06	5.516E+09	2.50E+05	2.88E+00	2.21E+10
3.00E+06	1.201E+09	5.00E+05	3.25E+00	2.40E+09
3.50E+06	7.884E+06	5.00E+05	3.75E+00	1.58E+07
4.00E+06	4.154E+06	5.00E+05	4.25E+00	8.31E+06
4.50E+06	2.409E+06	5.00E+05	4.75E+00	4.82E+06
5.00E+06	1.397E+06	5.00E+05	5.25E+00	2.79E+06
5.50E+06	8.097E+05	5.00E+05	5.75E+00	1.62E+06
6.00E+06	4.695E+05	5.00E+05	6.25E+00	9.39E+05
6.50E+06	2.722E+05	5.00E+05	6.75E+00	5.44E+05
7.00E+06	1.578E+05	5.00E+05	7.25E+00	3.16E+05
7.50E+06	9.152E+04	5.00E+05	7.75E+00	1.83E+05
8.00E+06	1.081E+05	2.00E+06	9.00E+00	5.41E+04
1.00E+07				

Table D.2: ORIGAMI photon results for a Westinghouse 17×17 PWR assembly burned to $57.535 \frac{MWd}{kg}$ and cooled for a combined time period of 5yr.

E [eV]	dS [$\frac{n}{sec}$]	dE [eV]	Bin Mid. E [MeV]	$\frac{dS}{dE}$ [$\frac{n}{MeV sec}$]
1.00E-05	8.130E-08	9.00E-05	5.50E-11	9.03E+02
1.00E-04	7.024E-07	4.00E-04	3.00E-10	1.76E+03
5.00E-04	6.636E-07	2.50E-04	6.25E-10	2.65E+03
7.50E-04	7.563E-07	2.50E-04	8.75E-10	3.03E+03
1.00E-03	7.004E-07	2.00E-04	1.10E-09	3.50E+03
1.20E-03	1.156E-06	3.00E-04	1.35E-09	3.85E+03
1.50E-03	2.192E-06	5.00E-04	1.75E-09	4.38E+03
2.00E-03	2.491E-06	5.00E-04	2.25E-09	4.98E+03
2.50E-03	2.735E-06	5.00E-04	2.75E-09	5.47E+03
3.00E-03	6.192E-06	1.00E-03	3.50E-09	6.19E+03
4.00E-03	7.045E-06	1.00E-03	4.50E-09	7.05E+03
5.00E-03	2.066E-05	2.50E-03	6.25E-09	8.27E+03
7.50E-03	2.447E-05	2.50E-03	8.75E-09	9.79E+03
1.00E-02	2.112E-04	1.53E-02	1.77E-08	1.38E+04
2.53E-02	8.187E-05	4.70E-03	2.77E-08	1.74E+04
3.00E-02	1.958E-04	1.00E-02	3.50E-08	1.96E+04
4.00E-02	2.221E-04	1.00E-02	4.50E-08	2.22E+04
5.00E-02	2.456E-04	1.00E-02	5.50E-08	2.46E+04

Continued on following page

E [eV]	dS [$\frac{n}{sec}$]	dE [eV]	Bin Mid. E [MeV]	$\frac{dS}{dE}$ [$\frac{n}{MeV sec}$]
6.00E-02	2.670E-04	1.00E-02	6.50E-08	2.67E+04
7.00E-02	2.869E-04	1.00E-02	7.50E-08	2.87E+04
8.00E-02	3.054E-04	1.00E-02	8.50E-08	3.05E+04
9.00E-02	3.229E-04	1.00E-02	9.50E-08	3.23E+04
1.00E-01	8.781E-04	2.50E-02	1.13E-07	3.51E+04
1.25E-01	9.709E-04	2.50E-02	1.38E-07	3.88E+04
1.50E-01	1.056E-03	2.50E-02	1.63E-07	4.23E+04
1.75E-01	1.135E-03	2.50E-02	1.88E-07	4.54E+04
2.00E-01	1.208E-03	2.50E-02	2.13E-07	4.83E+04
2.25E-01	1.277E-03	2.50E-02	2.38E-07	5.11E+04
2.50E-01	1.343E-03	2.50E-02	2.63E-07	5.37E+04
2.75E-01	1.405E-03	2.50E-02	2.88E-07	5.62E+04
3.00E-01	1.465E-03	2.50E-02	3.13E-07	5.86E+04
3.25E-01	1.523E-03	2.50E-02	3.38E-07	6.09E+04
3.50E-01	1.578E-03	2.50E-02	3.63E-07	6.31E+04
3.75E-01	1.631E-03	2.50E-02	3.88E-07	6.53E+04
4.00E-01	3.416E-03	5.00E-02	4.25E-07	6.83E+04
4.50E-01	3.612E-03	5.00E-02	4.75E-07	7.22E+04
5.00E-01	3.797E-03	5.00E-02	5.25E-07	7.59E+04
5.50E-01	3.974E-03	5.00E-02	5.75E-07	7.95E+04
6.00E-01	2.051E-03	2.50E-02	6.13E-07	8.20E+04
6.25E-01	2.092E-03	2.50E-02	6.38E-07	8.37E+04
6.50E-01	4.305E-03	5.00E-02	6.75E-07	8.61E+04
7.00E-01	4.462E-03	5.00E-02	7.25E-07	8.92E+04
7.50E-01	4.613E-03	5.00E-02	7.75E-07	9.23E+04
8.00E-01	4.760E-03	5.00E-02	8.25E-07	9.52E+04
8.50E-01	4.902E-03	5.00E-02	8.75E-07	9.80E+04
9.00E-01	2.503E-03	2.50E-02	9.13E-07	1.00E+05
9.25E-01	2.537E-03	2.50E-02	9.38E-07	1.01E+05
9.50E-01	2.571E-03	2.50E-02	9.63E-07	1.03E+05
9.75E-01	2.604E-03	2.50E-02	9.88E-07	1.04E+05
1.00E+00	1.051E-03	1.00E-02	1.01E-06	1.05E+05
1.01E+00	1.056E-03	1.00E-02	1.02E-06	1.06E+05
1.02E+00	1.061E-03	1.00E-02	1.03E-06	1.06E+05
1.03E+00	1.066E-03	1.00E-02	1.04E-06	1.07E+05
1.04E+00	1.071E-03	1.00E-02	1.05E-06	1.07E+05
1.05E+00	1.077E-03	1.00E-02	1.06E-06	1.08E+05
1.06E+00	1.082E-03	1.00E-02	1.07E-06	1.08E+05
1.07E+00	1.087E-03	1.00E-02	1.08E-06	1.09E+05
1.08E+00	1.092E-03	1.00E-02	1.09E-06	1.09E+05
1.09E+00	1.097E-03	1.00E-02	1.10E-06	1.10E+05
1.10E+00	1.102E-03	1.00E-02	1.11E-06	1.10E+05

Continued on following page

E [eV]	dS [$\frac{n}{sec}$]	dE [eV]	Bin Mid. E [MeV]	$\frac{dS}{dE}$ [$\frac{n}{MeV sec}$]
1.11E+00	1.107E-03	1.00E-02	1.12E-06	1.11E+05
1.12E+00	1.112E-03	1.00E-02	1.13E-06	1.11E+05
1.13E+00	1.117E-03	1.00E-02	1.14E-06	1.12E+05
1.14E+00	1.121E-03	1.00E-02	1.15E-06	1.12E+05
1.15E+00	3.394E-03	3.00E-02	1.17E-06	1.13E+05
1.18E+00	2.287E-03	2.00E-02	1.19E-06	1.14E+05
1.20E+00	3.466E-03	3.00E-02	1.22E-06	1.16E+05
1.23E+00	2.334E-03	2.00E-02	1.24E-06	1.17E+05
1.25E+00	5.917E-03	5.00E-02	1.28E-06	1.18E+05
1.30E+00	6.032E-03	5.00E-02	1.33E-06	1.21E+05
1.35E+00	6.144E-03	5.00E-02	1.38E-06	1.23E+05
1.40E+00	6.255E-03	5.00E-02	1.43E-06	1.25E+05
1.45E+00	6.364E-03	5.00E-02	1.48E-06	1.27E+05
1.50E+00	1.172E-02	9.00E-02	1.55E-06	1.30E+05
1.59E+00	1.206E-02	9.00E-02	1.64E-06	1.34E+05
1.68E+00	1.239E-02	9.00E-02	1.73E-06	1.38E+05
1.77E+00	1.271E-02	9.00E-02	1.82E-06	1.41E+05
1.86E+00	1.156E-02	8.00E-02	1.90E-06	1.44E+05
1.94E+00	8.825E-03	6.00E-02	1.97E-06	1.47E+05
2.00E+00	1.805E-02	1.20E-01	2.06E-06	1.50E+05
2.12E+00	1.388E-02	9.00E-02	2.17E-06	1.54E+05
2.21E+00	1.416E-02	9.00E-02	2.26E-06	1.57E+05
2.30E+00	1.282E-02	8.00E-02	2.34E-06	1.60E+05
2.38E+00	1.469E-02	9.00E-02	2.43E-06	1.63E+05
2.47E+00	1.664E-02	1.00E-01	2.52E-06	1.66E+05
2.57E+00	1.696E-02	1.00E-01	2.62E-06	1.70E+05
2.67E+00	1.728E-02	1.00E-01	2.72E-06	1.73E+05
2.77E+00	1.760E-02	1.00E-01	2.82E-06	1.76E+05
2.87E+00	1.791E-02	1.00E-01	2.92E-06	1.79E+05
2.97E+00	5.432E-03	3.00E-02	2.99E-06	1.81E+05
3.00E+00	9.113E-03	5.00E-02	3.03E-06	1.82E+05
3.05E+00	1.845E-02	1.00E-01	3.10E-06	1.85E+05
3.15E+00	6.687E-02	3.50E-01	3.33E-06	1.91E+05
3.50E+00	4.582E-02	2.30E-01	3.62E-06	1.99E+05
3.73E+00	5.562E-02	2.70E-01	3.87E-06	2.06E+05
4.00E+00	1.643E-01	7.50E-01	4.38E-06	2.19E+05
4.75E+00	5.784E-02	2.50E-01	4.88E-06	2.31E+05
5.00E+00	9.557E-02	4.00E-01	5.20E-06	2.39E+05
5.40E+00	1.501E-01	6.00E-01	5.70E-06	2.50E+05
6.00E+00	6.483E-02	2.50E-01	6.13E-06	2.59E+05
6.25E+00	6.614E-02	2.50E-01	6.38E-06	2.65E+05
6.50E+00	6.743E-02	2.50E-01	6.63E-06	2.70E+05

Continued on following page

E [eV]	dS [$\frac{n}{sec}$]	dE [eV]	Bin Mid. E [MeV]	$\frac{dS}{dE}$ [$\frac{n}{MeV sec}$]
6.75E+00	6.869E-02	2.50E-01	6.88E-06	2.75E+05
7.00E+00	4.181E-02	1.50E-01	7.08E-06	2.79E+05
7.15E+00	2.748E-01	9.50E-01	7.63E-06	2.89E+05
8.10E+00	3.072E-01	1.00E+00	8.60E-06	3.07E+05
9.10E+00	2.914E-01	9.00E-01	9.55E-06	3.24E+05
1.00E+01	5.152E-01	1.50E+00	1.08E-05	3.43E+05
1.15E+01	1.434E-01	4.00E-01	1.17E-05	3.58E+05
1.19E+01	3.690E-01	1.00E+00	1.24E-05	3.69E+05
1.29E+01	3.445E-01	9.00E-01	1.34E-05	3.83E+05
1.38E+01	2.361E-01	6.00E-01	1.41E-05	3.94E+05
1.44E+01	2.818E-01	7.00E-01	1.48E-05	4.03E+05
1.51E+01	3.720E-01	9.00E-01	1.56E-05	4.13E+05
1.60E+01	4.258E-01	1.00E+00	1.65E-05	4.26E+05
1.70E+01	6.624E-01	1.50E+00	1.78E-05	4.42E+05
1.85E+01	2.270E-01	5.00E-01	1.88E-05	4.54E+05
1.90E+01	4.629E-01	1.00E+00	1.95E-05	4.63E+05
2.00E+01	4.746E-01	1.00E+00	2.05E-05	4.75E+05
2.10E+01	7.333E-01	1.50E+00	2.18E-05	4.89E+05
2.25E+01	1.281E+00	2.50E+00	2.38E-05	5.12E+05
2.50E+01	1.349E+00	2.50E+00	2.63E-05	5.39E+05
2.75E+01	1.411E+00	2.50E+00	2.88E-05	5.64E+05
3.00E+01	7.575E-01	1.30E+00	3.07E-05	5.83E+05
3.13E+01	2.956E-01	5.00E-01	3.16E-05	5.91E+05
3.18E+01	9.006E-01	1.50E+00	3.26E-05	6.00E+05
3.33E+01	3.048E-01	5.00E-01	3.36E-05	6.10E+05
3.38E+01	4.923E-01	8.00E-01	3.42E-05	6.15E+05
3.46E+01	5.607E-01	9.00E-01	3.51E-05	6.23E+05
3.55E+01	9.502E-01	1.50E+00	3.63E-05	6.33E+05
3.70E+01	6.443E-01	1.00E+00	3.75E-05	6.44E+05
3.80E+01	7.185E-01	1.10E+00	3.86E-05	6.53E+05
3.91E+01	3.300E-01	5.00E-01	3.94E-05	6.60E+05
3.96E+01	9.351E-01	1.40E+00	4.03E-05	6.68E+05
4.10E+01	9.521E-01	1.40E+00	4.17E-05	6.80E+05
4.24E+01	1.107E+00	1.60E+00	4.32E-05	6.92E+05
4.40E+01	8.438E-01	1.20E+00	4.46E-05	7.03E+05
4.52E+01	1.287E+00	1.80E+00	4.61E-05	7.15E+05
4.70E+01	9.449E-01	1.30E+00	4.77E-05	7.27E+05
4.83E+01	6.616E-01	9.00E-01	4.88E-05	7.35E+05
4.92E+01	1.041E+00	1.40E+00	4.99E-05	7.44E+05
5.06E+01	1.056E+00	1.40E+00	5.13E-05	7.54E+05
5.20E+01	1.070E+00	1.40E+00	5.27E-05	7.64E+05
5.34E+01	4.418E+00	5.60E+00	5.62E-05	7.89E+05

Continued on following page

E [eV]	dS [$\frac{n}{sec}$]	dE [eV]	Bin Mid. E [MeV]	$\frac{dS}{dE}$ [$\frac{n}{MeV sec}$]
5.90E+01	1.630E+00	2.00E+00	6.00E-05	8.15E+05
6.10E+01	3.341E+00	4.00E+00	6.30E-05	8.35E+05
6.50E+01	2.141E+00	2.50E+00	6.63E-05	8.56E+05
6.75E+01	3.954E+00	4.50E+00	6.98E-05	8.79E+05
7.20E+01	3.620E+00	4.00E+00	7.40E-05	9.05E+05
7.60E+01	3.716E+00	4.00E+00	7.80E-05	9.29E+05
8.00E+01	1.894E+00	2.00E+00	8.10E-05	9.47E+05
8.20E+01	7.805E+00	8.00E+00	8.60E-05	9.76E+05
9.00E+01	1.025E+01	1.00E+01	9.50E-05	1.03E+06
1.00E+02	8.580E+00	8.00E+00	1.04E-04	1.07E+06
1.08E+02	7.773E+00	7.00E+00	1.12E-04	1.11E+06
1.15E+02	4.550E+00	4.00E+00	1.17E-04	1.14E+06
1.19E+02	3.463E+00	3.00E+00	1.21E-04	1.15E+06
1.22E+02	8.334E+01	6.40E+01	1.54E-04	1.30E+06
1.86E+02	1.013E+01	7.00E+00	1.90E-04	1.45E+06
1.93E+02	2.233E+01	1.50E+01	2.01E-04	1.49E+06
2.08E+02	3.039E+00	2.00E+00	2.09E-04	1.52E+06
2.10E+02	4.729E+01	3.00E+01	2.25E-04	1.58E+06
2.40E+02	7.661E+01	4.50E+01	2.63E-04	1.70E+06
2.85E+02	3.613E+01	2.00E+01	2.95E-04	1.81E+06
3.05E+02	5.307E+02	2.45E+02	4.28E-04	2.17E+06
5.50E+02	3.113E+02	1.20E+02	6.10E-04	2.59E+06
6.70E+02	3.554E+01	1.30E+01	6.77E-04	2.73E+06
6.83E+02	8.007E+02	2.67E+02	8.17E-04	3.00E+06
9.50E+02	6.808E+02	2.00E+02	1.05E-03	3.40E+06
1.15E+03	1.337E+03	3.50E+02	1.33E-03	3.82E+06
1.50E+03	2.052E+02	5.00E+01	1.53E-03	4.10E+06
1.55E+03	1.075E+03	2.50E+02	1.68E-03	4.30E+06
1.80E+03	1.878E+03	4.00E+02	2.00E-03	4.70E+06
2.20E+03	4.478E+02	9.00E+01	2.25E-03	4.98E+06
2.29E+03	1.502E+03	2.90E+02	2.44E-03	5.18E+06
2.58E+03	2.328E+03	4.20E+02	2.79E-03	5.54E+06
3.00E+03	4.506E+03	7.40E+02	3.37E-03	6.09E+06
3.74E+03	1.038E+03	1.60E+02	3.82E-03	6.48E+06
3.90E+03	1.547E+04	2.10E+03	4.95E-03	7.37E+06
6.00E+03	1.781E+04	2.03E+03	7.02E-03	8.77E+06
8.03E+03	1.441E+04	1.47E+03	8.77E-03	9.80E+06
9.50E+03	3.879E+04	3.50E+03	1.13E-02	1.11E+07
1.30E+04	5.112E+04	4.00E+03	1.50E-02	1.28E+07
1.70E+04	1.205E+05	8.00E+03	2.10E-02	1.51E+07
2.50E+04	8.604E+04	5.00E+03	2.75E-02	1.72E+07
3.00E+04	2.995E+05	1.50E+04	3.75E-02	2.00E+07

Continued on following page

E [eV]	dS [$\frac{n}{sec}$]	dE [eV]	Bin Mid. E [MeV]	$\frac{dS}{dE}$ [$\frac{n}{MeV sec}$]
4.50E+04	1.120E+05	5.00E+03	4.75E-02	2.24E+07
5.00E+04	4.634E+04	2.00E+03	5.10E-02	2.32E+07
5.20E+04	1.937E+05	8.00E+03	5.60E-02	2.42E+07
6.00E+04	3.411E+05	1.30E+04	6.65E-02	2.62E+07
7.30E+04	5.517E+04	2.00E+03	7.40E-02	2.76E+07
7.50E+04	1.984E+05	7.00E+03	7.85E-02	2.83E+07
8.20E+04	8.750E+04	3.00E+03	8.35E-02	2.92E+07
8.50E+04	4.583E+05	1.50E+04	9.25E-02	3.06E+07
1.00E+05	9.390E+05	2.80E+04	1.14E-01	3.35E+07
1.28E+05	8.048E+05	2.20E+04	1.39E-01	3.66E+07
1.50E+05	2.013E+06	5.00E+04	1.75E-01	4.03E+07
2.00E+05	3.164E+06	7.00E+04	2.35E-01	4.52E+07
2.70E+05	2.962E+06	6.00E+04	3.00E-01	4.94E+07
3.30E+05	3.681E+06	7.00E+04	3.65E-01	5.26E+07
4.00E+05	1.089E+06	2.00E+04	4.10E-01	5.44E+07
4.20E+05	1.103E+06	2.00E+04	4.30E-01	5.51E+07
4.40E+05	1.679E+06	3.00E+04	4.55E-01	5.60E+07
4.70E+05	1.705E+06	3.00E+04	4.85E-01	5.68E+07
5.00E+05	2.891E+06	5.00E+04	5.25E-01	5.78E+07
5.50E+05	1.348E+06	2.30E+04	5.62E-01	5.86E+07
5.73E+05	1.594E+06	2.70E+04	5.87E-01	5.90E+07
6.00E+05	4.183E+06	7.00E+04	6.35E-01	5.98E+07
6.70E+05	5.422E+05	9.00E+03	6.75E-01	6.02E+07
6.79E+05	4.302E+06	7.10E+04	7.15E-01	6.06E+07
7.50E+05	4.268E+06	7.00E+04	7.85E-01	6.10E+07
8.20E+05	2.505E+06	4.10E+04	8.41E-01	6.11E+07
8.61E+05	8.552E+05	1.40E+04	8.68E-01	6.11E+07
8.75E+05	1.527E+06	2.50E+04	8.88E-01	6.11E+07
9.00E+05	1.220E+06	2.00E+04	9.10E-01	6.10E+07
9.20E+05	5.472E+06	9.00E+04	9.65E-01	6.08E+07
1.01E+06	5.421E+06	9.00E+04	1.06E+00	6.02E+07
1.10E+06	5.937E+06	1.00E+05	1.15E+00	5.94E+07
1.20E+06	2.927E+06	5.00E+04	1.23E+00	5.85E+07
1.25E+06	4.044E+06	7.00E+04	1.29E+00	5.78E+07
1.32E+06	2.280E+06	4.00E+04	1.34E+00	5.70E+07
1.36E+06	2.258E+06	4.00E+04	1.38E+00	5.64E+07
1.40E+06	5.538E+06	1.00E+05	1.45E+00	5.54E+07
1.50E+06	1.806E+07	3.50E+05	1.68E+00	5.16E+07
1.85E+06	2.195E+07	5.00E+05	2.10E+00	4.39E+07
2.35E+06	4.961E+06	1.30E+05	2.42E+00	3.82E+07
2.48E+06	1.694E+07	5.20E+05	2.74E+00	3.26E+07
3.00E+06	2.567E+07	1.30E+06	3.65E+00	1.97E+07

Continued on following page

E [eV]	dS [$\frac{n}{sec}$]	dE [eV]	Bin Mid. E [MeV]	$\frac{dS}{dE}$ [$\frac{n}{MeV sec}$]
4.30E+06	5.419E+06	5.00E+05	4.55E+00	1.08E+07
4.80E+06	8.944E+06	1.63E+06	5.62E+00	5.49E+06
6.43E+06	2.870E+06	1.76E+06	7.31E+00	1.63E+06
8.19E+06	7.569E+05	1.81E+06	9.10E+00	4.18E+05
1.00E+07				

Table D.3: ORIGAMI photon results for a Westinghouse 17×17 PWR assembly burned to $57.535 \frac{MWd}{kg}$ and cooled for a combined time period of 15yr.

E [eV]	dS [$\frac{p}{sec}$]	dE [eV]	Bin Mid. E [MeV]	$\frac{dS}{dE}$ [$\frac{p}{MeV sec}$]
1.00E+04	6.656E+13	1.00E+04	1.50E-02	6.66E+15
2.00E+04	3.319E+13	1.00E+04	2.50E-02	3.32E+15
3.00E+04	4.687E+13	1.50E+04	3.75E-02	3.12E+15
4.50E+04	2.213E+13	1.50E+04	5.25E-02	1.48E+15
6.00E+04	8.508E+12	1.00E+04	6.50E-02	8.51E+14
7.00E+04	3.759E+12	5.00E+03	7.25E-02	7.52E+14
7.50E+04	1.474E+13	2.50E+04	8.75E-02	5.90E+14
1.00E+05	1.846E+13	5.00E+04	1.25E-01	3.69E+14
1.50E+05	9.208E+12	5.00E+04	1.75E-01	1.84E+14
2.00E+05	5.614E+12	6.00E+04	2.30E-01	9.36E+13
2.60E+05	2.317E+12	4.00E+04	2.80E-01	5.79E+13
3.00E+05	4.981E+12	1.00E+05	3.50E-01	4.98E+13
4.00E+05	1.763E+12	5.00E+04	4.25E-01	3.53E+13
4.50E+05	1.592E+12	6.00E+04	4.80E-01	2.65E+13
5.10E+05	4.075E+10	2.00E+03	5.11E-01	2.04E+13
5.12E+05	2.670E+12	8.80E+04	5.56E-01	3.03E+13
6.00E+05	2.836E+14	1.00E+05	6.50E-01	2.84E+15
7.00E+05	8.101E+12	1.00E+05	7.50E-01	8.10E+13
8.00E+05	2.021E+12	1.00E+05	8.50E-01	2.02E+13
9.00E+05	2.372E+12	1.00E+05	9.50E-01	2.37E+13
1.00E+06	1.329E+12	2.00E+05	1.10E+00	6.64E+12
1.20E+06	3.672E+12	1.30E+05	1.27E+00	2.82E+13
1.33E+06	2.016E+11	1.10E+05	1.39E+00	1.83E+12
1.44E+06	8.137E+10	6.00E+04	1.47E+00	1.36E+12
1.50E+06	1.723E+10	7.00E+04	1.54E+00	2.46E+11
1.57E+06	1.885E+11	9.00E+04	1.62E+00	2.09E+12
1.66E+06	9.230E+09	1.40E+05	1.73E+00	6.59E+10
1.80E+06	4.059E+09	2.00E+05	1.90E+00	2.03E+10
2.00E+06	7.196E+08	1.50E+05	2.08E+00	4.80E+09
2.15E+06	6.080E+07	2.00E+05	2.25E+00	3.04E+08

Continued on following page

E [eV]	dS [$\frac{p}{sec}$]	dE [eV]	Bin Mid. E [MeV]	$\frac{dS}{dE}$ [$\frac{p}{MeV sec}$]
2.35E+06	5.308E+07	1.50E+05	2.43E+00	3.54E+08
2.50E+06	9.814E+07	2.50E+05	2.63E+00	3.93E+08
2.75E+06	1.296E+07	2.50E+05	2.88E+00	5.18E+07
3.00E+06	9.757E+06	5.00E+05	3.25E+00	1.95E+07
3.50E+06	4.895E+06	5.00E+05	3.75E+00	9.79E+06
4.00E+06	2.836E+06	5.00E+05	4.25E+00	5.67E+06
4.50E+06	1.644E+06	5.00E+05	4.75E+00	3.29E+06
5.00E+06	9.532E+05	5.00E+05	5.25E+00	1.91E+06
5.50E+06	5.527E+05	5.00E+05	5.75E+00	1.11E+06
6.00E+06	3.205E+05	5.00E+05	6.25E+00	6.41E+05
6.50E+06	1.858E+05	5.00E+05	6.75E+00	3.72E+05
7.00E+06	1.077E+05	5.00E+05	7.25E+00	2.15E+05
7.50E+06	6.247E+04	5.00E+05	7.75E+00	1.25E+05
8.00E+06	7.378E+04	2.00E+06	9.00E+00	3.69E+04
1.00E+07				

Table D.4: ORIGAMI photon results for a Westinghouse 17×17 PWR assembly burned to $57.535 \frac{MWd}{kg}$ and cooled for a combined time period of 15yr.

E [eV]	dS [$\frac{n}{sec}$]	dE [eV]	Bin Mid. E [MeV]	$\frac{dS}{dE}$ [$\frac{n}{MeV sec}$]
1.00E-05	5.547E-08	9.00E-05	5.50E-11	6.16E+02
1.00E-04	4.790E-07	4.00E-04	3.00E-10	1.20E+03
5.00E-04	4.525E-07	2.50E-04	6.25E-10	1.81E+03
7.50E-04	5.158E-07	2.50E-04	8.75E-10	2.06E+03
1.00E-03	4.776E-07	2.00E-04	1.10E-09	2.39E+03
1.20E-03	7.881E-07	3.00E-04	1.35E-09	2.63E+03
1.50E-03	1.495E-06	5.00E-04	1.75E-09	2.99E+03
2.00E-03	1.699E-06	5.00E-04	2.25E-09	3.40E+03
2.50E-03	1.865E-06	5.00E-04	2.75E-09	3.73E+03
3.00E-03	4.222E-06	1.00E-03	3.50E-09	4.22E+03
4.00E-03	4.805E-06	1.00E-03	4.50E-09	4.80E+03
5.00E-03	1.409E-05	2.50E-03	6.25E-09	5.64E+03
7.50E-03	1.669E-05	2.50E-03	8.75E-09	6.67E+03
1.00E-02	1.440E-04	1.53E-02	1.77E-08	9.41E+03
2.53E-02	5.583E-05	4.70E-03	2.77E-08	1.19E+04
3.00E-02	1.336E-04	1.00E-02	3.50E-08	1.34E+04
4.00E-02	1.515E-04	1.00E-02	4.50E-08	1.51E+04
5.00E-02	1.675E-04	1.00E-02	5.50E-08	1.68E+04
6.00E-02	1.821E-04	1.00E-02	6.50E-08	1.82E+04
7.00E-02	1.956E-04	1.00E-02	7.50E-08	1.96E+04

Continued on following page

E [eV]	dS [$\frac{n}{sec}$]	dE [eV]	Bin Mid. E [MeV]	$\frac{dS}{dE}$ [$\frac{n}{MeV sec}$]
8.00E-02	2.083E-04	1.00E-02	8.50E-08	2.08E+04
9.00E-02	2.202E-04	1.00E-02	9.50E-08	2.20E+04
1.00E-01	5.988E-04	2.50E-02	1.13E-07	2.40E+04
1.25E-01	6.621E-04	2.50E-02	1.38E-07	2.65E+04
1.50E-01	7.206E-04	2.50E-02	1.63E-07	2.88E+04
1.75E-01	7.742E-04	2.50E-02	1.88E-07	3.10E+04
2.00E-01	8.241E-04	2.50E-02	2.13E-07	3.30E+04
2.25E-01	8.712E-04	2.50E-02	2.38E-07	3.48E+04
2.50E-01	9.159E-04	2.50E-02	2.63E-07	3.66E+04
2.75E-01	9.585E-04	2.50E-02	2.88E-07	3.83E+04
3.00E-01	9.993E-04	2.50E-02	3.13E-07	4.00E+04
3.25E-01	1.039E-03	2.50E-02	3.38E-07	4.15E+04
3.50E-01	1.076E-03	2.50E-02	3.63E-07	4.30E+04
3.75E-01	1.113E-03	2.50E-02	3.88E-07	4.45E+04
4.00E-01	2.330E-03	5.00E-02	4.25E-07	4.66E+04
4.50E-01	2.464E-03	5.00E-02	4.75E-07	4.93E+04
5.00E-01	2.590E-03	5.00E-02	5.25E-07	5.18E+04
5.50E-01	2.710E-03	5.00E-02	5.75E-07	5.42E+04
6.00E-01	1.399E-03	2.50E-02	6.13E-07	5.59E+04
6.25E-01	1.427E-03	2.50E-02	6.38E-07	5.71E+04
6.50E-01	2.937E-03	5.00E-02	6.75E-07	5.87E+04
7.00E-01	3.043E-03	5.00E-02	7.25E-07	6.09E+04
7.50E-01	3.147E-03	5.00E-02	7.75E-07	6.29E+04
8.00E-01	3.246E-03	5.00E-02	8.25E-07	6.49E+04
8.50E-01	3.343E-03	5.00E-02	8.75E-07	6.69E+04
9.00E-01	1.707E-03	2.50E-02	9.13E-07	6.83E+04
9.25E-01	1.730E-03	2.50E-02	9.38E-07	6.92E+04
9.50E-01	1.753E-03	2.50E-02	9.63E-07	7.01E+04
9.75E-01	1.776E-03	2.50E-02	9.88E-07	7.10E+04
1.00E+00	7.166E-04	1.00E-02	1.01E-06	7.17E+04
1.01E+00	7.202E-04	1.00E-02	1.02E-06	7.20E+04
1.02E+00	7.237E-04	1.00E-02	1.03E-06	7.24E+04
1.03E+00	7.272E-04	1.00E-02	1.04E-06	7.27E+04
1.04E+00	7.307E-04	1.00E-02	1.05E-06	7.31E+04
1.05E+00	7.342E-04	1.00E-02	1.06E-06	7.34E+04
1.06E+00	7.377E-04	1.00E-02	1.07E-06	7.38E+04
1.07E+00	7.411E-04	1.00E-02	1.08E-06	7.41E+04
1.08E+00	7.446E-04	1.00E-02	1.09E-06	7.45E+04
1.09E+00	7.480E-04	1.00E-02	1.10E-06	7.48E+04
1.10E+00	7.514E-04	1.00E-02	1.11E-06	7.51E+04
1.11E+00	7.548E-04	1.00E-02	1.12E-06	7.55E+04
1.12E+00	7.582E-04	1.00E-02	1.13E-06	7.58E+04

Continued on following page

E [eV]	dS [$\frac{n}{sec}$]	dE [eV]	Bin Mid. E [MeV]	$\frac{dS}{dE}$ [$\frac{n}{MeV sec}$]
1.13E+00	7.615E-04	1.00E-02	1.14E-06	7.62E+04
1.14E+00	7.649E-04	1.00E-02	1.15E-06	7.65E+04
1.15E+00	2.315E-03	3.00E-02	1.17E-06	7.71E+04
1.18E+00	1.560E-03	2.00E-02	1.19E-06	7.80E+04
1.20E+00	2.364E-03	3.00E-02	1.22E-06	7.88E+04
1.23E+00	1.592E-03	2.00E-02	1.24E-06	7.96E+04
1.25E+00	4.035E-03	5.00E-02	1.28E-06	8.07E+04
1.30E+00	4.114E-03	5.00E-02	1.33E-06	8.23E+04
1.35E+00	4.191E-03	5.00E-02	1.38E-06	8.38E+04
1.40E+00	4.266E-03	5.00E-02	1.43E-06	8.53E+04
1.45E+00	4.340E-03	5.00E-02	1.48E-06	8.68E+04
1.50E+00	7.995E-03	9.00E-02	1.55E-06	8.88E+04
1.59E+00	8.225E-03	9.00E-02	1.64E-06	9.14E+04
1.68E+00	8.448E-03	9.00E-02	1.73E-06	9.39E+04
1.77E+00	8.666E-03	9.00E-02	1.82E-06	9.63E+04
1.86E+00	7.881E-03	8.00E-02	1.90E-06	9.85E+04
1.94E+00	6.019E-03	6.00E-02	1.97E-06	1.00E+05
2.00E+00	1.231E-02	1.20E-01	2.06E-06	1.03E+05
2.12E+00	9.464E-03	9.00E-02	2.17E-06	1.05E+05
2.21E+00	9.659E-03	9.00E-02	2.26E-06	1.07E+05
2.30E+00	8.746E-03	8.00E-02	2.34E-06	1.09E+05
2.38E+00	1.002E-02	9.00E-02	2.43E-06	1.11E+05
2.47E+00	1.135E-02	1.00E-01	2.52E-06	1.13E+05
2.57E+00	1.157E-02	1.00E-01	2.62E-06	1.16E+05
2.67E+00	1.179E-02	1.00E-01	2.72E-06	1.18E+05
2.77E+00	1.200E-02	1.00E-01	2.82E-06	1.20E+05
2.87E+00	1.221E-02	1.00E-01	2.92E-06	1.22E+05
2.97E+00	3.704E-03	3.00E-02	2.99E-06	1.23E+05
3.00E+00	6.215E-03	5.00E-02	3.03E-06	1.24E+05
3.05E+00	1.258E-02	1.00E-01	3.10E-06	1.26E+05
3.15E+00	4.561E-02	3.50E-01	3.33E-06	1.30E+05
3.50E+00	3.125E-02	2.30E-01	3.62E-06	1.36E+05
3.73E+00	3.793E-02	2.70E-01	3.87E-06	1.40E+05
4.00E+00	1.121E-01	7.50E-01	4.38E-06	1.49E+05
4.75E+00	3.945E-02	2.50E-01	4.88E-06	1.58E+05
5.00E+00	6.518E-02	4.00E-01	5.20E-06	1.63E+05
5.40E+00	1.024E-01	6.00E-01	5.70E-06	1.71E+05
6.00E+00	4.421E-02	2.50E-01	6.13E-06	1.77E+05
6.25E+00	4.511E-02	2.50E-01	6.38E-06	1.80E+05
6.50E+00	4.598E-02	2.50E-01	6.63E-06	1.84E+05
6.75E+00	4.684E-02	2.50E-01	6.88E-06	1.87E+05
7.00E+00	2.851E-02	1.50E-01	7.08E-06	1.90E+05

Continued on following page

E [eV]	dS [$\frac{n}{sec}$]	dE [eV]	Bin Mid. E [MeV]	$\frac{dS}{dE}$ [$\frac{n}{MeV sec}$]
7.15E+00	1.874E-01	9.50E-01	7.63E-06	1.97E+05
8.10E+00	2.095E-01	1.00E+00	8.60E-06	2.10E+05
9.10E+00	1.987E-01	9.00E-01	9.55E-06	2.21E+05
1.00E+01	3.514E-01	1.50E+00	1.08E-05	2.34E+05
1.15E+01	9.777E-02	4.00E-01	1.17E-05	2.44E+05
1.19E+01	2.516E-01	1.00E+00	1.24E-05	2.52E+05
1.29E+01	2.350E-01	9.00E-01	1.34E-05	2.61E+05
1.38E+01	1.610E-01	6.00E-01	1.41E-05	2.68E+05
1.44E+01	1.922E-01	7.00E-01	1.48E-05	2.75E+05
1.51E+01	2.537E-01	9.00E-01	1.56E-05	2.82E+05
1.60E+01	2.904E-01	1.00E+00	1.65E-05	2.90E+05
1.70E+01	4.518E-01	1.50E+00	1.78E-05	3.01E+05
1.85E+01	1.548E-01	5.00E-01	1.88E-05	3.10E+05
1.90E+01	3.157E-01	1.00E+00	1.95E-05	3.16E+05
2.00E+01	3.237E-01	1.00E+00	2.05E-05	3.24E+05
2.10E+01	5.000E-01	1.50E+00	2.18E-05	3.33E+05
2.25E+01	8.734E-01	2.50E+00	2.38E-05	3.49E+05
2.50E+01	9.197E-01	2.50E+00	2.63E-05	3.68E+05
2.75E+01	9.623E-01	2.50E+00	2.88E-05	3.85E+05
3.00E+01	5.166E-01	1.30E+00	3.07E-05	3.97E+05
3.13E+01	2.016E-01	5.00E-01	3.16E-05	4.03E+05
3.18E+01	6.142E-01	1.50E+00	3.26E-05	4.09E+05
3.33E+01	2.078E-01	5.00E-01	3.36E-05	4.16E+05
3.38E+01	3.357E-01	8.00E-01	3.42E-05	4.20E+05
3.46E+01	3.823E-01	9.00E-01	3.51E-05	4.25E+05
3.55E+01	6.480E-01	1.50E+00	3.63E-05	4.32E+05
3.70E+01	4.394E-01	1.00E+00	3.75E-05	4.39E+05
3.80E+01	4.900E-01	1.10E+00	3.86E-05	4.45E+05
3.91E+01	2.250E-01	5.00E-01	3.94E-05	4.50E+05
3.96E+01	6.378E-01	1.40E+00	4.03E-05	4.56E+05
4.10E+01	6.498E-01	1.40E+00	4.17E-05	4.64E+05
4.24E+01	7.558E-01	1.60E+00	4.32E-05	4.72E+05
4.40E+01	5.759E-01	1.20E+00	4.46E-05	4.80E+05
4.52E+01	8.783E-01	1.80E+00	4.61E-05	4.88E+05
4.70E+01	6.451E-01	1.30E+00	4.77E-05	4.96E+05
4.83E+01	4.517E-01	9.00E-01	4.88E-05	5.02E+05
4.92E+01	7.108E-01	1.40E+00	4.99E-05	5.08E+05
5.06E+01	7.207E-01	1.40E+00	5.13E-05	5.15E+05
5.20E+01	7.304E-01	1.40E+00	5.27E-05	5.22E+05
5.34E+01	3.016E+00	5.60E+00	5.62E-05	5.39E+05
5.90E+01	1.113E+00	2.00E+00	6.00E-05	5.56E+05
6.10E+01	2.280E+00	4.00E+00	6.30E-05	5.70E+05

Continued on following page

E [eV]	dS [$\frac{n}{sec}$]	dE [eV]	Bin Mid. E [MeV]	$\frac{dS}{dE}$ [$\frac{n}{MeV sec}$]
6.50E+01	1.461E+00	2.50E+00	6.63E-05	5.85E+05
6.75E+01	2.699E+00	4.50E+00	6.98E-05	6.00E+05
7.20E+01	2.471E+00	4.00E+00	7.40E-05	6.18E+05
7.60E+01	2.537E+00	4.00E+00	7.80E-05	6.34E+05
8.00E+01	1.293E+00	2.00E+00	8.10E-05	6.46E+05
8.20E+01	5.328E+00	8.00E+00	8.60E-05	6.66E+05
9.00E+01	6.998E+00	1.00E+01	9.50E-05	7.00E+05
1.00E+02	5.857E+00	8.00E+00	1.04E-04	7.32E+05
1.08E+02	5.306E+00	7.00E+00	1.12E-04	7.58E+05
1.15E+02	3.106E+00	4.00E+00	1.17E-04	7.76E+05
1.19E+02	2.364E+00	3.00E+00	1.21E-04	7.88E+05
1.22E+02	5.688E+01	6.40E+01	1.54E-04	8.89E+05
1.86E+02	6.913E+00	7.00E+00	1.90E-04	9.88E+05
1.93E+02	1.524E+01	1.50E+01	2.01E-04	1.02E+06
2.08E+02	2.074E+00	2.00E+00	2.09E-04	1.04E+06
2.10E+02	3.227E+01	3.00E+01	2.25E-04	1.08E+06
2.40E+02	5.229E+01	4.50E+01	2.63E-04	1.16E+06
2.85E+02	2.466E+01	2.00E+01	2.95E-04	1.23E+06
3.05E+02	3.622E+02	2.45E+02	4.28E-04	1.48E+06
5.50E+02	2.125E+02	1.20E+02	6.10E-04	1.77E+06
6.70E+02	2.425E+01	1.30E+01	6.77E-04	1.87E+06
6.83E+02	5.464E+02	2.67E+02	8.17E-04	2.05E+06
9.50E+02	4.646E+02	2.00E+02	1.05E-03	2.32E+06
1.15E+03	9.128E+02	3.50E+02	1.33E-03	2.61E+06
1.50E+03	1.400E+02	5.00E+01	1.53E-03	2.80E+06
1.55E+03	7.336E+02	2.50E+02	1.68E-03	2.93E+06
1.80E+03	1.282E+03	4.00E+02	2.00E-03	3.20E+06
2.20E+03	3.056E+02	9.00E+01	2.25E-03	3.40E+06
2.29E+03	1.025E+03	2.90E+02	2.44E-03	3.54E+06
2.58E+03	1.589E+03	4.20E+02	2.79E-03	3.78E+06
3.00E+03	3.075E+03	7.40E+02	3.37E-03	4.16E+06
3.74E+03	7.081E+02	1.60E+02	3.82E-03	4.43E+06
3.90E+03	1.056E+04	2.10E+03	4.95E-03	5.03E+06
6.00E+03	1.215E+04	2.03E+03	7.02E-03	5.99E+06
8.03E+03	9.833E+03	1.47E+03	8.77E-03	6.69E+06
9.50E+03	2.648E+04	3.50E+03	1.13E-02	7.56E+06
1.30E+04	3.489E+04	4.00E+03	1.50E-02	8.72E+06
1.70E+04	8.227E+04	8.00E+03	2.10E-02	1.03E+07
2.50E+04	5.873E+04	5.00E+03	2.75E-02	1.17E+07
3.00E+04	2.044E+05	1.50E+04	3.75E-02	1.36E+07
4.50E+04	7.643E+04	5.00E+03	4.75E-02	1.53E+07
5.00E+04	3.162E+04	2.00E+03	5.10E-02	1.58E+07

Continued on following page

E [eV]	dS [$\frac{n}{sec}$]	dE [eV]	Bin Mid. E [MeV]	$\frac{dS}{dE}$ [$\frac{n}{MeV sec}$]
5.20E+04	1.322E+05	8.00E+03	5.60E-02	1.65E+07
6.00E+04	2.328E+05	1.30E+04	6.65E-02	1.79E+07
7.30E+04	3.766E+04	2.00E+03	7.40E-02	1.88E+07
7.50E+04	1.354E+05	7.00E+03	7.85E-02	1.93E+07
8.20E+04	5.971E+04	3.00E+03	8.35E-02	1.99E+07
8.50E+04	3.128E+05	1.50E+04	9.25E-02	2.09E+07
1.00E+05	6.409E+05	2.80E+04	1.14E-01	2.29E+07
1.28E+05	5.493E+05	2.20E+04	1.39E-01	2.50E+07
1.50E+05	1.374E+06	5.00E+04	1.75E-01	2.75E+07
2.00E+05	2.159E+06	7.00E+04	2.35E-01	3.08E+07
2.70E+05	2.021E+06	6.00E+04	3.00E-01	3.37E+07
3.30E+05	2.512E+06	7.00E+04	3.65E-01	3.59E+07
4.00E+05	7.429E+05	2.00E+04	4.10E-01	3.71E+07
4.20E+05	7.526E+05	2.00E+04	4.30E-01	3.76E+07
4.40E+05	1.145E+06	3.00E+04	4.55E-01	3.82E+07
4.70E+05	1.163E+06	3.00E+04	4.85E-01	3.88E+07
5.00E+05	1.972E+06	5.00E+04	5.25E-01	3.94E+07
5.50E+05	9.195E+05	2.30E+04	5.62E-01	4.00E+07
5.73E+05	1.088E+06	2.70E+04	5.87E-01	4.03E+07
6.00E+05	2.854E+06	7.00E+04	6.35E-01	4.08E+07
6.70E+05	3.699E+05	9.00E+03	6.75E-01	4.11E+07
6.79E+05	2.935E+06	7.10E+04	7.15E-01	4.13E+07
7.50E+05	2.912E+06	7.00E+04	7.85E-01	4.16E+07
8.20E+05	1.709E+06	4.10E+04	8.41E-01	4.17E+07
8.61E+05	5.835E+05	1.40E+04	8.68E-01	4.17E+07
8.75E+05	1.041E+06	2.50E+04	8.88E-01	4.17E+07
9.00E+05	8.325E+05	2.00E+04	9.10E-01	4.16E+07
9.20E+05	3.733E+06	9.00E+04	9.65E-01	4.15E+07
1.01E+06	3.698E+06	9.00E+04	1.06E+00	4.11E+07
1.10E+06	4.050E+06	1.00E+05	1.15E+00	4.05E+07
1.20E+06	1.997E+06	5.00E+04	1.23E+00	3.99E+07
1.25E+06	2.759E+06	7.00E+04	1.29E+00	3.94E+07
1.32E+06	1.556E+06	4.00E+04	1.34E+00	3.89E+07
1.36E+06	1.540E+06	4.00E+04	1.38E+00	3.85E+07
1.40E+06	3.779E+06	1.00E+05	1.45E+00	3.78E+07
1.50E+06	1.233E+07	3.50E+05	1.68E+00	3.52E+07
1.85E+06	1.500E+07	5.00E+05	2.10E+00	3.00E+07
2.35E+06	3.394E+06	1.30E+05	2.42E+00	2.61E+07
2.48E+06	1.159E+07	5.20E+05	2.74E+00	2.23E+07
3.00E+06	1.752E+07	1.30E+06	3.65E+00	1.35E+07
4.30E+06	3.681E+06	5.00E+05	4.55E+00	7.36E+06
4.80E+06	6.065E+06	1.63E+06	5.62E+00	3.72E+06

Continued on following page

E [eV]	dS [$\frac{n}{sec}$]	dE [eV]	Bin Mid. E [MeV]	$\frac{dS}{dE}$ [$\frac{n}{MeV sec}$]
6.43E+06	1.940E+06	1.76E+06	7.31E+00	1.10E+06
8.19E+06	5.098E+05	1.81E+06	9.10E+00	2.82E+05
1.00E+07				

Table D.5: ORIGAMI photon results for a Westinghouse 17×17 PWR assembly burned to $57.535 \frac{MWd}{kg}$ and cooled for a combined time period of 25yr.

E [eV]	dS [$\frac{p}{sec}$]	dE [eV]	Bin Mid. E [MeV]	$\frac{dS}{dE}$ [$\frac{p}{MeV sec}$]
1.00E+04	5.297E+13	1.00E+04	1.50E-02	5.30E+15
2.00E+04	2.566E+13	1.00E+04	2.50E-02	2.57E+15
3.00E+04	3.566E+13	1.50E+04	3.75E-02	2.38E+15
4.50E+04	1.888E+13	1.50E+04	5.25E-02	1.26E+15
6.00E+04	6.628E+12	1.00E+04	6.50E-02	6.63E+14
7.00E+04	2.962E+12	5.00E+03	7.25E-02	5.92E+14
7.50E+04	1.115E+13	2.50E+04	8.75E-02	4.46E+14
1.00E+05	1.292E+13	5.00E+04	1.25E-01	2.58E+14
1.50E+05	7.146E+12	5.00E+04	1.75E-01	1.43E+14
2.00E+05	4.144E+12	6.00E+04	2.30E-01	6.91E+13
2.60E+05	1.818E+12	4.00E+04	2.80E-01	4.54E+13
3.00E+05	3.881E+12	1.00E+05	3.50E-01	3.88E+13
4.00E+05	1.185E+12	5.00E+04	4.25E-01	2.37E+13
4.50E+05	1.121E+12	6.00E+04	4.80E-01	1.87E+13
5.10E+05	1.500E+10	2.00E+03	5.11E-01	7.50E+12
5.12E+05	8.362E+11	8.80E+04	5.56E-01	9.50E+12
6.00E+05	2.213E+14	1.00E+05	6.50E-01	2.21E+15
7.00E+05	1.701E+12	1.00E+05	7.50E-01	1.70E+13
8.00E+05	9.400E+11	1.00E+05	8.50E-01	9.40E+12
9.00E+05	1.145E+12	1.00E+05	9.50E-01	1.14E+13
1.00E+06	6.227E+11	2.00E+05	1.10E+00	3.11E+12
1.20E+06	1.675E+12	1.30E+05	1.27E+00	1.29E+13
1.33E+06	3.642E+10	1.10E+05	1.39E+00	3.31E+11
1.44E+06	4.013E+10	6.00E+04	1.47E+00	6.69E+11
1.50E+06	1.126E+10	7.00E+04	1.54E+00	1.61E+11
1.57E+06	8.850E+10	9.00E+04	1.62E+00	9.83E+11
1.66E+06	7.064E+09	1.40E+05	1.73E+00	5.05E+10
1.80E+06	3.129E+09	2.00E+05	1.90E+00	1.56E+10
2.00E+06	5.376E+08	1.50E+05	2.08E+00	3.58E+09
2.15E+06	1.938E+07	2.00E+05	2.25E+00	9.69E+07
2.35E+06	2.095E+06	1.50E+05	2.43E+00	1.40E+07
2.50E+06	8.458E+07	2.50E+05	2.63E+00	3.38E+08

Continued on following page

E [eV]	dS [$\frac{p}{sec}$]	dE [eV]	Bin Mid. E [MeV]	$\frac{dS}{dE}$ [$\frac{p}{MeVsec}$]
2.75E+06	4.819E+06	2.50E+05	2.88E+00	1.93E+07
3.00E+06	5.839E+06	5.00E+05	3.25E+00	1.17E+07
3.50E+06	3.385E+06	5.00E+05	3.75E+00	6.77E+06
4.00E+06	1.961E+06	5.00E+05	4.25E+00	3.92E+06
4.50E+06	1.137E+06	5.00E+05	4.75E+00	2.27E+06
5.00E+06	6.590E+05	5.00E+05	5.25E+00	1.32E+06
5.50E+06	3.821E+05	5.00E+05	5.75E+00	7.64E+05
6.00E+06	2.215E+05	5.00E+05	6.25E+00	4.43E+05
6.50E+06	1.285E+05	5.00E+05	6.75E+00	2.57E+05
7.00E+06	7.448E+04	5.00E+05	7.25E+00	1.49E+05
7.50E+06	4.318E+04	5.00E+05	7.75E+00	8.64E+04
8.00E+06	5.101E+04	2.00E+06	9.00E+00	2.55E+04
1.00E+07				

Table D.6: ORIGAMI photon results for a Westinghouse 17×17 PWR assembly burned to $57.535 \frac{MWd}{kg}$ and cooled for a combined time period of 25yr.

E [eV]	dS [$\frac{n}{sec}$]	dE [eV]	Bin Mid. E [MeV]	$\frac{dS}{dE}$ [$\frac{n}{MeVsec}$]
1.00E-05	3.834E-08	9.00E-05	5.50E-11	4.26E+02
1.00E-04	3.317E-07	4.00E-04	3.00E-10	8.29E+02
5.00E-04	3.132E-07	2.50E-04	6.25E-10	1.25E+03
7.50E-04	3.574E-07	2.50E-04	8.75E-10	1.43E+03
1.00E-03	3.307E-07	2.00E-04	1.10E-09	1.65E+03
1.20E-03	5.457E-07	3.00E-04	1.35E-09	1.82E+03
1.50E-03	1.035E-06	5.00E-04	1.75E-09	2.07E+03
2.00E-03	1.176E-06	5.00E-04	2.25E-09	2.35E+03
2.50E-03	1.292E-06	5.00E-04	2.75E-09	2.58E+03
3.00E-03	2.924E-06	1.00E-03	3.50E-09	2.92E+03
4.00E-03	3.327E-06	1.00E-03	4.50E-09	3.33E+03
5.00E-03	9.758E-06	2.50E-03	6.25E-09	3.90E+03
7.50E-03	1.156E-05	2.50E-03	8.75E-09	4.62E+03
1.00E-02	9.975E-05	1.53E-02	1.77E-08	6.52E+03
2.53E-02	3.866E-05	4.70E-03	2.77E-08	8.23E+03
3.00E-02	9.248E-05	1.00E-02	3.50E-08	9.25E+03
4.00E-02	1.049E-04	1.00E-02	4.50E-08	1.05E+04
5.00E-02	1.160E-04	1.00E-02	5.50E-08	1.16E+04
6.00E-02	1.261E-04	1.00E-02	6.50E-08	1.26E+04
7.00E-02	1.355E-04	1.00E-02	7.50E-08	1.35E+04
8.00E-02	1.442E-04	1.00E-02	8.50E-08	1.44E+04
9.00E-02	1.525E-04	1.00E-02	9.50E-08	1.52E+04

Continued on following page

E [eV]	dS [$\frac{n}{sec}$]	dE [eV]	Bin Mid. E [MeV]	$\frac{dS}{dE}$ [$\frac{n}{MeVsec}$]
1.00E-01	4.146E-04	2.50E-02	1.13E-07	1.66E+04
1.25E-01	4.585E-04	2.50E-02	1.38E-07	1.83E+04
1.50E-01	4.992E-04	2.50E-02	1.63E-07	2.00E+04
1.75E-01	5.364E-04	2.50E-02	1.88E-07	2.15E+04
2.00E-01	5.710E-04	2.50E-02	2.13E-07	2.28E+04
2.25E-01	6.036E-04	2.50E-02	2.38E-07	2.41E+04
2.50E-01	6.345E-04	2.50E-02	2.63E-07	2.54E+04
2.75E-01	6.640E-04	2.50E-02	2.88E-07	2.66E+04
3.00E-01	6.923E-04	2.50E-02	3.13E-07	2.77E+04
3.25E-01	7.194E-04	2.50E-02	3.38E-07	2.88E+04
3.50E-01	7.455E-04	2.50E-02	3.63E-07	2.98E+04
3.75E-01	7.708E-04	2.50E-02	3.88E-07	3.08E+04
4.00E-01	1.614E-03	5.00E-02	4.25E-07	3.23E+04
4.50E-01	1.707E-03	5.00E-02	4.75E-07	3.41E+04
5.00E-01	1.794E-03	5.00E-02	5.25E-07	3.59E+04
5.50E-01	1.878E-03	5.00E-02	5.75E-07	3.76E+04
6.00E-01	9.689E-04	2.50E-02	6.13E-07	3.88E+04
6.25E-01	9.884E-04	2.50E-02	6.38E-07	3.95E+04
6.50E-01	2.034E-03	5.00E-02	6.75E-07	4.07E+04
7.00E-01	2.108E-03	5.00E-02	7.25E-07	4.22E+04
7.50E-01	2.179E-03	5.00E-02	7.75E-07	4.36E+04
8.00E-01	2.249E-03	5.00E-02	8.25E-07	4.50E+04
8.50E-01	2.316E-03	5.00E-02	8.75E-07	4.63E+04
9.00E-01	1.182E-03	2.50E-02	9.13E-07	4.73E+04
9.25E-01	1.199E-03	2.50E-02	9.38E-07	4.79E+04
9.50E-01	1.214E-03	2.50E-02	9.63E-07	4.86E+04
9.75E-01	1.230E-03	2.50E-02	9.88E-07	4.92E+04
1.00E+00	4.963E-04	1.00E-02	1.01E-06	4.96E+04
1.01E+00	4.988E-04	1.00E-02	1.02E-06	4.99E+04
1.02E+00	5.013E-04	1.00E-02	1.03E-06	5.01E+04
1.03E+00	5.037E-04	1.00E-02	1.04E-06	5.04E+04
1.04E+00	5.061E-04	1.00E-02	1.05E-06	5.06E+04
1.05E+00	5.085E-04	1.00E-02	1.06E-06	5.09E+04
1.06E+00	5.109E-04	1.00E-02	1.07E-06	5.11E+04
1.07E+00	5.133E-04	1.00E-02	1.08E-06	5.13E+04
1.08E+00	5.157E-04	1.00E-02	1.09E-06	5.16E+04
1.09E+00	5.181E-04	1.00E-02	1.10E-06	5.18E+04
1.10E+00	5.204E-04	1.00E-02	1.11E-06	5.20E+04
1.11E+00	5.228E-04	1.00E-02	1.12E-06	5.23E+04
1.12E+00	5.251E-04	1.00E-02	1.13E-06	5.25E+04
1.13E+00	5.275E-04	1.00E-02	1.14E-06	5.27E+04
1.14E+00	5.298E-04	1.00E-02	1.15E-06	5.30E+04

Continued on following page

E [eV]	dS [$\frac{n}{sec}$]	dE [eV]	Bin Mid. E [MeV]	$\frac{dS}{dE}$ [$\frac{n}{MeV sec}$]
1.15E+00	1.603E-03	3.00E-02	1.17E-06	5.34E+04
1.18E+00	1.080E-03	2.00E-02	1.19E-06	5.40E+04
1.20E+00	1.637E-03	3.00E-02	1.22E-06	5.46E+04
1.23E+00	1.103E-03	2.00E-02	1.24E-06	5.51E+04
1.25E+00	2.795E-03	5.00E-02	1.28E-06	5.59E+04
1.30E+00	2.849E-03	5.00E-02	1.33E-06	5.70E+04
1.35E+00	2.903E-03	5.00E-02	1.38E-06	5.81E+04
1.40E+00	2.955E-03	5.00E-02	1.43E-06	5.91E+04
1.45E+00	3.006E-03	5.00E-02	1.48E-06	6.01E+04
1.50E+00	5.538E-03	9.00E-02	1.55E-06	6.15E+04
1.59E+00	5.697E-03	9.00E-02	1.64E-06	6.33E+04
1.68E+00	5.851E-03	9.00E-02	1.73E-06	6.50E+04
1.77E+00	6.002E-03	9.00E-02	1.82E-06	6.67E+04
1.86E+00	5.459E-03	8.00E-02	1.90E-06	6.82E+04
1.94E+00	4.169E-03	6.00E-02	1.97E-06	6.95E+04
2.00E+00	8.525E-03	1.20E-01	2.06E-06	7.10E+04
2.12E+00	6.555E-03	9.00E-02	2.17E-06	7.28E+04
2.21E+00	6.690E-03	9.00E-02	2.26E-06	7.43E+04
2.30E+00	6.057E-03	8.00E-02	2.34E-06	7.57E+04
2.38E+00	6.937E-03	9.00E-02	2.43E-06	7.71E+04
2.47E+00	7.858E-03	1.00E-01	2.52E-06	7.86E+04
2.57E+00	8.012E-03	1.00E-01	2.62E-06	8.01E+04
2.67E+00	8.163E-03	1.00E-01	2.72E-06	8.16E+04
2.77E+00	8.312E-03	1.00E-01	2.82E-06	8.31E+04
2.87E+00	8.458E-03	1.00E-01	2.92E-06	8.46E+04
2.97E+00	2.566E-03	3.00E-02	2.99E-06	8.55E+04
3.00E+00	4.304E-03	5.00E-02	3.03E-06	8.61E+04
3.05E+00	8.715E-03	1.00E-01	3.10E-06	8.71E+04
3.15E+00	3.159E-02	3.50E-01	3.33E-06	9.02E+04
3.50E+00	2.164E-02	2.30E-01	3.62E-06	9.41E+04
3.73E+00	2.627E-02	2.70E-01	3.87E-06	9.73E+04
4.00E+00	7.762E-02	7.50E-01	4.38E-06	1.03E+05
4.75E+00	2.732E-02	2.50E-01	4.88E-06	1.09E+05
5.00E+00	4.514E-02	4.00E-01	5.20E-06	1.13E+05
5.40E+00	7.089E-02	6.00E-01	5.70E-06	1.18E+05
6.00E+00	3.062E-02	2.50E-01	6.13E-06	1.22E+05
6.25E+00	3.124E-02	2.50E-01	6.38E-06	1.25E+05
6.50E+00	3.185E-02	2.50E-01	6.63E-06	1.27E+05
6.75E+00	3.244E-02	2.50E-01	6.88E-06	1.30E+05
7.00E+00	1.975E-02	1.50E-01	7.08E-06	1.32E+05
7.15E+00	1.298E-01	9.50E-01	7.63E-06	1.37E+05
8.10E+00	1.451E-01	1.00E+00	8.60E-06	1.45E+05

Continued on following page

E [eV]	dS [$\frac{n}{sec}$]	dE [eV]	Bin Mid. E [MeV]	$\frac{dS}{dE}$ [$\frac{n}{MeV sec}$]
9.10E+00	1.376E-01	9.00E-01	9.55E-06	1.53E+05
1.00E+01	2.433E-01	1.50E+00	1.08E-05	1.62E+05
1.15E+01	6.771E-02	4.00E-01	1.17E-05	1.69E+05
1.19E+01	1.743E-01	1.00E+00	1.24E-05	1.74E+05
1.29E+01	1.627E-01	9.00E-01	1.34E-05	1.81E+05
1.38E+01	1.115E-01	6.00E-01	1.41E-05	1.86E+05
1.44E+01	1.331E-01	7.00E-01	1.48E-05	1.90E+05
1.51E+01	1.757E-01	9.00E-01	1.56E-05	1.95E+05
1.60E+01	2.011E-01	1.00E+00	1.65E-05	2.01E+05
1.70E+01	3.128E-01	1.50E+00	1.78E-05	2.09E+05
1.85E+01	1.072E-01	5.00E-01	1.88E-05	2.14E+05
1.90E+01	2.186E-01	1.00E+00	1.95E-05	2.19E+05
2.00E+01	2.241E-01	1.00E+00	2.05E-05	2.24E+05
2.10E+01	3.463E-01	1.50E+00	2.18E-05	2.31E+05
2.25E+01	6.048E-01	2.50E+00	2.38E-05	2.42E+05
2.50E+01	6.368E-01	2.50E+00	2.63E-05	2.55E+05
2.75E+01	6.663E-01	2.50E+00	2.88E-05	2.67E+05
3.00E+01	3.577E-01	1.30E+00	3.07E-05	2.75E+05
3.13E+01	1.396E-01	5.00E-01	3.16E-05	2.79E+05
3.18E+01	4.253E-01	1.50E+00	3.26E-05	2.84E+05
3.33E+01	1.439E-01	5.00E-01	3.36E-05	2.88E+05
3.38E+01	2.325E-01	8.00E-01	3.42E-05	2.91E+05
3.46E+01	2.648E-01	9.00E-01	3.51E-05	2.94E+05
3.55E+01	4.487E-01	1.50E+00	3.63E-05	2.99E+05
3.70E+01	3.042E-01	1.00E+00	3.75E-05	3.04E+05
3.80E+01	3.393E-01	1.10E+00	3.86E-05	3.08E+05
3.91E+01	1.558E-01	5.00E-01	3.94E-05	3.12E+05
3.96E+01	4.418E-01	1.40E+00	4.03E-05	3.16E+05
4.10E+01	4.505E-01	1.40E+00	4.17E-05	3.22E+05
4.24E+01	5.240E-01	1.60E+00	4.32E-05	3.28E+05
4.40E+01	3.993E-01	1.20E+00	4.46E-05	3.33E+05
4.52E+01	6.090E-01	1.80E+00	4.61E-05	3.38E+05
4.70E+01	4.474E-01	1.30E+00	4.77E-05	3.44E+05
4.83E+01	3.133E-01	9.00E-01	4.88E-05	3.48E+05
4.92E+01	4.930E-01	1.40E+00	4.99E-05	3.52E+05
5.06E+01	4.998E-01	1.40E+00	5.13E-05	3.57E+05
5.20E+01	5.065E-01	1.40E+00	5.27E-05	3.62E+05
5.34E+01	2.092E+00	5.60E+00	5.62E-05	3.73E+05
5.90E+01	7.717E-01	2.00E+00	6.00E-05	3.86E+05
6.10E+01	1.581E+00	4.00E+00	6.30E-05	3.95E+05
6.50E+01	1.013E+00	2.50E+00	6.63E-05	4.05E+05
6.75E+01	1.872E+00	4.50E+00	6.98E-05	4.16E+05

Continued on following page

E [eV]	dS [$\frac{n}{sec}$]	dE [eV]	Bin Mid. E [MeV]	$\frac{dS}{dE}$ [$\frac{n}{MeV sec}$]
7.20E+01	1.713E+00	4.00E+00	7.40E-05	4.28E+05
7.60E+01	1.759E+00	4.00E+00	7.80E-05	4.40E+05
8.00E+01	8.965E-01	2.00E+00	8.10E-05	4.48E+05
8.20E+01	3.695E+00	8.00E+00	8.60E-05	4.62E+05
9.00E+01	4.852E+00	1.00E+01	9.50E-05	4.85E+05
1.00E+02	4.061E+00	8.00E+00	1.04E-04	5.08E+05
1.08E+02	3.679E+00	7.00E+00	1.12E-04	5.26E+05
1.15E+02	2.153E+00	4.00E+00	1.17E-04	5.38E+05
1.19E+02	1.639E+00	3.00E+00	1.21E-04	5.46E+05
1.22E+02	3.943E+01	6.40E+01	1.54E-04	6.16E+05
1.86E+02	4.792E+00	7.00E+00	1.90E-04	6.85E+05
1.93E+02	1.056E+01	1.50E+01	2.01E-04	7.04E+05
2.08E+02	1.438E+00	2.00E+00	2.09E-04	7.19E+05
2.10E+02	2.237E+01	3.00E+01	2.25E-04	7.46E+05
2.40E+02	3.625E+01	4.50E+01	2.63E-04	8.06E+05
2.85E+02	1.710E+01	2.00E+01	2.95E-04	8.55E+05
3.05E+02	2.511E+02	2.45E+02	4.28E-04	1.02E+06
5.50E+02	1.473E+02	1.20E+02	6.10E-04	1.23E+06
6.70E+02	1.681E+01	1.30E+01	6.77E-04	1.29E+06
6.83E+02	3.787E+02	2.67E+02	8.17E-04	1.42E+06
9.50E+02	3.221E+02	2.00E+02	1.05E-03	1.61E+06
1.15E+03	6.328E+02	3.50E+02	1.33E-03	1.81E+06
1.50E+03	9.708E+01	5.00E+01	1.53E-03	1.94E+06
1.55E+03	5.085E+02	2.50E+02	1.68E-03	2.03E+06
1.80E+03	8.884E+02	4.00E+02	2.00E-03	2.22E+06
2.20E+03	2.118E+02	9.00E+01	2.25E-03	2.35E+06
2.29E+03	7.106E+02	2.90E+02	2.44E-03	2.45E+06
2.58E+03	1.101E+03	4.20E+02	2.79E-03	2.62E+06
3.00E+03	2.131E+03	7.40E+02	3.37E-03	2.88E+06
3.74E+03	4.908E+02	1.60E+02	3.82E-03	3.07E+06
3.90E+03	7.319E+03	2.10E+03	4.95E-03	3.49E+06
6.00E+03	8.424E+03	2.03E+03	7.02E-03	4.15E+06
8.03E+03	6.817E+03	1.47E+03	8.77E-03	4.64E+06
9.50E+03	1.836E+04	3.50E+03	1.13E-02	5.24E+06
1.30E+04	2.419E+04	4.00E+03	1.50E-02	6.05E+06
1.70E+04	5.704E+04	8.00E+03	2.10E-02	7.13E+06
2.50E+04	4.072E+04	5.00E+03	2.75E-02	8.14E+06
3.00E+04	1.417E+05	1.50E+04	3.75E-02	9.45E+06
4.50E+04	5.299E+04	5.00E+03	4.75E-02	1.06E+07
5.00E+04	2.192E+04	2.00E+03	5.10E-02	1.10E+07
5.20E+04	9.164E+04	8.00E+03	5.60E-02	1.15E+07
6.00E+04	1.614E+05	1.30E+04	6.65E-02	1.24E+07

Continued on following page

E [eV]	dS [$\frac{n}{sec}$]	dE [eV]	Bin Mid. E [MeV]	$\frac{dS}{dE}$ [$\frac{n}{MeV sec}$]
7.30E+04	2.610E+04	2.00E+03	7.40E-02	1.31E+07
7.50E+04	9.387E+04	7.00E+03	7.85E-02	1.34E+07
8.20E+04	4.139E+04	3.00E+03	8.35E-02	1.38E+07
8.50E+04	2.168E+05	1.50E+04	9.25E-02	1.45E+07
1.00E+05	4.443E+05	2.80E+04	1.14E-01	1.59E+07
1.28E+05	3.808E+05	2.20E+04	1.39E-01	1.73E+07
1.50E+05	9.523E+05	5.00E+04	1.75E-01	1.90E+07
2.00E+05	1.496E+06	7.00E+04	2.35E-01	2.14E+07
2.70E+05	1.401E+06	6.00E+04	3.00E-01	2.33E+07
3.30E+05	1.741E+06	7.00E+04	3.65E-01	2.49E+07
4.00E+05	5.149E+05	2.00E+04	4.10E-01	2.57E+07
4.20E+05	5.216E+05	2.00E+04	4.30E-01	2.61E+07
4.40E+05	7.938E+05	3.00E+04	4.55E-01	2.65E+07
4.70E+05	8.061E+05	3.00E+04	4.85E-01	2.69E+07
5.00E+05	1.367E+06	5.00E+04	5.25E-01	2.73E+07
5.50E+05	6.372E+05	2.30E+04	5.62E-01	2.77E+07
5.73E+05	7.538E+05	2.70E+04	5.87E-01	2.79E+07
6.00E+05	1.978E+06	7.00E+04	6.35E-01	2.83E+07
6.70E+05	2.563E+05	9.00E+03	6.75E-01	2.85E+07
6.79E+05	2.034E+06	7.10E+04	7.15E-01	2.86E+07
7.50E+05	2.018E+06	7.00E+04	7.85E-01	2.88E+07
8.20E+05	1.184E+06	4.10E+04	8.41E-01	2.89E+07
8.61E+05	4.043E+05	1.40E+04	8.68E-01	2.89E+07
8.75E+05	7.217E+05	2.50E+04	8.88E-01	2.89E+07
9.00E+05	5.769E+05	2.00E+04	9.10E-01	2.88E+07
9.20E+05	2.587E+06	9.00E+04	9.65E-01	2.87E+07
1.01E+06	2.563E+06	9.00E+04	1.06E+00	2.85E+07
1.10E+06	2.807E+06	1.00E+05	1.15E+00	2.81E+07
1.20E+06	1.384E+06	5.00E+04	1.23E+00	2.77E+07
1.25E+06	1.913E+06	7.00E+04	1.29E+00	2.73E+07
1.32E+06	1.079E+06	4.00E+04	1.34E+00	2.70E+07
1.36E+06	1.068E+06	4.00E+04	1.38E+00	2.67E+07
1.40E+06	2.621E+06	1.00E+05	1.45E+00	2.62E+07
1.50E+06	8.554E+06	3.50E+05	1.68E+00	2.44E+07
1.85E+06	1.043E+07	5.00E+05	2.10E+00	2.09E+07
2.35E+06	2.362E+06	1.30E+05	2.42E+00	1.82E+07
2.48E+06	8.071E+06	5.20E+05	2.74E+00	1.55E+07
3.00E+06	1.217E+07	1.30E+06	3.65E+00	9.36E+06
4.30E+06	2.546E+06	5.00E+05	4.55E+00	5.09E+06
4.80E+06	4.191E+06	1.63E+06	5.62E+00	2.57E+06
6.43E+06	1.339E+06	1.76E+06	7.31E+00	7.61E+05
8.19E+06	3.516E+05	1.81E+06	9.10E+00	1.94E+05

Continued on following page

E [eV]	dS [$\frac{n}{sec}$]	dE [eV]	Bin Mid. E [MeV]	$\frac{dS}{dE}$ [$\frac{n}{MeVsec}$]
1.00E+07				

Table D.7: ORIGAMI photon results for a Westinghouse 17×17 PWR assembly burned to $57.535 \frac{MWd}{kg}$ and cooled for a combined time period of 35yr.

E [eV]	dS [$\frac{p}{sec}$]	dE [eV]	Bin Mid. E [MeV]	$\frac{dS}{dE}$ [$\frac{p}{MeVsec}$]
1.00E+04	4.260E+13	1.00E+04	1.50E-02	4.26E+15
2.00E+04	2.027E+13	1.00E+04	2.50E-02	2.03E+15
3.00E+04	2.771E+13	1.50E+04	3.75E-02	1.85E+15
4.50E+04	1.633E+13	1.50E+04	5.25E-02	1.09E+15
6.00E+04	5.196E+12	1.00E+04	6.50E-02	5.20E+14
7.00E+04	2.353E+12	5.00E+03	7.25E-02	4.71E+14
7.50E+04	8.661E+12	2.50E+04	8.75E-02	3.46E+14
1.00E+05	9.511E+12	5.00E+04	1.25E-01	1.90E+14
1.50E+05	5.599E+12	5.00E+04	1.75E-01	1.12E+14
2.00E+05	3.146E+12	6.00E+04	2.30E-01	5.24E+13
2.60E+05	1.432E+12	4.00E+04	2.80E-01	3.58E+13
3.00E+05	3.042E+12	1.00E+05	3.50E-01	3.04E+13
4.00E+05	9.064E+11	5.00E+04	4.25E-01	1.81E+13
4.50E+05	8.695E+11	6.00E+04	4.80E-01	1.45E+13
5.10E+05	7.866E+09	2.00E+03	5.11E-01	3.93E+12
5.12E+05	5.158E+11	8.80E+04	5.56E-01	5.86E+12
6.00E+05	1.756E+14	1.00E+05	6.50E-01	1.76E+15
7.00E+05	8.407E+11	1.00E+05	7.50E-01	8.41E+12
8.00E+05	5.177E+11	1.00E+05	8.50E-01	5.18E+12
9.00E+05	5.781E+11	1.00E+05	9.50E-01	5.78E+12
1.00E+06	3.487E+11	2.00E+05	1.10E+00	1.74E+12
1.20E+06	7.752E+11	1.30E+05	1.27E+00	5.96E+12
1.33E+06	2.367E+10	1.10E+05	1.39E+00	2.15E+11
1.44E+06	2.091E+10	6.00E+04	1.47E+00	3.49E+11
1.50E+06	7.881E+09	7.00E+04	1.54E+00	1.13E+11
1.57E+06	4.293E+10	9.00E+04	1.62E+00	4.77E+11
1.66E+06	5.492E+09	1.40E+05	1.73E+00	3.92E+10
1.80E+06	2.460E+09	2.00E+05	1.90E+00	1.23E+10
2.00E+06	4.226E+08	1.50E+05	2.08E+00	2.82E+09
2.15E+06	1.367E+07	2.00E+05	2.25E+00	6.83E+07
2.35E+06	1.603E+06	1.50E+05	2.43E+00	1.07E+07
2.50E+06	7.571E+07	2.50E+05	2.63E+00	3.03E+08
2.75E+06	3.352E+06	2.50E+05	2.88E+00	1.34E+07
3.00E+06	4.066E+06	5.00E+05	3.25E+00	8.13E+06

Continued on following page

E [eV]	dS [$\frac{p}{sec}$]	dE [eV]	Bin Mid. E [MeV]	$\frac{dS}{dE}$ [$\frac{p}{MeV sec}$]
3.50E+06	2.358E+06	5.00E+05	3.75E+00	4.72E+06
4.00E+06	1.365E+06	5.00E+05	4.25E+00	2.73E+06
4.50E+06	7.916E+05	5.00E+05	4.75E+00	1.58E+06
5.00E+06	4.589E+05	5.00E+05	5.25E+00	9.18E+05
5.50E+06	2.661E+05	5.00E+05	5.75E+00	5.32E+05
6.00E+06	1.543E+05	5.00E+05	6.25E+00	3.09E+05
6.50E+06	8.944E+04	5.00E+05	6.75E+00	1.79E+05
7.00E+06	5.186E+04	5.00E+05	7.25E+00	1.04E+05
7.50E+06	3.007E+04	5.00E+05	7.75E+00	6.01E+04
8.00E+06	3.551E+04	2.00E+06	9.00E+00	1.78E+04
1.00E+07				

Table D.8: ORIGAMI photon results for a Westinghouse 17×17 PWR assembly burned to $57.535 \frac{MWd}{kg}$ and cooled for a combined time period of 35yr.

E [eV]	dS [$\frac{n}{sec}$]	dE [eV]	Bin Mid. E [MeV]	$\frac{dS}{dE}$ [$\frac{n}{MeV sec}$]
1.00E-05	2.669E-08	9.00E-05	5.50E-11	2.97E+02
1.00E-04	2.316E-07	4.00E-04	3.00E-10	5.79E+02
5.00E-04	2.186E-07	2.50E-04	6.25E-10	8.74E+02
7.50E-04	2.498E-07	2.50E-04	8.75E-10	9.99E+02
1.00E-03	2.308E-07	2.00E-04	1.10E-09	1.15E+03
1.20E-03	3.810E-07	3.00E-04	1.35E-09	1.27E+03
1.50E-03	7.227E-07	5.00E-04	1.75E-09	1.45E+03
2.00E-03	8.211E-07	5.00E-04	2.25E-09	1.64E+03
2.50E-03	9.019E-07	5.00E-04	2.75E-09	1.80E+03
3.00E-03	2.041E-06	1.00E-03	3.50E-09	2.04E+03
4.00E-03	2.323E-06	1.00E-03	4.50E-09	2.32E+03
5.00E-03	6.813E-06	2.50E-03	6.25E-09	2.73E+03
7.50E-03	8.068E-06	2.50E-03	8.75E-09	3.23E+03
1.00E-02	6.964E-05	1.53E-02	1.77E-08	4.55E+03
2.53E-02	2.699E-05	4.70E-03	2.77E-08	5.74E+03
3.00E-02	6.457E-05	1.00E-02	3.50E-08	6.46E+03
4.00E-02	7.323E-05	1.00E-02	4.50E-08	7.32E+03
5.00E-02	8.099E-05	1.00E-02	5.50E-08	8.10E+03
6.00E-02	8.804E-05	1.00E-02	6.50E-08	8.80E+03
7.00E-02	9.459E-05	1.00E-02	7.50E-08	9.46E+03
8.00E-02	1.007E-04	1.00E-02	8.50E-08	1.01E+04
9.00E-02	1.065E-04	1.00E-02	9.50E-08	1.06E+04
1.00E-01	2.895E-04	2.50E-02	1.13E-07	1.16E+04
1.25E-01	3.201E-04	2.50E-02	1.38E-07	1.28E+04

Continued on following page

E [eV]	dS [$\frac{n}{sec}$]	dE [eV]	Bin Mid. E [MeV]	$\frac{dS}{dE}$ [$\frac{n}{MeVsec}$]
1.50E-01	3.488E-04	2.50E-02	1.63E-07	1.40E+04
1.75E-01	3.748E-04	2.50E-02	1.88E-07	1.50E+04
2.00E-01	3.989E-04	2.50E-02	2.13E-07	1.60E+04
2.25E-01	4.217E-04	2.50E-02	2.38E-07	1.69E+04
2.50E-01	4.433E-04	2.50E-02	2.63E-07	1.77E+04
2.75E-01	4.639E-04	2.50E-02	2.88E-07	1.86E+04
3.00E-01	4.836E-04	2.50E-02	3.13E-07	1.93E+04
3.25E-01	5.026E-04	2.50E-02	3.38E-07	2.01E+04
3.50E-01	5.208E-04	2.50E-02	3.63E-07	2.08E+04
3.75E-01	5.384E-04	2.50E-02	3.88E-07	2.15E+04
4.00E-01	1.128E-03	5.00E-02	4.25E-07	2.26E+04
4.50E-01	1.192E-03	5.00E-02	4.75E-07	2.38E+04
5.00E-01	1.253E-03	5.00E-02	5.25E-07	2.51E+04
5.50E-01	1.311E-03	5.00E-02	5.75E-07	2.62E+04
6.00E-01	6.767E-04	2.50E-02	6.13E-07	2.71E+04
6.25E-01	6.904E-04	2.50E-02	6.38E-07	2.76E+04
6.50E-01	1.421E-03	5.00E-02	6.75E-07	2.84E+04
7.00E-01	1.472E-03	5.00E-02	7.25E-07	2.94E+04
7.50E-01	1.522E-03	5.00E-02	7.75E-07	3.04E+04
8.00E-01	1.571E-03	5.00E-02	8.25E-07	3.14E+04
8.50E-01	1.617E-03	5.00E-02	8.75E-07	3.23E+04
9.00E-01	8.258E-04	2.50E-02	9.13E-07	3.30E+04
9.25E-01	8.370E-04	2.50E-02	9.38E-07	3.35E+04
9.50E-01	8.481E-04	2.50E-02	9.63E-07	3.39E+04
9.75E-01	8.590E-04	2.50E-02	9.88E-07	3.44E+04
1.00E+00	3.466E-04	1.00E-02	1.01E-06	3.47E+04
1.01E+00	3.484E-04	1.00E-02	1.02E-06	3.48E+04
1.02E+00	3.501E-04	1.00E-02	1.03E-06	3.50E+04
1.03E+00	3.518E-04	1.00E-02	1.04E-06	3.52E+04
1.04E+00	3.535E-04	1.00E-02	1.05E-06	3.53E+04
1.05E+00	3.552E-04	1.00E-02	1.06E-06	3.55E+04
1.06E+00	3.568E-04	1.00E-02	1.07E-06	3.57E+04
1.07E+00	3.585E-04	1.00E-02	1.08E-06	3.59E+04
1.08E+00	3.602E-04	1.00E-02	1.09E-06	3.60E+04
1.09E+00	3.618E-04	1.00E-02	1.10E-06	3.62E+04
1.10E+00	3.635E-04	1.00E-02	1.11E-06	3.63E+04
1.11E+00	3.651E-04	1.00E-02	1.12E-06	3.65E+04
1.12E+00	3.667E-04	1.00E-02	1.13E-06	3.67E+04
1.13E+00	3.684E-04	1.00E-02	1.14E-06	3.68E+04
1.14E+00	3.700E-04	1.00E-02	1.15E-06	3.70E+04
1.15E+00	1.120E-03	3.00E-02	1.17E-06	3.73E+04
1.18E+00	7.543E-04	2.00E-02	1.19E-06	3.77E+04

Continued on following page

E [eV]	dS [$\frac{n}{sec}$]	dE [eV]	Bin Mid. E [MeV]	$\frac{dS}{dE}$ [$\frac{n}{MeV sec}$]
1.20E+00	1.143E-03	3.00E-02	1.22E-06	3.81E+04
1.23E+00	7.700E-04	2.00E-02	1.24E-06	3.85E+04
1.25E+00	1.952E-03	5.00E-02	1.28E-06	3.90E+04
1.30E+00	1.990E-03	5.00E-02	1.33E-06	3.98E+04
1.35E+00	2.027E-03	5.00E-02	1.38E-06	4.05E+04
1.40E+00	2.064E-03	5.00E-02	1.43E-06	4.13E+04
1.45E+00	2.099E-03	5.00E-02	1.48E-06	4.20E+04
1.50E+00	3.867E-03	9.00E-02	1.55E-06	4.30E+04
1.59E+00	3.978E-03	9.00E-02	1.64E-06	4.42E+04
1.68E+00	4.086E-03	9.00E-02	1.73E-06	4.54E+04
1.77E+00	4.191E-03	9.00E-02	1.82E-06	4.66E+04
1.86E+00	3.812E-03	8.00E-02	1.90E-06	4.76E+04
1.94E+00	2.911E-03	6.00E-02	1.97E-06	4.85E+04
2.00E+00	5.953E-03	1.20E-01	2.06E-06	4.96E+04
2.12E+00	4.577E-03	9.00E-02	2.17E-06	5.09E+04
2.21E+00	4.672E-03	9.00E-02	2.26E-06	5.19E+04
2.30E+00	4.230E-03	8.00E-02	2.34E-06	5.29E+04
2.38E+00	4.844E-03	9.00E-02	2.43E-06	5.38E+04
2.47E+00	5.487E-03	1.00E-01	2.52E-06	5.49E+04
2.57E+00	5.595E-03	1.00E-01	2.62E-06	5.59E+04
2.67E+00	5.701E-03	1.00E-01	2.72E-06	5.70E+04
2.77E+00	5.805E-03	1.00E-01	2.82E-06	5.80E+04
2.87E+00	5.906E-03	1.00E-01	2.92E-06	5.91E+04
2.97E+00	1.792E-03	3.00E-02	2.99E-06	5.97E+04
3.00E+00	3.006E-03	5.00E-02	3.03E-06	6.01E+04
3.05E+00	6.086E-03	1.00E-01	3.10E-06	6.09E+04
3.15E+00	2.206E-02	3.50E-01	3.33E-06	6.30E+04
3.50E+00	1.511E-02	2.30E-01	3.62E-06	6.57E+04
3.73E+00	1.835E-02	2.70E-01	3.87E-06	6.79E+04
4.00E+00	5.420E-02	7.50E-01	4.38E-06	7.23E+04
4.75E+00	1.908E-02	2.50E-01	4.88E-06	7.63E+04
5.00E+00	3.152E-02	4.00E-01	5.20E-06	7.88E+04
5.40E+00	4.950E-02	6.00E-01	5.70E-06	8.25E+04
6.00E+00	2.138E-02	2.50E-01	6.13E-06	8.55E+04
6.25E+00	2.181E-02	2.50E-01	6.38E-06	8.73E+04
6.50E+00	2.224E-02	2.50E-01	6.63E-06	8.89E+04
6.75E+00	2.265E-02	2.50E-01	6.88E-06	9.06E+04
7.00E+00	1.379E-02	1.50E-01	7.08E-06	9.19E+04
7.15E+00	9.064E-02	9.50E-01	7.63E-06	9.54E+04
8.10E+00	1.013E-01	1.00E+00	8.60E-06	1.01E+05
9.10E+00	9.610E-02	9.00E-01	9.55E-06	1.07E+05
1.00E+01	1.699E-01	1.50E+00	1.08E-05	1.13E+05

Continued on following page

E [eV]	dS [$\frac{n}{sec}$]	dE [eV]	Bin Mid. E [MeV]	$\frac{dS}{dE}$ [$\frac{n}{MeV sec}$]
1.15E+01	4.728E-02	4.00E-01	1.17E-05	1.18E+05
1.19E+01	1.217E-01	1.00E+00	1.24E-05	1.22E+05
1.29E+01	1.136E-01	9.00E-01	1.34E-05	1.26E+05
1.38E+01	7.786E-02	6.00E-01	1.41E-05	1.30E+05
1.44E+01	9.294E-02	7.00E-01	1.48E-05	1.33E+05
1.51E+01	1.227E-01	9.00E-01	1.56E-05	1.36E+05
1.60E+01	1.404E-01	1.00E+00	1.65E-05	1.40E+05
1.70E+01	2.184E-01	1.50E+00	1.78E-05	1.46E+05
1.85E+01	7.484E-02	5.00E-01	1.88E-05	1.50E+05
1.90E+01	1.526E-01	1.00E+00	1.95E-05	1.53E+05
2.00E+01	1.565E-01	1.00E+00	2.05E-05	1.57E+05
2.10E+01	2.418E-01	1.50E+00	2.18E-05	1.61E+05
2.25E+01	4.223E-01	2.50E+00	2.38E-05	1.69E+05
2.50E+01	4.446E-01	2.50E+00	2.63E-05	1.78E+05
2.75E+01	4.652E-01	2.50E+00	2.88E-05	1.86E+05
3.00E+01	2.498E-01	1.30E+00	3.07E-05	1.92E+05
3.13E+01	9.745E-02	5.00E-01	3.16E-05	1.95E+05
3.18E+01	2.969E-01	1.50E+00	3.26E-05	1.98E+05
3.33E+01	1.005E-01	5.00E-01	3.36E-05	2.01E+05
3.38E+01	1.623E-01	8.00E-01	3.42E-05	2.03E+05
3.46E+01	1.849E-01	9.00E-01	3.51E-05	2.05E+05
3.55E+01	3.133E-01	1.50E+00	3.63E-05	2.09E+05
3.70E+01	2.124E-01	1.00E+00	3.75E-05	2.12E+05
3.80E+01	2.369E-01	1.10E+00	3.86E-05	2.15E+05
3.91E+01	1.088E-01	5.00E-01	3.94E-05	2.18E+05
3.96E+01	3.085E-01	1.40E+00	4.03E-05	2.20E+05
4.10E+01	3.150E-01	1.40E+00	4.17E-05	2.25E+05
4.24E+01	3.664E-01	1.60E+00	4.32E-05	2.29E+05
4.40E+01	2.792E-01	1.20E+00	4.46E-05	2.33E+05
4.52E+01	4.258E-01	1.80E+00	4.61E-05	2.37E+05
4.70E+01	3.130E-01	1.30E+00	4.77E-05	2.41E+05
4.83E+01	2.191E-01	9.00E-01	4.88E-05	2.43E+05
4.92E+01	3.448E-01	1.40E+00	4.99E-05	2.46E+05
5.06E+01	3.496E-01	1.40E+00	5.13E-05	2.50E+05
5.20E+01	3.543E-01	1.40E+00	5.27E-05	2.53E+05
5.34E+01	1.463E+00	5.60E+00	5.62E-05	2.61E+05
5.90E+01	5.397E-01	2.00E+00	6.00E-05	2.70E+05
6.10E+01	1.106E+00	4.00E+00	6.30E-05	2.76E+05
6.50E+01	7.087E-01	2.50E+00	6.63E-05	2.83E+05
6.75E+01	1.309E+00	4.50E+00	6.98E-05	2.91E+05
7.20E+01	1.198E+00	4.00E+00	7.40E-05	3.00E+05
7.60E+01	1.230E+00	4.00E+00	7.80E-05	3.07E+05

Continued on following page

E [eV]	dS [$\frac{n}{sec}$]	dE [eV]	Bin Mid. E [MeV]	$\frac{dS}{dE}$ [$\frac{n}{MeV sec}$]
8.00E+01	6.270E-01	2.00E+00	8.10E-05	3.13E+05
8.20E+01	2.584E+00	8.00E+00	8.60E-05	3.23E+05
9.00E+01	3.393E+00	1.00E+01	9.50E-05	3.39E+05
1.00E+02	2.840E+00	8.00E+00	1.04E-04	3.55E+05
1.08E+02	2.572E+00	7.00E+00	1.12E-04	3.67E+05
1.15E+02	1.506E+00	4.00E+00	1.17E-04	3.76E+05
1.19E+02	1.146E+00	3.00E+00	1.21E-04	3.82E+05
1.22E+02	2.757E+01	6.40E+01	1.54E-04	4.31E+05
1.86E+02	3.350E+00	7.00E+00	1.90E-04	4.79E+05
1.93E+02	7.382E+00	1.50E+01	2.01E-04	4.92E+05
2.08E+02	1.005E+00	2.00E+00	2.09E-04	5.03E+05
2.10E+02	1.564E+01	3.00E+01	2.25E-04	5.21E+05
2.40E+02	2.535E+01	4.50E+01	2.63E-04	5.63E+05
2.85E+02	1.195E+01	2.00E+01	2.95E-04	5.98E+05
3.05E+02	1.755E+02	2.45E+02	4.28E-04	7.16E+05
5.50E+02	1.029E+02	1.20E+02	6.10E-04	8.58E+05
6.70E+02	1.175E+01	1.30E+01	6.77E-04	9.04E+05
6.83E+02	2.647E+02	2.67E+02	8.17E-04	9.91E+05
9.50E+02	2.252E+02	2.00E+02	1.05E-03	1.13E+06
1.15E+03	4.424E+02	3.50E+02	1.33E-03	1.26E+06
1.50E+03	6.787E+01	5.00E+01	1.53E-03	1.36E+06
1.55E+03	3.555E+02	2.50E+02	1.68E-03	1.42E+06
1.80E+03	6.211E+02	4.00E+02	2.00E-03	1.55E+06
2.20E+03	1.481E+02	9.00E+01	2.25E-03	1.65E+06
2.29E+03	4.967E+02	2.90E+02	2.44E-03	1.71E+06
2.58E+03	7.698E+02	4.20E+02	2.79E-03	1.83E+06
3.00E+03	1.490E+03	7.40E+02	3.37E-03	2.01E+06
3.74E+03	3.431E+02	1.60E+02	3.82E-03	2.14E+06
3.90E+03	5.117E+03	2.10E+03	4.95E-03	2.44E+06
6.00E+03	5.889E+03	2.03E+03	7.02E-03	2.90E+06
8.03E+03	4.766E+03	1.47E+03	8.77E-03	3.24E+06
9.50E+03	1.283E+04	3.50E+03	1.13E-02	3.67E+06
1.30E+04	1.691E+04	4.00E+03	1.50E-02	4.23E+06
1.70E+04	3.988E+04	8.00E+03	2.10E-02	4.99E+06
2.50E+04	2.847E+04	5.00E+03	2.75E-02	5.69E+06
3.00E+04	9.909E+04	1.50E+04	3.75E-02	6.61E+06
4.50E+04	3.705E+04	5.00E+03	4.75E-02	7.41E+06
5.00E+04	1.533E+04	2.00E+03	5.10E-02	7.66E+06
5.20E+04	6.407E+04	8.00E+03	5.60E-02	8.01E+06
6.00E+04	1.128E+05	1.30E+04	6.65E-02	8.68E+06
7.30E+04	1.825E+04	2.00E+03	7.40E-02	9.12E+06
7.50E+04	6.562E+04	7.00E+03	7.85E-02	9.37E+06

Continued on following page

E [eV]	dS [$\frac{n}{sec}$]	dE [eV]	Bin Mid. E [MeV]	$\frac{dS}{dE}$ [$\frac{n}{MeVsec}$]
8.20E+04	2.894E+04	3.00E+03	8.35E-02	9.65E+06
8.50E+04	1.516E+05	1.50E+04	9.25E-02	1.01E+07
1.00E+05	3.106E+05	2.80E+04	1.14E-01	1.11E+07
1.28E+05	2.662E+05	2.20E+04	1.39E-01	1.21E+07
1.50E+05	6.658E+05	5.00E+04	1.75E-01	1.33E+07
2.00E+05	1.046E+06	7.00E+04	2.35E-01	1.49E+07
2.70E+05	9.791E+05	6.00E+04	3.00E-01	1.63E+07
3.30E+05	1.217E+06	7.00E+04	3.65E-01	1.74E+07
4.00E+05	3.598E+05	2.00E+04	4.10E-01	1.80E+07
4.20E+05	3.645E+05	2.00E+04	4.30E-01	1.82E+07
4.40E+05	5.548E+05	3.00E+04	4.55E-01	1.85E+07
4.70E+05	5.634E+05	3.00E+04	4.85E-01	1.88E+07
5.00E+05	9.553E+05	5.00E+04	5.25E-01	1.91E+07
5.50E+05	4.453E+05	2.30E+04	5.62E-01	1.94E+07
5.73E+05	5.268E+05	2.70E+04	5.87E-01	1.95E+07
6.00E+05	1.382E+06	7.00E+04	6.35E-01	1.97E+07
6.70E+05	1.791E+05	9.00E+03	6.75E-01	1.99E+07
6.79E+05	1.421E+06	7.10E+04	7.15E-01	2.00E+07
7.50E+05	1.410E+06	7.00E+04	7.85E-01	2.01E+07
8.20E+05	8.275E+05	4.10E+04	8.41E-01	2.02E+07
8.61E+05	2.826E+05	1.40E+04	8.68E-01	2.02E+07
8.75E+05	5.044E+05	2.50E+04	8.88E-01	2.02E+07
9.00E+05	4.032E+05	2.00E+04	9.10E-01	2.02E+07
9.20E+05	1.808E+06	9.00E+04	9.65E-01	2.01E+07
1.01E+06	1.792E+06	9.00E+04	1.06E+00	1.99E+07
1.10E+06	1.962E+06	1.00E+05	1.15E+00	1.96E+07
1.20E+06	9.676E+05	5.00E+04	1.23E+00	1.94E+07
1.25E+06	1.337E+06	7.00E+04	1.29E+00	1.91E+07
1.32E+06	7.543E+05	4.00E+04	1.34E+00	1.89E+07
1.36E+06	7.469E+05	4.00E+04	1.38E+00	1.87E+07
1.40E+06	1.833E+06	1.00E+05	1.45E+00	1.83E+07
1.50E+06	5.988E+06	3.50E+05	1.68E+00	1.71E+07
1.85E+06	7.317E+06	5.00E+05	2.10E+00	1.46E+07
2.35E+06	1.661E+06	1.30E+05	2.42E+00	1.28E+07
2.48E+06	5.678E+06	5.20E+05	2.74E+00	1.09E+07
3.00E+06	8.537E+06	1.30E+06	3.65E+00	6.57E+06
4.30E+06	1.775E+06	5.00E+05	4.55E+00	3.55E+06
4.80E+06	2.920E+06	1.63E+06	5.62E+00	1.79E+06
6.43E+06	9.320E+05	1.76E+06	7.31E+00	5.30E+05
8.19E+06	2.444E+05	1.81E+06	9.10E+00	1.35E+05
1.00E+07				

Table D.9: ORIGAMI photon results for a Westinghouse 17×17 PWR assembly burned to $57.535 \frac{MWd}{kg}$ and cooled for a combined time period of 45yr.

E [eV]	dS [$\frac{p}{sec}$]	dE [eV]	Bin Mid. E [MeV]	$\frac{dS}{dE}$ [$\frac{p}{MeVsec}$]
1.00E+04	3.450E+13	1.00E+04	1.50E-02	3.45E+15
2.00E+04	1.609E+13	1.00E+04	2.50E-02	1.61E+15
3.00E+04	2.171E+13	1.50E+04	3.75E-02	1.45E+15
4.50E+04	1.425E+13	1.50E+04	5.25E-02	9.50E+14
6.00E+04	4.081E+12	1.00E+04	6.50E-02	4.08E+14
7.00E+04	1.878E+12	5.00E+03	7.25E-02	3.76E+14
7.50E+04	6.788E+12	2.50E+04	8.75E-02	2.72E+14
1.00E+05	7.218E+12	5.00E+04	1.25E-01	1.44E+14
1.50E+05	4.395E+12	5.00E+04	1.75E-01	8.79E+13
2.00E+05	2.427E+12	6.00E+04	2.30E-01	4.05E+13
2.60E+05	1.131E+12	4.00E+04	2.80E-01	2.83E+13
3.00E+05	2.389E+12	1.00E+05	3.50E-01	2.39E+13
4.00E+05	7.066E+11	5.00E+04	4.25E-01	1.41E+13
4.50E+05	6.808E+11	6.00E+04	4.80E-01	1.13E+13
5.10E+05	4.133E+09	2.00E+03	5.11E-01	2.07E+12
5.12E+05	3.577E+11	8.80E+04	5.56E-01	4.06E+12
6.00E+05	1.394E+14	1.00E+05	6.50E-01	1.39E+15
7.00E+05	4.944E+11	1.00E+05	7.50E-01	4.94E+12
8.00E+05	3.104E+11	1.00E+05	8.50E-01	3.10E+12
9.00E+05	3.107E+11	1.00E+05	9.50E-01	3.11E+12
1.00E+06	2.129E+11	2.00E+05	1.10E+00	1.06E+12
1.20E+06	3.673E+11	1.30E+05	1.27E+00	2.83E+12
1.33E+06	1.810E+10	1.10E+05	1.39E+00	1.65E+11
1.44E+06	1.169E+10	6.00E+04	1.47E+00	1.95E+11
1.50E+06	5.760E+09	7.00E+04	1.54E+00	8.23E+10
1.57E+06	2.184E+10	9.00E+04	1.62E+00	2.43E+11
1.66E+06	4.290E+09	1.40E+05	1.73E+00	3.06E+10
1.80E+06	1.934E+09	2.00E+05	1.90E+00	9.67E+09
2.00E+06	3.322E+08	1.50E+05	2.08E+00	2.21E+09
2.15E+06	9.738E+06	2.00E+05	2.25E+00	4.87E+07
2.35E+06	1.260E+06	1.50E+05	2.43E+00	8.40E+06
2.50E+06	6.780E+07	2.50E+05	2.63E+00	2.71E+08
2.75E+06	2.355E+06	2.50E+05	2.88E+00	9.42E+06
3.00E+06	2.858E+06	5.00E+05	3.25E+00	5.72E+06
3.50E+06	1.657E+06	5.00E+05	3.75E+00	3.31E+06
4.00E+06	9.593E+05	5.00E+05	4.25E+00	1.92E+06
4.50E+06	5.562E+05	5.00E+05	4.75E+00	1.11E+06
5.00E+06	3.224E+05	5.00E+05	5.25E+00	6.45E+05
5.50E+06	1.869E+05	5.00E+05	5.75E+00	3.74E+05

Continued on following page

E [eV]	dS [$\frac{p}{sec}$]	dE [eV]	Bin Mid. E [MeV]	$\frac{dS}{dE}$ [$\frac{p}{MeV sec}$]
6.00E+06	1.084E+05	5.00E+05	6.25E+00	2.17E+05
6.50E+06	6.284E+04	5.00E+05	6.75E+00	1.26E+05
7.00E+06	3.643E+04	5.00E+05	7.25E+00	7.29E+04
7.50E+06	2.112E+04	5.00E+05	7.75E+00	4.22E+04
8.00E+06	2.495E+04	2.00E+06	9.00E+00	1.25E+04
1.00E+07				

Table D.10: ORIGAMI photon results for a Westinghouse 17×17 PWR assembly burned to $57.535 \frac{MWd}{kg}$ and cooled for a combined time period of 45yr.

E [eV]	dS [$\frac{n}{sec}$]	dE [eV]	Bin Mid. E [MeV]	$\frac{dS}{dE}$ [$\frac{n}{MeV sec}$]
1.00E-05	1.875E-08	9.00E-05	5.50E-11	2.08E+02
1.00E-04	1.634E-07	4.00E-04	3.00E-10	4.09E+02
5.00E-04	1.541E-07	2.50E-04	6.25E-10	6.16E+02
7.50E-04	1.764E-07	2.50E-04	8.75E-10	7.05E+02
1.00E-03	1.627E-07	2.00E-04	1.10E-09	8.14E+02
1.20E-03	2.686E-07	3.00E-04	1.35E-09	8.95E+02
1.50E-03	5.097E-07	5.00E-04	1.75E-09	1.02E+03
2.00E-03	5.789E-07	5.00E-04	2.25E-09	1.16E+03
2.50E-03	6.361E-07	5.00E-04	2.75E-09	1.27E+03
3.00E-03	1.440E-06	1.00E-03	3.50E-09	1.44E+03
4.00E-03	1.638E-06	1.00E-03	4.50E-09	1.64E+03
5.00E-03	4.805E-06	2.50E-03	6.25E-09	1.92E+03
7.50E-03	5.690E-06	2.50E-03	8.75E-09	2.28E+03
1.00E-02	4.911E-05	1.53E-02	1.77E-08	3.21E+03
2.53E-02	1.904E-05	4.70E-03	2.77E-08	4.05E+03
3.00E-02	4.553E-05	1.00E-02	3.50E-08	4.55E+03
4.00E-02	5.165E-05	1.00E-02	4.50E-08	5.16E+03
5.00E-02	5.711E-05	1.00E-02	5.50E-08	5.71E+03
6.00E-02	6.209E-05	1.00E-02	6.50E-08	6.21E+03
7.00E-02	6.670E-05	1.00E-02	7.50E-08	6.67E+03
8.00E-02	7.101E-05	1.00E-02	8.50E-08	7.10E+03
9.00E-02	7.507E-05	1.00E-02	9.50E-08	7.51E+03
1.00E-01	2.042E-04	2.50E-02	1.13E-07	8.17E+03
1.25E-01	2.258E-04	2.50E-02	1.38E-07	9.03E+03
1.50E-01	2.462E-04	2.50E-02	1.63E-07	9.85E+03
1.75E-01	2.645E-04	2.50E-02	1.88E-07	1.06E+04
2.00E-01	2.816E-04	2.50E-02	2.13E-07	1.13E+04
2.25E-01	2.976E-04	2.50E-02	2.38E-07	1.19E+04
2.50E-01	3.129E-04	2.50E-02	2.63E-07	1.25E+04

Continued on following page

E [eV]	dS [$\frac{n}{sec}$]	dE [eV]	Bin Mid. E [MeV]	$\frac{dS}{dE}$ [$\frac{n}{MeV sec}$]
2.75E-01	3.274E-04	2.50E-02	2.88E-07	1.31E+04
3.00E-01	3.413E-04	2.50E-02	3.13E-07	1.37E+04
3.25E-01	3.547E-04	2.50E-02	3.38E-07	1.42E+04
3.50E-01	3.675E-04	2.50E-02	3.63E-07	1.47E+04
3.75E-01	3.800E-04	2.50E-02	3.88E-07	1.52E+04
4.00E-01	7.957E-04	5.00E-02	4.25E-07	1.59E+04
4.50E-01	8.411E-04	5.00E-02	4.75E-07	1.68E+04
5.00E-01	8.842E-04	5.00E-02	5.25E-07	1.77E+04
5.50E-01	9.253E-04	5.00E-02	5.75E-07	1.85E+04
6.00E-01	4.775E-04	2.50E-02	6.13E-07	1.91E+04
6.25E-01	4.871E-04	2.50E-02	6.38E-07	1.95E+04
6.50E-01	1.002E-03	5.00E-02	6.75E-07	2.00E+04
7.00E-01	1.039E-03	5.00E-02	7.25E-07	2.08E+04
7.50E-01	1.074E-03	5.00E-02	7.75E-07	2.15E+04
8.00E-01	1.108E-03	5.00E-02	8.25E-07	2.22E+04
8.50E-01	1.141E-03	5.00E-02	8.75E-07	2.28E+04
9.00E-01	5.826E-04	2.50E-02	9.13E-07	2.33E+04
9.25E-01	5.905E-04	2.50E-02	9.38E-07	2.36E+04
9.50E-01	5.984E-04	2.50E-02	9.63E-07	2.39E+04
9.75E-01	6.061E-04	2.50E-02	9.88E-07	2.42E+04
1.00E+00	2.446E-04	1.00E-02	1.01E-06	2.45E+04
1.01E+00	2.458E-04	1.00E-02	1.02E-06	2.46E+04
1.02E+00	2.470E-04	1.00E-02	1.03E-06	2.47E+04
1.03E+00	2.482E-04	1.00E-02	1.04E-06	2.48E+04
1.04E+00	2.494E-04	1.00E-02	1.05E-06	2.49E+04
1.05E+00	2.506E-04	1.00E-02	1.06E-06	2.51E+04
1.06E+00	2.518E-04	1.00E-02	1.07E-06	2.52E+04
1.07E+00	2.529E-04	1.00E-02	1.08E-06	2.53E+04
1.08E+00	2.541E-04	1.00E-02	1.09E-06	2.54E+04
1.09E+00	2.553E-04	1.00E-02	1.10E-06	2.55E+04
1.10E+00	2.564E-04	1.00E-02	1.11E-06	2.56E+04
1.11E+00	2.576E-04	1.00E-02	1.12E-06	2.58E+04
1.12E+00	2.587E-04	1.00E-02	1.13E-06	2.59E+04
1.13E+00	2.599E-04	1.00E-02	1.14E-06	2.60E+04
1.14E+00	2.610E-04	1.00E-02	1.15E-06	2.61E+04
1.15E+00	7.898E-04	3.00E-02	1.17E-06	2.63E+04
1.18E+00	5.322E-04	2.00E-02	1.19E-06	2.66E+04
1.20E+00	8.066E-04	3.00E-02	1.22E-06	2.69E+04
1.23E+00	5.432E-04	2.00E-02	1.24E-06	2.72E+04
1.25E+00	1.377E-03	5.00E-02	1.28E-06	2.75E+04
1.30E+00	1.404E-03	5.00E-02	1.33E-06	2.81E+04
1.35E+00	1.430E-03	5.00E-02	1.38E-06	2.86E+04

Continued on following page

E [eV]	dS [$\frac{n}{sec}$]	dE [eV]	Bin Mid. E [MeV]	$\frac{dS}{dE}$ [$\frac{n}{MeV sec}$]
1.40E+00	1.456E-03	5.00E-02	1.43E-06	2.91E+04
1.45E+00	1.481E-03	5.00E-02	1.48E-06	2.96E+04
1.50E+00	2.728E-03	9.00E-02	1.55E-06	3.03E+04
1.59E+00	2.806E-03	9.00E-02	1.64E-06	3.12E+04
1.68E+00	2.883E-03	9.00E-02	1.73E-06	3.20E+04
1.77E+00	2.957E-03	9.00E-02	1.82E-06	3.29E+04
1.86E+00	2.689E-03	8.00E-02	1.90E-06	3.36E+04
1.94E+00	2.054E-03	6.00E-02	1.97E-06	3.42E+04
2.00E+00	4.200E-03	1.20E-01	2.06E-06	3.50E+04
2.12E+00	3.229E-03	9.00E-02	2.17E-06	3.59E+04
2.21E+00	3.295E-03	9.00E-02	2.26E-06	3.66E+04
2.30E+00	2.984E-03	8.00E-02	2.34E-06	3.73E+04
2.38E+00	3.417E-03	9.00E-02	2.43E-06	3.80E+04
2.47E+00	3.871E-03	1.00E-01	2.52E-06	3.87E+04
2.57E+00	3.947E-03	1.00E-01	2.62E-06	3.95E+04
2.67E+00	4.021E-03	1.00E-01	2.72E-06	4.02E+04
2.77E+00	4.095E-03	1.00E-01	2.82E-06	4.09E+04
2.87E+00	4.166E-03	1.00E-01	2.92E-06	4.17E+04
2.97E+00	1.264E-03	3.00E-02	2.99E-06	4.21E+04
3.00E+00	2.120E-03	5.00E-02	3.03E-06	4.24E+04
3.05E+00	4.293E-03	1.00E-01	3.10E-06	4.29E+04
3.15E+00	1.556E-02	3.50E-01	3.33E-06	4.45E+04
3.50E+00	1.066E-02	2.30E-01	3.62E-06	4.64E+04
3.73E+00	1.294E-02	2.70E-01	3.87E-06	4.79E+04
4.00E+00	3.823E-02	7.50E-01	4.38E-06	5.10E+04
4.75E+00	1.346E-02	2.50E-01	4.88E-06	5.38E+04
5.00E+00	2.223E-02	4.00E-01	5.20E-06	5.56E+04
5.40E+00	3.491E-02	6.00E-01	5.70E-06	5.82E+04
6.00E+00	1.508E-02	2.50E-01	6.13E-06	6.03E+04
6.25E+00	1.539E-02	2.50E-01	6.38E-06	6.15E+04
6.50E+00	1.568E-02	2.50E-01	6.63E-06	6.27E+04
6.75E+00	1.598E-02	2.50E-01	6.88E-06	6.39E+04
7.00E+00	9.725E-03	1.50E-01	7.08E-06	6.48E+04
7.15E+00	6.393E-02	9.50E-01	7.63E-06	6.73E+04
8.10E+00	7.147E-02	1.00E+00	8.60E-06	7.15E+04
9.10E+00	6.778E-02	9.00E-01	9.55E-06	7.53E+04
1.00E+01	1.198E-01	1.50E+00	1.08E-05	7.99E+04
1.15E+01	3.334E-02	4.00E-01	1.17E-05	8.34E+04
1.19E+01	8.581E-02	1.00E+00	1.24E-05	8.58E+04
1.29E+01	8.014E-02	9.00E-01	1.34E-05	8.90E+04
1.38E+01	5.491E-02	6.00E-01	1.41E-05	9.15E+04
1.44E+01	6.555E-02	7.00E-01	1.48E-05	9.36E+04

Continued on following page

E [eV]	dS [$\frac{n}{sec}$]	dE [eV]	Bin Mid. E [MeV]	$\frac{dS}{dE}$ [$\frac{n}{MeV sec}$]
1.51E+01	8.653E-02	9.00E-01	1.56E-05	9.61E+04
1.60E+01	9.903E-02	1.00E+00	1.65E-05	9.90E+04
1.70E+01	1.541E-01	1.50E+00	1.78E-05	1.03E+05
1.85E+01	5.278E-02	5.00E-01	1.88E-05	1.06E+05
1.90E+01	1.077E-01	1.00E+00	1.95E-05	1.08E+05
2.00E+01	1.104E-01	1.00E+00	2.05E-05	1.10E+05
2.10E+01	1.705E-01	1.50E+00	2.18E-05	1.14E+05
2.25E+01	2.978E-01	2.50E+00	2.38E-05	1.19E+05
2.50E+01	3.135E-01	2.50E+00	2.63E-05	1.25E+05
2.75E+01	3.281E-01	2.50E+00	2.88E-05	1.31E+05
3.00E+01	1.761E-01	1.30E+00	3.07E-05	1.35E+05
3.13E+01	6.872E-02	5.00E-01	3.16E-05	1.37E+05
3.18E+01	2.094E-01	1.50E+00	3.26E-05	1.40E+05
3.33E+01	7.086E-02	5.00E-01	3.36E-05	1.42E+05
3.38E+01	1.145E-01	8.00E-01	3.42E-05	1.43E+05
3.46E+01	1.304E-01	9.00E-01	3.51E-05	1.45E+05
3.55E+01	2.209E-01	1.50E+00	3.63E-05	1.47E+05
3.70E+01	1.498E-01	1.00E+00	3.75E-05	1.50E+05
3.80E+01	1.670E-01	1.10E+00	3.86E-05	1.52E+05
3.91E+01	7.671E-02	5.00E-01	3.94E-05	1.53E+05
3.96E+01	2.177E-01	1.40E+00	4.03E-05	1.55E+05
4.10E+01	2.226E-01	1.40E+00	4.17E-05	1.59E+05
4.24E+01	2.589E-01	1.60E+00	4.32E-05	1.62E+05
4.40E+01	1.973E-01	1.20E+00	4.46E-05	1.64E+05
4.52E+01	3.009E-01	1.80E+00	4.61E-05	1.67E+05
4.70E+01	2.213E-01	1.30E+00	4.77E-05	1.70E+05
4.83E+01	1.549E-01	9.00E-01	4.88E-05	1.72E+05
4.92E+01	2.438E-01	1.40E+00	4.99E-05	1.74E+05
5.06E+01	2.472E-01	1.40E+00	5.13E-05	1.77E+05
5.20E+01	2.505E-01	1.40E+00	5.27E-05	1.79E+05
5.34E+01	1.034E+00	5.60E+00	5.62E-05	1.85E+05
5.90E+01	3.815E-01	2.00E+00	6.00E-05	1.91E+05
6.10E+01	7.816E-01	4.00E+00	6.30E-05	1.95E+05
6.50E+01	5.009E-01	2.50E+00	6.63E-05	2.00E+05
6.75E+01	9.250E-01	4.50E+00	6.98E-05	2.06E+05
7.20E+01	8.467E-01	4.00E+00	7.40E-05	2.12E+05
7.60E+01	8.691E-01	4.00E+00	7.80E-05	2.17E+05
8.00E+01	4.431E-01	2.00E+00	8.10E-05	2.22E+05
8.20E+01	1.826E+00	8.00E+00	8.60E-05	2.28E+05
9.00E+01	2.398E+00	1.00E+01	9.50E-05	2.40E+05
1.00E+02	2.007E+00	8.00E+00	1.04E-04	2.51E+05
1.08E+02	1.818E+00	7.00E+00	1.12E-04	2.60E+05

Continued on following page

E [eV]	dS [$\frac{n}{sec}$]	dE [eV]	Bin Mid. E [MeV]	$\frac{dS}{dE}$ [$\frac{n}{MeV sec}$]
1.15E+02	1.064E+00	4.00E+00	1.17E-04	2.66E+05
1.19E+02	8.097E-01	3.00E+00	1.21E-04	2.70E+05
1.22E+02	1.948E+01	6.40E+01	1.54E-04	3.04E+05
1.86E+02	2.366E+00	7.00E+00	1.90E-04	3.38E+05
1.93E+02	5.214E+00	1.50E+01	2.01E-04	3.48E+05
2.08E+02	7.101E-01	2.00E+00	2.09E-04	3.55E+05
2.10E+02	1.105E+01	3.00E+01	2.25E-04	3.68E+05
2.40E+02	1.791E+01	4.50E+01	2.63E-04	3.98E+05
2.85E+02	8.446E+00	2.00E+01	2.95E-04	4.22E+05
3.05E+02	1.240E+02	2.45E+02	4.28E-04	5.06E+05
5.50E+02	7.269E+01	1.20E+02	6.10E-04	6.06E+05
6.70E+02	8.295E+00	1.30E+01	6.77E-04	6.38E+05
6.83E+02	1.869E+02	2.67E+02	8.17E-04	7.00E+05
9.50E+02	1.591E+02	2.00E+02	1.05E-03	7.95E+05
1.15E+03	3.126E+02	3.50E+02	1.33E-03	8.93E+05
1.50E+03	4.795E+01	5.00E+01	1.53E-03	9.59E+05
1.55E+03	2.512E+02	2.50E+02	1.68E-03	1.00E+06
1.80E+03	4.387E+02	4.00E+02	2.00E-03	1.10E+06
2.20E+03	1.046E+02	9.00E+01	2.25E-03	1.16E+06
2.29E+03	3.508E+02	2.90E+02	2.44E-03	1.21E+06
2.58E+03	5.437E+02	4.20E+02	2.79E-03	1.29E+06
3.00E+03	1.053E+03	7.40E+02	3.37E-03	1.42E+06
3.74E+03	2.424E+02	1.60E+02	3.82E-03	1.51E+06
3.90E+03	3.615E+03	2.10E+03	4.95E-03	1.72E+06
6.00E+03	4.160E+03	2.03E+03	7.02E-03	2.05E+06
8.03E+03	3.367E+03	1.47E+03	8.77E-03	2.29E+06
9.50E+03	9.067E+03	3.50E+03	1.13E-02	2.59E+06
1.30E+04	1.195E+04	4.00E+03	1.50E-02	2.99E+06
1.70E+04	2.818E+04	8.00E+03	2.10E-02	3.52E+06
2.50E+04	2.012E+04	5.00E+03	2.75E-02	4.02E+06
3.00E+04	7.002E+04	1.50E+04	3.75E-02	4.67E+06
4.50E+04	2.618E+04	5.00E+03	4.75E-02	5.24E+06
5.00E+04	1.083E+04	2.00E+03	5.10E-02	5.41E+06
5.20E+04	4.526E+04	8.00E+03	5.60E-02	5.66E+06
6.00E+04	7.969E+04	1.30E+04	6.65E-02	6.13E+06
7.30E+04	1.289E+04	2.00E+03	7.40E-02	6.45E+06
7.50E+04	4.636E+04	7.00E+03	7.85E-02	6.62E+06
8.20E+04	2.044E+04	3.00E+03	8.35E-02	6.81E+06
8.50E+04	1.071E+05	1.50E+04	9.25E-02	7.14E+06
1.00E+05	2.194E+05	2.80E+04	1.14E-01	7.84E+06
1.28E+05	1.881E+05	2.20E+04	1.39E-01	8.55E+06
1.50E+05	4.703E+05	5.00E+04	1.75E-01	9.41E+06

Continued on following page

E [eV]	dS [$\frac{n}{sec}$]	dE [eV]	Bin Mid. E [MeV]	$\frac{dS}{dE}$ [$\frac{n}{MeVsec}$]
2.00E+05	7.387E+05	7.00E+04	2.35E-01	1.06E+07
2.70E+05	6.914E+05	6.00E+04	3.00E-01	1.15E+07
3.30E+05	8.591E+05	7.00E+04	3.65E-01	1.23E+07
4.00E+05	2.541E+05	2.00E+04	4.10E-01	1.27E+07
4.20E+05	2.574E+05	2.00E+04	4.30E-01	1.29E+07
4.40E+05	3.918E+05	3.00E+04	4.55E-01	1.31E+07
4.70E+05	3.979E+05	3.00E+04	4.85E-01	1.33E+07
5.00E+05	6.746E+05	5.00E+04	5.25E-01	1.35E+07
5.50E+05	3.145E+05	2.30E+04	5.62E-01	1.37E+07
5.73E+05	3.720E+05	2.70E+04	5.87E-01	1.38E+07
6.00E+05	9.760E+05	7.00E+04	6.35E-01	1.39E+07
6.70E+05	1.265E+05	9.00E+03	6.75E-01	1.41E+07
6.79E+05	1.004E+06	7.10E+04	7.15E-01	1.41E+07
7.50E+05	9.957E+05	7.00E+04	7.85E-01	1.42E+07
8.20E+05	5.843E+05	4.10E+04	8.41E-01	1.43E+07
8.61E+05	1.995E+05	1.40E+04	8.68E-01	1.43E+07
8.75E+05	3.561E+05	2.50E+04	8.88E-01	1.42E+07
9.00E+05	2.847E+05	2.00E+04	9.10E-01	1.42E+07
9.20E+05	1.277E+06	9.00E+04	9.65E-01	1.42E+07
1.01E+06	1.265E+06	9.00E+04	1.06E+00	1.41E+07
1.10E+06	1.386E+06	1.00E+05	1.15E+00	1.39E+07
1.20E+06	6.835E+05	5.00E+04	1.23E+00	1.37E+07
1.25E+06	9.448E+05	7.00E+04	1.29E+00	1.35E+07
1.32E+06	5.329E+05	4.00E+04	1.34E+00	1.33E+07
1.36E+06	5.278E+05	4.00E+04	1.38E+00	1.32E+07
1.40E+06	1.296E+06	1.00E+05	1.45E+00	1.30E+07
1.50E+06	4.237E+06	3.50E+05	1.68E+00	1.21E+07
1.85E+06	5.193E+06	5.00E+05	2.10E+00	1.04E+07
2.35E+06	1.181E+06	1.30E+05	2.42E+00	9.09E+06
2.48E+06	4.044E+06	5.20E+05	2.74E+00	7.78E+06
3.00E+06	6.055E+06	1.30E+06	3.65E+00	4.66E+06
4.30E+06	1.249E+06	5.00E+05	4.55E+00	2.50E+06
4.80E+06	2.053E+06	1.63E+06	5.62E+00	1.26E+06
6.43E+06	6.543E+05	1.76E+06	7.31E+00	3.72E+05
8.19E+06	1.713E+05	1.81E+06	9.10E+00	9.47E+04
1.00E+07				

APPENDIX E

SUMMARY NEUTRON TABLES

Table E.1: Dose from neutrons in $\frac{Rad(Si)}{hr}$ taken as an average on the multi-purpose canister wall.

	5 yr	15 yr	25 yr
MPC-24	1.677E-02	-	7.927E-03
MPC-32	2.449E-02	1.670E-02	1.158E-02
MPC-68	3.281E-04	2.387E-04	1.774E-04

Table E.2: Cobalt activation from neutrons in $\frac{Bq}{gm}$ per hr exposure taken as an average on the multi-purpose canister wall.

	5 yr	15 yr	25 yr
MPC-24	1.581E-01	-	7.520E-02
MPC-32	2.177E-01	1.495E-01	1.036E-01
MPC-68	2.785E-03	2.034E-03	1.514E-03

Table E.3: Dose from neutrons in $\frac{Rem}{hr}$ taken as an average on the METCON wall.

	5 yr	15 yr	25 yr
MPC-24	3.268E-03	-	1.536E-03
MPC-32	5.432E-03	3.706E-03	2.552E-03
MPC-68	7.443E-05	5.427E-05	4.042E-05

Table E.4: Dose from neutrons in $\frac{Rad(Si)}{hr}$ taken as an average on the multi-purpose canister lid.

	5 yr	15 yr	25 yr
MPC-24	8.535E-04	-	4.051E-04
MPC-32	1.423E-03	9.747E-04	6.795E-04
MPC-68	4.633E-05	3.366E-05	2.516E-05

Table E.5: Dose from neutrons in $\frac{Rad(Si)}{hr}$ taken behind a 4-side, 5mm, Pb shield as an F4 tally in the annulus formed by the multi-purpose canister and the METCON.

	5 yr	15 yr	25 yr
MPC-24	1.896E-02	-	8.778E-03
MPC-32	2.921E-02	2.019E-02	1.377E-02
MPC-68	3.404E-04	2.490E-04	1.890E-04

APPENDIX F

SUMMARY PHOTON TABLES

Table F.1: Dose from photons in $\frac{Rad(Si)}{hr}$ taken as an average on the multi-purpose canister wall.

	5 yr	15 yr	25 yr
MPC-24	8.961E+03	-	2.448E+03
MPC-32	1.435E+04	5.446E+03	3.960E+03
MPC-68	3.396E+03	2.000E+03	1.535E+03

Table F.2: Dose from photons in $\frac{Rem}{hr}$ taken as an average on the METCON wall.

	5 yr	15 yr	25 yr
MPC-24	3.949E-02	-	4.035E-03
MPC-32	6.316E-02	1.234E-02	6.779E-03
MPC-68	1.092E-02	2.686E-03	1.641E-03

Table F.3: Dose from photons in $\frac{Rad(Si)}{hr}$ taken as an average on the multi-purpose canister lid.

	5 yr	15 yr	25 yr
MPC-24	1.662E+00	-	4.358E-01
MPC-32	5.240E+00	1.909E+00	1.370E+00
MPC-68	3.956E+00	2.260E+00	1.616E+00

Table F.4: Dose from photons in $\frac{Rad(Si)}{hr}$ taken behind a 4-side, 5mm, Pb shield as an F4 tally in the annulus formed by the multi-purpose canister and the METCON.

	5 yr	15 yr	25 yr
MPC-24	3.147E+03	-	7.693E+02
MPC-32	6.619E+03	2.379E+03	1.707E+03
MPC-68	1.643E+03	9.283E+02	7.542E+02